UNIVERSIDAD DE MURCIA
FACULTAD DE MEDICINA

New Eutectoid Materials in the System Dicalcium Silicate-Tricalcium Phosphate as scaffolds for Bone Tissue Engineering

Nuevos Materiales Eutectoides en el Sistema Fosfato Tricálcico-Silicato Dicálcico para Regeneración Ósea

Cragnolini Francesca

2012

Cada trecho recorrido enriquece al peregrino y lo acerca un poco más a hacer realidad sus sueños.

El Alquimista

to my grandfather,

and my family

ACKNOWLEDGEMENTS

During these years not only I learned many new things in the fields of the biotechnology, the orthopaedic medicine, and tissue regeneration based on stem cell research, also I learned many things about life and people y met on the way show me new ways of life and different manners to approach the troubles presenting in the life like in the science. So now I have new attitudes and I feel enrich.

For this reason I would like to start saying that it has been a wonderful experience and I hope to go on in the field of the research in my life.

First I would like to thanks my Directors: Dr. Luis Meseguer Olmo from the University of Murcia, and Dra. Piedad Nieves De Aza Moya from the University of Elche, for give me the opportunity to realize this project and support me during its realization.

A special gratitude is directed to Luis, for transmitting me his knowledge and great practical experience, for his patience, and for the hours spent for the realization of this research work. Very important for me was the freedom he gives me to propose and realize my own ideas and for his helpful criticism; because this attitude stimulates my participation in the project, with equivocations, but I could correct the errors to progress. But above all, I will thanks him because in every moment I feel like home, the very important think when you are far from your own home.

I would also like to extend my gratitude to my laboratory companions from the group of Cellular Therapy of Universitary Hospital Virgen de la Arrixaca, for their valuable help during my research work. Between them special thanks to Paola Romecín Duran and David García Bernal for help me in flow cytometry studies, Carlos Bueno for cell transfection, and Ana Belen Meseguer Henarejos for samples collection and storing. Many thanks also to all the Doctors/Professors of the group, that first of all contracted me in the group giving me the possibility to realize my thesis and incorporate in the MSCs Bone Regeneration Therapy line, discovering a new and interesting world, and help during this years working together.

I would like to express my sincerely thanks to the Cellular Cultures Service of the University of Murcia (SACE), for the important guidance its personal gives to me

and helpfulness; especially I whant to name Antonia Bernabeu for the essential help gave me and suggestions based in her large experience.

Least but not last, I would like to express my warmest and deepest gratitude to my Mom and Papi, for believing in me and for their unconditional emotional and economic support throughout my academic career. Especially I want to mention my grandparents that always repeat me that they would be there for anything y need, and so it has been until now. I hope my family will be proud, and above of all, my grandfather Francesco, because I have reached my purpose, the one he desired for me. I thanks my sister and her family, to help me when I was in need, and for give me a nieces that love me so much.
Finally I would like to thanks my friends, the Italians and the Spanish ones and the others from all the countries: I will always remember your encouragement, kindness and friendship, because without these things it would not have been possible to finish my thesis.

I conclude remembering all the people that even if we leave apart, we never will be distant.

You know

Francesca Cragnolini

Index

Abbreviations

HA: Hydroxyapatite

ALP: Alkaline Phosphatase

AR: Alizarin Red

BMP: Bone Morphogenetic Proteins

BSP: Bone sialoprotein

C_2S: (Ca_2SiO_4) Dicalcium Silicate

Ca: Calcium

CBFβ: small protein core binding factor β

COLI: Collagen type I

COLIAI: α1(I) collagen

CT: Threshold Cycle

ECM: Extracellulare Matrix

EDS: Energy-dispersive X-ray spectroscopy

ERK/12: Extracellular Signal-regulated Kinases 1/2

FC: Flow Cytometry

FGF: Fibroblast growth factor

FGF-2: Fibroblast growth factor 2,

GAPDH: Glyceraldehyde-3-phosphate dehydrogenase

GM: Growth Medium

HS: Heparan Sulfate

ICP-OES: Inductively Coupled Plasma Optical Emission Spectrometry

IF: Immunofluorescence

MAPK: Mitogen-activated Protein Kinase

MSCs: Mesenchymal stem cells

NPP1: Nucleotide Pyrophosphatase Phosphodiesterase

OM: Osteogenic Medium

OPN: Osteopontin

OSC: Osteocalcin

OSE2: Osteoblast Specific Element 2

OSN: Osteonectin

P: Phosphorous

Pi: Inorganic phosphate

PPi: Pyrophosphate

Ppm: Part per million

Real time RT-PCR: Reverse-Transcription Polymerase Chain Reaction In Real Time,

RT: Room temperature

RUNX2: Runt-related transcription factor 2

SBF: Fetal Bovine Serum

SEM: Scanning Electron Microscopy

Si: Silicon

TCP: Tricalcium Phosphate

TGFβ: Transforming Growth Factor β

TNAP: Tissue Non Specific Alkaline Phosphatase

Introduction

1. INTRODUCTION

1.1 BONE TISSUE

1.1.1 DEVELOPMENTAL SKELETOGENESIS

Skeletogenesis in the developing embryo involves the distinct processes of cellular differentiation leading to the formation of cartilage and bone. Because the skeleton represents the scaffolding of the vertebrate animal and provides the general architecture of the body, developmental skeletogenesis must follow a highly programmed pathway and is regulated by multiple cellular and humoral control mechanism.

1.1.2 INTRAMEMBRANOUS AND ENDOCHONDRAL OSSIFICATION

Embryonic skeletal development occurs through two major pathways: (1) the endochondral pathway, such as in the long bones of the limb; (2) and the intramembranous pathway, which takes place predominantly in the bones of the craniofacial structures. In the endochondral ossification sequence, mesenchymal cells, such as those in the embryonic limb bud, condense and differentiate into cartilage, which becomes an anlage of the future skeletal components. Bone Morphogenetic Proteins (BPS), as well as Fibroblast Growth Factors (FGFs) appear to be essential in the process of mesenchymal cell condensation. Briefly, the cartilage anlage subsequently matures, undergoes hypertrophy, mineralizes, and is then invaded by blood vessels and osteoprogenitor cells. These cells differentiate into osteoblasts and form spicules of bone by the production and mineralization of an osteoid matrix. In detail, under the influence of a different set of factors and local conditions, mesenchymal cells undergo division and differentiate into prechondroblasts and then into chondroblasts rather than directly into osteoblasts. These cells secrete the cartilaginous matrix, where the predominant collagen is collagen type II. Like osteoblasts, the chondroblasts become progressively embedded

within their own matrix, where they lie within lacunae, and they are then called chondrocytes. Unlike osteocytes however, chondrocytes continue to proliferate for some time, this being allowed in part by the gel-like consistency of cartilage. At the periphery of this cartilage (in the perichondrium), the mesenchymal cells continue to proliferate and differentiate through appositional growth. Another type of growth is observed in the cartilage by cell proliferation and synthesis of new matrix between the chondrocytes (interstitial growth). Beginning in the centre of the cartilage model, at what is to become the primary ossification center, chondrocytes continue to differentiate and become hypertrophic. During this process, hypertrophic cells deposit a mineralized matrix, where cartilage calcification is initiated by matrix vesicles. Once this matrix is calcified, it is partially resorbed by osteoclasts. After resorption and a reversal phase, osteoblasts differentiate in this area and form a layer of woven bone on top of the remaining cartilage. This woven bone will later be remodeled into lamellar bone. The growth plate demonstrates, from the epiphyseal area to the diaphyseal area, the different stages of chondrocyte differentiation involved in endochondral bone formation. In contrast, intramembranous bone formation involves direct differentiation of mesenchymal cells into osteoblasts. The newly differentiated osteoblasts will synthesize a woven bone matrix, while at the periphery, mesenchymal cells continue to differentiate into osteoblasts. Blood vessels are incorporated between the woven bone trabeculae and will form the hematopoietic bone marrow. Later this woven bone will be remodeled through the classical remodeling process, resorbing woven bone and progressively replacing it with mature lamellar bone. No cartilage intermediate is found in the intramembranous pathway. Thus, although the final bony tissue in the intramembranous bone and that in the endochondral bone resemble each other, the pathways leading to their formation are distinctly different. The mechanistic basis underlying the progression of the embryonic mesenchyme along the endochondral or intramembranous pathway is currently unknown. However, it is noteworthy that, in most cases, the origins of the mesenchymal cells, which give rise to the endochondral long bones and the intramembranous craniofacial bones, are most likely also different. Osteoblasts in many of the craniofacial bones in vertebrates are descendents of the neural crest cells, a mesenchymal cell type that is unique to vertebrates and is derived from the

neural ectoderm. By contrast, osteoblasts in the rest of the axial skeleton and the appendicular skeleton are derived from the paraxial mesoderm (somites) and the lateral plate mesoderm, respectively.

Nevertheless, it should be pointed out that neural crest cells will differentiate into cartilage, provided that they interact with the appropriate epithelium during their migration to the rostral part of the developing embryo. For example, differentiation of cranial neural crest mesenchymal cells that have anchorin CII receptors for type II collagen may be influenced by interactions with type II collagen on neuroepithelial tissues encountered during migration. These studies, therefore, clearly indicate that both mesenchymally-derived cells and their interactions with adjacent epithelial cells play important roles in skeletal development.

Under certain conditions, the normally intramembranous calvarium also displays a phenotype resembling that of cartilage. For example, in chick embryos that have been made calcium-deficient via long-term maintenance in culture without their eggshells, the calvarium expresses type II collagen, a cartilage-associated matrix molecule, and cells with a chondrocyte-like phenotype. Another example is the formation in the calvarium of a fracture callus, which also undergoes chondrogenesis. Thus, the two pathways of ossification, intramembranous and endochondral, may actually share some commonalities, particularly with regard to the cellular differentiation potential of the initial mesenchymal cell population.

Mesenchymal cells appear to have the potential to undergo chondrogenesis; therefore, in developing intramembranous bone, there must exists a set of conditions that would either enhance osteogenesis or inhibit chondrogenesis. Understanding the nature of these conditions should shed light on the underlying mechanisms that lead to birth defects involving intramembranous bones, such as those of the craniofacial skeleton. Such knowledge should also facilitate designing protocols to enhance bone formation in endochondral bones, especially during fracture repair, because diaphyseal bone growth proceeds via the intramembranous pathway. (Bone formation and repair, Brighton CT, Friedlaender G, Lane JM).

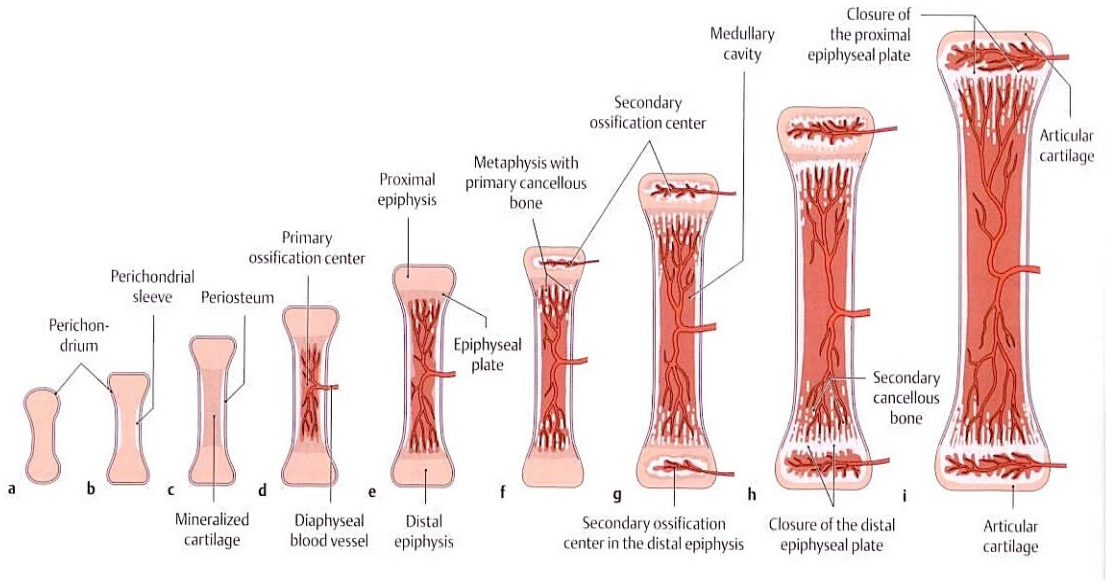

Fig. 1: Skeletogenesis: long bone grow up during development.

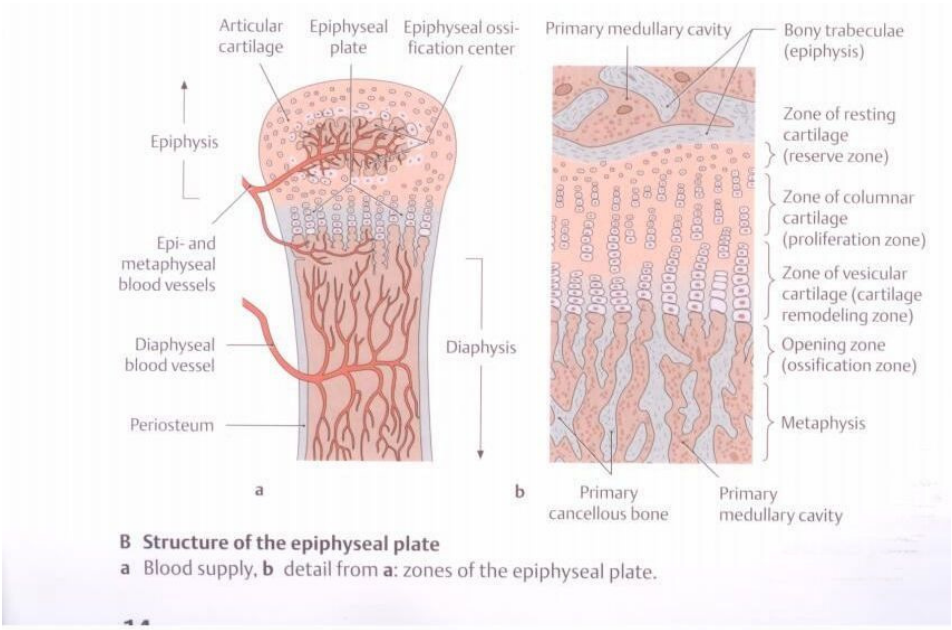

Fig. 2: Structure of the ephifiseal growth plate.

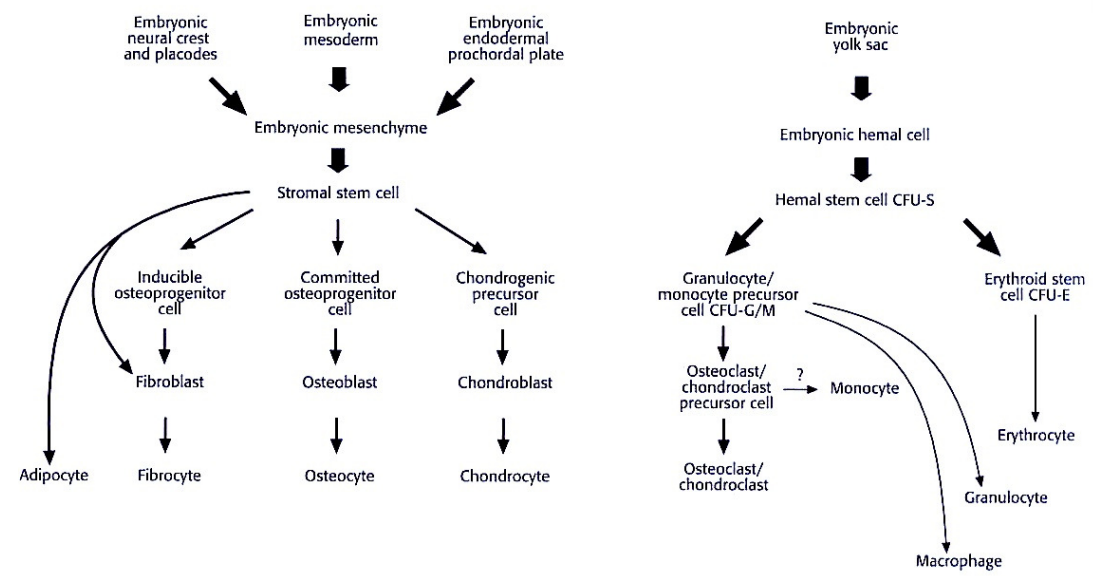

Fig. 3: Schematic representation of stromal stem cells potential differentiation destinies.

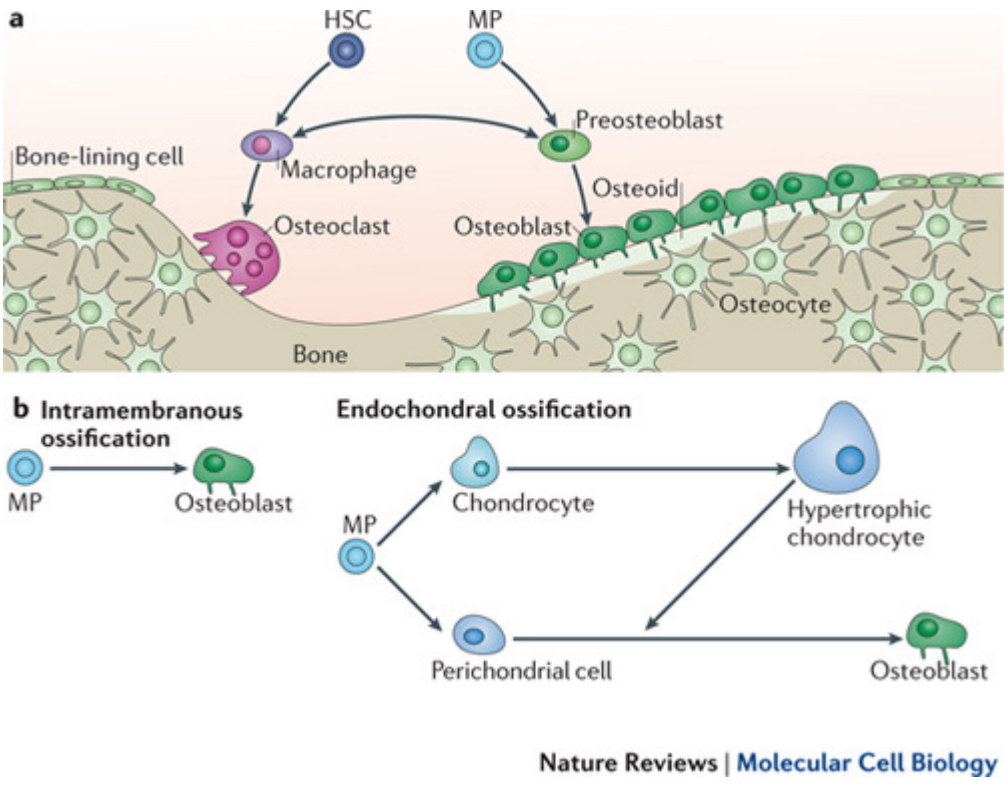

Fig. 4: Intramembranous and endochondral ossification. MP (Mesenchymal precursor) direct differentiation in osteoblast in intramembranous ossification, and MP previous differentiation in chondroblast or perichondral cells in endochondrañ ossification.

1.1.3 BONE FUNCTIONS

Bone intercellular substance, secreted by osteoblasts, becomes calcified for added strength; as a result, bone is the most highly developed of the supporting connective tissue. Since metabolites and gases are unable to diffuse through calcified bone matrix, a direct blood supply is necessary. Bone function as a supporting endoskeleton and for the attachment of tendons and ligaments necessary for locomotion. Bone encloses and protects the brain and spinal cord, and all vital organs. The interior of some bones serves as the site of bone marrow and hematopoiesis (blood cell formation). In addition, bone is a storage depot for calcium and phosphate, which can be mobilized to enter the blood when levels fall below normal, to maintain serum homeostasis which is essential for life. Bone is very hard yet has some elasticity, can be compressed, and has considerable tensile strength. Bone responds to changing stresses and external forces by modifying its organization.

1.1.4 BONE GENERAL ORGANIZATION

Bone is a supporting connective tissue consisting of cells, called osteoblasts, that synthesize and export a product called extracellular matrix or bone matrix. Bone matrix contains collagen fibers and an amorphous component with a high concentration of sulphated proteogycans. In addition, bone matrix becomes calcified following secretion, and the calcium salts take the form of hydroxyapatite crystals. As osteoblasts become surrounded by their secretory product, they develop long, slender extensions, cease the secretion of bone matrix, and are called osteocytes. Large multinucleated cells called osteoclasts are able to erode bone matrix, and are important in bone remodelling and regulating plasma calcium levels. Finally, osteogenic or osteoprogenitor cells derived from embryonic mesenchymal cells persist in certain regions and have the capacity to differentiate into osteoblasts.

MACROSCOPIC STRUCTURE

Bones exist in a variety of shapes and sizes. Long bones such as the femur, have a thick-walled tubular portion in the middle (diaphyses) that expand at each end into two wider extremities (the epiphysis), and between them there is a transition zone (the metaphysis). The epiphysis on the one hand and the metaphysis and midshaft on the other hand originate from two independent ossification centers, and are separated by a layer of cartilage, the epiphyseal cartilage (which constitutes the growth plate) during the period of development and growth. This layer of proliferative cells and expanding cartilage matrix is responsible for the longitudinal growth of bones; it progressively mineralizes and is later remodeled and replaced by bone tissue by the end of the growth period. Articular cartilage covers the epiphysis at the synovial joint. By gross observation it is possible to distinguish two forms of bone: compact and cancellous. Compact bone, which constitutes the external part of the bones in the diaphysis (cortex), is formed by a thick and dense layer of calcified tissue, and encloses the medullary cavity where the hematopoietic bone marrow is housed. Compact bone, that appears solid, actually contains microscopic canals and channels. Toward the metaphysis and the epiphysis, the cortex becomes progressively thinner and the internal space is filled with a network of thin, calcified trabeculae forming the cancellous or trabecular bone. The spaces enclosed by these thin trabeculae are also filled with hematopoietic bone marrow and are continuous with the diaphyseal medullary cavity. The outer cortical bone surfaces at the epiphyses are covered with a layer of articular cartilage that does not calcify. Cancellous bone can be converted into compact bone directly by the continued secretion of layers of bone matrix by osteoblasts onto of the surface of the cancellous bone, but blood vessels must be brought into the interior of compact bone by the formation of osteons or haversian systems. Both compact and cancellous bone undergoes remodelling in response to tension or applied loads, the degree of activity and hormonal fluctuations.

So cortical and trabecular bone are made up of the same cells and the same matrix elements, but there are structural and functional differences. The primary structural difference is quantitative: 80% to 90% of the volume of compact bone is calcified, whereas only 15% to 25% of the trabecular volume is calcified (the remainder being

occupied by bone marrow, blood vessels, and connective tissue). The result is that 70% to 85% of the interface with soft tissues is at the endosteal bone surface, including all trabecular surfaces, leading to the functional difference: the cortical bone fulfills mainly a mechanical and protective function and the trabecular bone mainly a metabolic function, albeit trabeculae definitively participate in the biomechanical function of bones, particularly in bones like the vertebrae. (Chapter 1. ANATOMY AND ULTRASTRUCTURE OF BONE - HISTOGENESIS, GROWTH AND REMODELING. Ronals Baron. Updated: May 13, 2008).

Periosteum and endosteum

Except at articular surfaces, bone possesses a fibrocellular sheath called periosteum. Periosteum consists of an outer fibrous layer containing collagen fibers and fibroblasts that form the collagen fibers and an inner layer called the osteogenic layer. This name means that it contains osteoprogenitor cells with the potential to become osteoblasts and secrete additional bone matrix. Bone can grow only from the surface, oppositional growth; bone cannot grow by interstitial because osteocytes cannot divide. Osteocytes once trapped by bone matrix, cease the synthesis and export of bone matrix. Endosteum consists of osteoprogenitor cells and fine reticular fibers. Endosteum lines both Haversian and Volkmann's canals and is continuous with the periosteum.

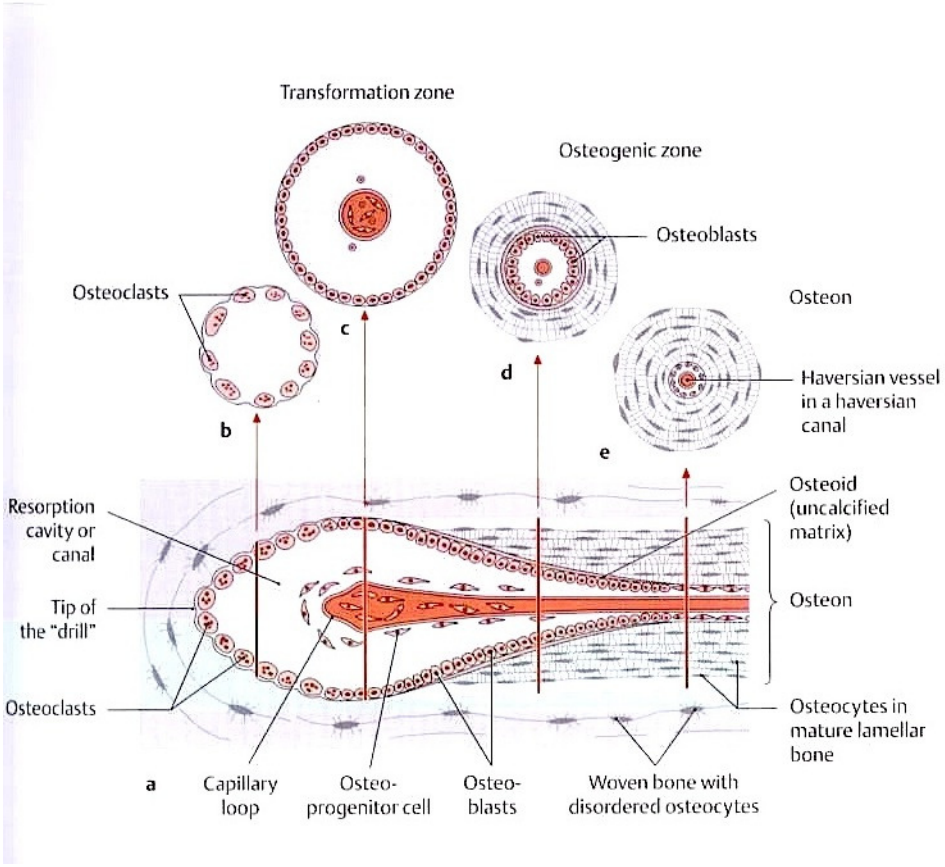

Fig. 5: Detail of bone tissue structure.

Woven and lamellar bone

There are two forms of mineralized bone: woven (immature) and lamellar (mature). Woven bone is initially formed in the embryonic skeleton, but with continued development it is replaced by mature bone. Woven bone forms on the calcified cartilage during endochondral ossification. Subsequently, osteoclasts and chondroclasts erode the woven bone and calcified cartilage matrix, which are replaced by mature lamellar bone. Woven bone is not generally present in humans after about 5 years age, but it may be formed in certain diseases (tumors and some metabolic bone diseases) and during healing of fractures. Woven bone has a higher rate of formation and turnover, a more random pattern of collagen fibrils orientation, and more numerous osteocytes per unit volume compared to lamellar bone. Further, mineralization of woven bone is more irregular than that of lamellar bone. Woven bone is more easily deformed and flexible but weaker than mature bone.

MICROSCOPIC ORGANIZATION

Osteons are cylinders of bone consisting of concentric lamellae (layers) of bone matrix around a central canal called haversian canal (Havers, 1691), that contains blood vessels, lymphatic vessels, endosteum, and an occasional nerve. Osteons comprise most of the mature diaphyseal compact bone. The collagen fibrils in adjacent lamellae run in different directions, which confer additional strength to the bone. Osteons range from 3 to 5 mm in length, and are approximately 0,3 mm in diameter, and have up to six bone lamellae. Osteons can branch and anastomose. Transverse or oblique vessel channels called Volkmann's canals interconnect the haversian canals. The vascular channels also communicate with both periosteal and endosteal surfaces. The cells bodies of bone cells (osteocytes) reside in spaces of bone matrix called lacunae. Many long fingers like extensions of the osteocyte cell body extend into narrow channels called canaliculi. Canaliculi radiate from the haversian canals and interconnect this canal with all the osteocytes in the osteonal lamellae. Canaliculi do not usually cross the cement lines that marked the outer extent of osteons. The lamella bone consists mainly of haversian systems containing osteonal lamellae. The outer and inner circumferential lamellae, as well as interstitial lamellae, complete the regional differentiation of compact bone lamellae. The intraosseus vascular system extends through the Haversian and Volkmann canals and supplies the osteocytes that reside within lacunae and canaliculi of the bone matrix. The blood vessels in the haversian and Volkmann canals are continuous with periosteal and medullary vessels; thus the vascular channels of bone communicate with both the periosteal and endosteal surfaces.

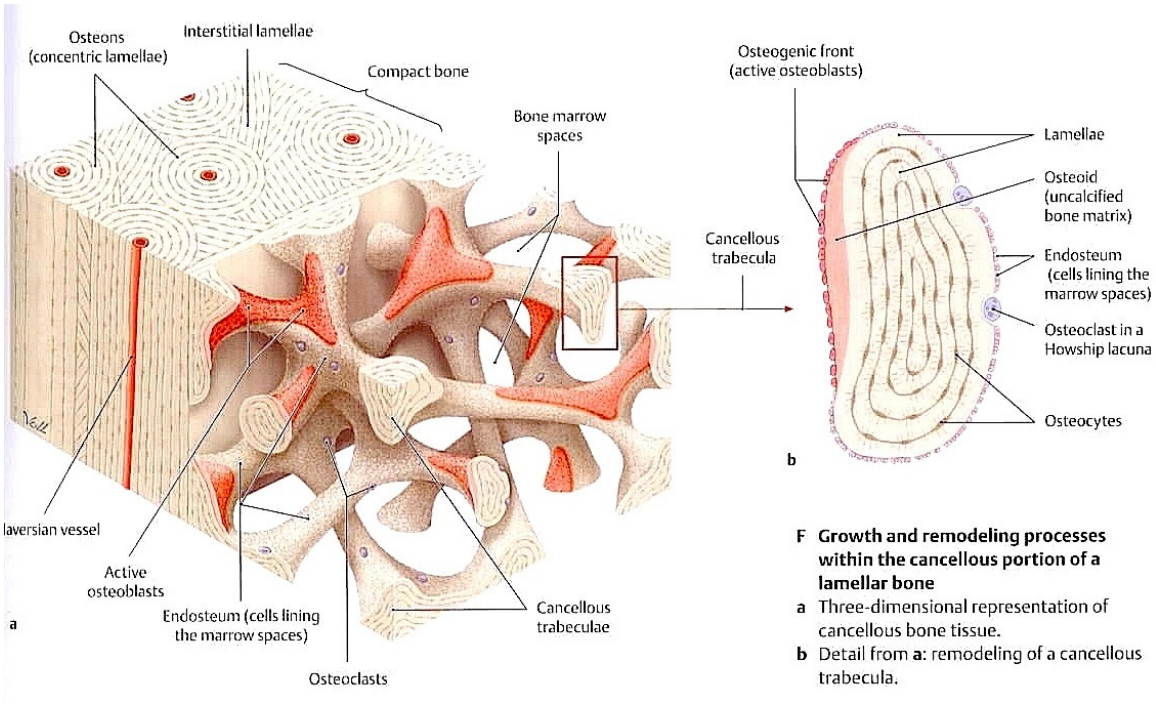

F Growth and remodeling processes within the cancellous portion of a lamellar bone

a Three-dimensional representation of cancellous bone tissue.

b Detail from **a**: remodeling of a cancellous trabecula.

Fig 6: Compact and spongy bone structure.

Cancellous/spongy bone

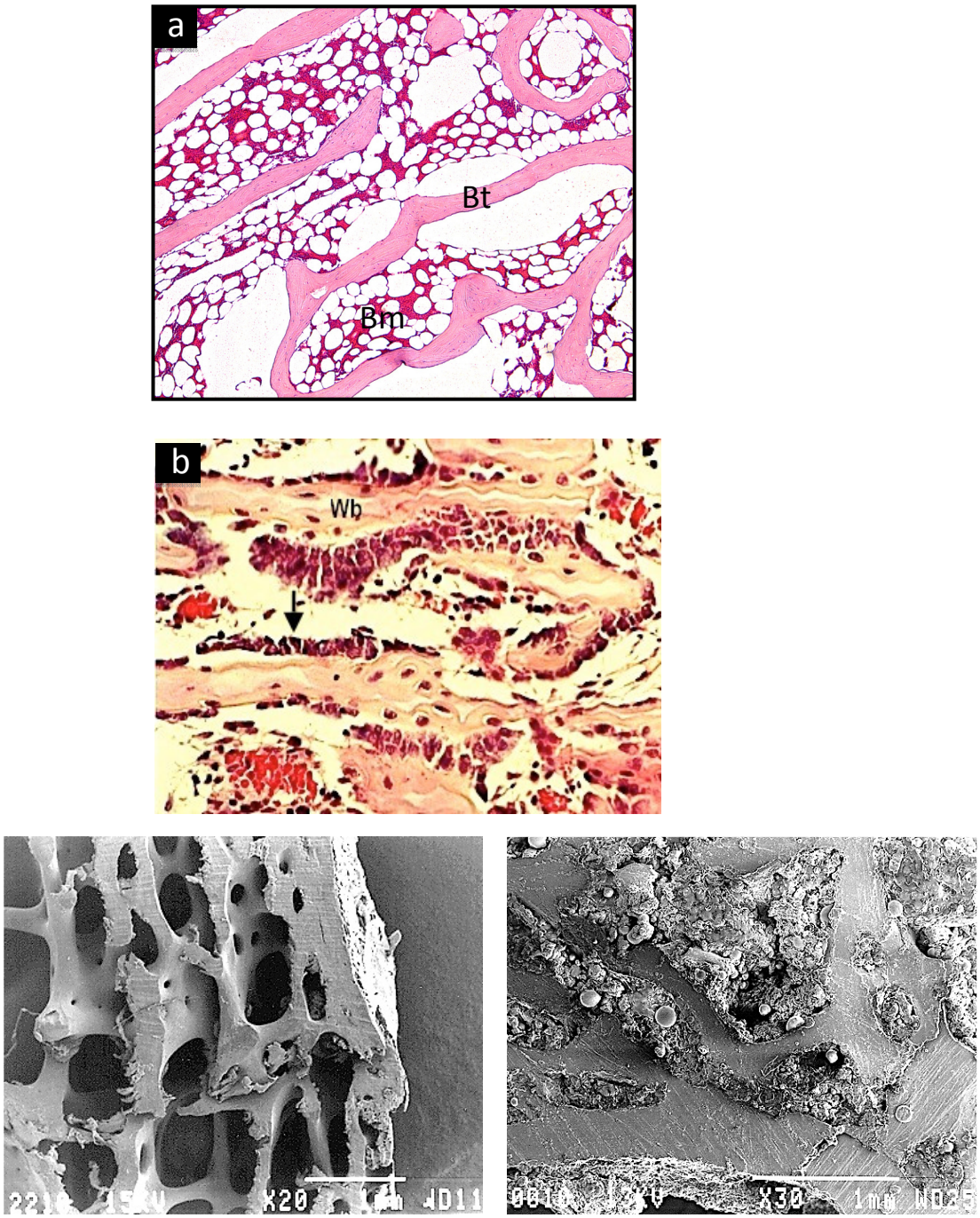

Fig. 7: (a) Bony trabeculae (Bt) characteristics of cancellous bone and bone marrow (Bm) occupying spaces between them. (HE, X40). (b) Woben bone (Wb) and osteoblast lining on the surface (arrow) (HE, X125). (c y d) SEM micrography of organuzation of the trabeculae in the cancellous bone tissue. Bone marrow occupying the spaces between trabeculae (bar 1 μ m).

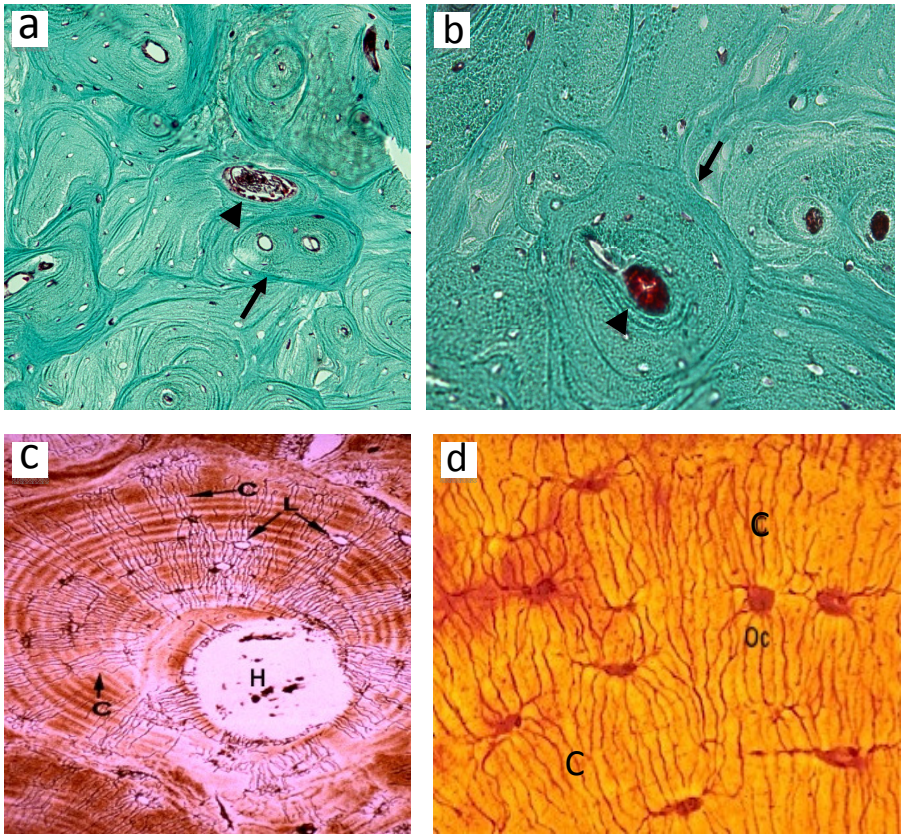

Fig. 8: Light photomicrography of normal compact bone in cross-secction from the cortex showing: (a,b) multiple osteons (arrow) arranged arround Haversian canals (arrow head).(c) Haversian canal detail (H) and osteocytes into lacunae (L) and (c) radiating canaliculi. (d) Innumerable fine cytoplasmatic processes-canaliculi (c) radiating from the ostecytes housed in lacunaes (Oc). (a-b) Trichrome Masson, X120, X150. (c-d) Haematoxylin & Eosin (H & E) (with colour filter), X200, X250, respectivelly.

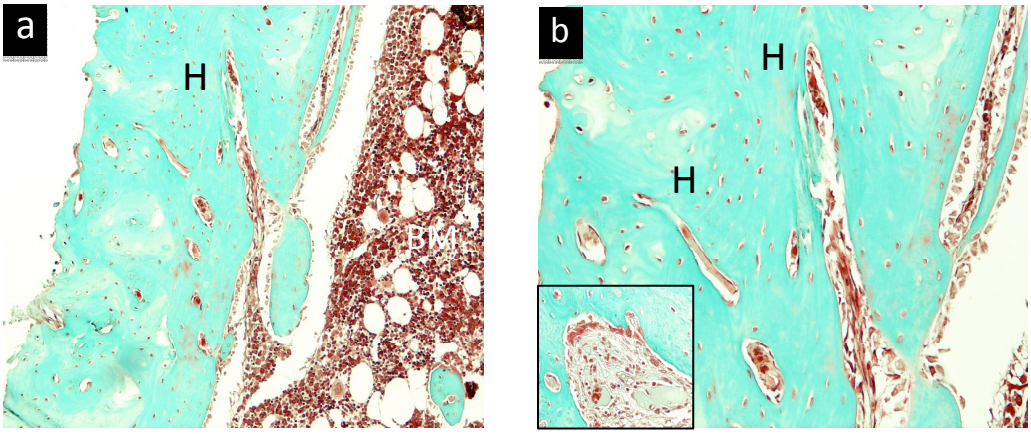

Fig. 9: Light photomicrography of cortical bone cross section. (a) Development of an Havers canal (H) and bone marrow (BM). (b) Detail of the previous figure. (Trichrome Masson, X30 and X80 respectivelly).

1.1.5 BONE CELLS

OSTEOPROGENITOR CELLS

A population of mesenchyme-derived cells, called osteoprogenitor cells, can proliferate and differentiate into osteoblasts and chondroblasts in some cases. Osteoprogenitors are found in bone surfaces; and become activated during bone fractures and are involved in repair.

OSTEOBLASTS

Osteoblasts arise from mesenchyme cells and are responsible for bone formation (osteogenesis). The principle tissues that are capable of giving rise to osteoblasts are bone marrow, periosteum, endosteum, and the periodontal membrane. Bone cell formation and bone deposition appear to include the production of osteoblast-derived growth factors that are involved in both autocrine and paracrine regulation.
Osteoblasts line bone surfaces; they synthesize, package, and export the organic constituents of bone matrix including type I collagen and sulphated proteoglycans. Recent studies indicate that the secretory products of osteoblasts are quite diverse.

At the light microscope level, the osteoblast is characterized morphologically by a round nucleus at the base of the cell (away from the bone surface), an intensely basophilic cytoplasm, and a prominent Golgi complex located between the nucleus and the apex of the cell. The osteoblast is characterized by the presence of a well-developed rough endoplasmic reticulum with dilated cisternae and a dense granular content. These organelles are involved in the major activity of the osteoblast: the production and secretion of collagenous and non-collagenous bone matrix proteins, including type I collagen. The osteoblast secretes in a polarized fashion. Osteoblasts also produce a range of growth factors under a variety of stimuli, including the insulin-like growth factors (IGFs), platelet-derived growth factors (PDGFs), basic fibroblast growth factor (bFGF), transforming growth factor-beta (TGF-β), interleukins, FGFs, BMPs and Wnt_s (LRP5/6 and Frizzled) and retinoids.

Receptors for paracrine and autocrine effectors include those for epidermal growth factor (EGF), IGFs, PDGF and TGF. Osteoblasts also have receptors for several adhesion molecules (integrins) involved in cell attachment to the bone surface.
Osteoblasts are responsive to parathyroid hormone (PTH).
Among the markers for osteoblasts are alkaline phosphatase (ALP), prostaglandin-E2 (PGE-2), collagenase and collagenase inhibitor, transforming growth factor-β (TGF-β), and matrix components such as type I collagen (ColI), osteonectin (ON) and osteocalcin (OCN).

The microenvironment of bone cells is important in their differentiation. Among the molecules that are suggested to be osteoinductive are fibronectin, collagen, procollagen peptides, and larger proteoglycans. Once bone matrix secretion as been initiated, additional bone matrix is secreted on preexisting bone surfaces. Some new matrix comes to surround the osteoblast. The ultimate fate of osteoblasts is to become enclosed and trapped by their secretory products. However, the osteoblast undergoes a pronounced shape change as it becomes surrounded by bone matrix. Osteoblasts that are inactive in bone matrix secretion tend to be smaller and more flattened or oval in shape than actively secreting osteoblasts.

Among the cytokines secreted by the osteoblast are the main regulators of osteoclast differentiation, i.e. M-CSF, RANKL and Osteoprotegerin (OPG). M-CSF is essential in inducing the commitment of monocytes to the osteoclast lineage whereas RANKL promotes the differentiation and activity of osteoclasts.

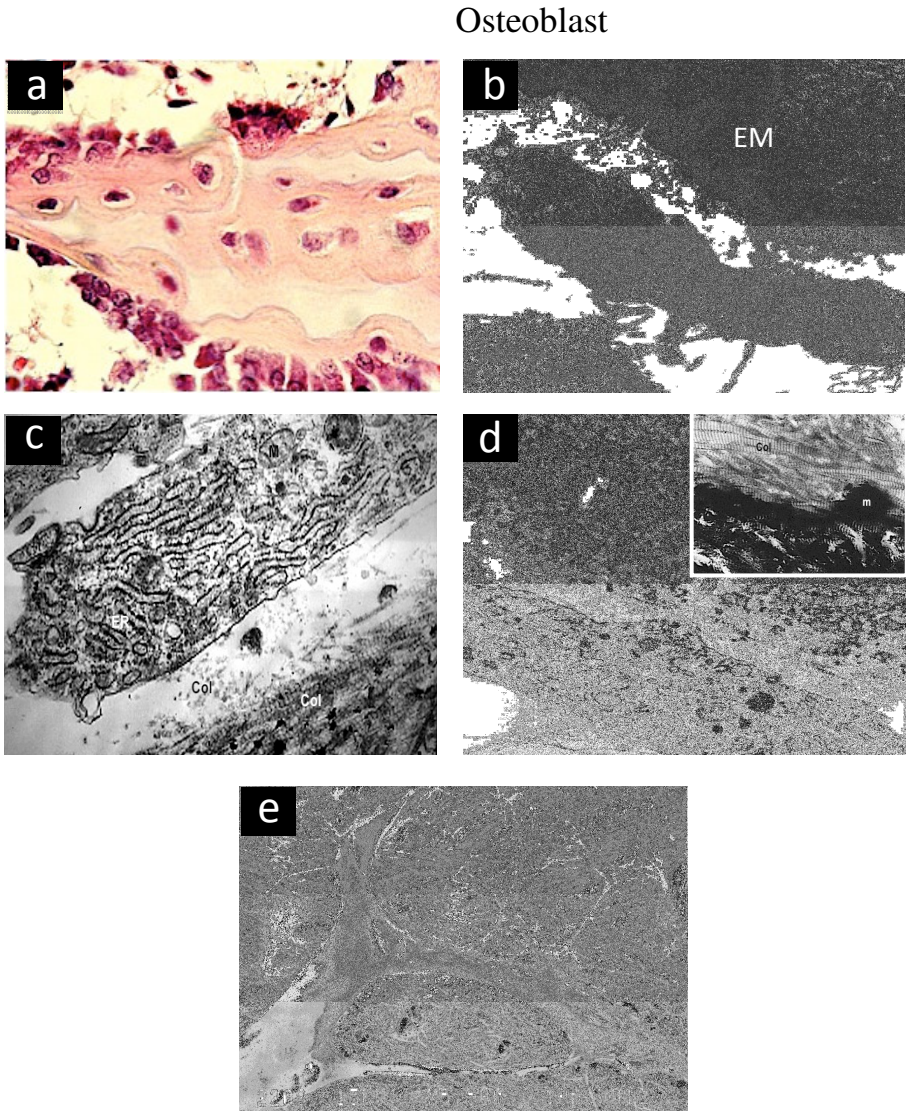

Fig. 10: (a) Light photomicrography of newly formed woven with peripheral osteoblasts and plump osteocytes. A multinucleated osteoclast lining the surface can be seen at the top (HE, X200). (b) Transmission electron microscopy (TEM) micrgraph of an elongated-shape osteoblast near to mineralized bone matrix (EMM)(X30.000). (c) Clear and well defined endoplasmic reticulum (ER) and mitochondria (M). (d) Transmission electro micrograph of osteoblast and patches of calcification in osteoid. Some of the mimeral is aligned with the callagen fibrils (X 20.000). Both the apatite crystals and the collagen fibrils are haphazardly arranged. Some of the cristal appear thin and needle-shaped but others are wider and plaque-shaped (X 30.000). Inset: collagen fibrils in a wide osteoid (X 50.000). (e) SEM micrograph of an osteoblast spreading on a network of collagen fibres layer (bar 1 μ m).

OSTEOCYTES

When osteoblasts deposit bone on preexisting surfaces, they eventually become surrounded by bone matrix and are called osteocytes. Osteocyte cell bodies reside in spaces called lacunae, which are especially evident in ground bone preparations in which the osteocytes are removed. As osteoblasts become surrounded by intercellular matrix, they extend many long, slender, finger-like extensions (tendrils) that contact those of nearby osteocytes. This results in many small channels (canaliculi), that extend throughout the bone matrix and create a canalicular circulatory system that provides nourishment for osteocytes. ECF flow through the canalicular network is altered during bone matrix compression and tension and is believed not only to allow exchanges with the extracellular fluids in the surrounding tissues but also to create shear forces that are directly involved in mechanosensing and regulation of bone remodeling. In turn, the activation of the mechanosensing cilium may determine the local concentration of cytokines capable of regulating bone formation and/or bone resorption, such as RANKL, OPG or sclerostin. (see below) The extensions of one osteocyte touch those from others nearby osteocytes or processes from the cells lining the bone surface (osteoblasts or flat lining cells), and gap junctions are formed. Osteocyte morphology varies according to cell age and functional activity. A young osteocyte has most of the ultrastructural characteristics of the osteoblast from which it was derived, except that there has been a decrease in cell volume and in the importance of the organelles involved in protein synthesis (rough endoplasmic reticulum, Golgi). An older osteocyte, located deeper within the calcified bone, shows a further decrease in cell volume and organelles, and an accumulation of glycogen in the cytoplasm. These cells synthesize small amounts of new bone matrix at the surface of the osteocytic lacunae, which can subsequently calcify. Osteocytes express, in low levels, a number of osteoblast markers, including OC, OP, and ON.

It is likely that osteocytes respond to bone tissue strain and influence bone remodeling activity by recruiting osteoclasts to sites where bone remodeling is required. Osteocyte cellular activity is increased after bone loading; studies in cell culture have demonstrated increased calcium influx and prostaglandin production by osteocytes after mechanical stimulation, but there is no direct evidence for osteocytes

signaling to cells on the bone surface in response to bone strain or microdamage to date. Osteocytes can become apoptotic and their programmed cell death may be one of the critical signals for induction of bone remodeling. Ultimately, the fate of the osteocyte is to be phagocytosed and digested together with the other components of bone during osteoclastic bone resorption.

The discoveries that osteocytes can secrete the Wnt antagonist Sclerostin and that this secretion is inhibited both by PTH treatment and by mechanical loading establishes the first direct link between biomechanics, endocrine hormones, bone formation and osteocytes. Similarly, osteocytes can secrete RANKL and OPG, contributing also to the regulation of bone resorption. Thus, osteocytes are emerging as the critical cell type linking mechanical forces in bone to the regulation of bone mass and shape through remodeling.

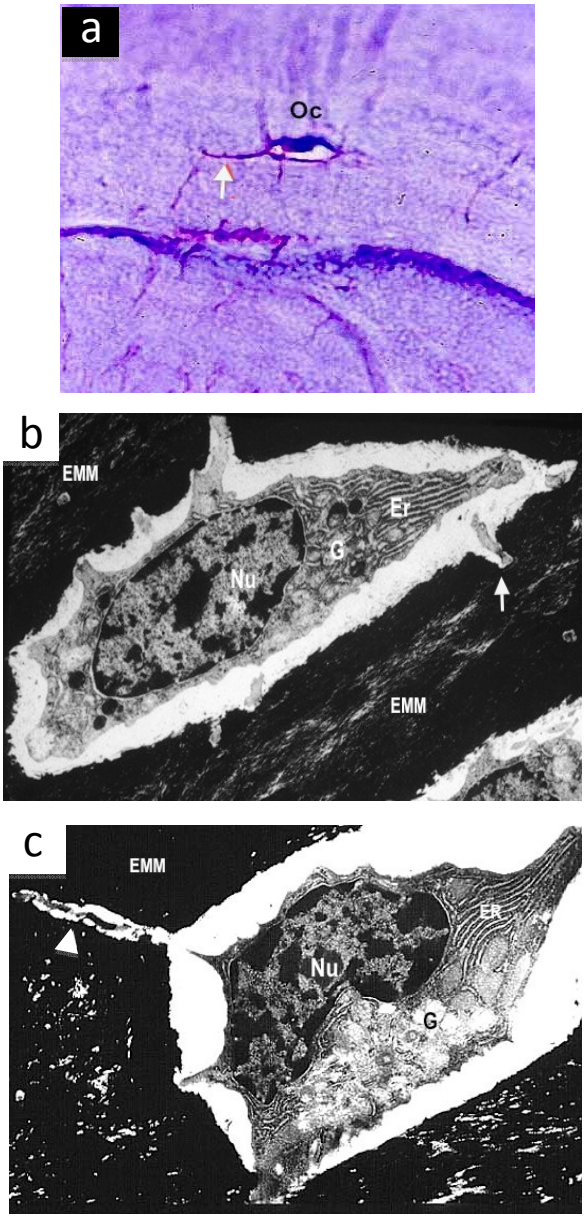

Fig. 11: (a) Light photomicrography of an osteocyte (Oc) and extensive fine canalicular channelling (HE, X200). (b) TEM micrograph of an osteocyte. The ER is sparse and the Golgi apparatus nor well developed. The irregularities on the cell surface are the origins of osteocyte processes (arrow). The lacunar wall is not fully mineralized. An osteocyte process is entering a canaliculus at the top left (arrow head). (X10.000).

OSTEOCLASTS

The source of osteoclasts is not completely clear, but one possibility is that they form from the fusion of monocytes that come in contact with bone matrix. Another possibility is that osteoclasts can develop from mesenchyme cells through a "pre-osteoclast" intermediate.

The osteoclast is the bone lining cell responsible for bone resorption. The osteoclast is a giant multinucleated cell, up to 100mm in diameter and containing four to 20 nuclei. It is usually found in contact with a calcified bone surface and within a lacuna (Howship's lacunae) that is the result of its own resorptive activity. It is possible to find up to four or five osteoclasts in the same resorptive site, but there are usually only one or two. The cytoplasm is "foamy" with many vacuoles. The zone of contact with the bone is characterized by the presence of a ruffled border with dense patches on each side (the sealing zone). The most prominent features of the osteoclast are, however, the deep foldings of the plasma membrane in the area facing the bone matrix (ruffled border) and the surrounding zone of attachment (sealing zone). The sealing zone is formed by a ring of focal points of adhesion (podosomes) with a core of actin and several cytoskeletal and regulatory proteins around it, that attach the cell to the bone surface, thus sealing off the subosteoclastic bone-resorbing compartment. The attachment of the cell to the matrix is performed via integrin receptors, which bind to specific RGD (Arginine-Glycine-Aspartate) sequences found in matrix proteins (see table sopra/anteriore).

The osteoclast is morphologically and functionally polarized. Its membrane has an apical and a basolateral surface. Osteocalsts contain mitochondria, lysosomes, and free polyribosomes. The osteoclast is able to produce a variety of secretory products.

Na+/K+-ATPase is present in the osteoclast ruffled border and may act as a sodium or calcium exchanger for hydrogen ions in regulating the acidity of this region. Carbonic anhydrase, an enzyme that may also participate in acidification adjacent to the ruffled border, has been localized within the osteoclast. Hydrogen ion transport by ATPase across the ruffled border is important in the production of an acidic environment for resorption.

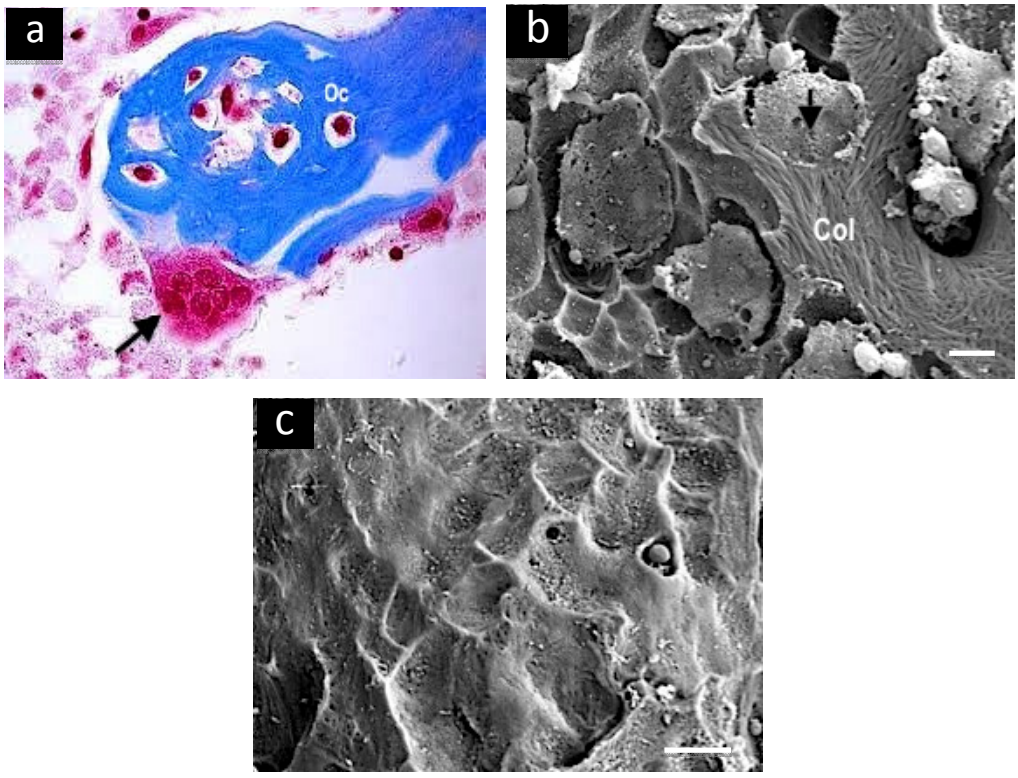

Fig. 12: (a) Light photomicrography of multinucleated osteoclast (six nuclei) on the trabeculae surface (arrow) (Trichrome Masson X150). (b) SEM micrography of osteoclasts (arrow) destroying collagen fibers during the process of remodeling and (c) final results (bar 1 μ m).

1.1.6 EXTRACELLULAR BONE MATRIX

The unique mechanical qualities that permit bone to serve as a supporting connective tissue are due to the nature of the intercellular or extracellular substance, which contains both inorganic and organic components. The inorganic portion is about 65% of bone dry weight, and the organic component comprises about 32% of the dry weight.

ORGANIC COMPONENT

Nearly 90% of the organic matrix of bone is collagen, principally type I collagen, which causes acidophilic staining. Roughly 10% of the organic content consists of proteins and glycoproteins, as well as hepran-sulphate, keratin sulphate, chondroitin

sulphate, and hyaluronic acid, largely in the form of proteoglycan aggregates. The organic component, collagen, enables bone to resist tension, while the mineral component, permits bone to resist compression. The various calcium slats in bone matrix provide hardness and rigidity. The initial organic matrix that is secreted is called osteoid. As osteoid becomes mineralized, it is than converted into bone. The osteoid matrix contains molecules that bind both collagen and mineral. Collagen contains regions that stimulate or catalyze the nucleation of mineral crystals.

Numerous noncollagenous proteins present in bone matrix have been purified and sequenced, but their role has been only partially characterized (Table). Most non-collagenous proteins within the bone matrix are synthesized by osteoblasts, but not all: approximately a quarter of the bone non-collagenous proteins are plasma proteins which are preferentially absorbed by the bone matrix, such as a_2-HS-glycoprotein, which is synthesized in the liver. The major non-collagenous protein produced is osteocalcin (OC), which makes up 1% of the matrix, and may play a role in calcium binding and stabilization of hydroxyapatite in the matrix and/or regulation of bone formation, as suggested by increased bone mass in osteocalcin knockout mice. Another negative regulator of bone formation found in the matrix is matrix gla-protein, which appears to inhibit premature or innapropriate mineralization, as demonstrated in a knockout mouse model. In contrast to this, biglycan, a proteoglycan, is expressed in the bone matrix, and positively regulates bone formation, as demonstrated by reduced bone formation and bone mass in biglycan knockout mice.

Protein	**MW**	**Role**
Osteonectin (SPARC)	32K	Calcium, apatite and matrix protein binding Modulates cell attachment
α-2-HS-Glycoprotein	46-67K	Chemotactic for monocytes. Mineralization via matrix vesicles
Osteocalcin (Bone GLA protein)	6K	Involved in stabilization of hydroxyapatite. Binding of calcium. Chemotactic for monocytes. Regulation of bone formation.
Matrix-GLA-protein	9K	Inhibits matrix mineralization
Osteopontin (Bone Sialoprotein I)	50K	Cell attachment (via RGD sequence). Calcium binding
Bone Sialoprotein II	75K	Cell attachment (via RGD sequence). Calcium binding
24K Phosphoprotein (α-1(I) procollagen N-propeptide)	24K	Residue from collagen processing
Biglycan (Proteoglycan I)	45K core	Regulation of collagen fiber growth. Mineralization and bone formation. Growth factor binding
Decorin (Proteoglycan II)	36K core + side chains	Collagen fibrillogenesis. Growth factor binding
Thrombospondin, Fibronectin		Cell attachment (via RGD sequence). Growth factor binding. Hydroxyapatite formation
Growth Factors IGFI & IGFII ,TGFβ, Bone morphogenetic proteins (BMPs)		Differentiation, proliferation and activity of osteoblasts. Induction of bone and cartilage in osteogenesis and fracture repair

Table. 1: Non-collagenous Proteins in Bone

The principal non-collagenous proteins of bone can be classified as glycosamminoglycan-containing molecules, the proteoglycans, and alpha-carboxyglutamic acid-containing molecules, and phosphoproteins (Wiessmann HP, 2005). Of phosphoproteins recent interest has focused on a subset of these proteins termed small integrin-binding ligand N-linked glycoproteins (SIBLING). SIBLINGs include OPN, BSP, enamelin and MEPE ().

Osteopontin (OPN)

Also known as Bone sialoprotein 1 (BSP-1) or secreted phosphoprotein I (SPP1), OPN is SIBLING glycoprotein encoded on Chr4, that was first identified in 1986 in osteoblasts.
The protein is composed of ~300 amino acids residues and has ~30 carbohydrate residues attached including 10 sialic acid residues, which are attached to the protein during post-translational modification in the Golgi apparatus. The protein is rich in acidic residues: 30-36% is either aspartic or glutamic acid. OPN is a highly negatively charged, extracellular matrix protein that lacks an extensive secondary structure (Wang KX, 2008).

The prefix "osteo" means that OPN is express in bone, although it is also express in other tissues, at lower levels, including: kidney, nervous tissue, uterus, macrophages and it is found in human plasma. OPN is an extracellular (secreted) structural protein and therefore an organic component of bone, it corresponds the 2% of non-collagenous protein of the bone ECM. OPN is important in cell growth as it can promote collagen independent cell spreading and cell attachment through its RGD motifs (implicated in binding to integrins). (Merry K, 1993)

As the others phosphorylated sialoproteins, it has affinity for Ca^{++} ions and is able to bind to hydroxyapatite crystals and crystal nuclei, presumably via an acid-rich stretch of nine aspartic acid residues (Merry K, 1993), blocking their growth (Boskey AL, 1993), so it is important in the biomineralization process. OPN is produced at late stages of osteoblastic maturation, corresponding to stages of matrix formation just prior to mineralization. OPN secretion by osteoblasts also precedes the secretion of other phosphorylated sialoproteins, indicating OPN role in regulating the mineralization process by preventing the advancement of the mineralization front which permits osteoblasts proliferation and growth before the beginning of the mineralization process. Data about OPN as HA nucleator are discrepant; OPN has many of the features expected of a nucleator of mineral-crystal formation, so there is

the possibility that OPN acts as a nucleator involved in a secondary nucleation phase if properly oriented (Boosley, 1993). Osteopontin has been implicated as an important factor in bone remodeling (Choi ST, 2008). Specifically, research suggests it plays a role in anchoring osteoclasts to the mineral matrix of bones, due to OPN ultrastructural localization in areas adjacent to resorptive osteoclasts (Reinholt, 1990) OPN serves to initiate the process by which osteoclasts develop their ruffled borders to begin bone resorption. In addition, osteoclasts have been shown to synthesize OPN during active remodeling (Dodds, 1995), which further demonstrate that OPN has a major role in the maintenance of bone homeostasis.

Dodds RA, Connor JR, James IE. Human osteoclasts, not osteoblasts, deposit osteopontin onto resorption surfaces: an in vitro and ex vivo study of remodeling bone. J Bone Miner Res. 10: 1666-1680, 1995.

OPN expression is induced by osteoblastic cell adhesion to ColI, and signal transduction appears mediated by integrins containing β_1.
Selective adhesion of osteoblastic cells to different integrin ligands induce osteopontin gene expression. (Carvalho RS, 2003).

While calcium is a divalent cation used by cells as a second messenger to control a great variety of cellular processes, it is also well acknowledged as a specific extracellular signal able to regulate proliferation, activity and differentiation of skeletal cells. In contrast, the role of inorganic phosphate (P_i) as an extracellular signal able to regulate gene expression in skeletal cells has only recently been shown. It is now evident that Pi is able to stimulate the expression of mineralization-regulating proteins such as MGP and OPN in chondrocytes and bone forming cells through the activation of specific signalling molecules including the MAP kinases ERK1/2 pathway. Due to the concomitant presence of P_i and Ca^{++} in the vicinity of the bone cells, we question whether calcium might modulate the affects of extracellular P_i in osteoblasts. In conclusion, this study demonstrates for the first time that calcium plays a pivotal role in regulating the effects of P_i on bone cells. The mechanisms by which calcium modulates the osteoblastic effects of P_i do not seem to involve the activity of a calcium recaptor but more likely require the formation of calcium-phosphate precipitates that in turn induce ERK1/2 phosphorilation and OPN stimulation. This study also highlights the potential existence of calcium-phosphate negative feedback loop to control excessive calcification through the regulation of mineralization-inhibiting proteins such as OPN.
Phosphate dependent stimulation of MGP and OPN expression in osteoblasts via the ERK1/2 pathway is modulated by calcium. (Khoshniat S, 2011)

Acts as a cytokine involved in enhancing production of interferon-gamma and interleukin-12 and reducing production of interleukin-10 and is essential in the pathway that leads to type I immunity.

Runx2 (Cbfa1) and osterix (Osx) transcription factors are required for the expression of OPN (Nakashima, 2002) Runx2 and Osx bind promoters of *Opn* upregulating OPN gene transcription (Ducy P, 1997). Due to the presence of a high-specificity vitamin D response element (VDRE) in the OPN gene promoter, vitamin D fluctations influence OPN gene transcription. Extracellular inorganic phosphate (P_i) has also been identified as a modulator of OPN expression. (Fatherazi S, 2009).Stimulation of OPN expression also occurs upon exposure of cells to pro-inflammatory cytokines,classical mediators of acute inflammation (e.g. tumour necrosis factor α [TNFα], infterleukin-1β [IL-1β]), angiotensin II, transforming growth factor β (TGFβ) and parathyroid hormone (PTH), although a detailed mechanistic understanding of these regulatory pathways are not yet known.

Bone sialoportein

BSP (IBSP) is a calcium binding, anionic phosphoprotein normally expressed only in mineralized tissues and at sites of new mineral formation. BSP ... high sialic acid content of the mineralized tissues extracellular matrix and constitutes from 8 to 12% of the total non-collagenous proteins in bone (22). BSP has a flexible conformation, with very little, if any, secondary structure, that has been proposed to be required for its function as a bridging molecule with multiple binding partners. BSP has been shown to be involved in cell attachment through its RGD motifs, cell signaling, hydroxyapatite binding, hydroxyapatite nucleation, and collagen binding.

The binding of BSP to fibrillar collagen induces not only osteoblasts proliferation and differentiation but is thought to be important for the initiation of bone mineralization and in the adhesion of bone cells to the mineralized matrix. (22). BSP has a high affinity to Ca^{++} ions and hydorxyapatite and acts as a nucleus for the formation of the first apatite crystals. As the apatite forms along the collagen fibers within the extracellular matrix, BSP could direct, redirect or inhibit the crystal growth (ref. 15 di WIKI). BSP interacts with fibrillar collagen in the ‘‘hole-zones’’ of type I collagen fibrils, a site associated with early mineral deposition, and tend to be oriented parallel to the fibril axes (22). The binding of BSP to collagen is suggested not to be simply a non specific interaction between BSP post-translational modifications and collagen, but a more specific interaction between the residues of BSP and collagen is involved. Moreover the binding to collagen is calcium-dependent; increases in calcium in the environment decrease BSP binding to collagen. This is explained by the previous formation of long range electrostatic interactions that stabilize the formation of an initial low affinity complex prior to the formation of more specific short range interactions (22). The glutamic acid-rich sequences of BSP may be of particular importance in the nucleation of hydroxyapatite. This polyglutamic acid sequences are predicted to form an αhelical structure which could provide an appropriate spacing of the γ-carboxylate groups for binding Ca^{++} ions in the dimension of the hydroxyapatite crystals.

Osteocalcin

OSC, also known as bone gamma-carboxyglutamic acid-containing protein (BGLAP), is a noncollagenous protein found in bone. OSC is secreted solely by osteoblasts and its concentration in serum is closely linked to bone metabolism and serves as a biological marker for the clinical assessment of bone diseases (28). Although its precise mechanism of action is unclear, OSC influences bone mineralization, in part due to its functions in cell signaling that leads to the recruitment of osteoclasts and osteoblasts, which have active roles in bone resorption and deposition, and in part through its ability to bind with high affinity to the mineral component of bone. In fact OSC has no known enzyme activity and its function depends on its structure: a negatively charged protein surface that places five Ca++ ions in positions complementary to those in hydroxyapatite. Using this recognition mechanism, OSC could potentially modulate the crystal morphology and growth of hydroxyapatite. And in this complex, the carboxy terminus of OSC, which promotes the adhesion of osteoblasts in bone replacement, is readily accessible (28).

Heperan Sulfate

Although most of the organic component of osteoblast ECM is comprised of collagen, growing evidence suggests the most bioactive element of a developing matrix is its heparan sulfate glycosaminoglycan complement. HS is a linear, highly variable, highly sulfated glycosaminoglycan polysaccharide found in all animal tissues. HS biological activity largely depends on internal sulfated domain that regulate the flow of an astonishing number of mitogenic influences that coordinate MSC commitment and growth, and ultimately, osteoblast phenotype (29). Among the heparan sulfate-binding factors known to be important to this process are the FGFs and their receptors, members of the transforming growth factor superfamily, as well as the collagens, laminins and fibronectins. This binding may results in the activation of the ERK1/2 pathway, and the consequent phosphorylation of the RUNX2 transcription factors and the expression of gene specific of the osteoblast lineage, suggesting the potential for HS to shift cells from proliferative to differentiative phenotypes (29).

Colagen type I

Collagen type I is the most common of the collagens in vertebrates. It comprises up to 90% of the skeletons of the mammals and is also widespread all over the body: in addition to bones, it is found in skin, tendons, ligaments, cornea,

intervertebral disks, dentine and granulation tissues. It is one of the main components of the osteoid matrix, and can transduce intracellularly various types of signals through its binding to integrins, serves as a scaffold for calcification and plays an important role in orienting the newly formed apatite crystals during mineralization. It is composed of 3 single α-chains, that contain a signal peptide that is cleaved when the molecules reach the rough endoplasmatic reticulum. Here, in the lumen, some modification occurs as the hydroxylation of the proline and lysine residues due to the action of an enzyme called prolyl-hydroxylase that works with ascorbic acid, iron and silicon as cofactors. After the glycosylation of some specific hydroxylated amino acids, a triple helical structure is formed inside the endoplasmatic reticulum from two α-1 chains (produced by Col1AI gene) and one α2 chain. This molecule of procollagen contains extension proteins on each end that make it very soluble and therefore easy to move within the cell as it undergoes further modifications. Procollagen is then shipped to the Golgi apparatus, where it is packaged and secreted by exocytosis. In the extracellular spaces, the N-and C-terminal extensions are cleaved and the triple helical collagen molecules line up and begin to form fibrils and subsequently fibers. This reaction places stable crosslinks (intramolecular crosslinks) within and between (intermolecular crosslinks) the molecules. This is the critical step that gives the collagen fibers its strength.

Osteonectin

Osteonectin (ON) also known as secreted protein, acidic and rich in cysteine (SPARC), is a calcium binding matricellular glycoprotein that is secreted by many different types of cells and that can have intracellular or extracellular localization (21). Matricellular proteins are extracellular regulatory macromolecules that mediate cell-matrix interactions but may not contribute significantly to extracellular matrix structure.

OSN is constitutively present in cells and tissues involved in morphogenesis, wound repair and remodeling, such as osteoblasts, platelets and endothelial cells. OSN plays a role in the tissue repair/remodeling process by influencing matrix formation and metalloproteinase production, cell adhesion and spreading (inhibitor), cell proliferation (inhibits cell cycle), migration, facilitation of acquisition of differentiated phenotype (Yan Q, 1999). OSN, in fact, exhibits counteradhesive effects that lead to cell rounding and changes in cell shape and result in the disruption of cell/matrix interactions, that are

temporarily necessary for cells undergoing migration and proliferation (21). For this reason, OSN is necessary for normal bone remodeling, maintenance of bone mass, and bone quality, but not contribute significantly to ECM structure (21). OSN binds to collagen type I and hydroxyapatite, through separate areas of its molecule, forming the link between the mineral and organic phases of bone tissue and also has the ability to inhibit the growth of hydroxyapatite crystals helping the regulation of bone mineralization. It seems to block the growth sites of nucleated calcium phosphate, resulting in the formation of smaller crystallites.
There are two calcium binding sites; an acidic domain that binds 5 to 8 Ca^{2+} with a low affinity and an EF-hand loop that binds a Ca^{2+} ion with a high affinity. Calcium ions regulate both the function and the structure of SPARC. Binding of calcium causes an increase in the α-helicity and hence a change in conformation the reduces the susceptibility of the extracellular domain to proteinases and alters its affinity for collagen (Yan Q, 1999). OSN is highly expressed early in osteoblastic differentiation, but its expression decreases as the cells acquire characteristics of mature osteoblasts. In contrast, its transcript levels change little during osteoblastic differentiation, indicating regulation at the level of translation.

High levels of immunodetectable osteonectin are found in active osteoblasts and marrow progenitor cells, odontoblasts, periodontal ligament and gingival cells and some chondrocytes and hypertrophic chondrocytes. Osteonectin is also detectable in osteoid, bone matrix proper and dentin.

SPARC is encoded by a single gene in all species studied today. Is a 32 KDa protein, that consists of 286 residues divided in three distinct domains. The N-terminal domain (resitues 1-52) is an acidic region rich in Asp and Glu; domain I binds several calcium ions with low affinity and interact with hydroxyapatite. The second domain is a Cys-rich, follistatin-like (FS) domain (residues 53-137); the FS domain contains two copper binding sites. Domain III (residues 138-286) is the extracellular domain, is largely α-helical and contains a canonical pair of EF-hands, with high affinity calcium binding sites (Yan Q, 1999).

Alkaline phosphatase

ALP is a hydrolase enzyme responsible for removing phosphate groups from many types of molecules (including nucleotides, proteins and alkaloids) in a process called dephosphorylation. As the name suggests, ALP is more affective in an alkaline environment. ALP exists as several tissue-specific isozymes encoded by separate genes. Humans have four ALP genes corresponding to intestinal (ALPI), placental (ALPP), placental-like and liver/bone/kidney (tissue non-specific alkaline phosphatase; ALPL) gene products. ALP has many different functions in the many organisms and tissues where it occurs, but the same mechanism of action. It is attached to the outer face of the plasma membrane through a phosphatidyl inositol-glycophospholipid anchor covalently attached to the C-terminus of the enzyme. The catalytic mechanism involves the formation of a serine phosphate at the active site which reacts with water at alkaline pH to release Pi from the enzyme (24). In bone, the free phosphate can now precipitate with calcium in the formation of hydoxyapatite crystals or enter the cells and act as a signal molecule promoting the expression of other osteoblast related genes (23). ALP is expressed early in development, and is soon observed on the cell surface and in matrix vesicles. Later in the developmental program, while other genes are upregulated, ALP expression declines. For this reason ALP must function in the initial phases of the process (24). It seems that Pi increases ALP activity while decreases ALP mRNA, in fact the concentration of Pi in the culture medium is proportional to the amount of ALP activity because regulates the stability of the enzyme, but is negatively correlate with the mRNA expression of the ALP gene (25).

MINERAL COMPONENT

The final mineral product in bone matrix is similar to crystalline hydroxyapatite ($Ca_5(PO_4)_3OH$), and the mineral deposits form in close spatial relation to matrix vesicles and collagen fibrils. Noncrystalline calcium phosphate is also present in bone matrix. Bone mineral also contains citrate and bicarbonate ions, as well as fluoride, magnesium, potassium, and sodium ions. Relatively little water is present in bone (8-9%) compared to cartilage (75%).

Calcification process

Calcification of bone matrix is required for its proper function but limits diffusion. Chondrocytes respond to matrix calcification by dying; osteocytes adapt by forming connections via canaliculi to a blood supply. Many details about bone matrix calcification are unclear, but several important events are associated with the process. The proteins OC and ON bind extracellular Ca^{++} ions to produce a locally high concentration of these ions. OP is present in osteoid at the mineralizing front and appears to play a role in the mineralization process. Osteoblasts elaborate matrix vesicles by budding from the plasma membrane and are involved in initial stages of hydroxyapatite formation.

Collagen fibers in bone matrix may also be important for the precipitation of calcium and phosphate into an insoluble salt. Under certain conditions, solutions of calcium and phosphate form apatite crystals in the presence of collagen. In addition, early calcium phosphate deposits appear at the periphery of staggered procollagen molecules in TEM. However, calcification does not occur in other tissues that have considerable amounts of collagen. While initial stages of crystalline calcium deposites in bone matrix are closely associated with collagen fibrils, their precise role in the calcification process remains unclear. Many questions remain about mechanisms involved in the calcification of bone.

Calcium in bone

Newly deposited calcium is somewhat labile; thus calcium can be mobilized to enter an adjacent capillary or it can be removed from the blood and deposited in bone matrix as needed. Labeling studies indicate that during every minute in the life of an adult human, one of every four calcium ions present in blood exchanges with calcium ions in bone; thus some interchange of calcium ions between blood and bone matrix occurs without osteoclast intervention. Bone resorption is important in remodeling bones and making them stronger and serves as a reservoir of calcium. A stable concentration of calcium ions in the blood is extremely important. The normal calcium concentration is about 10mg/ml of blood plasma. Bone matrix serves as a reservoir for excess calcium ions or as a source of calcium ions, as needed.

Bones and bone tissue exhibit a virtually continuous process of structural change beginning in the embryo and continuing throughout adult life. This is carried out by removal and deposition of bone in a selective manner.
It is convenient to divide the modelling and remodelling into external and internal kinds though the cellular mechanisms are the same in both and the processes overlap in time. External modelling is concerned with bones shape, geometry, form, whilst the internal process alters bone at histological level. External remodelling ends with cessation of growth whilst internal remodelling continues until death. (Capitulo 2. Libro fotoc. Luis).

1.1.7 BONE RESORPTION

Osteoclasts actively acidify the extracellular space in a resorption bay. The intracellular source of the protons results from the carbonic anhydrase-dependent hydration of CO_2 to H_2CO_3. The hydrogen ions resulting from the dissociation are secreted into the resorbing compartment by a proton pump. The bicarbonate (HCO_3^-) leaves the cell by the Cl-/ HCO_3^- exchanger located in the basolateral membrane. The basolateral membrane also contains Na^+/K^+-ATPase as well a Ca^{++}-ATPase.
Located in the periphery of the ruffled border is a region called the clear zone, which contains principally actin micorfilaments, vinculin and talin. This region completely encircles the ruffled border. It is an area where the osteoclasts firmly adheres to the

adjacent substratum and may assist in sealing off the acidic compartment adjacent to the ruffled border. Vacuoles and coated and uncoated vesicles in osteoclasts are involved in both endocytosis and exocytosis. Enzymes packaged in the Golgi move to the ruffled border, where they are released into the space adjacent to the mineralized bone. Products of the resorption are taken into the cell, further digested in secondary lysosomes, and released in adjacent blood vessels.

Osteoclasts are essential for the proper growth, remodeling, and repair of bone, and normally their activity is tightly coupled to bone formation by osteoblasts.

When blood calcium levels becomes elevated (hypercalcemia), calcitonin, an hormone produced by thyroid gland, is released. Calcitonin have an oppesed action to PTH. Calcitonin bond to its receptors on osteoclast membrane and decrease osteoclast activity and motility. Calcitonin stimulates bone deposition by osteoblasts. As new bone matrix is calcified, the blood calcium level is reduced.

PTH and other hormones don't seem to act directly on osteoclasts; they act on osteoblasts. Osteoblasts then secrete specific substances such as macrophage colony-stimulating factor (M-CSF) or IL-6, which are involved in osteoclast maturation and recruitment. It appears that osteoblasts can initiate bone resorption by neutral protease digestion of the unmineralized surface (osteoid), exposing resorption-stimulating mineralized bone to osteoclast contact.

Prostaglandins may act to reduce or terminate resorption by osteoclasts. (Kessel)

1.1.8 BONE MOLECULAR REGULATION

TRANSCRIPTIONAL FACTORS

The differentiation of osteoblasts from mesenchymal progenitors requires the activity of specific transcription factors. These transcription factors are expressed and function at distinct time points during the differentiation process, thereby defining various developmental stages of the osteoblast lineage.

SOX9: marks all osteoblast progenitor

SOX9, a transcription factor of the sex-determining region Y (SRY)-related high mobility group box family of proteins, is crucial for skeletal development. SOX9 is indispensable for chondrogenesis and also marks the mesenchymal progenitors that

give rise to all osteoblasts. However, SOX9 is not expressed by mature osteoblasts. The role of SOX9 in osteoblast differentiation is not well understood. Conditional deletion of SOX9 in the limb bud mesenchyme led to the absence of chondrocytes and osteoblasts, but it is not known whether the loss of osteoblasts reflected a direct requirement for SOX9 in this lineage or a secondary effect owing to the lack of cartilage. By contrast, when SOX9 was deleted in the neural crest cells that contribute to the craniofacial skeleton, the cells that normally form chondrocytes instead expressed markers for osteoblasts, indicating that the bipotential cells probably switched fates in the absence of SOX9. The reason for the different outcomes for SOX9 deletion in the limb bud mesenchyme versus neural crest cells is not clear, but a potential explanation is that, in the limb mesenchyme, but not the neural crest cell, conditional knockout mice SOX9 was deleted before the bipotential progenitor was established. Alternatively, it is possible that the bipotential nature of neural crest cells could be established independently of SOX9 but that SOX9 is important for preventing these cells from differentiating into osteoblasts.

RUNX2 is integral to the osteoblast lineage

Cbfa1/RUNX2, a Runt domain-containing transcription factor (RUNX2 is homologous to the Drosophila protein Runt), is indispensable for osteoblasts differentiation from mesenchymal precursors during both endochondral and intramembranous ossification. In fact, homozygous deletion of *Runx2* in mice resulted in a complete lack of osteoblasts, whereas haploinsufficiency of *Runx2* (or mutations in Cbfa1 locus) in mice or *RUNX2* in humans led to hypoplastic clavicles and delayed closure of the fontanelles, defects that are characteristic of cleidocranial dysplasia in humans. Furthermore, deletion of a nuclear targeting signal located at the carboxyl terminus of RUNX2 led to an identical phenotype to that of RUNX2-null mice, highlighting the importance of proper nuclear localization of this transcription factor. In addition to being needed for osteoblasts differentiation, RUNX2 is necessary for the proper function of mature osteoblasts, including the synthesis of bone matrix.

During limb development in the embryo, RUNX2 is expressed within the chondrogenic mesenchyme, subsequent to and dependent on SOX9 expression.

Following the formation of cartilage, RUNX2 becomes more restricted to the perichondrial cells and osteoblasts, but it is re-expressed in the early hypertrophic chondrocytes (playing positively to regulate hypertrophic chondrocyte differentiation). Interestingly, in the absence of RUNX2, the perichondrium (which normally contains bipotential cells known as osteochondroprogenitors) becomes hypoplastic, indicating that RUNX2 may be necessary for the production and/or maintenance of the progenitors.

Numerous nuclear factors have been shown to synergize with RUNX2 to promote osteoblast differentiation. These are MAF, TAZ (transcriptional co-activator with PDZ-binding motif; also known as WWTR1), SATB2 (special AT-rich sequence-binding 2), RB (retinoblastoma), GLI2, DLX5, MSX2 and BAPX1 (Bagpipe homeobox protein homologue 1), which function in different ways, including stimulating RUNX2 expression, enhancing RUNX2 activity or acting as co-activators. Conversely, some other nuclear factors (TWIST1, HAND2 (heart and neural crest derivatives expressed 2), ZFP521 (zinc-finger protein 521), STAT1 (signal transducer and activator of transcription 1), Schnurri 3, GLI3, HOXA2 and the HES (Hairy and Enhancer of Split) and HEY (HES-related with YRPW motif) proteins) have been found to suppress RUNX2 levels or activity. These factors also use a range of mechanisms, including blocking *RUNX2* DNA binding, nuclear translocation and protein expression. Finally, RUNX2 regulation of target gene expression is likely to be modulated by proteins that govern chromatin structures. For instance, histone deacetylase 4 (HDAC4) was shown to suppress RUNX2 function in chondrocytes to inhibit hypertrophy.

The fact that RUNX2 is activated either by a posttranslational modification and through an accessory factor implies that its mRNA level is poorly correlated with its activity (Franceschi & Xiao, 2003).

RUNX2 binds to DNA interacting with the small protein core binding factor β (CBFβ), a common partner of all Runx proteins. CBFβ does not binds DNA itself, but allosterically enhances the DNA-binding capacity of Runx proteins and increases their half-life by stabilizing them against proteolytic degradation by the ubiquitin-proteasome system (Komori, 2002).

Inconsistencies between RUNX2 mRNA or protein levels and its transcriptional activity suggest that posttranslational modifications and/or protein protein interactions may regulate this factor. RUNX2 can be phosphorilated and activated by the mitogen-activated protein kinase (MAPK) pathway. This pathway can be stimulated by a variety of signals including those initiated by extracellular matrix (ECM) via interactions between collagen type I and integrins β_1, osteogenic growth factors like bone morphogenic proteins (BMPs) and fobroblast growth factor-2 (FGF-2), mechanical loading and hormones such as parathyroid hormone (PTH). Protein kinase A (PKA) may also phosphorilate/activate RUNX2 under certain conditions. When RUNX2 is phosphorilated, can migrate to the nucleus and directly stimulate transcription of osteoblast-related genes such as those encoding alkaline phosphatase, osteocalcin, osteopontin, collagen type I, bone sialoprotein, which have in their promoter the Osteoblast Specific Element-2 (OSE2). In addition, RUNX2 activity is enhanced by protein-protein interactions as are seen with PTH-induced RUNX2/AP1 and BMP-mediated RUNX2/SMADs interactions. Mechanisms of interaction with RUNX2 are complex including binding of distinct components such as AP-1 factors and Smads proteins to separate DNA regions in target gene promoters and direct physical interactions between RUNX2 and AP-1/Smad factors. Post-translational modifications such as phosphorylation may influence interactions between RUNX2 and other nuclear factors. These findings suggest that RUNX2 plays a central role in coordinating multiple signals involved in osteoblast differentiation. (Franceschi & Xiao, 2003)

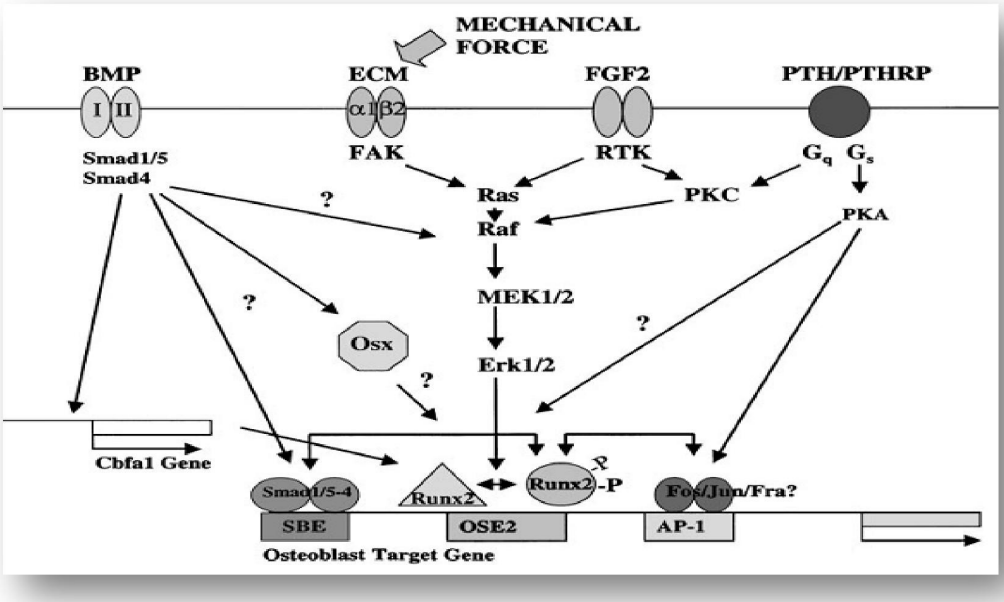

Fig. 13 OSE sequence stimulation in the promoter of many osteoblastic genes, inducted by diverse signals.

OSX is required downstream of RUNX2

Osterix (OSX), a transcription factor containing three C_2H_2-type zinc-fingers, is necessary for osteoblast differentiation. *OSX* was discovered as a BMP-induced gene in C2C12 cells, and its deletion resulted in complete absence of osteoblasts in mouse embryos, despite the relatively normal expression of RUNX2. These results, together with the observation that OSX expression was abolished in RUNX2-null mice, indicate that OSX functions downstream of RUNX2 during osteoblast differentiation. In contrast to RUNX2 deletion, which leads to a hypoplastic perichondrium, loss of OSX results in ectopic cartilage formation beneath a thickened perichondrium at the diaphysis (where a bone collar normally forms), presumably owing to a fate switch of progenitors to chondrocytes instead of osteoblasts. Beyond its role in differentiation during embryogenesis, OSX is crucial for postnatal osteoblast and osteocyte differentiation and function. Thus, OSX has important roles at multiple stages within the osteoblast lineage, both during embryonic development and in postnatal life.

Several transcription factors regulate osteoblast differentiation by regulating OSX. These include the tumour suppressor p53, which decreases OSX levels through an unknown mechanism, and NFATC1 (nuclear factor of activated T cells, cytoplasmic 1), a calcium-sensitive transcription factor that stimulates osteoblast differentiation by enhancing OSX transcriptional activity.

Oct4: TF of non-differentiated cells

Octamer binding protein factor 4 (Oct4) encodes a POU-domain transcription factor (Scholer et al., 1990). The gene is specifically express in embryonic stem (ES) cells but can also be detected in adult stem cells such as bone marrow-derived mesenchymal stem cells (Pochampally et al., 2004). Expression of Oct4 is down-regulated during stem cell differentiation. Oct4 plays a critical role in maintaining pluripotency and self-renewal of ES cells (Niwa et al., 2000; Pesce and Scholer, 2001) but its utility as a marker of pluripotency has been challenged recently by studies suggesting that it is express in a variety of differentiated cells, including peripheral blood mononuclear cells (PBMCs) (Tai et al., 2005). However, detection of Oct4 by RT-PCR could be prone to artificial generated by pseudogene transcripts (genomic DNA sequences similar to normal genes and are regarded as defunct, relatives of functional genes).

ATF4 is important in more mature cells

Activating transcription factor 4 (ATF4), a member of the basic Leu zipper (bZIP) family of transcription factors, has important roles in the more mature osteoblast lineage cells, and its effects seem to be antagonized by the ZIP-containing nuclear protein FIAT (factor inhibiting ATF4-mediated transcription)75 (TABLE 1). Misregulation of ATF4 activity has been linked with the skeletal abnormalities seen in human patients with Coffin–Lowry syndrome and neurofibromatosis type I76,77. ATF4 may function in osteoblast lineage cells through two distinct mechanisms. First, it directly regulates the expression of the osteoblast-derived molecules osteocalcin (a bone matrix protein with newly reported roles in glucose homeostasis

and male fertility (BOX 1)) and receptor activator of nuclear factor-κB ligand (RANKL; also known as TNFSF11), which promotes osteoclast differentiation and function[76,78]. Second, ATF4 promotes efficient amino acid import to ensure proper protein synthesis by osteoblasts[76]; members of the forkhead box O (FOXO) family of transcription factors regulate postnatal bone homeostasis partly by interacting with ATF4 to promote amino acid import[79,80] (TABLE 1).

Moreover, ATF4 was shown to act in chondrocytes to stimulate the expression of IHH (an inducer of osteoblast differentiation, see below)[81]. It is therefore possible that ATF4 may indirectly regulate the osteoblast lineage through its role in chondrocytes.

AP1 family transcription factors

Members of the activator protein 1 (AP1) transcription factor family have been shown to regulate osteoblast differentiation or function; however, their relationship with RUNX2, OSX and ATF4 is not yet clear. Interestingly, different AP1 transcription factors have been shown to have differential effects on these processes. In particular, loss of the AP1 protein FOS-related antigen 1 (FRA1) in the mouse embryo led to low bone mass owing to reduced production of bone matrix proteins[82], whereas transgenic overexpression of FRA1 resulted in high bone mass caused by increased osteoblast differentiation[83]. Similarly, transgenic overexpression of ΔFOSB, a naturally occurring isoform of the AP1 protein FOSB, increased bone mass through cell-autonomous stimulation of osteoblast differentiation and function[84,85]. Conversely, genetic deletion of the AP1 factor JUNB reduced osteoblast differentiation in a cell-autonomous manner[86].

DEVELOPMENTAL REGULATORY SIGNALS

The transcription factors described above are regulated by a range of developmental signals, which have important roles at various stages of osteoblast lineage cell development. Several signalling pathways act on *ah*MSCs promoting proliferation and differentiation.

HH signaling

Hedgehog (HH) proteins, upon binding to the receptor Patched homologue 1 (PTCH1), signal through the seven-pass transmembrane protein Smoothened (SMO) to regulate gene transcription through both derepression and activation of the GLI family of transcription factors (87). GLI2 and GLI3 are the primary effectors of HH signalling in the embryo, whereas GLI1 is generally dispensable for normal embryogenesis (88,89).

Of the three HH proteins in the mammalian genome, IHH is specifically expressed by the prehypertrophic and early hypertrophic chondrocytes within the endochondral cartilage primordium, and signals to chondrocytes and the adjacent perichondrial cells to promote osteoblast differentiation (90). Indeed, mice deficient in IHH completely lack osteoblasts within the endochondral skeleton, although the intramembranous osteoblasts form; this indicates that IHH signalling is dispensable for intramembranous osteoblast differentiation (90). Subsequent genetic studies of SMO revealed that IHH signalling is directly required in perichondrial cells for them to initiate osteoblast differentiation (91). In the absence of IHH signalling, the perichondrial progenitors failed to express RUNX2, which, as discussed above, is indispensible for osteoblast differentiation. However, RUNX2 does not seem to be the sole effector for IHH signalling, as forced expression of RUNX2 did not rescue osteoblast differentiation in IHH-deficient mouse embryos (92). Activation of RUNX2 expression by IHH in the perichondrial cells can be achieved through removal of the GLI3 repressor, but induction of OSX, and hence the entire osteogenic programme, requires both the depression of GLI3 and the activation of GLI2 (93,94). The mechanism through which GLI2 and GLI3 regulate the expression of RUNX2 and OSX is not understood at present. In addition to osteoblast differentiation in the

perichondrium, HH signalling is also necessary for trabecular bone formation, as evidenced by genetic studies of SMO in mouse embryos (91). Thus, IHH, an indispensable signal emanated from the prehypertrophic and early hypertrophic chondrocytes, controls the onset of osteoblast differentiation in the endochondral skeleton.

In contrast to endochondral ossification, intramembranous osteoblast differentiation does not seem to require HH signalling. This was suggested by the finding that ossification of the skull is relatively normal in IHH-null mice, although the result did not rule out the potential importance of other HH proteins, such as Sonic hedgehog. More importantly, in chimeric embryos developed from SMO-null and wild-type embryonic stem cells, SMO-null cells contributed to osteoblasts in the mandible (the lower jaw bone), which is formed through intramembranous ossification (91). The differential requirement for HH between the two ossification processes is not understood, but it implies that HH signalling may have evolved to couple cartilage development with bone formation, whereas a different mechanism is used to activate osteoblast differentiation directly from mesenchyme.

The role for HH signalling in osteoblast lineage cells in postnatal life is less clear. Deletion of IHH from the growth plate chondrocytes in newborn mice resulted in disruption of the growth plate and a continuous loss of trabecular bone in older mice (95). Similarly, pharmacological inhibition of HH signalling in 1–2-week-old mice led to cessation of growth and disruption of bone structure (96). However, these studies did not distinguish direct effects on osteoblasts from those secondary to the chondrocyte defects. In a separate study, genetic disruption of HH signalling in mature osteoblasts resulted in an increase in bone mass in postnatal mice owing to suppressed osteoclast differentiation97. By contrast, pharmacological inhibition of HH signalling in postnatal mice led to a decrease in bone mass, coupled with reduced osteoblast numbers and function, although diminished osteoclast numbers were also noticed68. Thus, HH signalling seems to have complex roles in chondrocytes, osteoblasts and osteoclasts in postnatal mice, and alteration of HH signalling may result in variable outcomes depending on the timing and cell specificity of the manipulation.

Notch signaling

Notch signalling mediates communication between neighbouring cells through direct cell–cell contact. Following binding to their ligands on the neighbouring cell surface (Jagged 1 (JAG1), JAG2, Delta-like 1 (DLL1), DLL3 and DLL4 in mammals), Notch receptors (Notch 1–Notch 4 in mammals) undergo a proteolytic cleavage that is catalysed by the γ-secretase complex, which requires either presenilin 1 (PS1) or PS2 (REFS 98–101). As a result, the Notch intracellular domain (NICD) is released from the plasma membrane and translocates to the nucleus, where it interacts with the CSL family transcription factor RBPJκ (also known as CBF1 in mammals). Together, they activate the transcription of target genes, such as the *HES* and *HEY* family of transcription factors, which in turn control the expression of other genes102.

Mouse genetic studies suggest that Notch signalling suppresses osteoblast differentiation. Removal of either PS1 and PS2 or Notch 1 and Notch 2 in the embryonic limb mesenchyme markedly enhanced osteoblast formation, resulting in high bone mass in adolescent mice67. The high bone mass in the Notch-deficient mice coincided with decreased numbers of bone marrow mesenchymal progenitors, supporting a model in which Notch signalling normally suppresses osteoblast differentiation from the progenitors. The suppression seems to occur at a stage before OSX activation, as deletion of Notch signalling in RUNX2+OSX+ cells did not cause a similar phenotype (F.L., unpublished observations) (FIG. 3b). Mechanistically, Notch signalling seems to inhibit osteoblast differentiation in part by inducing HEY1 and HEY-like (HEYL). These, in turn, decrease RUNX2 transcriptional activity67.

Consistent with the negative role of Notch signalling in osteoblast differentiation, *NOTCH1* haploinsufficiency in humans causes ectopic ossification in the aortic valves66,103, whereas gain-of-function mutations in *NOTCH2* are responsible for Hadju–Cheney syndrome, a disorder of severe and progressive bone loss104,105. Similarly, transgenic mice globally overexpressing the Notch target gene *Hey1* show progressive osteopenia106. Interestingly, whereas Notch activation was found to suppress osteoblast differentiation from early precursors107, at a later stage it caused

pathological overproduction of immature osteoblasts, similar to what occurs in certain human osteosarcomas108–110. Thus, these studies have highlighted the stage-specific functions of constitutive Notch activation in the osteoblast lineage.

WNT signaling

The WNT family of glycoproteins has important roles in regulating osteoblast lineage cells. Upon engaging various membrane receptors, WNT ligands activate numerous intracellular pathways that are either dependent or independent on β-catenin111,112.

In β-catenin-dependent WNT signalling, WNT binds to Frizzled receptors and their co-receptors low-density lipoprotein receptor-related protein 5 (LRP5) or LRP6 to stabilize cytosolic β-catenin (FIG. 3c). β-catenin then enters the nucleus and stimulates the transcription of WNT target genes by interacting with lymphoid enhancer-binding factor 1 (LEF1), T cell factor 1 (TCF1), TCF3 and TCF4. The mechanism responsible for the nuclear localization of β-catenin is not fully understood, but JUN N-terminal kinase (JNK)-mediated phosphorylation of β-catenin triggered by activation of the small GTPase RAC1 was shown to be important in certain contexts113.

Genetic evidence from both humans and mice has implicated β-catenin-dependent WNT signalling in the regulation of bone accrual during postnatal life. In humans, loss-of-function mutations in the gene encoding the WNT co-receptor LRP5 cause osteoporosis-pseudoglioma syndrome114, a form of juvenile-onset osteoporosis. Conversely, a different set of mutations in *LRP5* that render the co-receptor refractory to extracellular WNT inhibitors, such as Dickopff-related 1 (DKK1) and sclerostin, cause high bone mass syndrome115–119. In addition, loss-of-function or loss-of-expression mutations in *SOST* (which encodes sclerostin) result in the bone-thickening diseases sclerosteosis or Van Buchem disease, respectively120–123. Furthermore, in mice, *Lrp5* (REF. 124) or *Wnt10b*125 deletion leads to reduced bone mass postnatally, and *Lrp6* haploinsufficiency further decreases bone mass in LRP5-null mice126. By contrast, mice engineered to express a mutant form of *LRP5* that causes high bone mass in humans also exhibit a high bone mass127,128. Analyses of LRP5-mutant mice revealed that LRP5 predominantly affects osteoblast

numbers and function, with no clear effect on osteoclasts124,127,128. Moreover, *Lrp5* mutations mainly affect postnatal bone accrual with no obvious effect in the embryo; the exact reason for this is not clear.

The mechanism through which LRP5 controls postnatal bone accrual is not well understood. Because deletion of β-catenin in mature osteoblasts by independent groups did not produce a similar bone phenotype to LRP5-deficient mice (that is, increase in osteoblast number and activity with no obvious effect on osteoclasts)129,130, LRP5 could function independently of β-catenin, at an earlier stage within the osteoblast lineage, or beyond the skeletal tissue. The potential stage specificity of LRP5 function was addressed by two different groups but with conflicting results. One group reported that deletion of *Lrp5* either in mature osteoblasts128 or in mesenchymal progenitors131 (and therefore all cells of the osteoblast lineage) did not produce any bone phenotype, whereas a second group showed that deletion of *Lrp5* predominantly in osteocytes resulted in less bone127. Supported by their respective findings, the two groups proposed competing models: the first group argues that LRP5 functions in the duodenum to suppress circulating levels of serotonin, which in turn directly inhibits osteoblast proliferation128; whereas the second group suggests that LRP5 acts directly in the osteoblast lineage127. Thus, further work is needed to better understand how LRP5 functions.

It is worth noting that serum serotonin levels were shown to inversely correlate with bone mass in patients harbouring disease-causing *LRP5* mutations131,132, and administration of a chemical inhibitor that reduces serum serotonin levels increased bone mass in both LRP5-deficient mice and in ovariectomized mice133,134. It is of great interest to see in the future whether reducing serum serotonin levels can be a useful strategy for treating osteoporosis in humans.

In contrast to what occurs in the postnatal stage, β-catenin has been shown to have an integral role in osteoblast differentiation in the embryo. Indeed, genetic deletion of β-catenin in embryonic mesenchymal progenitors abolishes mature osteoblast generation135–138. Specifically, β-catenin is required for the progression from the RUNX2+ stage to the RUNX2+OSX+ stage and from RUNX2+OSX+ cells to mature osteoblasts135,136 (FIG. 2), although the molecular mechanisms underlying these regulations are not understood. This requirement for β-catenin in osteoblast

differentiation seems to be linked to its role in WNT signalling, as deletion of both LRP5 and LRP6 in mesenchymal progenitors, similarly to the removal of β-catenin, results in loss of osteoblasts139. Interestingly, deletion of β-catenin in either mesenchymal progenitors or RUNX2+OSX+ cells caused ectopic cartilage formation in the place of bone, possibly owing to a fate switch for the bipotential progenitors94,136–138, but the mechanism underlying this fate switch is not understood (FIG. 2). Furthermore, β-catenin signalling has been shown to be downstream of IHH signalling, as β-catenin deletion does not impair IHH signalling in the perichondrium (which contains osteoblast progenitors), whereas IHH removal abolishes β-catenin signalling in that compartment135,140.

β-catenin-independent WNT signalling has also been implicated in regulating the osteoblast lineage. For instance, WNT-induced G protein-coupled phosphatidylinositol signalling and protein kinase Cδ (PKCδ) activation have been shown to promote osteoblast differentiation by stimulating the progression from RUNX2+ to RUNX2+OSX+ cells through an unknown mechanism141 (FIG. 3c). In addition, WNT5A is thought to promote osteoblast differentiation by inducing suppressive histone methylation at the promoters of peroxisome proliferator-activated receptor-γ (PPARγ) target genes, thereby inhibiting the adipogenic programme142. Thus, WNT5A seems to inhibit adipogenesis through a different mechanism from that of another WNT ligand, WNT10B, which suppresses the expression of the adipogenic transcription factors PPARγ and CCAAT/enhancer-binding protein-α (C/EBPα) in a β-catenin and TCF-dependent manner143. Exactly how inhibition of adipogenesis in either case leads to osteoblast differentiation is not clear.

Finally, deletion of Frizzled 9 was shown to cause decreased bone mass in part through downregulation of ISG15, a ubiquitin-like protein modifier, without impairing β-catenin signalling144. Overall, with a better understanding of other signalling cascades activated by WNT, it is anticipated that additional mechanisms through which WNT proteins regulate the osteoblast lineage will be uncovered.

BMP signaling

BMPs, which are members of the transforming growth factor-β (TGFβ) superfamily, have essential roles in a wide range of biological processes145. In the most studied mechanism, BMPs bind to receptor complexes composed of heterotetramers of type I and type II Ser/Thr kinase receptors, and activate SMADs (SMAD1, SMAD5 or SMAD8) through site-specific phosphorylation. The phosphorylated SMADs form a complex with their common partner, SMAD4, and enter the nucleus to regulate gene expression (FIG. 3d).

Genetic studies have uncovered important roles for BMP2 and BMP4 in promoting osteoblast differentiation. Knockout experiments showed that a critical threshold level of BMP2 and BMP4 signalling is required for differentiation to mature osteoblasts and that this is mediated by controlling the transition from RUNX2+ to RUNX2+OSX+ cells through an unknown mechanism146 (FIG. 3d). Furthermore, mice lacking only BMP2 in the limb mesenchyme formed bone during embryogenesis but exhibited a clear defect in bone mineral density shortly after birth, resulting in frequent fractures that failed to heal147. Thus, BMP2 has a unique role in postnatal bone formation, although it is not clear whether this is due to its specific signalling property or to the insufficient levels of other BMPs with similar functions. Mouse genetic studies of the BMP receptors have also revealed important roles for BMP signalling in controlling bone mass. Deletion of BMP receptor 1A (BMPR1A) in preosteoblasts and osteoblasts, either *in utero* or postnatally, resulted in an unexpected increase in bone mass148–150. These studies indicated that, although BMPR1A loss decreased bone formation, it also reduced bone resorption to a greater extent, resulting in a net increase in bone mass. Thus, BMP signalling in osteoblast lineage cells seems to also have an important role in regulating osteoclasts.

In addition to its role in osteoblast differentiation, BMP signalling regulates the function of mature osteoblasts. Deletion of BMPR1A in mature osteoblasts decreased osteoblast function151, whereas overexpression of noggin, a secreted inhibitor for BMPs, caused a reduction in osteoblast function and a lower bone mass in mice post-natally152. Similarly, deletion of SMAD4, a downstream effector of BMP signalling, in mature osteoblasts led to reduced osteoblast function153.

Interestingly, BMP3 may counteract the activities of BMP2 and BMP4 to maintain a proper bone mass *in vivo*, as BMP3-null mice had more trabecular bone than wild-type mice. However, the cellular basis for the phenotype is not clear154. Recent studies have shown that BMP3 engages the BMP type II receptor activin receptor 2B (ACVR2B) to inhibit signalling by BMP2 or BMP4 (REF. 155). In the postnatal skeleton, BMP3 is mainly produced by osteoblasts and osteocytes and it in turn reduces differentiation from the earlier-stage osteoblast lineage cells155. Thus, BMP3 seems to function in a negative feedback mechanism to ensure the production of a correct number of osteoblasts.

FGF signallin

FGFs are a large family of proteins (22 members in humans and mice) that carry out diverse biological functions in vertebrates156. Most FGFs function by binding to cell surface Tyr kinase FGF receptors (FGFRs; FGFR1–FGFR4 in humans and mice), leading to the phosphorylation of a range of signalling proteins and the activation of multiple signalling modules, including mitogen-activated protein kinase (MAPK), phosphoinositide 3-kinase (PI3K), STAT1 and PKC157 (FIG. 3e). Mutations in FGFRs are responsible for a large range of congenital skeletal disorders in humans (for a more detailed discussion, see REF. 158).

Genetic studies in mice have revealed diverse roles for FGF signalling in osteoblast lineage cells, both in embryonic and postnatal stages. For example, mice lacking FGF2 showed a reduction in total bone mass at the adult stage, which was probably due to reduced preosteoblast proliferation and decreased osteoblast function159, whereas FGF18-null embryos exhibited defects in the formation of mature osteoblasts despite normal RUNX2 expression160,161. Similarly, FGFR1 signalling at an early developmental stage promotes osteoblast differentiation without affecting RUNX2 expression, but FGFR1 signalling in mature osteoblasts inhibits their mineralization activity though an unknown mechanism162. By contrast, FGFR2 promotes the proliferation of preosteoblasts and the function of mature osteoblasts163, although the mesenchymal splice form of FGFR2 stimulates osteoblast differentiation partly through upregulation of RUNX2 expression[164,165]. Finally, mice lacking FGFR3 showed an increase in osteoblast number but a decrease

in osteoid mineralization[166]. Thus, FGF signalling through different receptors has diverse roles in regulating preosteoblast proliferation and osteoblast differentiation, as well as the activity of mature osteoblasts, but the precise stages at which FGFs regulate proliferation and differentiation, and the intracellular signalling cascades responsible for each function, remain to be elucidated.

(*Fanxin Long,* Building strong bones: molecular regulation of the osteoblast lineage, Volume 13: 27-38, January 2012).

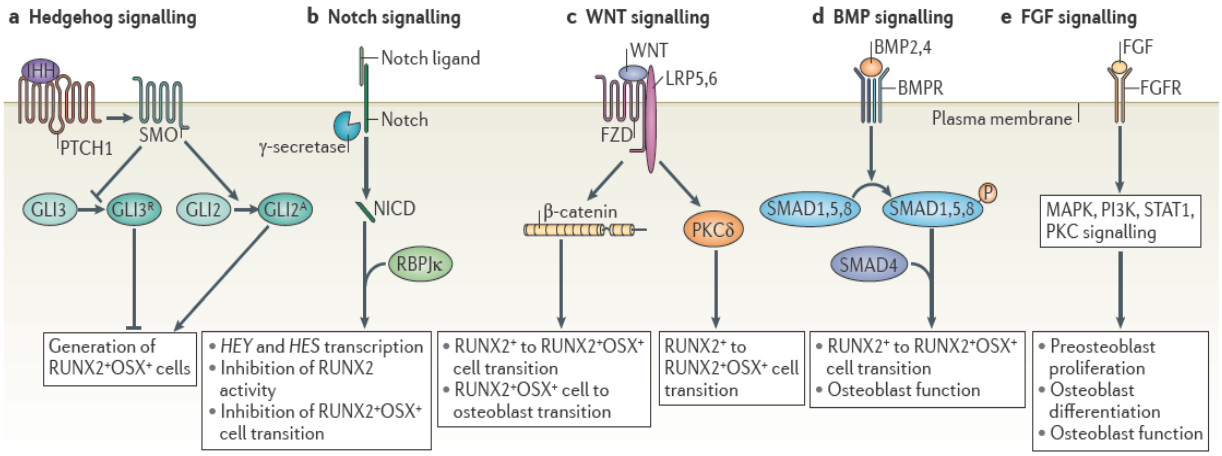

Fig. 14 Developmental signals regulating key steps of osteoblast differentiation.

1.2 MESENCHYMAL STEM CELLS

1.2.1 ADULT HUMAN STEM CELLS

Any adult tissue with repair and/or regenerative capabilities is likely to harbour tissue-specific stem cells defined as cells that self-renew and retain the sufficient proliferative and differentiation potential to be able to repair and/or reconstitute a specific tissue. It is well known that adult bone has an impressive ability to repair: therefore, it is not surprising that the identification and characterisation of the stem cells responsible for this process is an active field of investigation (Bianco, 2008; Caplan, 2007; Kolf, 2007; Prockop 1997).

An orderly chain of highly regulated processes involving cell proliferation, migration, differentiation, and maturation, leads to the production and sustenance of most cell lineages in adult organism. The earliest cell type on this chain has been called a stem cell. Together with their extensive capacity for self-renewal, stem cells display a broad potential for giving rise to diverse differentiated progenies. Adult organisms contain several classes of stem cells: hematopoietic, neural, mesenchymal.

For a long time, adult stem cells have been considered to be developmentally committed in such a way that they appear restricted to produce specific cell lineages, namely those from the tissue in which the stem cell resides (i.e. bone marrow forms blood cells). This deterministic concept has been recently challenged by several findings; reports have shown that a particular stem cell originates not only the predicted collection of cells characteristic of the tissue in which they reside in, but may also give rise to a set of unacquainted progenitors (Petersen, 1999).

Moreover, to suit the elevated demand of precursors that occurs during tissue growth and repair, adult organisms should have the ability to recruit uncommitted progenitors from other tissue sources. Thus, it seems that in addition to their ability to divide without limits (self-renewal) and to give rise to distinctive cells (multipotent), adult stem cells are remarkably malleable and exhibit a higher degree of plasticity.

Another feature of stem cells is their ability to leave their tissue niche and circulate in the blood stream, as occurs with the mesenchymal stem cells (Reading, 2000).

However, to express its differentiation program, a circulating stem cell must home into an appropriate microenvironment (Watt FM, 2000).

Bone marrow contains not only the hematopoietic stem cell, but also the stem cell for tissues that can roughly be defined as mesenchymatic. The multipotencial of mesenchymal stem cells, their easy isolation and culture, as well as their high ex-vivo expansive potential make these cells an attractive therapeutic tool capable of playing a role in a wide range of clinical applications in the context of both cell and gene therapy strategies (Minguell JJ, 2001).

1.2.1.1 MESENCHYMAL STEM CELLS (MSCS)

In the early 1970's, the pioneering work of Friedestein et al. demonstrated that the rodent bone marrow had fibroblastoid cells with clonogenic potential *in vitro* (Friedenstein 1970 and 1980). Friedenstein isolated spindle-like cells from whole bone marrow for their capacity to adhere to plastic. Adherent cells were heterogeneous in appearance but capable of forming colonies (Colony-forming unit fibroblastic, CFU-F). Friedenstein demonstrate that these cells could make bone and reconstitute a hematopoietic microenvironment in subcutaneous transplants, and that CFU-F could regenerate heterotopic bone tissue in serial transplants providing evidence in support of their self-renewal potential. Over the years, numerous laboratories have confirmed and expanded these findings showing that cells isolated according to Friedenstein's protocol were also present in the human bone marrow stroma; and that these cells could be sub-passaged and differenciated in vitro into a variety of cells of the mesenchymal lineages such as osteoblasts, chondrocytes, adipocytes and myoblasts (Bianco, 2008; Caplan, 2007; Kolf, 2007; Pittenger 1999; Prockop 1997).

Was demonstrated later their multilineage differentiation capacity being capable also to non-mesenchymal cells like neural cells (Marrow into Brain) (Kopen, 1999; Reyes, 1999). Cells isolated by Friedenstein were later renamed by Caplan et al. "mesenchymal stem cells" or "MSC" (Caplan, 2007). MSC (or MSC like cells) are not a unique feature of the bone marrow, as they were subsequently isolated from adult connective tissues (Punto, 2005; Puntos, 2006) and are also found in tissues

such as fat (Lee RH), pre-natal tissue, such as placenta (In't Anker PS), umbilical cord blood (Erices A), fetal bone marrow, blood, lung, liver and spleen (In't Anker PS) dental pulp, periodontal ligament (Trubiani O), tendon, synovial membrane and skeletal muscle, thymus and spleen (Krampera), Circulating MSCs can be detected in peripheral blood (Roufosse CA), similarly to what happens for haematopoietics stem cells. Though the complete equivalency of such populations has not been formally demonstrated using robust scientific methods. Therefore, our knowledge of MSCs is virtually entirely based on the characterization of cultured cells, and our definition of MSCs is indeed an "operational" definition based on the potential to self-renew and differentiate in vitro. Little is known about the phenotypic characteristics of MSCs in vivo, their developmental origin, their contribution to organogenesis and postnatal tissue homeostasis normally, and their anatomical localization. Moreover there isn't a test that rigorously shows their ability to self-renew in vivo, so proving their "stemness" (Schipani, 2009).

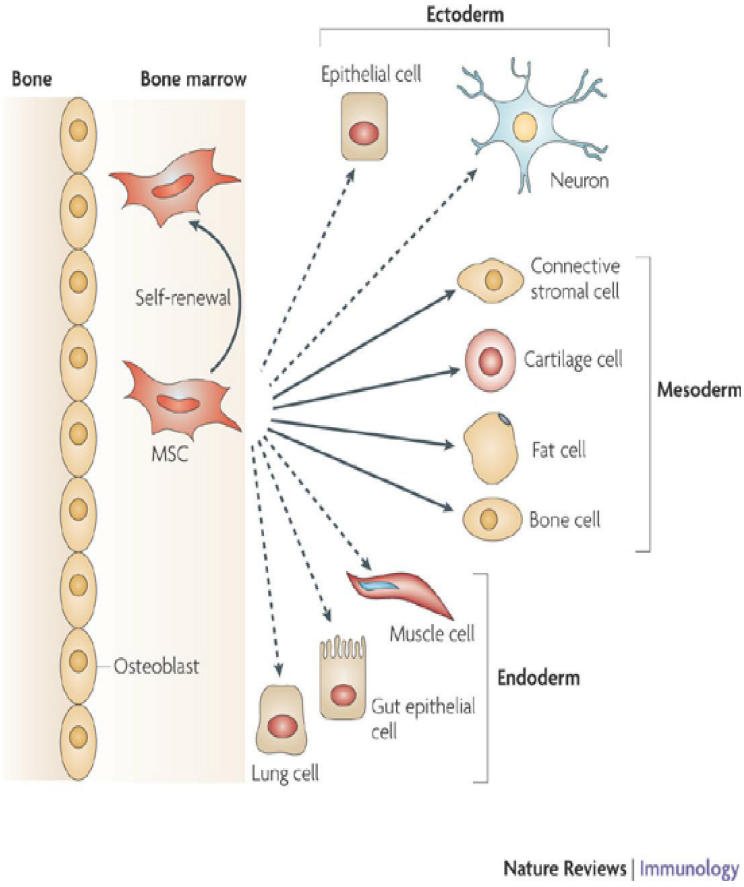

Fig. 15: The figure shows the ability of ahMSCs in the bone marrow stroma, to self-renew (curved arrow), to differentiate towards the mesodermal lineage (straight, solid arrow) and to transdifferentiate (dashed arrows) into cells of other lineages.

1.2.2 STEM CELL NICHE

A costellation of intrinsic and extrinsic cellular mechanisms regulates the balance of self-renewal *ah*MSCs and differentiation potential. Many works propose the existence of sites in the body that provide a sheltering environment that sequesters stem cells from differentiation stimuli, apoptotic stimuli and other stimuli that would dissipate stem cell reserves, which have been defined with the name of "niches". Stem cells must periodically activate to produce progenitors or "transit amplifying cells", which are committed to produce mature cell lineages. Thus, maintaining a balance of stem cell quiescent and active is a hallmark of a functional niche (Augello, 2010).

An extensive literature has pointed to pericytes as a potential source of MSCs (Tavian, 2005). Pericytes reside in the wall of the sinusoidal blood vessels of the bone marrow. Crisan et al. suggested that multipotent MSCs with perivascular localization exist in numerous human organs. Whether the vascular setting provides a true niche for pericytic MSC-like cells and is the main source of MSCs in vivo, remains to be established. (stembook.org) In this regard, however, it is important to note that an increasing amount of evidence has recently linked angiogenesis to osteoblastogenesis, suggesting that blood vessels could be a source of osteoprogenitors or of MSCs with osteogenic potential (Wang et al., 2007).
Another extremely important but yet unanswered question in regard to MSCs and their site of origin is whether the bone periosteal compartment, which is critical for fracture repair, is also as a source of MSCs and whether this periosteal population shares significant similarities with the MSCs isolated from bone marrow (Modder and Khosla, 2008).

1.2.3 DENOMINATION USED TO REFER TO MESENCHYMAL STEM CELLS

It has been proposed that a heterogeneous population of non-hematopoietic stem cells exists in the bone marrow of both humans and rodents, with MSCs being just a subset of this complex cellular make-up. The heterogeneity is exemplified by the different cell pools investigators over the years have isolated from the bone marrow

using different methodology and by the different names that have been assigned to the diverse populations: “Endothelial Progenitor Cells (EPCs)”, “Multipotent Adult Progenitor Cells (MAPCs)”, “Marrow-Isolated Adult Multilinage Inducible cells (MIAMI)”, “Mesenchymal Stem Cells (MSCs)” and “Very Small Embryonic-Like stem cells (VSELs)”. EPCs are considered endothelial precursors that reside in the bone marrow and are released into the bloodstream to contribute to vasculogenesis in injured organs. MAPCs were isolated from bone marrow mononuclear cells and exhibit a fibroblastic morphology; after in vitro expansion are the only one that can contribute to all three germ layers upon injection into blastocysts at least in rodents; this term refers not only to the stem cell per se, but to a vast repertoire of committed progenitors exhibiting at least more than one differentiation potential and describes to be present both in the bone as well as in several mesenchymal tissues. MIAMI cells were also shown to express markers for cells derived from all three germ layers. VSEL cells are the only ones characterised in vivo, were found during embryogenesis in the epiblast and were found to express markers characteristic of pluripotent stem cells, (steembook.org).

We will refer to adult human bone marrow isolated mesenchymal like stem cells as *ah*MSCs, in this work.

1.2.4 CHARACTERISTICS OF *ah*MSCS

Bone marrow stroma is the most recurrent tissue source utilized in growing mesenchymal progenitors; in humans, the starting material frequently consists of aliquots of bone marrow obtained from normal donors undergoing marrow aspiration for purposes of transplantation. Mesenchymal stem cells represent a very small fraction, 0.001-0.01% of the total population of nucleated cell in the marrow. After plating low-density mononuclear cells in a basal medium supplemented with selected batches of fetal bovine serum (Prockop, 1997; Conget, 1999), the plastic-adherent cells is considered the primary ex-vivo source of MPCs.

By light or phase contrast microscopy, MPCs cultures display a rathr homogenous population of fibroblast-like cells (Castro-Malaspina 1980). Cell cycle studies revealed that the vast majority of cells are standing at the G_0/G_1 phase of the cell

cycle (Conget, 1999). After subcultivation MPCs exhibit a large but highly variable expansive potential. While some preparations of MPCs can be expanded through over 15 cell dublings, others cease replicating after about four cell doublings (Digirolamo CM, 1999). This is due to several determinants, among them the procedure used to harvest the marrow (Digirolamo, 1999), the low frequency of MPCs in marrow harvests, the age or condition of the donor from which the MPCs were extracted (Digirolamo, 1999). Despite the high ex-vivo expansive potential, MPC do not loose their normal karyotype and telomerase activity (Pittenger, 1999). However, extensive subcultivation impairs cell function by the onset of evident signs of senescence (Digirolamo, 1999) and or apoptosis (Conget, 1999).

Surface markers

The development of a series of monoclonal antibodies raised towards surface MPCs antigens, along with other antibodies developed to characterise bone marrow stromal cells, has been crucial for the immunophenotyping of these cells. Results have shown that the antigenic phenotype of MPCs is not unique, but borrows features of mesenchymal, endothelial, epithelial, and muscle cells. Specific antigens are: SH2, SH3, SH4, STRO-1, a-smooth muscle actin, MAB1740 (Conget, 1999; Haynesworth 1992; Galmiche 1993; Simmons 1991). The SH2 antibody (Haynesworth, Baber, Caplan 1992), raised against human MSCs, reacts with an epitope present on the transforming growth factor-beta receptor endoglin (CD105) (Barry, 1999). Both the SH3 and SH4 antibodies (Heynesworth, 1992) recognise distinct epitopes on the membrane-bound ecto-5'-nucleotidase (CD73) (Barry, 2001); these antibodies do not react with haematopoietic cells or osteocytes. Stro-1 was identified as an antibody that reacted with non-haematopoietic progenitor bone marrow stromal cells (Simmons and Torok-Storb, 1991). CD-166 (activated leukocyte-cell adhesion molecule, ALCAM) is present on undifferenciated MSCs, which disappeared once the cells embarked upon the osteogenic pathway and began to express cell surface alkaline phosphatase (Bruder, 1997). Majumdar en 2003 determines that MSCs express a large spectrum of cell adhesion molecules of potential importance in cell binding and homing interactions. MSCs exhibit high expression of integrins α1, α5 and β1, low expression of α2, α3, α6, αV, β2 and β4, and no expression of α4, α L

and β2; and express VCAM-1(CD106) AND ICAM-1 (CD54). Human MSCs also express HLA-ABC and not HLA-DR. The results of this analysis point to several potentially key interactions in vivo between MSCs and other cell types.
MPCs do not express the typical hematopoietic antigens, CD45 and CD 34 (Conget, 1999; Pittenger, 1999; Jiang 2002).

At present well-defined phenotypic criteria to characterize MSCs do not exist. This is because till today there is not a single marker that specifically delineates the in vivo MSCs. Therefore positive and negative phenotypic staining is performed which results in a loose phenotypic definition with significant controversies in this area. This task is further aggravated by the fact that MSCs share features with other types of cells including endothelial, epithelial and muscle cells (Minguell, 2001).

1.2.5 COMMITTED PROGENITORS IN *ah*MSCS CULTURES

Studies utilising distinct experimental approaches have established that cultures of bone-derived *ah*MSCs contain uncommitted mesenchymal progenitors as well as committed osteoprogenitors. All together, this evidence puts forward the contention that uncommitted, mesenchymal stem cells are not only located in the marrow, but are also ubiquitously positioned in bones where, under appropriate stimuli (microenvironment?), may self-renew, commit, and generate cells exhibiting the phenotypic and functional characteristic of the resident tissue (Liu F, 1994).

Muraglia et al. shown that while 30% of all clones of bone marrow deriving cells exhibit a tri-lineage (osteo/condro/adipo) differentiation potential, the rest exhibit either a bi-lineage (osteo/chondro) or a pure osteogenic potential. This data strengthen the concept that cultures of bone marrow-derived *ah*MSCs are not homogenous, but consist of an assortment of uncommitted and committed progenitors exhibiting divergent stemness. The letter concept discloses that as progenitors progress towards the terminal phenotype, self-renewal is gradually lost and commitment increases.

Proliferation, differentiation, and maturation are in principle independent, in other words: stem cell divides without maturation, while a cell close to functional competence may mature but not divide. However, the committed cell population divides and matures, showing intermediate properties between stem cells and functional mature cells. Therefore the stemness of mesenchymal progenitors is not a property of a particular cell type, but a spectrum of capabilities of cell types within a population (Minguell JJ, 2001).

Single cell clonal cultures show also a wide variation in the proliferation rates that are directly related with differentiation potential. Fast growing clones have multipotential characteristics, whereas slow growing clones have a limited differentiation potential, and start to show changes in cell morphology and signs of cell senescence (Xiao Y, 2010).

1.2.6 ISOLATION OF *ah*MSCS

To date there is no established procedure for the isolation of *ah*MSCs but a wide number of protocols exist providing non-comparable data (Puntos, 2007). The first and simple method implies the adherence properties of MSCs which where first identified by the pioneer work of Friedenstein et al. (Friedenstein, 1976). In that study whole bone marrow was placed in plastic culture dishes and after 4 hours the non-adherent cells were washed out. They observed that the cells remained dormant for 2-4 days and than they proliferated rapidly. A modification of this protocol includes the density centrifugation of BM. This technique involves the use of high density low viscosity and low osmotic pressure solutions (i.e. Ficoll, Percoll) to obtain the mononucleated fraction of BM which contains *ah*MSCs (Lennon, 2006); subsequently, after Ficoll/Percoll centrifugation cells are plated at densities ranging from $1 \cdot 10^4$ to $0.4 \cdot 10^6$ cells/cm^2 (Lodie, 2002; Pittenger, 1999), adherence to plastic occurs giving a population of *ah*MSCs. The initial number of *ah*MSCs can be increased as much as 36,6% by simple collection and replating of the initially non-adherent cell population which is washed out during the first feeding (Wan, 2006). *ah*MSCs from solid tissues, like bone, could be isolated using the above mentioned philosophy. In this method a small piece of bone is placed directly inside the flask or

plate and cells grow out of bone explants onto the plastic substratum (Simmons, 1991). Primary cultures are usually maintained for 12-16 days, during which time the non-adherent hematopoietic cell fraction is depleted (Barry, 2004). An alternative to this technique is the collagenase digestion process. Collagenases are enzymes that are able to cleave the peptide bounds in the triple helical collagen molecule. In this way cells are released from the tissue and can be easily collected by wash and centrifugation. This isolation technique is used for more than two decades (Lennon, 1983; Wong 1986). Unfortunately, there is not a standardised protocol for its use, resulting in a variety of concentrations and digestion times (Pountos, 2007). The yield of *ah*MSCs using enzymatic digestion appears to be higher than that of BM aspirates: 100-fold more *ah*MSCs (Sakaguchi Y, 2005). Some authors suggested that these cells are identical to those isolated from BM both, in terms of differentiation potential and phenotypic characteristics (Sakaguchi Y, 2005); others suggest that enzymatic treatment could result in alterations of the metabolic profile of *ah*MSCs (Thomas CB, 2004).

The plastic adherence itself is not sufficient to allow for the purification of *ah*MSCs, as many studies demonstrate (Jiang, 2002; Phinney 1999, Lodie 2002), because these cells reported substantial variation in the cell numbers and levels of expression of ALP and other markers. These results illustrate the complexity of subpopulations of bone marrow cells, the need to evaluate isolation techniques with care, and the need to identify new cell-specific markers (Barry, 2004).

The issue arising from the above mentioned techniques is the purity of the *ah*MSCs sample. The contamination of the cells with other types of cells (like haematopoietic stem cells) results in a heterogeneity of the preparations. Techniques like the magnetic bed sorting and fluorescent-activated cell sorting have been developed. These techniques are based on the use of antibodies directed to *ah*MSCs surface markers epitopes (phenotypic profile of the *ah*MSCs discussed above).

1.2.7 EXPANSION OF *ah*MSCS

The next step, after *ah*MSCs in vivo isolation, is the ex-vivo expansion. This stage allows *ah*MSCs replication, targeting sufficient numbers for clinical use. Several factors could influence the yield of ex-vivo expansion of *ah*MSCs. These factors are either donor dependent or technique dependent. Donor dependent include the age of the donor and the sex, the presence of trauma, and the presence of a systemic disease. The technical issues are mainly related to the target number of cells that is the number of passages of *ah*MSCs, the method of culture and media that are used for expansion. *ah*MSCs proliferate rapidly resulting in an expansion of a thousand-fold in two to three weeks time (Chen, 2004). In addition *ah*MSCs could proliferate for about 19 doublings in culture without losing their property to proliferate and differentiate (Muraglia, 2000). However, expansion has shown to gradually reduce the maximal differentiation potential of *ah*MSCs (Banfi A, 2000). Extensive subcultivation also impairs the cell's function resulting in cellular senescence that is associated with growth arrest and apoptosis (Digirolamo,1999; Stenderup, 2003). There are data suggesting that prolonged culture could result in spontaneous transformation acquiring tumorigenic potential (Rubio, 2005).

Media and Serum

The most important component of successful expansion of *ah*MSCs is the media used. Culture medium consists of a basal medium (Dulbecco's Modified Eagle's Medium, DMEM) containing glucose, ions including calcium, magnesium, potassium, sodium, and phosphate, as well as fetal animal sera in concentrations of 10% or 20%. Commonly the most used is the heat inactivated Fetal Bovine Sera (FBS). However, there are two main issues arising from their use: their efficacy compared with human serum, and their potential side effects like transmission of diseases and immune reactions (Pountos, 2007). Results are divergent at the moment.

Monolayer and three-dimensional static cultures

Monolayer is the basic and the most economical technique for *ah*MSCs expansion; cells are grown in polystyrene culture Petri dishes or flasks. Plastic vessels used in tissue cultures are specially treated to ensure good adherence of cells to the vessels.

Culture conditions include incubation in a maintained temperature of 37ºC, in a humidified atmosphere with 95% O_2 and 5-7% CO_2. When cells reach confluency they are treated with tripsin and seeded into new flasks, following the desired cell concentration for expansion or for the experiment.

Three dimensional static cultures, are not fully explored. A variety of systems has been developed in the last years. Different materials have been used as structural frameworks to encapsulate and support *ah*MSCs. Monolayer culture is simple to perform but includes several disadvantages. Several studies have been shown that *ah*MSCs grown in 2D systems compared to 3D systems, have reduced differentiation capacity, reach senescence earlier, ALP activity and osteocalcin content were significantly lower (Banfi, 2000; Na K, 2007). 3D dynamic systems, also called bioreactors, are a good alternative, because they produce a unique environment mimicking the in-vivo condition of the cells. Their advantages include minimal shear stress, microgravity, efficient nutrient supply and metabolite removal (Xi Chen, 2006).

1.2.8 DIFFERENTIATION INTO OSTEOGENIC LINEAGE

The differentiation of *ah*MSCs into bone, cartilage and fat has been described and characterized by multiple laboratories (Barry, 2001; Bruder 1998; Digirolamo 1999, Johnstone 1998; Muraglia 2000; Pittenger 1999). Among others, osteogenic activation requires the presence of β-glycerol-phosphate, ascorbic acid-2-phosphate, dexamethasone and fetal bovine serum. When cultured in monolayer in the presence of these supplements the cells acquire an osteoblastic morphology with up-regulation of ALP activity and deposition of a calcium-rich mineralized extracellular matrix.

1.2.9 THERAPEUTIC APPLICATIONSOF *ah*MSCS

Stem cell therapy involves the transplantation of autologous or allogenic stem cells into patients, either through local delivery or systemic infusion.

In the area of orthopaedic medicine there are also many examples of applications involving local delivery of marrow stem cells. These include the repair of segmental bone defects (Quarto, 2001) and… (mettere lavori di Luis).

There is accumulating evidence of the hypoimmunogenic nature of MSCs and this has implications in terms of allogenic therapy, or the delivery to a recipient of cells derived from an unmatched donor. There are several reports describing the clinical use of allogenic donor-mismatched cells with little evidence of host immune rejection or GVHD. For example, allogenic bone marrow transplantation in children with Osteogenesis Imperfecta resulted in engraftment of donor-derived MSCs and an increase in new bone formation (Horwitz, 1999).

Implanted cell-host interactions

The question of the host response to implanted MSCs is critical and receiving attention as these cells are being considered in a variety of clinical applications. There are several aspects to the implanted cell-host interaction that need to be addressed as we attempt to understand the mechanism underlying stem cell therapies. These are: 1. the host immune response to implanted cells, 2. the homing mechanism that guide delivered cells to a site of injury and 3. differentiation of implanted cells under the influence of local signs (Barry, 2004).

Host immune response. An additional but not less important property of MSCs is their immunomodulatory effect towards a large number of immune effector cells, including $CD4^+$ and $CD8^+$ T cells. Di Nicola et al. found in 2002 that human T cell proliferation, stimulated by the addition of irradiated allogenic peripheral blood lymphocyted, dendritic cells or phytohaemaglutinin, was greatly suppressed when the cultures also contain MSCs. The immunomodulatory effect seems to depend, at least in humans, mainly on soluble factors rather than cell-cell contact; this evidence suggests that local or systemic therapeutical benefit of MSC infusion may be achieved also with low numbers of MSCs. (Krampera M, 2006; Krampera M, 2003).

There is some convincing evidence, as discusse above, that human MSCs, by virtue of their distinct immunophenotype, associated with the absence of HLA Class II expression, as well as low expression of co-stimulatory molecules (Majumdar, 2003),

may be nonimmunogenic or hypoimmunogenic. HLA Class II expression is also absent from the surface of differentiated MSCs and these cells did not elicit an alloreactive lymphocyte proliferative response (Le Blanc, 2003).

Homing mechanism. Seems clear that MSCs when delivered by intravenous infusion, are capable of specific migration to a site of injury. This ability of implanted cells to seek out the site of tissue damage has been demonstrated in the case of bone fracture (Shake, 2002), myocardial infarction, and others pathologies. The mechanisms that guide homing of implanted cells are unclear (Wang el al. demonstrate the role of chemokines in cerebral ischemic tissues).

Interestingly, Wang et al. (2002) also noted that the efficiency of homing of these cells was decreased following long-term culture, an effect that will influence the preparation if these cells for therapeutic use (Barry, 2004).

In vivo differentiation. The fundamental principle of stem cell therapy is that undifferentiated cells, following delivery to the injured host and migration to the site of injury, will, under the influence of local signals, differentiate to cells of the appropriate phenotype. These differentiated cells then contribute to the repair of the injured tissue. There is evidence to indicate that this is the case, but little or no data concerning the specific signals that give rise to differentiation in situ. For instance, cells implanted in an osseus defect, such as a large segmental gap in the femur, stimulate formation of new bone that con be assessed both radiologically and histologically (Bruder, 1998).

Therapeutic callenges

Considering together regenerative potential and immunoregulatory effect of MSCs, it is easy to imagine what powerful tool for the therapy these cells may become in degenerative and inflammatory diseases.

Although early pre-clinical data demonstrate the safety and effectiveness of MSC therapy there are still many questions to be answered surrounding the mechanism of action. Additional information is required concerning the therapeutic efficacy of transplanted cells and the mechanisms of engraftment, homing and in vivo differentiation. There is also a need to carry out appropriately designed toxicology studies to demonstrate the long-term safety of these therapies. The widespread use of

stem cell therapy will also depend upon the availability of validated methods for large-scale cultures, storage and distribution. However, the reconstruction of any tissue requires not only repairing cells, but also adequate scaffolds where the implanted MSCs can proliferate and interact with specific growth factors and cytokines. There is a need for novel engineered devices for tissue-specific delivery of cells. Thus, regenerative medicine has become discipline that joins cell biology, tissue engineering and surgery to renew tissues with vital cells, bio-matrices and signalling molecules (Dominici M, 2001; Tuan RS, 2003).

1.2.11 *ah*MSCs AND BONE REGENERATIVE MEDICINE

On the basis of in vitro observation that *ah*MSCs can differentiate into osteocytes and chondrocytes, many attempts have been made to use expanded *ah*MSCs for in vitro tissue repair (Fibbe WE, 2002; Long MW, 2001; Barry FP, 1997).

Bone tissue engineering is an emerging interdisciplinary field that combines the principles of biology and engineering. This is a new approach for bone regeneration and endeavours to repair large bone losses using biomaterials to deliver stem cells to the defective site. These stem cells can be induced to differentiate into osteoblasts by the proper local conditions encountered in the defective site and also by the release of a set of specific ions by the biomaterials used as scaffolds (Ferguson, 1999). This form of therapy differ from standard drug therapy or permanent implants in that the engineered bone becomes integrated within the patient, affording a potentially permanent and specific cure of the disease state.

Bone marrow-derived *ah*MSCs have been seeded on extracellular matrices such as hydroxyapatite and then implanted in vivo into various animal models to repair segmental bone defects of critical size, subsequently observing bone formation (Krebsbach PH, 1997; Kon, 2000; Petite, 2000). Normal marrow-derived stromal cells have been also infused into animals or children with osteogenesis imperfecta (Horwitz EM, 1999; Pereira, 1995).

Particularly promising for orthopedic applications, especially for bone formation, is the use of natural or synthetic biomaterials as carriers for MSCs delivery (Cancedda

R, 2003). Recent advances in the field of biomaterials have determined a transition from the use of non-porous, biologically inert materials (i.e. ceramics or titanium) to porous, resorbable and osteoconductive biomaterials (i.e. hydroxyapatite and tricalcium phosphate) (Rose, 2002; Vats 2003). Cell-matrix composites, made of hydroxyapatite/tricalcium phosphate ceramics loaded with autologous MSCs expanded in vitro, have been successfully used in vivo, leading to resolution of critical segmental bone defects that had been not healed by resident cells or the addition of the osteoconductive device alone (Bruder, 1997). A number of clinical studies have shown the efficacy of this approach in humans. Porous ceramic scaffolds loaded with in vitro expanded autologous bone-marrow-derived *ah*MSCs were successfully implanted in 3 patients with large bone defects (Quarto R, 2001). More recently, an extended mandible discontinuity was successfully repaired through a heterotopic bone induction with biomaterials, patient's bone marrow and growth factors (Warnke PH, 2004). Consequently, an efficient approach to repair bone defects seems to be the local implantation of porous cell-matrix composites loaded with autologous bone marrow *ah*MSCs, previously collected from the patient and expanded in vitro under stringent culture conditions (Europ Commission-Health, 2004).

There are at least three different modes that have been studied for using stem cells in scaffolds. Cells can be loaded into the scaffolds *in vitro* and, after a short incubation to ensure attachment, the cell-scaffold composites can be implanted in the patient. Second, the cell-scaffold composite is incubated in differentiation media to stimulate stem cell progression into the osteoblastic lineage, and than the composite is implanted into the defective site. The last approach is to implant scaffolds functionalized with factors that facilitate regenerative cells recruitment at the defective site (Caplan, 2007).

Conclusions and future perspectives of bone regeneration therapies

The knowledge of the biology and the potential clinical use of MSCs have dramatically improved in the last few years. On the basis of in vitro evidence of MSC multilineage differentiation, most experiments with engineering have been carried out with small size defects. However, human defects are normally larger and

more complicated, thus requiring larger repair tissues and structural and mechanical properties similar to human normal tissues. For this reason, bioreactors have been developed in the last few years. Within the bioreactor, cells are continuously loaded into the scaffold and nutrients dynamically provided through the cell-scaffold composite. Moreover, bioreactors can also expose forming tissue to specific physical stimuli that may improve tissue growth and maturation (Cancedda R, 2003). In the next future, the ex vivo formation of complex tridimentional hybrid tissues (i.e. joint cartilage with subchondral bone and integrated vascular access for implantation) would revolutionize the treatment of damaged skeletal tissue.

1.3 BIOMATERIALS

In the last few years the biomedical research area is going towards materials science aiming applications of materials to health care, the so-called biomaterials. They can be defined as implantable materials that must be in contact with living tissues with the final aim of achieving a correct biological interaction between the material and the host (Vallet-Regí M, 2008). In the first Consensus Conference of the European Society for Biomaterials (ESB) in 1976, a biomaterial was defined as "a nonviable material used in a medical device, intended to interact with biological systems"; however the ESB's current definition is a "material intended to interface with biological systems to evaluate, treat, augment or replace any tissue, organ or function of the body". This subtle change in definition is indicative of how the field of biomaterials has evolved. Biomaterials have moved from merely interacting with the body to influencing biological processes toward the goal of tissue regeneration. However, a more recent definition has been published: "*a biomaterial is a substance that has been engineered to take a form which, alone or as part of a complex system, is used to direct, by control of interactions with components of living systems, the course of any therapeutic or diagnostic procedure, in human or veterinary medicine* (Williams DF, 2009).

Different types of materials can be found depending on the function to perform or the tissue to be replaced (Vallet-Regí M and Ruiz-Hernández E, 2011).

When trying to understand the evolution of biomaterials research and their clinical availability during the last 60 years, three different generations seem to be clearly marked (Hench and Polak 2002): bioinert materials (first generation), bioactive and biodegradable materials (second generation), and materials designed to stimulate specific cellular responses at the molecular level (third generation). These three generations should not be interpreted as chronological, but conceptual, since each generation represents an evolution on the requirements and properties of the materials involved. This means that at present, research and development is still devoted to biomaterials that, according to their properties, could be considered to be of the first or the second generation. The materials that each new generation brings in do not necessarily override the use of those of a previous one (Navarro M, 2008).

First generation

In engineering design, the selection of a material for a specific application is governed by matching the material properties with the requirements of this application. In the case of biomaterials, biological requirements have to be added to the common ones (mechanical, chemical and physical). Consequently, concepts such as foreign body reaction (particularly due to wear debris), stress shielding, biocompatibility, and, more recently, bioactivity and osteoinduction have been gradually introduced as requirements for biomaterials in the design of implantable devices. When synthetic materials were first used in biomedical applications, the only requirement was to 'achieve a suitable combination of physical properties to match those of the replaced tissue with a minimal toxic response of the host' (Hench 1980). They were the 'first-generation biomaterials', according to Hench's classification, because they were 'inert' so as to reduce the immune response and the foreign body reaction to a minimum.

Second generation

The second generation of biomaterials should be considered to have appeared between 1980 and 2000, and was defined by the development of bioactive materials' ability to interact with the biological environment to enhance the biological response and the tissue/surface bonding, as well as by the development of bioabsorbable materials' ability to undergo a progressive degradation while new tissue regenerates and heals. Bioactivity refers to any interaction or effect that materials exert on cells with the aim of leading or activating them to specific responses and behaviours. Mineralization and binding between the bone tissue and the implant is one of the most currently known processes to increase bioactivity in bone repair and fixation applications. Bioactive biomaterials designed for bone fixation, repair and regeneration led to the in vivo deposition of a layer of HA at the material surface. By the mid-1980s, these bioactive materials had reached clinical use in a variety of orthopaedic and dental applications, including several bioactive glasses (BGs), ceramics, glass–ceramics and composites.

Third generation

The third-generation biomaterials are meant to be new materials that are able to stimulate specific cellular responses at the molecular level (Hench & Polak 2002). For these biomaterials, the bioactivity and biodegradability concepts are combined, and bioabsorbable materials become bioactive and vice versa. These materials' properties should merge with their ability to signal and stimulate specific cellular activity and behaviour. Temporary three-dimensional porous structures that stimulate cells' invasion, attachment and proliferation, as well as functionalized surfaces with peptide sequences that mimic the ECM components so as to trigger specific cell responses are being developed (Hutmacher et al. 2000; Temenoff & Mikos 2000; Agrawal & Ray 2001). Deliveries of biochemical factors and medical drugs, as well as control of cell behaviour through mechanotransduction are some fields of interest.

1.4 BIOCERAMICS

Bioceramics are those engineered materials that find their applications in the field of medicine (Williams FD, 1987). Traditionally, the brittleness, the low mechanical fracture toughness and the low resistance to the impact have limited the applications of the ceramic materials. Nevertheless, a strong interest in the use of ceramics for biomedical engineering applications were developed at the end of the years sixty. New ceramics, with very improved properties, contributed to increase the possibilities of using ceramics in biomedicine and their use has extended considerably since then (Schackelford JF, 1999; Dubok VA, 2000). The great chemical inertia of the ceramics, their high compression strength and their aesthetic appearance, made that these materials began to be used in dentistry, mainly in dental crowns. Later their use extended to orthopaedic applications (Vallet-Regí M, 2001; Williams DF, 1985; Hulbert SF, 1987). Used initially as alternatives to metallic materials in order to increase the biocompatibility of implants, bioceramics can be classified from different points of views (Hench LL, 1991; Hulbert SF, 1983):

(a) According to the type of answer of the living host

(b) According to the application to which they are destined (Hench LL, 1975 Ann Rev Mater Sci)

(c) According to the characteristics of the material (De Groot K, 1991)
However, in this review, the classification, according to the answer of the living host, is going to be followed, because it is considered more in accordance with the application of the bioceramic materials. Then, according with this, bioceramics can be divided in Bioinert; Bioactive or Surface Reactive and Biodegradable or Resorbable Materials.

Bioinert

Relatively Bioinert ceramics undergo little or no Chemicals changes when they are exposed to physiological environments. They maintain their physical and mechanical properties while in the host. The answer of the host to these bioceramics is the formation of a very fine fibrous tissue capsule of varying thickness, several micrometers or less, that surround implant materials. The fixation of implants in the body is made through a strong mechanical interlocking, by tissue ingrowth into undulating surfaces (Hayashi K, 1992). When high strength is required, the bond is made by perforations in the implants using threads, cements, etc. When so high strength are not required can be used porous inert bioceramics, with sizes of pore between 100 and 150 μm, which guarantee the growth of the tissue towards within implants assuring its fixation (Hulbert SF, 1970; De Groot K, 1988; Cheung HS, 1989). Typical examples of these bioinert ceramics are: Alumina (α-Al_2O_3); Zirconia (ZrO_2), Alumina-Zirconia and Pyrolytic Carbon.

Bioactive

Generally, when an artificial material is implanted in the body, it is encapsulated by uncalcified fibrous tissue that isolates it from the surrounding. This is a normal reaction intended to protect the body from foreign substances. However, in the early 1970s, Hench et al. (Hench LL,1971) found that a glass, called Bioglass®; of the complex system Na2O-CaOSiO2-P2O5, induced the formation of no fibrous tissue, but rather came into direct contact with the surrounding bone and formed a tight chemical bond with it. Since then, other types of glasses and glass-ceramics have also been found to bind to living bone (Blenke BA, 1973; Kokubo T, 1993; Berger G 1989), Hench et al.(Hench LL,1981; Hench LL, 1978), Gross et al. (Gross UM,

1993; Gross UM, 1982), Karlon et al. (Karlsson KH, 1989; Anderson OH, 1990) and Kokubo et al. (Kokubo T, 1993; Kokubo T, 1986). These bone-binding materials are called bioactives materials. The appearance of this type of bioceramics born of the need to eliminate the interfacial movement that takes place with the implantation of bioinert ceramics. Consequently, L. L. Hench proposes in 1967 to the U.S.A. Army Medical Research and Development Command, a research based on the modification of the Chemicals composition of ceramics, and glasses so that they have chemical reactivity with the physiological system and form chemical bond between the surfaces of implant materials and the adjacent tissue. Upon implantation in the host, bioactive ceramics form a strong bond with adjacent tissue. Except hydroxyapatite, which bond directly to living bone, the rest of bioactive materials bond to bone through a carbohydroxyapatite layer (CHA) biologically active, which provides the interfacial union with the host. This phase is chemical and structurally equivalent to the mineral phase of the bone, and the responsible of the interfacial union. The interface of union between bioactive materials and tissue is usually extremely strong. In many cases, the interfacial strength of adhesion is equivalent to or greater than the cohesive strength of the implant material or the tissue bonded to the bioactive implant. Generally, the break takes place in the implant or in the bone but almost never in the interface (Hench LL, 1984; Hench LL, 1988; Gross U, 1988). However, not only certain types of glasses and glassceramics are bioactives. Other ceramic materials "sensus stricto" are also bioactives. The typical example is the hydroxyapatite, which is the only one that bond directly to bone and other examples are: certain silicates (diopside and wollastonite) and a new group of ceramic materials denominated Bioeutéctics®, as it will be exposed next.

Biodegradable or resorbable

The resorbable ceramics began to be used in 1969. These types of bioceramics are dissolved with time and are gradually replaced by natural tissues. A very thin or non-existent interfacial thickness is the final results. They would be the ideals implants, since only remain in the body while their function is necessary and disappear as the tissue regenerates. Their greater disadvantage is that their mechanical strength diminishes during the reabsorption process. Consequently, the function of these

materials is to participate in the dynamic process of formation and reabsorption that takes place in bone tissues; so they are used like scaffolding or filling spaces allowing to the tissues their infiltration and substitution (Neo M, 1992). All the resorbable ceramics, except plaster ($CaSO_4^{½}H_2O$), are based on calcium phosphates, varying their biodegradability in the sense: α-TCP > β-TCP >>>> HA

The biodegradation rate is increased, as it is logical, as: a) specific surface increases (powders are more quickly biodegraded that porous solids and these more quickly than dense solids); b) when crystallinity decreases; c) when grain and crystal size decrease; d) when e.g. there are ionic substitutions of CO_3^{--}, Mg^{++} and Sr^{++} in HA.

The factors that tend to decrease the rate of biodegradation include e.g.: a) F^- substitution F^- in HA; b) Mg^{++} substitution in β - TCP and c) lower β - TCP/HA ratios in biphasic compounds. The biodegradation or reabsorption of calcium phosphates is caused by three factors:

1) Physiochemical dissolution, which depends on the solubility product of the material and local pH of its environment. New phases may be formed, such as amorphous calcium phosphates, dicalcium phosphate dihydrate, octacalcium phosphate, and anionic substituted HA.

2) Preferential attack of the grain boundaries and physical disintegration in small particles.

3) Biological factors, such as phagocytosis, which causes a decrease in local pH concentration, the cellular activity and the site of implantation. One of the few bioceramics that satisfy partially these requirements is the tricalcium phosphate (TCP).

1.5 Si SOSTITUTION IN CALCIUM-PHOSPHATE BIOCERAMICS

Due to the high demand for synthetic biomaterials to assist and replace skeletal tissues, and the high failure rate of these medical implants, a great deal of research focuses on improving the strength of the implant–tissue interface, and in the design of implants that degrade in concert with the natural healing process (Driessens F, 1990).

In 1970, Carlisle (Carlisle EM, 1970) suggested that ‘‘Silicon may be allied to the initiation of mineralization of preosseous tissues’’. Since then, numerous articles have confirmed the metabolic effect of Si on bone (Pietak AM, 2007), so it can be considered as an accepted fact. The positive effect of Si on bone metabolism has raised the interest of research groups working on Si-containing bone graft substitutes, in particular those working with bioglass (Hench LL, 2004). In the 1990’s, researchers started making efforts to develop Silicon substituted calcium phosphates (also named ‘‘silicated calcium phosphate’’ and ‘‘silicate-substituted calcium phosphate’’) (Gibson IR, 1999; Langraff S, 1999; Ruys AJ, 1993).

It is not surprising that bioceramics that incorporate Si into their composition realize higher bioactivity. These include materials with very high Si levels such as Bioglass (Hench LL, 1991) and Pseudowollastonite (CaSiO3) (R.G. Carrodeguas, 2008; Piedad De Aza, Bol. Soc. Esp. Ceram. Vidr. 2005) as well as CaP-based materials with trace levels of Si doping such as hydroxyapatite (Si-HA) and tricalcium phosphate (Si TCP) (J.W. Reid, 2006; J.W. Reid, 2008). Thus apatite ceramics containing Si are expected to be useful as biodegradable biomaterials to increase the speed of bony regeneration (A.E. Porter, 2003; A.M. Minarelli-Gaspar, 2009). Hydroxyapatite (HA) has been used for many years as bone repairing material. Recently, many attempts to introduce Silicon into its network as a way to improve the bioactivity level of the material has been carried out. However, HA is the less soluble of all calcium phosphates and less reactive. HA is denser and more packed of all calcium phosphates of biological relevance. On the other hand, tricalcium phosphate (TCP) is more soluble and biodegradable than HA, and is expected that Si ions occupying P sites in TCP network are more labile than in the HA network as well.

Martinez et al. demonstrate that silicon substitute TCP (Si-TCP) promotes the formation of a carbo-hydroxyapatite type B precipitate and increases the reactivity of the materials, enhancing the formation of the interface between the ceramic and the media, possibly contributing to quick bonding of the material to the bone in vivo and promoting bone regeneration. Also confirm that (Si-TCP) promotes cellular

proliferation and differentiation to osteoblasts. (Martinez IM, Velásquez PN, De Aza PN.)

Implanted bioactive ceramics materials interact with the body, and the main reactions mainly take place on the surface of the material, leaving the remaining bulk material unchanged, which usually leads to a harmful shear stress. To make possible the ingrowth of new bone into implants, the materials must present appropriate interconnected porous structure (Hench LL, 1998, Bioceramics). Bearing in mind the lack of mechanical properties of the porous biomaterials and the difficulties to react of the bulk implant, the idea of a dense well-structured biphasic material to overcome both problems has been developed. The material would consist of a bioactive phase, which is easily dissolved obtaining the interconnected structure; and another resorbable phase, which maintains the mechanical properties during the resorptio and slowly releases Ca, P, and Si ions to the environment for new bone formation (De Aza PN, 1997; De Aza PN, 1998; De Aza AH, 2007; De Aza PN, 2000). Considering this a new biphasic material is proposed, which is composed of a resorbable and osteoconductive phase (TCP) and another bioactive phase that is a silico-phosphate.

The present work focused on the system $2CaO{\cdot}SiO_2$ – $3CaO{\cdot}P_2O_5$ (C_2S-TCP) in order to obtain and characterize eutectoids materials.

Tricalcium Phosphate

TCP is one of the most important biomaterials based on phosphates, currently recognized as ceramic material, that significantly simulates the mineralogical structure of bone (Albee F, 1920; Hench LL., 1998; De Aza PN, 2007; Roy S, 2008). TCP is more soluble and biodegradable than HA because less dense and packed, is the pre-eminently biodegradable phosphate. TCP has three polymorphic forms, β, α and α′. The latter is of no interest because it transforms into the α form during cooling. β-TCP is stable at room temperature and reconstructively transforms to 1125 °C into α-TCP, which is metastably retained until room temperature during the cooling (Trömel G., 1932; Welch JH, 1961; Carrodeguas RG, 2010). TCP ceramics implanted *in vivo* are non toxic, antigenically inactive, not carcinogenic and bound directly to the bone without intervening connective tissue. So TCP ceramics show

good biological compatibility and osteoconductive characteristics when implanted in living tissues, for these reasons and for their mechanical characteristics are therefore used clinically for hard tissue replacement (Best SM, 2008).

Dicalcium Silicate

Dicalcium silicate exists in several polymorphic forms. The most widely known polymorphs include α', α, β, ɤ, and among them only ɤ-form is stable at room temperature without stabilizers. The β-form of dicalcium silicate is commonly found in ordinary Portland cement in association with stabilizing ions, refractories and heat-resistant coatings. (Ghosh SN, …)

Recent studies have shown that Ca2S as the potential to be used as biomaterial. Ceramics of C2S are found to support mesenchymal stem cell adhesion and spreading, and the cells establish close contacts with the ceramics after 1 day in culture. These findings indicate that Ca2S ceramics possesses good biocompatibility and mechanical properties, and might be a promising bone implant material (Liu X, Morra M., 2008)

Ca2S can spontaneously bond to living bone, without forming a fibrous tissue around them, due to the formation of a bone-like apatite layer on their surface. Liu X et al. (Liu X, 2005) demonstrate the formation of an apatite layer after 24 h immersion of Ca2S ceramics in SBF, indicting excellent bioactivity.

1.6 IONS

1.6.1 INORGANIC PHOSPHATE (P_i)

Like explained in the bone general description, bone is the main reservoir for calcium and phosphate, with 99% of calcium and 85% of phosphate being stored in the skeleton. Their homeostasis depends not only on their absorption from the gut and its retention or excretion by the kidneys, but is tightly coupled to bone remodeling. This process requires a balance between osteoblast and osteoclast activities, leading to bone formation or bone resorption respectively. The resorption

of the bone matrix results in the dissolution of the apatitic bone mineral, which ultimately triggers a local increase in inorganic phosphate (P_i) and Ca^{++} in the vicinity of bone cells. The local increase in Pi also results from the activity of the tissue non-specific alkaline phosphatase (TNAP), an enzyme expressed during the differentiation of the osteoblastic bone-forming cells. TNAP regulates mineralization by hydrolyzing pirophosphate, a potent inhibitor of calcification, which in turn leads to the production of the mineralization promoter P_i (Terkeltaub RA. et al., 2001). The increase Pi resulting from the TNAP activity and bone remodeling is believed to act as a specific signal for skeletal cells affacting different genes expresión (Bellow CG et al., 1991) and various functions such as proliferation (Kanatani M et al., 2002), differentiation (Beck GR et al., 2000), mineralization (Julien M et al., 2007), or apoptosis (Magne D et al., 2003).

Khoshniat S et al. and others (Beck GR, 2000; Julien M, 2007), have recently shown that extracellular Pi regulates expresión of the mineralization-associated genes osteopontin (OPN) and matrix gla protein (MGP) through the ERK1/2 pathway (Khoshniat S et al., 2011).

1.6.2 SILICON

Carlisle (Carlisle EM, 1972) demonstrated that silicon is an essential mineral for growth and skeletal development and a Si-deficient diet causes significantly diminished weight gain, cartilage and bone development.

The primary effect of Si in bone and cartilage is thought to be associated with matrix synthesis, although its influence on calcification may be an indirect phemomenon through its effect on matrix components (Seaborn CD et al., 2002). Silicon has been found to promote colI synthesis, enhance osteoblast differentiation (Reffitt DM et al., 2003) and prevent poor host bone metabolism in defect repair (Hing K et al., 2006).

Reffitt et al. propose a possible function of Si as a cofactor of prolyl-hydroxylase enzyme, which hydrolyzes the proline residues of collagen pro-α chains, and so fundamental for the collagen synthesis. It has also been proposed that Si binds endogenous toxic metals such as aluminium, thus leading to optimal enzyme activity. Si is also known to bind to glycosaminoglycans macromolecules, such as heparan

sulfate, playing an important role in the formation of cross-links between collagen and proteoglycans resulting in the stabilizing of the bone matrix molecules and preventing their enzymatic degradation (Schwarz KA, 1973).

1.6.3 CALCIUM

While Ca^{++} is a divalent cation used by cells as a second messenger to control a great variety of cellular processes, it is also well acknowledged as a specific extracellular signal able to regulate proliferation, activity and differentiation of skeletal cells (Dvorak MM et al., 2004). Ca^{++} acts through binding to a G-protein coupled extracellular calcium sensing receptor, activating the ERK 1/2 pathway and inducing the expression of osteoblast differentiation markers as RUNX2, ALP, COlI, OPN, BSP, OSC, and stimulates the formation of mineralized nodules (Khoshniat, 2011).

Calcium ions (Ca^{++}) serve as an important regulator of a variety of physiologic and cellular processes. The intracellular free Ca^{++} concentration (Ca^{++}_i), which undergoes large transient changes upon cellular stimulation, plays a major role in signal transduction, exocytosis, cell migration, and cell differentiation (Pietrobon D, Di Virgilio F, PozzanT. Structural and functional aspects of calcium homeostasis in eukaryotic cells. Eur J Biocem 193: 599-622, 1990). The extracellular free calcium concentration (ca++e) in contrast, is maintained within a narrow physiological range and is crucial for a spectrum of physiological phenomena, including blood coagulation, neurotransmitter release and maintenance of skeletal integrity (Brown EM. Extracellular Ca++ sensing, regulation of pharathyroid cell function, and role of Ca++ and other ions as extracellular (first) messenger. Physiol Rev 71: 371-411, 1991).

Extracellular Ca++ homeostasis is accomplished by the regulation of Ca++ absorption from the gastrointestinal tract, Ca++ excretion by the kidney, and Ca++ deposition and/or mobilization from mineralized bone. The regulation of Ca++e is contributed to by an intricate system of calcium sensing cells that respond to minute fluctuations in Ca++e (Brown EM, 1990). House et al. (House MG, Kohlmeier L, Chattopadhyay N, Kifor O, Yamaguchi T, Leboff MS, Glowacki J, Brown EM.

Expression of an extracellular calcium-sensing receptor (CaR) in human and mouse bone marrow cells. J of Bone and Min Res 12:1959-1970, 1997) with their studies indicate that the calcium-sensing receptor is present in low-density mononuclear bone marrow cells as well as in cells of several hematopoietic lineages and could potentially play a role in controlling the functions of various cell types within the marrow space.

CaR is also present in osteoblasts (Chang W, Tu C, Chen TH, Komuves L, Oda Y, Pratt SA, Miller S, Shoback D. … Endocrinology 140: 5883-5893, 1999), but its functional role is still debated, if CaR is a true regulator of bone function or whether its expression is vestigial (Raisz LG. J Clin Invest 111: 945-947, 2003). Dvorak MM et al. (Dvorak MM, 2004) show that osteoblasts sense and respond to extracellular free ionized calcium concentrations (Ca^{++}_o) (accompanying bone remodeling) independently of systemic calciotropic factors in a time- and concentration-dependent manner. The local fluctuation of Ca^{++}_o may therefore regulate osteoblasts activity during both Ca^{++} load and buffering by bone, where the cells are exposed to large increases in Ca^{++}_o, and remodeling, when the local elevation in Ca^{++}_o are more moderate. Dvorak et al in this study demonstrate that Ca^{++}_o ,most likely acting through the CaR, is a key regulator of osteoblasts cell fate (expression of the osteoblast differentiation markers ostoeclacin, osteopontin and ColI mRNAs was increased by Ca^{++}_o , when Ca^{++} concentration in the medium was duplicated, as was mineralized nodule formation and ALP activity.

1.6.4 CALCIUM-PHOSPHATES PRECIPITATES

There are some evidences in which it seems that the cell must balance the calcium-to-phosphate ratio to avoid apoptosis and that calcium is necessary to modulate phosphate action. The hipótesis is related to the formation of calcium phosphate precipitates that occur in the concomitant presence of Ca^{++} and P_i *in vitro*. These crystals can trigger the activation of specific cellular processes like the stimulation of ERK1/2 phosphorylation that induce the expression of mineralization associated genes as osteopontin. Calcium phosphate precipitates are not endocytosed, but they

transduce their signal intracellularly, binding to specific sites on the plasma membrane that request the integrity of the lipid rafts (Khoshniat S et al., 2011).

Aims

2. AIMS

2.1. GENERAL OBJECTIVE

This work intend to evaluate the properties of three ceramic materials in the system dicalcium silicate-tricalcium phosphate, which differ for the C_2S and TCP composition percentage (EC1…., EC2 ….EC3 ….), to be considered adequate as scaffolds for bone tissue engineering, with an *in vitro* study.

2.2. SPECIFIC OBJECTIVES

3.2.1. To elaborate and set up an adequate *in vitro* experimental model that permits to study the effect of three different composition ceramics in the system dicalcium silicate-tricalcium phosphate with these composition percentages: EC1 , EC2 , EC3 , on ahMSCs responses.

3.2.2. The Isolation, characterization and establishment of an ahMSCs line.

3.2.3. To study with quantitative methods, proliferation kynetics/rate of the ahMSCs seeded on the three ceramics EC1, EC2, EC3.

3.2.4. To study the biocompatibility level of the three ceramics EC1, EC2, EC3.

3.2.5. To determine osteoinductive influence of these three materials (EC1, EC2, EC3) upon *ah*MSCs, studing their osteoblastic differentiation.

3.2.6. To analyse the dinamic characteristics of the EC1, EC2, and EC3 materials surface, after immersion in basal growth medium.

3.2.7. Evaluate if there is a coorelation between the ionic concentrations present in the culture medium after materials soaking, and the behaviour of *ah*MSCs seeded in the same well of the materials or on EC1, EC2 and EC3 pieces.

We expect to (pretendemos), determine the utility of the methodology used in this research work, to use it in the future as an in Vitro model that permits análisis of specific parameters of the *ah*MSCs behaviour and activity as a consequence of cells culture in presence of eutectoids matherials of different compositions like. EC1, EC2 and EC3.

Materials and Methods

3. MATERIALS AND METHODS

3.1 MATERIAL SYNTHERING

The raw materials for the present study were C_2S and TCP previously synthesized. C_2S and TCP were synthesized using solid state reaction made by Isabel Maria Martínez Pérez PhD. from the Miguel Hernandez University ("Bioceramics in the sub-system α-tricalcium phosphate-silicocarnotite. *In vitro* and *in vivo* characterization", 2011).

Mixtures with compositions show in table … were selected and prepared bearing in mind the phase equilibra diagram of C_2S and TCP. (Nurse, 1959; Virtudes The system Ca3….2011; Matinez I, 2012).

The three materials were synthesized in the Biomaterials Unit of UMH.

Composition

The three biomaterials tested in this work (EC1, EC2, EC3) are ceramics composed of α-tricalcium phosphate (TCP), which chemical formula is $Ca_3(PO_4)$, doped with different amounts of dicalcium silicate (C_2S), which formula is Ca_2SiO_4. They are prepared by solid state reaction, at high temperature and slowly cooled to room temperature. This system was chosen because the TCP is a widely used biomaterial due to its bioactivity, biocompatibility, osteoconductivity and osteoinductivity (Hench LL, 1991). Moreover the silicon or silicate addition to calcium phosphates have demonstrated to promote osteogenesis and to enhance the in vivo material behaviour (See below).

	Wt% TCP	Wt% C_2S
EC 1	31	69
EC 2	55	45
EC 3	83	17

Table 2: Weight percent of TCP and C_2S of the ECs coating by addition of some undissolvable components or in association with materials with strong mechanical properties (9).

Matherials pieces production

They are round-shaped and used as pieces of two sizes: 7 mm in diameter and 3 mm in thickness and 2.4 cm in diameter and 2 mm in thickness.

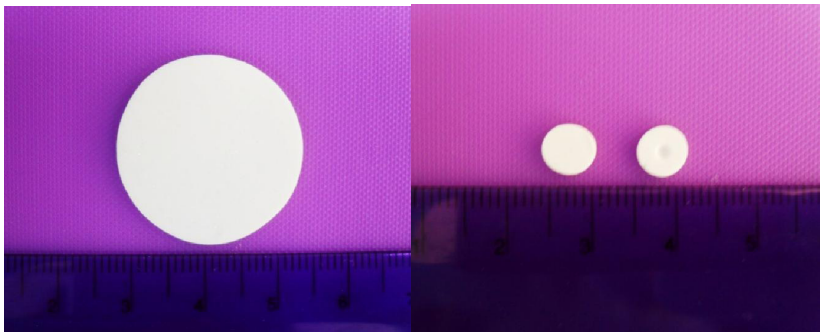

Fig. 16: EC materials: a) 2.4 cm diameter, 2mm thickness b) 7 mm diameter, 3 mm thickness.

3.2 PREVIOUS MATERIALS CHARACTERIZATION

Surface characterization. EC1, EC2, EC3 materials were characterized just after synthesis by SEM microscopy, to characterize materials surface.

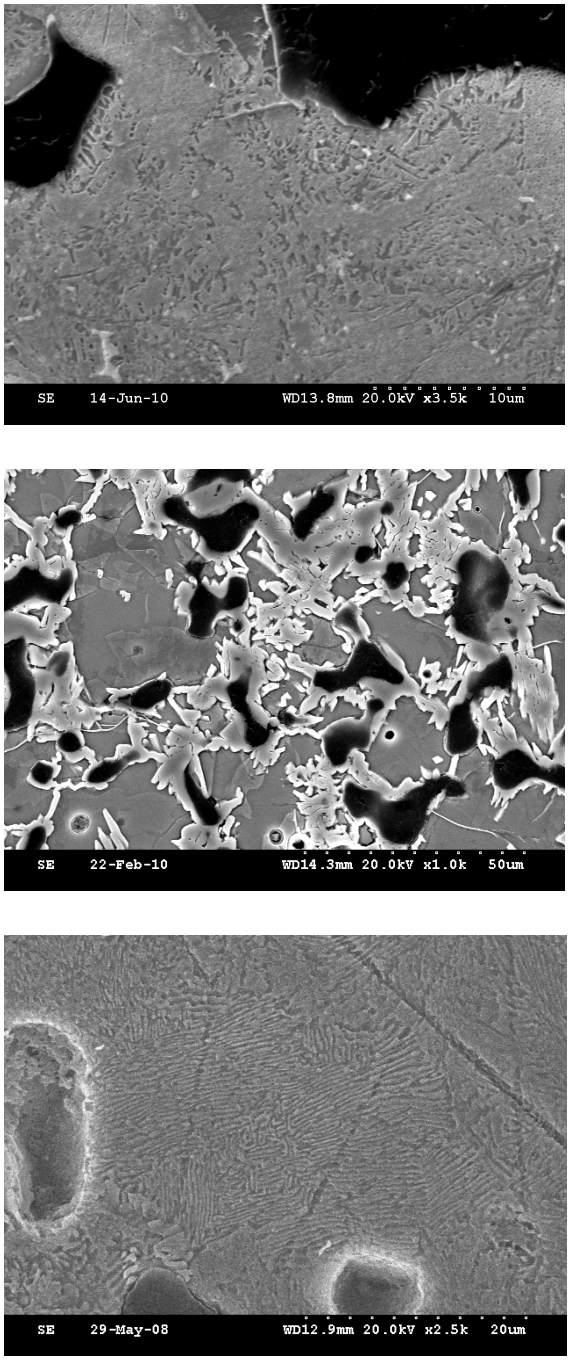

Fig. 17: SEM images of EC1, EC2, EC3 (from the top respectively) materials. Images show differences in the aspect of the surface of the three materials.

Confirmation of the materials bioactivity

Bioactivity was proved after materials synthesis for the same laboratory that synthesized the materials, by Simulated Body Fluid immersion (by the productor).

3.3 THE CELLS: CELLS ISOLATION AND PROPAGATION

What is a cell culture

Cell culture refers to the removal of cells from an animal or plant and their subsequent growth in a favorable artificial environment. The cells may be removed from the tissue directly and disaggregated by enzymatic or mechanical means before cultivation, or they may be derived from a cell line or cell strain that has already been established.

Primary culture refers to the stage of the culture after the cells are isolated from the tissue and proliferated under the appropriate conditions until they occupy all of the available substrate (i.e., reach confluence). At this stage, the cells have to be subcultured (i.e., passaged) by transferring them to a new vessel with fresh growth medium to provide more room for continued growth.

Cell Strain. If a subpopulation of a cell line is positively selected from the culture by cloning or some other method, this cell line becomes a **cell strain**. A cell strain often acquires additional genetic changes subsequent to the initiation of the parent line.

Cell line. After the first subculture, the primary culture becomes known as a cell line or subclone. Cell lines derived from primary cultures have a limited life span (i.e., they are finite; see below), and as they are passaged, cells with the highest growth capacity predominate, resulting in a degree of genotypic and phenotypic uniformity in the population.

Finite vs continue cell line. Normal cells usually divide only a limited number of times before losing their ability to proliferate, which is a genetically determined event known as senescence; these cell lines are known as finite. However, some cell lines become immortal through a process called transformation, which can occur spontaneously or can be chemically or virally induced. When a finite cell line

undergoes transformation and acquires the ability to divide indefinitely, it becomes a continuous cell line.

Culture conditions

Culture conditions vary widely for each cell type, but the artificial environment in which the cells are cultured invariably consists of a suitable vessel containing the following:

- a substrate or medium that supplies the essential nutrients (amino acids, carbohydrates, vitamins, minerals)
- growth factors
- hormones
- gases (O_2, CO_2)
- a regulated physico-chemical environment (pH, osmotic pressure, temperature)

Most cells are anchorage-dependent and must be cultured while attached to a solid or semi-solid substrate (adherent or monolayer culture), while others can be grown floating in the culture medium (suspension culture).

3.3.1 ISOLATION OF HUMAN BONE MARROW MESENCHYMAL STEM CELLS

Bone marrow was aspirated under local anesthesia at the iliac crest a*h*MSCs were isolated from bone marrow obtained by percutaneous direct aspiration from iliac crest of three male human volunteers (50 ml/patient) in good physical condition ranging from 27 to 35 years old, who were undergoing elective surgery for slipped disc and a vascular necrosis of the femoral head as result of posterior dislocation. The volunteers signed previously an informed consent. The study was approved by the ethics and clinical trials committee of our institution (University Hospital V. Arrixaca, Murcia).

Bone marrow aspirate was conserved in the siringe used for the aspiration and containing sodium heparin (20 U/ml of aspirated material). Mononuclear cells were separated by Ficoll density gradient through a SEPAX™ System device (Biosafe, Eysines, Switzerland), from the entire bone marrow aspirate.
The SEPAX™ system is a modern cell separation device for fast and automated processing of blood and bone marrow aspirates. It extracts from the sample in succession are: plasma, buffy coat and red blood cells, and separates them in different chambers. The buffy coat, containing the mononuclear cells, was than used to obtain a primary culture of bone marrow adherent mesenchymal stem cells.

Primary culture of hMSCs

Procedure:

- Centrifuge the bone marrow samples processed by SEPAX™ System at 1000 rpm for 10 minutes at 20°C and discard the supernatant.
- Resuspend the cell pellet in a minimal volume of complete culture medium and, under sterile conditions, remove 100-200µl of cell suspension.

For the majority of manipulations using cell cultures, such as transfections, cell fusion techniques, cryopreservation and subculture routines it is necessary to quantify the number of cells prior to use. Using a consistent number of cells will maintain optimum growth and also help to standardise procedures using cell cultures. This in turn gives results with better reproducibility.

- Add an equal volume of Trypan Blue (prepare a 0.4% solution of trypan blue in buffered isotonic salt solution, pH 7.2 to 7.3, i.e. DPBS) (dilution factor =2) and mix by gentle pipetting. Trypan blue is a diazo dye used to selectively stain dead cells. Since cells are very selective in the compounds that pass through the membrane, in a viable cell trypan blue can't enter, however it pass the membrane in a dead cell. Hence, dead cells are shown as a distinctive blue colour under a microscope.
- Clean the Neubauer chamber.
- Moisten the coverslip with water or exhaled breath. Slide the coverslip over the chamber back and forth using slight pressure. Fill both sides of the chamber with cell suspension (approximately 10 µl) and view under an inverted phase contrast microscope using x20 magnification.
- Count the number of viable (seen as bright cells) and non-viable cells (stained blue) over the large squares. Note the number of cells per squares counted.
- Calculate the % of viable cells using the formula below:

% viable cells = [1.00 – (Number of blue cells ÷ Number of total cells)] × 100

- Calculate the concentration of viable and non-viable cells and the percentage of viable cells using the equations below:

[(N tot cells/2)/4]x ml of suspension x 10000 x trypan blue dilution factor

- Dilute the cell suspension to have 1 million cells/mL
- Seed 3000 cell/cm² in cultures flasks (225.000 cells per 75 cm^2 flask)

- Add the appropriate volume of complete growth medium and incubate at 37º C in a 7.5% CO□ atmosphere and 95% of relative humidity.
- Change the growth medium every three days.

Isolation and primary culture of human osteoblasts

Human osteoblasts (OBs) were isolated from a*h*MSCs bone from iliac crest of three male human volunteers (50 ml/patient) in good physical condition ranging from 27 to 35 years old, who were undergoing elective surgery for slipped disc and a vascular necrosis of the femoral head as result of posterior dislocation.

When fragments of spongeous bone are placed in culture, osteoblats migrate out from the explants, adhere to the plastic surface of the flask, proliferate and grow in monolayer forming nodules of calcium deposits.

Procedure:

- ✓ Remove fragments of spongeus bone of approximately 1-2 mm x1-2 mm, put them in a Falcon tube and washe three times in Dulbecco's Phosphate Buffered Saline (DPBS), containing no calcium, magnesium, or phenol red (DPBS) supplemented with routine antibiotics: 1% penicillin/streptomycin and amphotericinB.
- ✓ Incubate twice the bone fragments for 15 minutes at 37°C with type XI Collagenase (Sigma) prepared to 1,25 mg/mL in DPBS (A).
- ✓ Place the fragments in culture flasks or Petri dishes and add complete growth medium.
- ✓ Incubate at 37ºC in a 7.5 Co2 atmosphere and 95% of relative humidity.
- ✓ Change the growth medium every 3 days.
- ✓ Monitor the explants in culture to observe the quantity of osteoblasts that migrate out of the explants.
- ✓ When cells reach the confluence, discard bone fragments (and subculture cells)

Subculturing and expanding of hMSCs and hOBs

Both MSCs and OBs grow in monolayer. Adherent cell lines will grow *in vitro* until they have covered the surface area available or the medium is depleted of nutrients. At this point the cell lines should be sub-cultured in order to prevent the culture dying. To subculture the cells they need to be brought into suspension. The degree of adhesion varies from cell line to cell line but in the majority of cases proteases such as trypsin, are used to release the cells from the flask by loosing cells to flasks surface bounds. Such enzymes are usually combined in solution with divalent cation chelators lsuch as EDTA (that binds calcium and magnesium ions). However, this may not be appropriate for some lines where exposure to proteases is harmful, in these cases cells should be brought into suspension mechanically with the aid of cell scrapers. In our case Trypsin with common concentrations are indicated.

Cells attach to the plate, grow up and divide until confluence. At this point, the subcultivation cycle will be repeated (A). Each cycle of subcultivation is marked with a "passage number". The passage number refers to the number of times the cell line has been re-plated and allowed to grow back to confluency. We define the first seeding $P_{0.}$

Materials:

- Media– pre-warmed to 37°C
- 70% (v/v) isopropanol in sterile water
- DPBS
- 0.25% trypsin/ 0.25% EDTA in DPBS,
- SBF
- Trypan blue and Neubauer chamber

Equipment:

- Waterbath set to 37ºC

- Microbiological safety cabinet level 2
- Incubator
- Pre-labelled flasks
- Inverted phase contrast microscope
- Centrifuge
- Haemocytometer

Procedure:

- ✓ View cultures using an inverted microscope to assess the degree of confluency and confirm the absence of bacterial and fungal contaminants.
- ✓ Remove spent medium.
- ✓ Wash the cell monolayer with DPBS using a volume equivalent to half the volume of culture medium. Repeat this wash step because these cells are known to adhere strongly. Moreover trypsin is inactivated in the presence of serum, therefore it is essential to remove all traces of serum from the culture medium by washing the monolayer of cells with PBS.
- ✓ Pipette trypsin/EDTA (previously activated during 20 minutes at 37º C) onto the washed cell monolayer using 2mL per 75cm^2 of surface area. Rotate flask to cover the monolayer with trypsin.
- ✓ Return flask to the incubator and leave for 5 minutes. Cells should only be exposed to trypsin/EDTA long enough to detach cells. Prolonged exposure could damage cell surface receptors or kill cells.
- ✓ Examine the cells using an inverted microscope to ensure that all the cells are detached (round shape) and floating. The side of the flasks may be gently tapped to release any remaining attached cells.
- ✓ Resuspend the cells in a double volume of fresh serum-containing medium (DMEM) respect to trypsin to inactivate these one. Centrifuge cells at 1000 rpm for 10 minutes at 20°C, to eliminate the trypsin.
- ✓ Remove 100-200 µl and perform a cell count (like expose previously).
- ✓ Seed 3000 cell/cm2 (if necessary centrifuge and resuspend cells 1 million/mL after counting to facilitate divide cells between new flasks) in new labelled

flasks containing pre-warmed medium, and incubate at 37ºC in a 7,5% CO2 atmosphera and 95% of relative humidity.

- ✓ Change the medium every three days.
- ✓ When the cells reach again the confluence repeat cell subculture.

Key Points:

Although most cells will detach in the presence of trypsin alone the EDTA is added to enhance the activity of the enzyme. And when the cells were cultured in presence of the materials, was necessary increase EDTA concentration (0.5%) because the highly concentrations of the calcium ions in the dissolution.

hMSCs and hOBs cryopreservation

The aim of cryopreservation is to enable stocks of cells to be stored to prevent the need to have all cell lines in culture at all times. It is invaluable when dealing with cells of limited life span. The other main advantages of cryopreservation are: to reduce risk of microbial contamination, to reduce risk of cross contamination with other cell lines, to reduce risk of genetic drift and morphological changes, permit to work using cells at a consistent passage number and to reduce costs.

The basic principle of successful cryopreservation and resuscitation is a slow freeze and quick thaw. Although the precise requirement may vary with different cell lines as a general guide cells should be cooled at a rate of –1°C to –3°C per minute (with the help of alcools like isopropanol alcool) and thawed quickly by incubation in a 37°C water bath for 3-5 minutes. Other important points that should be follow are:

1. Cultures should be in log phase of growth (this can be achieved by using pre-confluent cultures i.e. cultures that are below their maximum cell density and by changing the culture medium 24 hours before freezing).
2. A high concentration of serum (>20%) should be used.
3. Use a cryoprotectant such as dimethyl sulphoxide (DMSO) or glycerol to help protect the cells from rupture by the formation of ice crystals. The most

commonly used cryoprotectant is DMSO at a final concentration of 10%, however, this is not appropriate for all cell lines e.g. where DMSO is used to induce differentiation. In such cases an alternative such as glycerol should be used.

Following controlled rate freezing in the presence of cryoprotectants, cell lines can be cryopreserved in a suspended state for indefinite periods provided a temperature of less than -135°C is maintained.

Storage in liquid phase nitrogen allows the lowest possible storage temperature to be maintained with absolute consistency, but requires the use of large volumes (depth) of liquid nitrogen which is a potential hazard.

Freezing procedure:

- ✓ After trypsinization, count the cells using trypan blue for a viable cell count. The viability should be over 90% to ensure the cells are healthy enough for freezing.
- ✓ Dilute the cell suspension to have 2 million cells/ml.
- ✓ Place the cryovials in the isopropanol freezing box previously cooled. Isopropanol is chosen to allow gradual freezing.
- ✓ Aliquot 1 ml of cell suspension in a cryovial.
- ✓ Add 10% of DMSO. DMSO is a cryoprotective agent that reduce the freezing point of the medium and also allow a slower cooling rate, greatly reducing the risk of ice crystal formation, which cause cell damage and/or death.
- ✓ Promptly put the box at -80°C. After 24 hours the vials can be put in a storing box at -80°C, if using them in months, or kept in liquid nitrogen if need to conserve them for a longer time.

Towing rocedure:

- ✓ Prepare the flasks - label with cell line name, passage number and date.

- ✓ Collect an ampoule of cells from liquid nitrogen storage and transfer to the laboratory on dry ice. It is important to handle the ampoules with care
- ✓ Quickly transfer the ampoule to a 37°C waterbath until only one or two small ice crystals, if any, remain (1-2 minutes). It is important to thaw rapidly to minimise any damage to the cell membranes. Note: Do not totally immerse the ampoule as this may increase the risk of contamination.
- ✓ Wipe ampoule with a tissue soaked in 70% alcohol prior to opening.
- ✓ Pipette the whole content of the ampoule into a sterile tube (e.g. 15 ml capacity). Then slowly add 5ml pre-warmed medium that has already been supplemented with the appropriate constituents. Determine the viable cell density. Transfer the appropriate volume of cell suspension to a flask to achieve the cell seeding density.

For adherent cell lines: Adjust the volume of the medium, and if necessary the flask size, to achieve the cell seeding density recommended on the cell line data sheet. A pre-centrifugation step to remove cryoprotectant is not normally necessary as the first media change will remove residual cryoprotectant. If it is, then this will be specified on the data sheet. If the cells are to be used immediately (e.g. for a cell based assay), rather than subcultured, it may be advisable to perform a pre-centrifugation step to remove cryoprotectant.

Key Points:

1. Most text books recommend washing the thawed cells in media to remove the cryoprotectant. This is only necessary if the cryoprotectant is known to have an adverse effect on the particular cell type. For example, some cell types are known to differentiate in the presence of DMSO. In such cases the cells should be washed in media before being added to their fi nal culture flasks.
2. The addition of the thawed cell suspension to culture medium effectively dilutes the cryoprotectant (e.g. DMSO) reducing the toxicity of the cryoprotectant. That is why it is important to add the thawed cell suspension to a larger volume of culture medium immediately after the ampoule has

thawed; do not allow thawed ampoules to sit at room temperature for long periods.

3. For most cultures it is best practice to subculture before confluence is reached so that the cells are harvested during their log phase of growth and are at optimum viability ready for seeding into new flasks. Some hybridomas may be slow to recover post resuscitation therefore start in 20% (v/v) FBS and 10% (v/v) hybridoma enhancement supplement in the appropriate medium.

3.4 EXPERIMENT DESIGN

3.4.1 THE INCUBATION OF THE BIOMATERIALS

Biomaterials are placed in 6, 24 or 96-well plate in order to execute different types of experiments. They are incubated for 24 h in fetal bovine serum (FBS). FBS acts as a tampon, begins the formation of the apatite layer and contains adhesión molecules, like fibronectin and vitronectin, that will be absorbed during the nucleation of apatite and will promote cell adhesion. These adhesion molecules mediate the cell attachment, binding to cell integrins, that begin to cluster and initiate the signaling cascade and regulate events such as cell spreading, migration, proliferation and differentiation (32). Then they are left one week in the culture medium, that is changed regularly every three days. In this way the pH of the medium, reaches the value of ~7 that is compatible with cell survival. The volume of medium added to every well is calculated to put 1 ml of culture medium every 3 cm² of total surface of the biomaterial according to the International Organization for Standardization (ISO10993-12:2007):

 Total surface 2.4cmx2mm material:(2x3.14x1.2x0.2)+(3.14x1.2²)x2=10.5 cm².

Volume of culture medium: 10.5/3 = 3.5 ml

 Total surface 7mmx3mm material:(2x3.14x0.35x0.3)+(3.14x0.35²)x2=1.4 cm².

Volume of culture medium: 1.4/3=0.47 500 µl

For the biomaterials placed in 96-well plates, 200 µl of culture medium is added

to every well.

3.4.2 CULTURE CONDITIONS

Flow cytometry (FC) and qPCR:

5000 cells/cm² are seeded over the biomaterials with a diameter of 2.4 cm and a thickness of 2 mm placed in a six-well plate. The volume of medium added is 3.5 ml. At the end of every week the cells are trypsinized and processed.

MTT and SEM microscopy:

5000 cells/cm² are seeded over the biomaterials with a diameter of 7 mm and a thickness of 3 mm placed in a 96-well plate. The volume of medium added is 200 µl.

Immunofluorescence (IF), Alizarin Red (AR) and Alkaline Phosphatase (ALP) assays:

Biomaterials with a diameter of 7 mm and a thickness of 3 mm are placed in a 24-well plate. 500 µl of cell suspension is seeded globally inside the well covering the biomaterial. Cells are seeded at a concentration of 5000 cells/cm². Immunofluorescence needs to be visualized with a microscope and the thickness of the material would be an obstacle in the detection of the target proteins of cells seeded on the biomaterial while the Alizarin Red is a colorimetric assay and the biomaterial could interfere in the detection of the resulting coloured product. For 30
these reasons, these experiments are not performed on cells seeded directly over the biomaterials

3.4.3 THE INCUBATION PERIOD

The incubation period is of four weeks, at the end of every week the experiments are performed. Starting with the third week, when cells are calculated to reach confluence, in addition to the normal growth medium (GM), samples are

incubated also with an osteogenic medium (OM) supplemented with:

$1 10^{-8}$ M Dexametasone, a synthetic glucocorticoid, capable of inducing human bone marrow stromal cells to express an osteoblastic phenotype.

50μg/ml L-ascorbic acid-2-phosphate, a cofactor of the prolyl hydroxylase that increases the proline hydroxylation in the intracellular procollagen pool and the rate of procollagen secretion

0.01 M β-glicerophosphate, used as a local source of inorganic phosphate

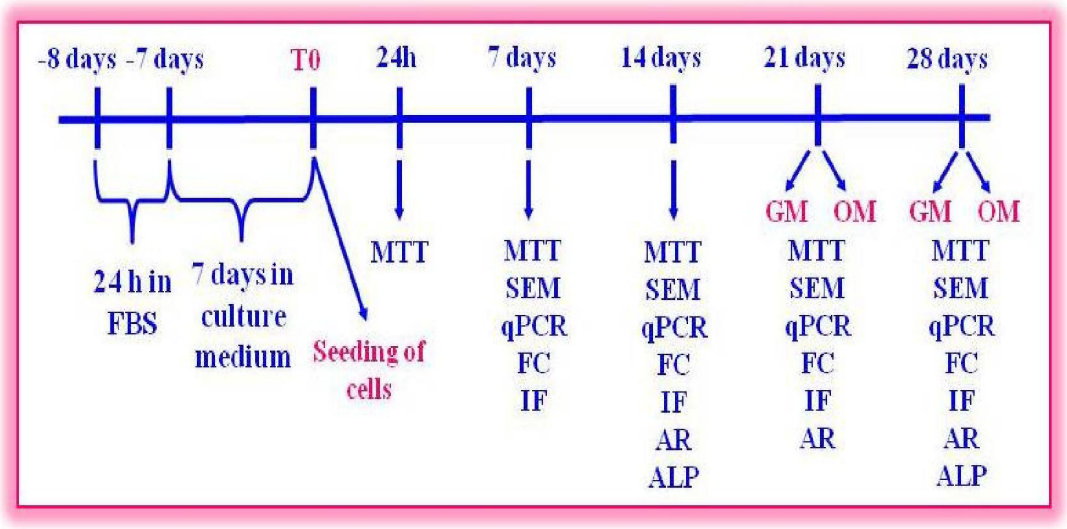

Fig. 18: The incubation period and the specific experiments performed at the end of every week.

3.5 INDUCTIVELY COUPLED PLASMA OPTICAL EMISSION SPECTROMETRY (ICP-OES)

Inductively coupled plasma optical emission spectrometry, is an analytical technique used for the detection of chemical elements. It is a type of emission spectroscopy that

uses the inductively coupled plasma, to produce excited atoms and ions that emit electromagnetic radiation at wavelengths characteristic of a particular element.
The intensity of this emission is proportional to the concentration of the element within the sample. The ICP-OES is composed of two parts: the ICP and the optical spectrometer. The ICP torch consists of three concentric tubes, usually made of quartz. The end of this torch is placed inside the coil of a radio frequency (RF) generator. The argon gas is typically used to create plasma.

When the torch is turned on, an intense electromagnetic field is created within the coil by the high power radio frequency signal flowing in the coil. This RF signal is created by the RF generator which is, effectively, a high power radio transmitter. The argon gas flowing through the torch is ignited with a Tesla unit that creates a brief discharge arc through the argon flow to initiate the ionization process. Once the plasma is "ignited", the Tesla unit is turned off.

The argon gas is ionized in the intense electromagnetic field and flows in a particular rotationally symmetrical pattern towards the magnetic field of the RF coil. A stable, high temperature plasma of about 7000 K is then generated as the result of the inelastic collisions created between the neutral argon atoms and the charged particles.

A peristaltic pump delivers an aqueous or organic sample into a nebulizer where it is changed into mist and introduced directly inside the plasma flame. The sample immediately collides with the electrons and charged ions in the plasma and is itself broken down into charged ions. The various molecules break up into their respective atoms which then lose electrons and recombine repeatedly in the plasma, giving off radiation at the characteristic wavelengths of the elements involved. A shear gas, typically nitrogen or dry compressed air is used to 'cut' the plasma at a specific spot. One or two transfer lenses are then used to focus the emitted light on a diffraction grating where it is separated into its component wavelengths in the optical spectrometer. In other designs, the plasma impinges directly upon an optical interface which consists of an orifice from which a constant flow of argon emerges, deflecting the plasma and providing cooling while allowing the emitted light from the plasma to

enter the optical chamber. Still other designs use optical fibers to convey some of the light to separate optical chambers.

Within the optical chamber(s), after the light is separated into its different wavelengths (colors), the light intensity is measured with a photomultiplier tube or tubes physically positioned to "view" the specific wavelength(s) for each element line involved, or, in more modern units, the separated colors fall upon an array of semiconductor photodetectors such as charge coupled devices (CCDs). In units using these detector arrays, the intensities of all wavelengths (within the system's range) can be measured simultaneously, allowing the instrument to analyze for every element to which the unit is sensitive all at once. Thus, samples can be analyzed very quickly.

The intensity of each line is then compared to previously measured intensities of known concentrations of the elements, and their concentrations are then computed by interpolation along the calibration lines.

In addition, special software generally corrects for interferences caused by the presence of different elements within a given sample matrix.

Procedure:

Both types of biomaterials with a diameter of 2,4 cm and a thickness of 1,5 mm and with a diameter of 7 mm and a thickness of 3 mm were incubated for 24 hours in SBF and for 36 days at 37°C in normal culture medium (respectively in 3,5 ml and 0,5 ml). Culture medium was removed after 3h, 6h, 12h, 24h, 4d, 8d, 12d, 16d, 20d, 24d, 28d, 32d and 36d of incubation and analyzed using Inductively Coupled Plasma Optical Emission Spectrometry OPTIMA 2000™ (PerkinElmer) to obtain the elemental concentrations of Si, Ca, and P. The relative abundance of dissolved ions in culture medium is measured in part per million (ppm).

Instrument parameters:

Generator power: 1300 W.

Generator frequence: 40MHz.

Argon plasma flux: 15 $L.min^{-1}$

Auxiliar argon flux: 0.2 $L.min^{-1}$

Argon nebulizator flux: 0.83 $L.min^{-1}$

Peristaltic pump flux: 1.5 $L.min^{-1}$.

Instrument calibration:

The calibration of the instrument was realized previously samples processing, with the use of monoelement and/or multyelement patrones diluted in milliQ water. Analitic determinations were done in triplicate, including blanks in the calibration and in the sample quantification analysis. Calibration equation used was lineal. In every analite the correlation coefficient of the rectas was always mayor to 0.999.

Los patrones and their concentrations, used for the calibration, were:

Phosphor: 5 mg/L, 15 mg/L and 50 mg/L.

Calcium: 20 mg/L, 50 mg/L, 100 mg/L, 200 mg/L.

Silicium: 1 mg/L, 10 mg/L, 16 mg/L, 25 mg/L.

3.6 MTT ASSAY

The MTT assay is a colorimetric assay that allows to assess cell viability and proliferation. It can also be used to determine cytotoxicity of drugs and toxic materials, since those agents would stimulate or inhibit cell viability and growth. 3-

(4,5-Dimethylthiazol-2-yl)-2,5-diphenyltetrazolium bromide, thiazolyl blue (MTT) is a tetrazolium salt that is reduced by the mitochondrial dehydrogenase present in living cells to a formazan dye, giving a purple colour. This product is representative of the dehydrogenase enzyme activity, present in active state in all living cells, and so of the number of living cells.

MTT and related tetrazolium salts

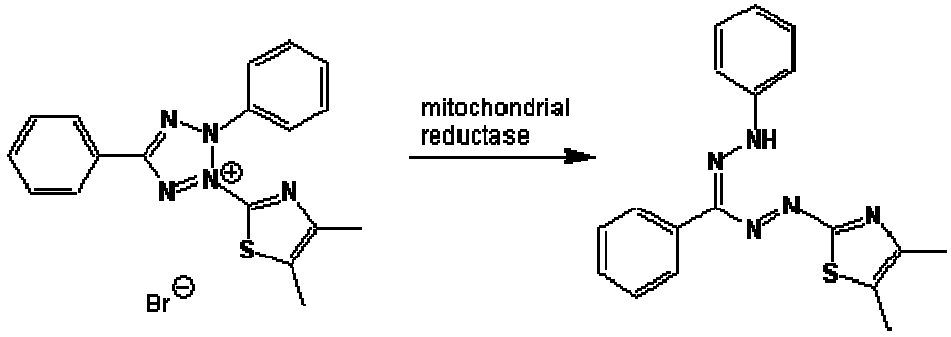

Fig. 19 MTT and related tetrazolium salts.

MTT (3-(4,5-Dimethylthiazol-2-yl)-2,5-diphenyltetrazolium bromide), a yellow tetrazole, is reduced to purple formazan in living cells.[1] A solubilization solution, usually either dimethyl sulfoxide (as in our case), an acidified ethanol solution, or a solution of the detergent sodium dodecyl-sulfate in diluted hydrochloric acid, is added to dissolve the insoluble purple formazan product into a colored solution, and with shaking. The absorbance of this colored solution can be quantified by measuring at a certain wavelength (usually between 500 and 600 nm) by a spectrophotometer. The absorption maximum is dependent on the solvent employed (Mosmann T, 1983). These reductions take place only when reductase enzymes are active, and therefore conversion is often used as a measure of viable (living) cells. However, it is important to keep in mind that many different conditions can increase or decrease metabolic activity. Changes in metabolic activity can give large changes in MTT results while the number of viable cells is constant. When the amount of purple formazan produced by cells treated with an agent is compared with the amount of

formazan produced by untreated control cells, the effectiveness of the agent in causing death, or changing metabolism of cells, can be deduced through the production of a dose-response curve.

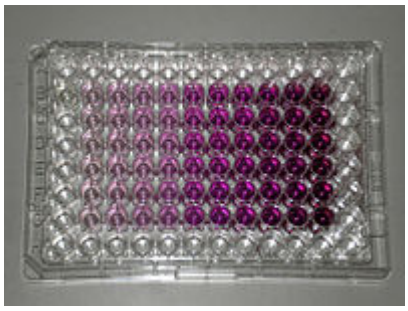

Fig. 20: microtiter plate after an MTT assay. Increasing amounts of cells resulted in increased purple colouring.

Procedure:

5000 cells/cm² are seeded over every piece of biomaterial before placed in a 96-well plate and on the surface of the wells as controls. Five pieces are used for every material.

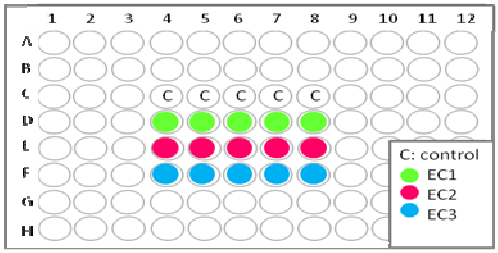

Prepare the MTT solution dissolving MTT 1mg/ml in DMEM without phenol red and incubate at 37°C to help the dissolution. Protect it from the light.

- Aspirate the culture medium from each well.
- Add 200 µl of MTT solution to each well (work in dark).
- Incubate for 4 hours in dark at 37°C.
- Remove MTT solution from each well to discard the unmetabolized MTT.
- Add 100 µl of DMSO to each well to solubilize amount of insoluble purple formazan. Add 100 µl of DMSO also to 5 unused wells as blank.
- Put the plates on a shaking table at 150 rpm for 5 minutes in dark , to thoroughly mix the formazan into the solvent.

- The presence of the biomaterial makes the lecture of the absorbance impossible, so it's necessary to transfer the DMSO from each well with the biomaterials to a clean one.
- Read the absorbance, directly correlated with cell quantity, in a plate reader (Labsystem, Multiscan MCC 340) at 570 nm, using 690 nm as reference wavelength.

Determination of cell proliferation:

To determine the cell proliferation rate, a calibration line is necessary as a reference. The same cell population used for the experiment, is seeded at different cell concentration (1000, 2000, 4000, 6000, 8000, 10000, 15000, 20000, 25000, 30000, 40000, 50000 cells/well, in duplicates) in a 96-well plate and the MTT assay is performed after 12 h, in order to know the value of absorbance relative to every cell concentration, before cells start to proliferate. The known cell concentrations are plotted against their value of absorbance to create a calibration line. Plotting the value of absorbance of the unknown samples against the calibration curve is possible to determine their cellular concentration.

3.7 PE-ANNEXIN V APOPTOSIS QUANTIFICATION ASSAY

Apoptosis is a normal physiologic process which occurs during embryonic development as well as in maintenence of tissue homeostasis. The apoptotic program is characterized by certain morphologic features, including loss of plasma membrane

asymmetry and attachment, condensation of the cytoplasm and nucleus, and internucleosomal cleavage of DNA. Loss of plasma membrane is one of the earliest features. In apoptotic cells, the membrane phospholipid phosphatidylserine (PS) is translocated from the inner to the outer leaflet of the plasma membrane, thereby exposing PS to the external cellular environment (Koopman G, Reutelingsperger CP, Kuijten GAM. Annexin V for flow cytometric detection of phosphatidylserine expression on B cells undergoing apoptosis. Blood 84 (5): 1415–20, 1994; Vermes I, Haanen C, Steffens-Nakken H, Reutelingsperger C. A novel assay for apoptosis—flow cytometric detection of phosphatidylserine expression on early apoptotic cells using fluorescein labelled Annexin V. *J* Immunol Methods 184 (1): 39–51, 1995)

Annexin V is a 35-36 kDa Ca^{++} dependent phospholipid-binding protein that has a particularly high affinity for PS, and binds to cells with exposed PS, like physiologically do in the inner leaflet of the cell membrane. Annexin V function is unknown, however has been proposed (in vitro experiments and established role in antiphospholipid syndrome) to play a role in the inhibition of blood coagulation by competing for phosphatidylserine binding sites with prothrombin and also to inhibit the activity of phospholipase A1 (Raynal P, Pollard HB. Annexins: the problem of assessing the biological role for a gene family of multifunctional calcium- and phospholipid-binding proteins. Biochim Biophys Acta 1197(1):63-93, 1994).

Annexin V may be conjugated to fluorochromes, including Phycoerythrin (PE), enzymatic labels such as biotin, or radioelements. PE-Annexin V conjugate format used in this experiment retains its high affinity for PS and thus serves as a sensitive probe for flow cytometric analysis of cells that are undergoing apoptosis.

Since externalization of PS occurs in the earlier stages of apoptosis, PE Annexin V staining can identify apoptosis at an earlier stage than assays based on nuclear changes such as DNA fragmentation. PE Annexin V staining precedes the loss of membrane integrity which accompanies the latest stages of cell death resulting from either apoptotic or necrotic processes. Therefore, staining with PE Annexin V is typically used in conjunction with a cell nucleus stainer like Propidium-iodure or a vital dye such as 7-Amino-Actinomycin (7-AAD) chosen in this study. Viable cells with intact membranes exclude 7-AAD, whereas the membranes of dead and

damaged cells are permeable to 7-AAD. Cells that are considered viable are PE Annexin V and 7-AAD negative; cells that are in early apoptosis are PE Annexin V positive and 7-AAD negative; and cells that are in late apoptosis or already dead are both PE Annexin V and 7-AAD positive. This assay does not distinguís between cells that have undergone apoptotic death versus those that have died as a result of a necrotic pathway (Van Engeland M, Ramaekers FC, Schutte B, Reutelingsperger CP. A novel assay to measure loss of plasma membrane asymmetry during apoptosis of adherente cells in culture. Cytometry 24(2):131-139, 1996).

Assay Procedure:

PE Annexin V binding is calcium dependent and defined calcium and salt concentrations are required for optimal staining.

Cells culture

Cells was seeded at a density of 2.0 x 10^5 cells/cm^2 in 24 wells plates and cultured in GM medium for 24 hours at 37ºC to allow the adherence of the cells. Following, sterile biomaterials pieces was incorporated on upper chambers of 8 µm-pore-size cell culture inserts (BD Bioscience, San José, CA) and incubated in wells in presence of *ah*MSCs for 0, 12, 24 hours and 3 and 7 days. Later, cells were detached using 0,25% w/v tripsin-EDTA solution (Sigma).

PE Annexin V staining protocol

Cells were wash twice with cold DPBS and then resuspended in 1X Binding Buffer at a concentration of 1 x 10^6 cells/ml. Than 100 µl of the solution (1 x 10^5 cells) were transfered to a 5 ml culture tube. 5 µl of PE Annexin V and 5 µl 7-AAD were added

each tube. After gently vortexing, the cells were incubated for 15 min at RT (25°C) in the dark. Finally 400 µl of 1X Binding Buffer were added to each tube.

Analisys

Percentage of live (Annexin-V^- / 7-AAD^-), early apoptotic ($Annexin^+$ / 7-AAD^-) or late apoptotic and necrotic cells (Annexin-V^+ / 7-AAD^+) was analyzed in a Beckman Coulter Navios flow cytometer (Fullerton, CA, USA). Subsequently, the percentage of each population was calculated and statistical tStudent test performed ($p<0.05$). All determinations were performed in triplicate.

Controls for setting up flow cytometr

The following controls were used to set up compensation and quadrants:

1. Unstained cells.

2. Cells stained with PE Annexin V (no 7-AAD).

3. Cells stained with 7-AAD (no PE Annexin V).

3.8 ALKALINE PHOSPHATASE ASSAY

Quantitative Alkaline Phosphatase ES Characterization Kit (Millipore) was used to determine the presence of Alkaline Phosphatase in cell cultures. Alkaline phosphatase (ALP) is a hydrolase enzyme responsible of the dephosphorilation of various cell mulecules such as nucleotides, proteins, and alkaloids under alkaline conditions. ALP in humans is an obiquitous enzyme but it levels are more elevated in cells of the liver, kidney, bone, placenta, embryo and under specific disease states.
Under alkaline conditions, ALP can catalyze the reaction of hydrolysis of p-nitrophenylphosphate (p-NPP) into phosphate and p-nitrophenol, a yellow product. The amount of p-nitrophenol produced is proportional to the amount of the enzyme

alkaline phosphatase present in the sample, so ALP amount can be inferred by the quantification of p-nitrophenol accumulated after the catalytic reaction. P-nitrophenol amount can be quantified with a spectrophotometer set at 405 nm.

p-nitrophenylphosphate $\xrightarrow{\text{ALP}}$ **phosphate + p-nitrophenol (yellow product)**

The experiment was performed in duplicate (two pieces for every material were used).

Procedure:

Was done an 8-point standard curve for alkaline phosphatase (including blank) in triplicate for every assay run. Total reaction volume was 100 µL. (Recombinant alkaline phophatase is provided in the kit).

Standard curve was done by serial dilutions of the ALP standard in triplicates, corresponding to 5, 2.5, 1.25, 0.625, 0.3125, 0.15625 and 0.078125 ng ALP and a blank control.

Before starting the experiment was determined the total reaction volumes (p-NPP Buffer) required to carry out the experiments in replicates and to include the 8-point standard curve with blank in replicates:

4 conditions (EC1, 2, 3, Ctrl) x 2 pieces x 3 replicates = 24 total reactions

8 reactions (8-point standard curve) x 3 replicates = 24 total reactions

48 total reactions x 100 µL reaction volume = 4800 µL total volume

Assuming ~ 20% volume overage = 4800 + 960 = 5760 µL or ~ 5,8 mL total reaction volume. Just before starting the assay was prepared a 2X p-NPP substrate solution such that the total volume is one half of the total reaction volume above calculated. 2,9 mL of 2X p-NPP Substrate solution were done by diluting 116 µL of 50X p-NPP Substrate Concentrate with 2784 µL of p-NPP Buffer. The medium was remuved from each well of the 24-well plate and the biomaterial piece removed. The cell monolayer was washed twice with DPBS solution, to remove residual serum. Cells were than trypsinyzed to detach them from the wells and

were centrifuged in a 15 mL falcon tube at 2000 rpm for 5 minutes at RT to pellet the cells. The supernatant was removed and the cell pellet resuspended in 1 mL 1X Wash Solution, supplied with the kit. Cells were counted using a Neubauer chamber and trypan blue staining, to aliquot 20000 cells in each one of three 1,5 mL microcentrifuge tubes (three replicates). The operation was done for each of the cell samples to be analyzed. Eppendorf tubes were spin at 2000 rpm for 5 minutes at RT to pellet the cells. The supernatant was eliminated taking care do not touch cell pallets, and than the pellets were resuspended in 50 µL p-NPP Buffer. Each one of the triplicates suspensions were transferred to one well of a 96-well assay plate provided by the kit. The first 3 columns (A1-3 through H1-3), of the 96-well plate, were reserved to run the 8-point alkaline phosphatase standard curve. At this time, the enzymatic reaction has not been initiated. Enzymatic reaction is initiated when 50 µL 2X p-NPP Substrate Solution is added to the cell suspension.

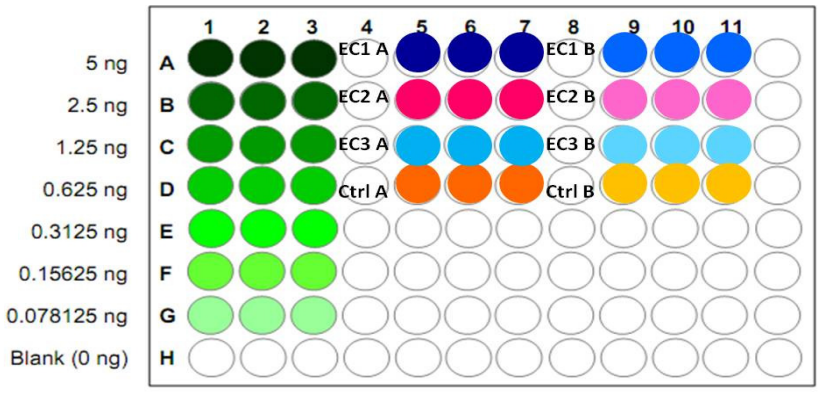

Fig. 21: well-plate showing the position of the set of 8 ALP known concentration in triplicate (green) and the unknown samples in triplicate (EC1blue, EC2 pink, EC3 light blue, Ctrl orange)

Using a multichannel micropipette, 50 µL of p-NPP Buffer were aliquoted into the first three columns (A1-3 through H1-3) of the 96-well plate. (Total number = 24 wells). Than an additional of 49 µL of p-NPP Buffer were putted into the first three wells (A1, A2, A3). 1 µL of ALP standard were putted into each of the three wells, A1, A2, A3, changing tip for each transfer.

Using a multichannel micropipette set to 50 µL, the contents of wells were carefully mixed and then 50 µL were transferred to the next row of wells (B1, B2, B3). The mixing and transfer of 50 µL to the next row of wells (C1, C2, C3) were repeated to obtain in total seven serial dilutions of the ALP standard, in triplicates, corresponding to 5, 2.5, 1.25, 0.625, 0.3125, 0.15625 and 0.078125 ng ALP per well. The excess 50 µL solution were discarded from wells G1, G2, G3. Wells H1, H2, and H3 should contain only the p-NPP Buffer and serve as blank (0 ng AP control).

Using a multichannel pipette 50 µL of the 2X p-NPP Substrate Solution were added into each of the wells containing the 8-point standard curve (A1-3 to H1-3) and also to each of the unknown samples so that the final reaction volume was 100 µL. Addition of 2X p-NPP Substrate Solution initiates the enzymatic reaction. Starting form this moment 96 wells plate was incubated for 20 minutes at room temperature in the dark. After 20 minutes incubation 50 µL of Reaction Stop Solution were added to each reaction well to stop the reaction. Final volume per well = 150 µL. The absorbance was red at 405 nm. The set of ALP known concentrations were plotted versus their values of absorbance to obtain a standard curve.

Plotting samples absorbance values to the standard curve was determined the samples unknown concentration.

3.9 ALIZARIN RED STAINIGN AND QUANTIFICATION

Osteogenesis kit assay (Millipore) was used to detect the presence of mineralization nodules. The kit functioning is based on alizarin red compound, a dye used to evaluate the calcium-rich deposits by cells in culture. Alizarine red dye can be

extracted from the stained monolayer and assayed, permitting a qualitative and quantitative analysis. The experiment was performed in duplicate (two pieces for every material).

Alizarin Red Staining Protocol

Carefully the medium was aspirate from 24-well plate wells and the biomaterial piece exctracted without disturbing the monolayer. Cells were washed with DPBS twice. First of all cells were 8% paraformaldehyde fixed and incubate at RT for 15 minutes. Carefully, without disrupting the monolayer, the fixative was removed and cells rinsed three times (at least 5 minutes each) with an excess of distilled water. 1 mL/well Alizarin Red Stain Solution was added and samples incubated at RT for 20 minutes. The excess of dye was eliminated and wells were washed four times (at least 5 minutes each with a gentle rocking) with deionized H_2O. 1 mL water to each well was leaved to prevent the cells from drying. Samples were inspected under an optical microscope and images acquired. Differentiated cells containing mineral deposits appeared stained bright red by the Alizarin Red Solution.

Protocol for quantitative analysis of Alizarin Red Staining

Quantitative analysis of Alizarin Red Staining can be performed by determining the absorbance at 405 nm of a set of known Alizarin Red concentrations and comparing these values to those obtained from unknown samples. The dye can be extracted from the stained monolayer and quantified directly. The sensitivity of the assay is improved by the extraction of the calcified mineral at low pH.

400 µL 10% acetic acid were added, after images acquisition, to each well of the 24-well plate and samples were incubated for 30 minutes with shaking.
The monolayer, loosely attached after the treatment, was gently scraped with the aid of a cell scraper, from the plate and transferred with acetic acid solution added before to a 1.5 mL microcentrifuge tube. Before starting the treatment of dye extraction, samples in the Eppendorf were vigorously mix with a Vortex for 30 seconds.
Samples were sealed with parafilm to avoid evaporation and heated to 85°C for 10 minutes putting them in a heatbath. Than tubes were transferred to ice for 5 minutes.

Subsequent centrifugation at 20,000 xg for 15 minutes permits calcium deposits recovery.

While centrifuging, Alizarin Red standards were prepared. The 10X ARS dilution buffer contained in the kit was first diluted 1:10 in distilled H_2O to obtain a 1X working ARS dilution buffer. Than the 40 mM Alizarin Red solution was diluted 1:20 in 1X ARS dilution buffer, obtaining a 2 mM working stock. The standard set was realized by diluting the 2 mM working stock in 2-fold serial dilutions in 1.5 ml microcentrifuge tubes (2mM, 1mM, 500 µM, 250 µM, 125 µM, 62,5 µM, 31,3 µM, blank). The blank will consist of just the 1X ARS dilution buffer.

After centrifugation step 400 µL of the supernatant of each sample were withdraw and transfer to a new 1.5 ml microcentrifuge tube. The pH was neutralized with 150 µL 10% Ammonium hydroxide. The pH felt down within the range of 4,1 - 4,5. 150 µL of the standards and the samples were transferred to a transparent bottom 96-well plate. The absorbance was red at 405 nm in a plate reader (Labsystem, Multiscan MCC 340). The set of Alizarin Red known concentrations were plotted again their values of absorbance to obtain a standard curve. Determine the concentration of the unknown sample plotting their value of absorbance to the standard curve.

3.10 FLOW CYTOMETRY MARKER EXPRESSION ANALYSIS

Flow cytometry is a technique that uses the principles of light scattering, light excitation, and emission of fluorochorme molecules to generate specific multi-parameter data from particles and cells in the size range of 0.5 to 40 µm of diameter, and permits analyze up to thousand particles per second. Cells are hydrodinamically

focused in a sheath of PBS before intercepting an optimally focused light source. Lasers are most often used as a light source in flow cytometry.

Principles of the flow cytometer

Fluidics system:

One of the fundamentals of flow cytometry is the ability to measure the properties of individual particles. When a sample in solution is injected into a flow cytometer, the particles are randomly distributed in three-dimensional space. The sample must therefore be ordered into a stream of single particles to be interrogated by the machine. Flow cytometer use the principle of hydrodynamic focusing for presenting cells to a laser. The sample is injected into a central channel/core, enclosed by an outer sheath that contains a faster flowing fluid. As the sheath fluid moves, it creates a massive drag effect on the narrowing central chamber. This alters the velocity of the central fluid whose flow front becomes parabolic with greatest velocity at its center and zero velocity at the wall. The effect creates a single file of particles and is called hydrodynamic focusing, that is what permits to analyze one cell at a time. Under optimal conditions (laminar flow) the fluid in the central chamber will not mix with the sheath fluid.

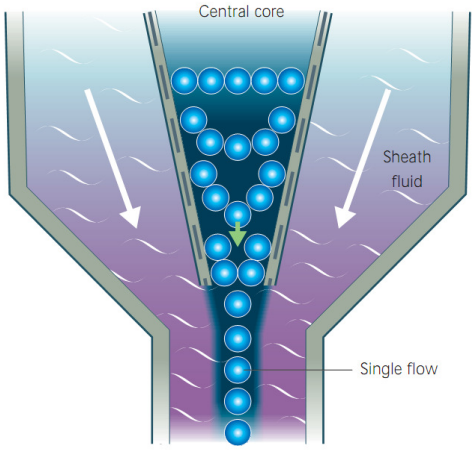

Fig 22: Hydrodynamic focusing produces a single stream of particles. (A)

Optics and detection:

After hydrodynamic focusing, each particle passes through one or more beams of light. Cell light scattering or fluorescence emission, if the particle is labeled with a fluorochrome, provides information about the particle's characteristics. Light scattering occurs when a particle deflects incident laser light. The extent to which

this occurs depends on the physical properties of a particle, namely its size and internal complexity. Factors that affect light scattering are the cell's membrane, nucleus, and granular material inside the cell; cell shape and surface topography also contribute to the total light scatter.

Lasers are the most commonly used light sources in modern flow cytomatry. Lasers produce a single wavelength of light at one or more discreet frequancies (coherent light).

Light that is scattered in the forward direction, typically up to 20° offset from the laser beam's axis, is collected by a lens known as the forward scatter channel (FSC). The FSC intensity roughly equates to the particle's size and can also be used to distinguish between cellular debris and living cells. Light measured approximately at a 90° angle to the excitation line is called side scatter. The side scatter channel (SSC) provides information about the granular content (internal complexity) of a particle. Both FSC and SSC values obtained are unique for every particle, and a combination of the information may be used to differentiate different cell types in a heterogeneous sample.

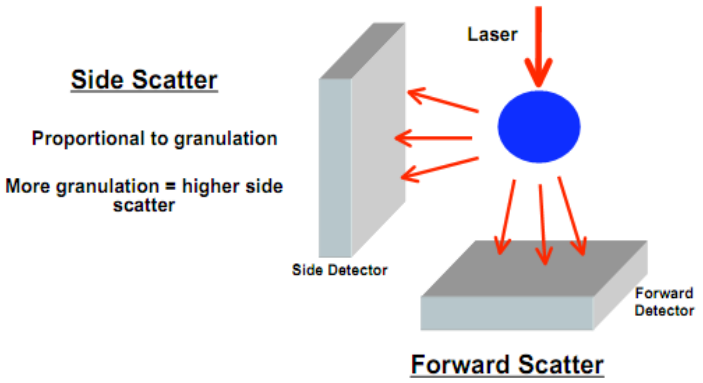

Fig 23. Principles of light scatter. (B)

Fluorescence measurements taken at different wavelengths can provide quantitative and qualitative data about fluorochrome-labeled cell surface receptors or intracellular molecules such as DNA and cytokines.

Flow-cytometers use separate fluorescence (FL-) channels to detect light emitted. The number of detectors will vary according to the machine. Detectors are either silicon photodiodes or photomultiplier tubes (PMTs). PMTs are more sensitive instruments and are ideal for scatter and fluorescence readings.

The specifivity of detection is controlled by optical filters, which block certain wavelengths while transmitting (passing) others.

Signal processing

When light hits a photodetector a small current (a few microamperes) is generated, and light signals are converted to electronic signals and than assigned a channel number on a data plot. Current associated voltage has an amplitude proportional to the total number of light photons received by the detector. The electrical pulses originating from light detected by the detector is then amplified by a series of linear or logarithmic amplifiers. Log amplification is most often used to measure fluorescence in cells. This type of amplification expands the scale for weak signals and compresses the scale for strong signals, resulting in a distribution that is easy to display on a histogram. Linear scaling is preferable where there is not such a broad range of signals as in DNA analysis. After the different signals or pulses are amplified they are processed by an Analog to Digital Converter (ADC) which in turn allows for events to be plotted on a graphical scale (One parameter, two parameter histograms). The measurement from each detector is referred to as a 'parameter' like forward scatter, side scatter or fluorescence. The data acquired in each parameter are known as the 'events' and refer to the number of cells displaying the physical feature or marker of interest.

Single-parameter histograms

The one-parameter graphs display a measurement parameter (relative fluorescence or light scatter intensity) on the x-axis and the cell count (number of events) on the y-axis. All one-parameter histograms have 1,024 channels. These channels correspond to the original voltage generated by a specific "light" event detected by the PMT detector. In other words, the ADC assigns a channel number based on the pulse height for individual events. Therefore, brighter specific fluorescence events will yield a higher pulse height and thus a higher channel number when displayed as a histogram. They are useful for evaluating the total number of cells in a sample that possess the physical properties selected for or which express the marker of interest.

Cells with the desired characteristics are known as the positive dataset. Ideally, flow cytometry will produce a single distinct peak that can be interpreted as the positive dataset. However, in many situations, flow analysis is performed on a mixed population of cells resulting in several peaks on the histogram. In order to identify the positive dataset, flow cytometry should be repeated in the presence of an appropriate negative isotype control that is a control for non-specific binding of the labeled antibody.

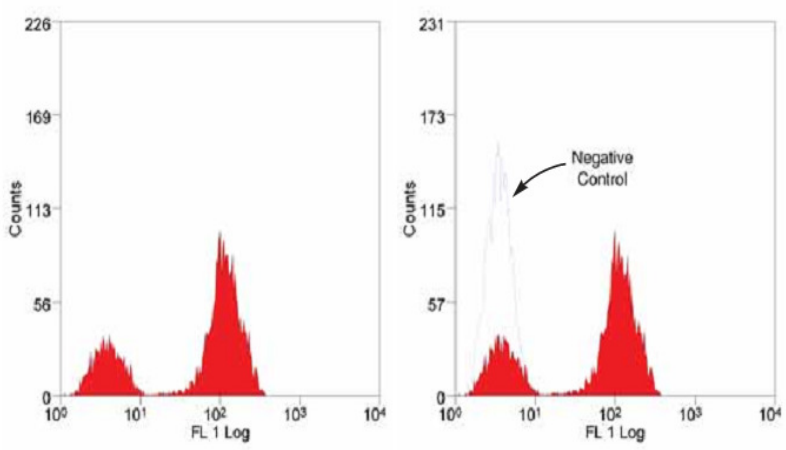

Fig 24. Histograms of positive (A) and negative (B) signals. A: Using rat anti-mouse F4/80 conjugated to FITC to stain mouse peritoneal macrophages produces two peaks. **B:** By running an appropriate isotype control (rat IgG2b negative control conjugated to FITC) and overlaying its image on the histogram (blue outline) the positive dataset is identified as the taller red peak on the right. (A)

Two-parameter histograms

The two-parameter graphs display two measurement parameters, one and one on the y-axis, and the cell count height on a density gradient. This is similar to a topographical map. You can select 64 or 256 channels on each axis of two-parameter histograms. Particle counts are shown by dot density or by contour plot.

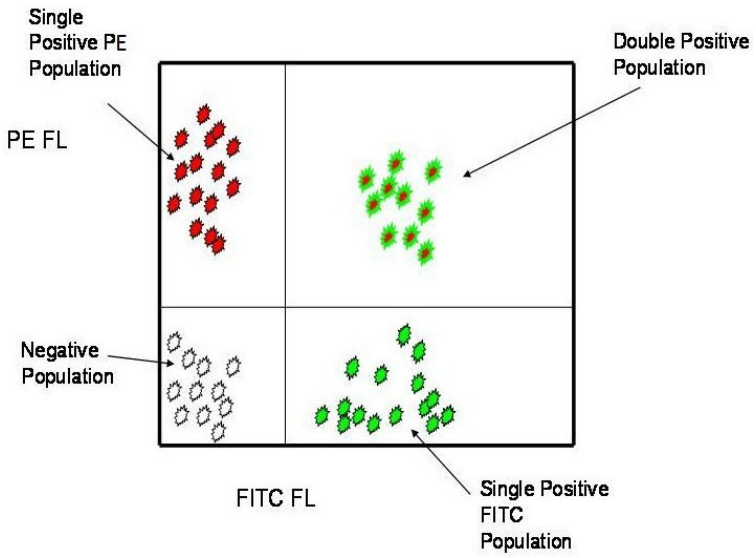

Fig. 25: Dual color fluorescence histogram: The top left quadrant encompasses PE-labeled cells, the right down quadrant contains the FITC-labeled cells and the top right quadrant comprises a double positive population both for PE (Phycoerythrin) and FITC (Fluorescein isothiocyanate). (C)

The parameters could be SSC, FSC or fluorescence. Another example is the dual-color fluorescence histogram that offers a double analysis discriminating cells labeled with both fluorochromes, with only one of them or none. Different cluster of cells are positioned in different quadrants of the histogram.

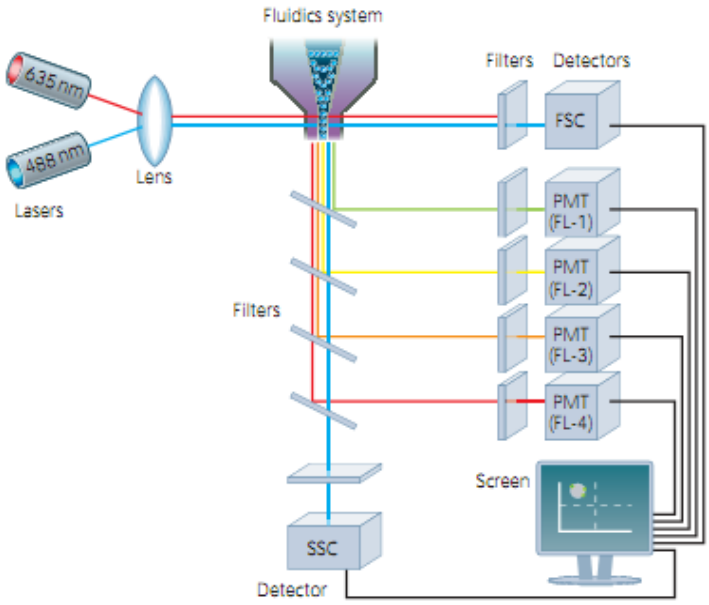

Fig 26: Schematic overview of a typical flow cytometer setup. (A)

Fluorescence compensation

One consideration to be aware of when performing multicolor fluorescence studies is the possibility of spectral overlap. When two or more fluorochromes are used during a single experiment there is a chance that their emission profiles will coincide, making measurement of the true fluorescence emitted by each difficult. This can be avoided by using fluorochromes at very different ends of the spectrum; however, this

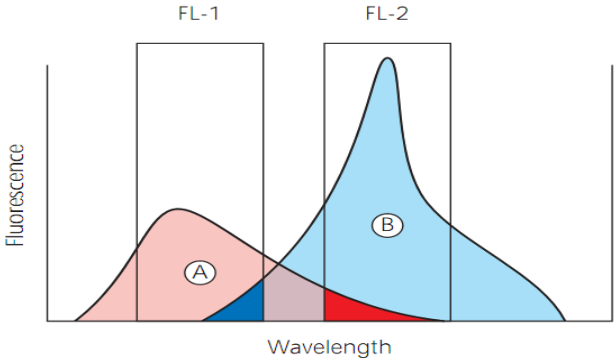

Fig 27: Spectral overlap: Dark blue shade represents the proportion of that overlaps into the FL-1 channel. Red shade represents the proportion of that interferes with FL-2 channel measurements. (A)

is not always practical. Instead, a process called fluorescence compensation is applied during data analysis, which calculates how much interference (as a %) a fluorochrome will have in a channel that was not assigned specifically to measure it. To calculate how much compensation needs to be applied to the dataset if both dyes are used simultaneously, some control readings must first be taken. Fluorochrome A should be run through the flow cytometer on its own and the % of its total emission that is detectable in the wrong channel (spillover) determined.

Data analysis

Gates and regions

An important principle of flow cytometry data analysis is to selectively visualize the cells of interest while eliminating results from unwanted particles e.g. dead cells and debris. This procedure is called gating.

Cells have traditionally been gated according to physical characteristics. For instance, subcellular debris and clumps can be distinguished from single cells by size, estimated by forward scatter. Also, dead cells have lower forward scatter and side scatter than living cells. On the density plot, each dot or point represents an individual cell that has passed through the instrument.

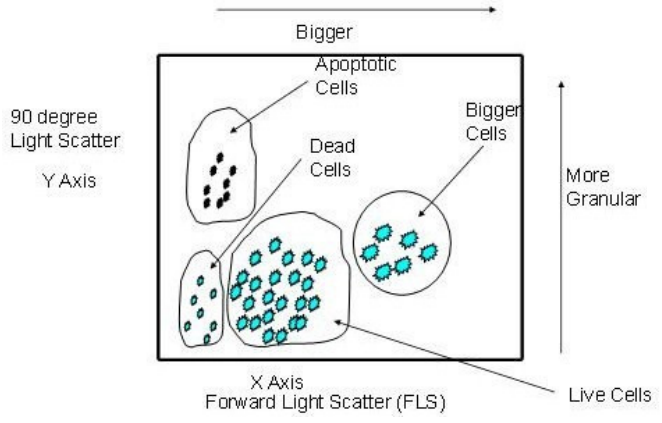

Fig 28. Light Scattering, two-parameter Histogram: Thanks to the cell sorting, living cells can be distinguished from dead and apoptotic cells. (C)

Newer gating strategies utilize fluorescence parameters along with scatter parameters.

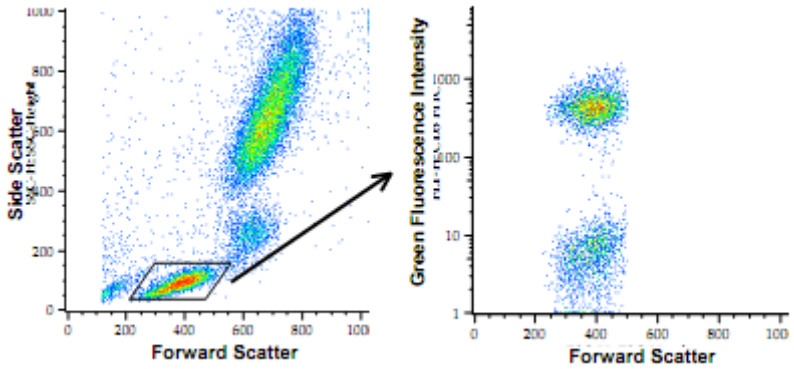

Fig 29. Selected distinct populations for further data analysis or sorting. (B)

Data generated in flow cytometry is displayed using Multiparamater Acquisition and Display software platforms. Histograms corresponding to each of the parameters of interest can be analyzed using statistical tools to calculate percentage of cells manifesting specific fluorescence, and fluorescence intensity. This information can be used to look at fluorescence expression within subpopulations of cells in a sample (gating). (C)

Flow cytometry protocol

Preparation of cells:

The culture media was removed and discarded from the wells and cells washed two times with culture medium. 2 ml of prewarmed (20 minutes at 37°C) 0,25% Trypsin/0,25% EDTA were added in the wells and samples were incubate for 5 minutes at 37°C. Trypsin was inactivated adding 4 ml culture medium supplemented with 20 % FBS or FBS. Cells were transfered in a 50 ml tube.

Cells were centrifuged at 1000 rpm for 10 minutes at 4°C, and keep on ice all time during manipulation.

Than cells were resuspended in a volume 1% FBS in DPBS to obtain a concentration of 2800 cell/µl (2800000 cell/ml).

Calibration

Control = cells

Control + CD90

Control + CD73

Control + CD105

Control + CD90 + CD73

Control + CD73 + CD105

Control +CD90 + CD73 + CD105

Samples + Ab-antiCD90 + Ab-antiCD73 + Ab-antiCD105

Direct immunofluorescence staining of cells:

In this technique the fluorochrome is directly linked to the primary antibody.

Fluorochromes used:

- APC: Allophycocyanin→Excitation: 635 nm; Maximal emission: 661nm
- FITC: Fluorescein isothiocyanate→Excitation: 488nm; Maximal emission: 525 nm
- PE: Phycoerythrin→Excitation: 488 nm; Maximal emission: 627nm

- **Sample:** cells incubated with the antibody of interest coniugated with a fluorocrome.
- **Blank:** sample not incubated with antibody to measure the background and the auto-fluorescence of the samples, due to intrinsic sample characteristics.
- **Negative control:** sample incubated with antibody directed to a marker that is presumed to be absent from the sample, to test the homogeneity of the sample and the presence of auto-fluorescence.
- **Isotype control:** sample incubated with an antibody that has no relevant specificity. It helps to distinguish non-specific background staining from specific antibody staining and to confirm that the binding of the antibody,

chosen to detect the protein of interest, is specific and not a result of non-specific Fc receptor binding or due to some other protein interactions. The most common antibodies used as isotype control are IgG1, IgG2a, IgG2b, IgG3, IgM, and IgA; this antibodies should be the same antibody isotype as the specific antibody.

45 µl of cell suspension were aliquoted into as many tubes as required. The antibodies were diluted at the recommended (and pre-standardized by our laboratory) dilution in DPBS.

- Blank: 45 µl of cell suspension and 5 µl of DPBS.
- Sample: 45 µl of cell suspension and 5 µl of each antibody: 5 µl of CD90-APC (1/100), 5 µl of CD105-FITC (1/10) and 5 µl of CD 73-PE (1/10). (typical MSC markers)
- Negative control: 45 µl of cell suspension and 5 µl of each antibody: 5 µl of CD45-FITC (1/10) and 5 µl of CD34-PE (1/10). (typical haematopoyetic markers).
- Isotype control: 45 µl of cell suspension and 5 µl of each isotype control: 5 µl of APC-Mouse IgG1k (1/10), 5 µl of PE-Mouse IgG1k (1/10) and 5 µl of FITC-Mouse IgG2ak (1/10).

All samples were incubated for 30 minutes at 4°C in the dark.
After the incubation cells were washed adding 500 µl of fetal calf serum (FCS; Gibco) 1% in DPBS and centrifuging samples at 180 xg for 10 min at 4°C. Cells were resuspended in 0.2 ml of PBS/BSA solution. After passing the cleaning solution (Coulter Clenz TM) in the cytometer, the samples containing cells marked with antibodies and blanks were passed in sequence.

Data were achived with Beckman Coulter Navios flow cytometer and analyzed with Navios flow cytometry software.

Biblio.

Flow Cytometry: a practical approach, 3rd Edition. Ed. By MG Ormerod Oxford University Press (2000).

Practical Flow Cytometry, 4th Edition. Howard M Shapiro, Wiley Liss (2003).

3.11 ACHIEVEMENT, MANIPULATION AND ANALYSIS OF NUCLEIC ACIDS

Purification of Total RNA from Animal Cells

For purification of total RNA from cells Quiagen RNeasy Mini Kit (Qiagen) was used.

This technology combines the selective binding properties of a silica-based membrane with the speed of microspin technology. A specialized high-salt buffer system allows up to 100 µg of RNA longer than 200 bases to be isolated.

Protocol.

After removing the culture media and washing the wells with DPBS, cells were detach from the plastic with tripsine (0,25% Trypsin/0,25% EDTA) treatment for 5 min at 37ºC. EDTA sequesters calcium ions in the solution, so cells can be easily detached because the integrin bonds are weakened. A higher concentration of EDTA is used for the trypsinization of cells seeded on biomaterials with respect to the cells seeded in a normal culture vessel because of the large amount of calcium liberated from biomaterials. (See the liberation of calcium in ICP results). Cells were centrifuged at 1000 rpm (Heraus FRESCO 21 centrifuge, Thermo Scientifics) for 10 minutes at 20° C, to eliminate tripsine and culture media residue. Biological samples are first lysed and homogenized with 350 µl of a highly denaturing guanidine-

thiocyanate-containing buffer (RLT), containing 0,01% β-mercaptoethanol to minimize degradation, which immediately inactivates RNases to ensure purification of intact RNA. The lysate of every well was pipet(ed) into a QIAshredder spin column and was centrifuged for 2 min at 8000 Xg; this step permits to homogenize the sample as it passes through the spin column. One volume of 70% ethanol was added and the sample was then applied to an RNeasy Mini spin column, and centrifuged for 1 min at 8000 Xg; the total RNA binds to the membrane in the column. Subsequently RW1 and RPE buffers were added in the column to wash the membrane by centrifugation. Purified RNA was finally eluted by adding 30 µl RNAse free water in the column and centrifuging for 2 min t 8000 Xg. These columns efficiently remove most of the DNA without needing DNase treatment. With this procedure, all RNA molecules longer than 200 nucleotides are purified. The procedure provides an mRNA enrichment since most RNAs < 200 nucleotides (such as 5.8S rRNA, 5S rRNA and tRNA, which together comprise 15-20% of total RNA) are selectively excluded. RNA can be conserved at -80ºC up to 1 year.

RNA quantification

The concentration (µg/ml) of RNA was determined by measuring the absorbance at 260 nm (A_{260}) in a BioPhotometer plus spectrophotometer de Eppendorf (A_{260}=1 → 44 µg/ml). Sample dilution was 2 µl RNA in 98 µl RNase-free water; blank was the RNAse free water used for samples dilution.

The absorbance at 280 nm was also red, providing the ratio (A_{260}/A_{280}), that is an estimation of the *purity* of the RNA with respect to contaminants like proteins, that absorb the UV spectrum. Pure RNA has a A_{260}/A_{280} ratio of 1.9-2.1.

cDNA synthesis

Retrotranscription of RNA to cDNA was performed using BIORAD iScript cDNA Synthesis Kit following manufacturer's protocol.

iScript cDNA synthesis kit components:

- the RNase H^+ iScript reverse transcriptase, a modified MMLV-derived reverse transcriptase, optimized for reliable cDNA synthesis over a wide

dynamic range of input RNA, with RNase H enzymatic activity that removes RNA in RNA:DNA hybrids to allow primer binding and second-strand DNA synthesis;

- a premixed RNase inhibitor to prevent indiscriminate degradation of RNA template;
- a unique blend of oligo(dT) and random primers that works well with a wide variety of targets, optimized for the production of targets < 1kb in lengths.

Table 3. *Reaction mixture:*

Reagents	**Volume per reaction**
5x iScript reaction mix	4 µl
iScript reverse transcriptase	1 µl
Nuclease-free water	x µl
RNA template (1µg total RNA)	x µl
Total volume	20 µl

Reaction protocol:

With the use of a termocycler, samples were subjected to 3 cycles of different temperatures, that permit respectively the denaturation of the RNA in the samples, the cDNA synthesis and finally to complete the synthesis of eventually incomplete templates:

- 5 min at 25°C
- 30 min at 42°C
- 5 min at 85°C

Since RT-PCR quantification of RNA is based on amplification of cDNAs, the amount of cDNA produced by the reverse transcriptase must accurately represent original amounts to enable accurate quantification, and this is what this kit ensures us. In this study was used 1 µg or RNA as starting sample.

Determining the integrity of RNA templates

After retrotranscription, the integrity of total RNA of all samples, was checked performing a PCR (Polymerase Chain Reaction). The gene amplified was β-actin, as a housekeeping internal control.

PCR (Polymerase Chain Reaction) is a simple and powerful method to amplify only a target molecule of nucleic acid of a tiny amount by cycling three incubation steps at different temperatures: double-stranded target is heat denatured (denaturation step), the two primers complementary to the target segment are annealed at lower temperature (annealing step), and the annealed primers are then extended at an intermediate temperature (extension step) with a DNA polymerase. As the target copy number doubles upon each cycle, PCR can thereby amplify DNA fragments up to 10^6-fold in a short period (exponential amplification). It is an end point assay, who measures the amount of accumulated PCR product at the end of the PCR cycle.

PCR was performed with Promega GoTaq® Hot Start Polymerase kit that contains:

- the high-performance GoTaq® DNA polymerase bound to a proprietary antibody that blocks polymerase activity. The polymerase activity is restored during the initial denaturation step when amplification reactions are heated at 94°C for one minute. This allows for hot-start PCR in which polymerase activity is inhibited at temperatures below 70°C, allowing convenient, room-temperature reaction setup. Hot-start PCR is advantageous because it may eliminate or minimize primer-dimer and secondary products.
- The 5X Green GoTaq® Flexi Buffer contains two dyes (a blue dye and a yellow dye) that separate during electrophoresis to monitor migration progress. The blue dye migrates at the same rate as a 3–5kb DNA fragment in a 1% agarose gel. The yellow dye migrates at a rate faster than primers (<50bp) in a 1% agarose gel. Green GoTaq® Flexi Buffer also increases the density of the sample, so it will sink into the well of the agarose gel, allowing direct loading without adding dye (to the mix).

The pair of primers used in this study were designed by the program Primer3 (http://biotools.umassmed.edu/bioapps/primer3-WWW.cgi) and synthesized by Roche (Roche Diagnostics S.L., Barcelona, España).

B-ACTIN	FW		*TM ºC*
	Rv		*TM ºC*

Table 4. *Reaction Mixture:*

Reagents	**Volume per Reaction**	**Final concentration**
5X Green GoTaq® Flexi Buffer	5 µl	1X
MgCl 25 mM	2,5 µl	2,5 mM
dNTPs 2,5 mM (each)	2 µl	0,2 mM (each dNTP)
Forward primer 10 µM	1 µl	400 nM
Reverse primer 10 µM	1µl	400 nM
cDNA (1µg/µl)	1 µl	40 ng
Taq polymerase (5u/µl)	0,5 µl	2,5 u
Nuclease-free water	12 µl	
Total volume	**25 µl**	

Table 5. *Cycling conditions:*

Step	**Time**	**Temperature**	
Activation	3 minutes	95°C	
Activation	4 minutes	94°C	
Denaturation	1 minute	94°C	
Annealing	1 minute	57°C	**x 40 cycles**
Extension	1 minute	72°C	
Final extension	10 minute	72°C	
Refrigeration	Forever	4°C	

Hibridation of primer at cDNA templates: 1 min at melting temperature. The hybridization temperature is cold melting temperature (Tm) and was calculated for

every oligonucleotide (primer) with the formula Tm (ºC) = 4x(G+C)+2x(A+T). Was chosen the minor temperature of the two calculated for every pair of primers, 58 ºC in this case.

Agarose Gel Electrophoresis

To visualize the PCR products all samples were then loaded on a 1,5X agarose gel to perform an electrophoresis. Agarose gel electrophoresis in denaturating conditions (presence of SDS) is used to separate nucleic acid fragments by length. Nucleic acid molecules are separated by applying an electric field, negatively charged molecules moves through an agarose matrix to the catode. Shorter molecules move faster than longer ones because they pass easily through the pores of the gel.

Preparation of an 1,5% agarose gel and electrophoresis.

200 ml of TBE 1X (40 mM Tris, q.0 mM EDTA, 30mM acetic acid) were mix with 3 g of agarose in a glass becker and heat in a microwave since it becomes transparent and reach the temperature of 65°C. When cooled the solution was pour in the electrophoresis chamber. 10 µl of Red Safe (20000X) were added and mixed with a comb. (Red Safe final concentration was 1X). The combs were placed and the gel let cool down and solidify.

20 µl of every sample were charged in the wells created by the comb. 10 µl of marker was charged in the first well.

An electric field of 120 V was applied for 30 minutes. Finally the gel were place in a the transilluminator (SYNGENE) and visualized under a blue light (… lenght). Photos were captured with GeneSnap software.

Real-time PCR (RT-PCR) or Quantitative PCR

Starting from cDNA, gene expression was analyzed with two-step RT-PCR.

Real time PCR is a highly sensitive technique enabling amplification and quantification of a specific nucleic acid sequence with detection of the PCR product in real time, that means at the same time that the reaction take place. So the data are collected throughout the PCR process, rather than at the end of the amplification. In real-time PCR, reaction are characterized by the point in time during cycling when amplification of a target is first detect rather than the amount of target accumulated after a fixed number of cycles. This is in contrast with end-point detection in conventional PCR, which does not enable accurate quantification of a sample of nucleic acids. If PCR products are analyzed by end-point analysis, quantification is not possible as most reactions have reached the plateau phase of amplification. During this phase, no significant increase in the amount of PCR product takes place. This is mainly due to depletion of PCR components and renaturation of PCR product strands caused by the high concentration of end products, which prevent further primer annealing. If identical template amounts are used, this may not necessarily result in identical yields of PCR products; it makes the quantification impossible. Real-time PCR overcome this problem by determining the actual amount of PCR product present at a given cycle, indicated by the intensity of fluorescence.

Detection of PCR products in real-time

In this thesis, real time PCR was used for an accurate quantification of starting amount of cDNA target. PCR products can be detected using fluorescent dyes that bind to double-stranded DNA. Applied Biosystems supplies the reactive Power SYBR® Green Master Mix.

The fluorescent dye SYBR Green I binds all double-stranded DNA molecules, emitting a fluorescent signal of a defined wavelength when bounded (Fig.1.). The excitation and emission maxima of SYBR Green I is at 494 nm and 521 nm, respectively. Detection takes place in the extension step of real-time PCR. Signal

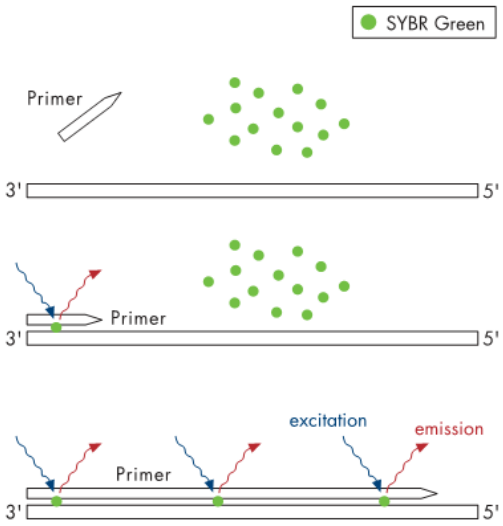

Fig. 30. SYBR Green principle. Principle of SYBR Green-based detection of PCR products in real-time PCR (A).

intensity increases with increasing cycle number due to the accumulation of PCR product. Unfortunately, nonspecific PCR products and primer–dimers will also contribute to the fluorescent signal. Therefore, high PCR specificity is required when using SYBR Green. **E quindi come ottengo la specificità???? Adjust reaction conditions! Aggiungere.**

Basic terms used in real-time PCR

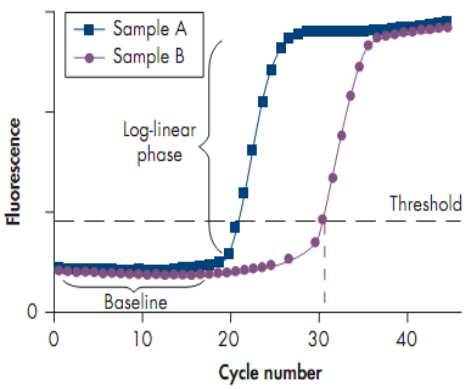

Fig. 31. Typical amplification plot (A).

Before levels of nucleic acid target can be quantified in real-time PCR, the raw data must be analyzed and baseline and threshold values set. Analysis of different PCR products from a single experiment requires threshold adjustment for each individual assay. Data are displayed as a sigmoidal-shaped amplification plots, in which the fluorescence is plotted against the cycle number (Fig 2.).

Baseline. Baseline is the noise level in early cycles, tipically measured between cycle 3 to 15, where there is no detectable increase in fluorescence due to the amplification products. This refers to nonspecific fluorescence in the reaction, for example, due to the presence of large amounts of double-stranded DNA template when using SYBR Green. The background component in this case is mathematically removed by the software algorithm of the real-time cycler.

Threshold. Threshold is adjusted to a value above the background and significantly below the plateau of an amplification plot, within the linear region of the amplification curve, which represents the detectable log-linear range of the PCR. The threshold value should be set within the logarithmic amplification plot view to enable easy identification of the log-linear phase of the PCR. If several targets are used in the real-time experiment, the threshold must be set for each target.

Threshold cycle (C_T). Is the cycle at which the amplification plot crosses the threshold line. C_T allows calculation of the starting template amount. Major is the abundance of a transcript, minor is the C_T obtained, because the sigmoidal curve shifts to the left.

Endogenous reference gene. An endogenous control is a genepresent in each experiment, and whose expression level should not differ between samples, such as a housekeeping gene. The expression level of this gene, should also not vary under experimental conditions. Comparing the CT value of a target gene with that of the endogenous reference gene, allows normalization of the expression level of the target gene to the amount of input RNA or cDNA. So an endogenous reference gene corrects for possible RNA degradation or presence of inhibitors in the RNA sample, and for variation in RNA content, reverse-transcription efficiency, nucleic acid recovery, and sample handling. In this case was utilized GAPDH.

No template control (NTC): A control reaction that contains all essential components of the amplification reaction except the template. Detection of fluorescence in an NTC reaction indicates the presence of contaminating nucleic acids.

Standard curve: To generate a standard curve, CT values/crossing points of different standard dilutions are plotted against the logarithm of input amount of standard material. The standard curve is commonly generated using a dilution series of at least 4 different concentrations of the standard. Each standard curve should be checked for validity, with the value for the slope falling between –3.3 to –3.8. Standards which give a slope differing greatly from these values should be discarded.

Efficiency and slope: The slope of a standard curve provides an indication of the efficiency of the real-time PCR. It can be calculated plotting the Ct values (Y axis) against the log template amount (cDNA) (X axis). A slope of –3.322 means that the PCR has an efficiency of 1, or 100%, and the amount of PCR product doubles during each cycle. A slope of less than –3.322 is indicative of a PCR efficiency <1. Generally, most amplification reactions do not reach 100% efficiency due to experimental limitations. A slope of greater than –3.322 (e.g., –3.0) indicates a PCR efficiency which appears to be greater than 100%. This can occur when values are measured in the nonlinear phase of the reaction or it can indicate the presence of inhibitors in the reaction. From the slope (S), efficiency can be calculated using the following formula:

$$\textbf{PCR efficiency (\%)} = (10^{(-1/S)} - 1) \times 100$$

Melting curve analysis

After PCR is completed, melting curve analysis can be performed to check the specificity of the reaction, for example detecting the presence of primer dimer. The energy required to break the base-base hydrogen bonding between two strands of DNA depends on their length, GC content and their complementarity. By heating a reaction-mixture that contains double-stranded DNA sequences and measuring dissociation against temperature, these attributes can be inferred.(si può togliere).

This dissociation between two DNA-strands can be measured using SYBR green thanks to the large reduction in fluorescence that results. Primer dimer usually consist of short sequences, so denaturate at lower temperature than the target sequence and hence can be distinguished giving a different melting curve.

Quantification of target amounts

By selecting the threshold within the log-linear phase for all samples, it is possible to calculate the actual amount of starting molecules since the fluorescence intensity is directly proportional to the amount of PCR product in the exponential phase.

Comparative method or ΔC_T method of relative quantification

In relative quantification, the ratio between the amounts of a target gene and an endogenous reference gene is determined. This ratio is then compared between different samples. The C_T of every gene was compared with the C_T of an endogenous reference gene. Relative quantification permits, after showing that the efficiencies of the target and endogenous control amplifications are approximately equal, eliminate the need of a standard curve. With this method the exact amount of template in the reaction is not determined.

The ΔCT value for each sample is determined by calculating the difference between the CT value of the target gene and the CT value of the endogenous reference gene.

ΔC_T(sample) = C_T target gene – C_T endogenous reference gene

If the PCR efficiencies of the target gene and endogenous reference gene are comparable, the normalized level of target gene expression is calculated by using the formula:

Normalized target gene expression level in sample = $2^{-\Delta CT}$

Components

- **Qiagen Rotor-Gene Q.** For performing real time RT-PCR was used Qiagen Rotor-Gene Q, an innovative real-time cycler that enables high-precision real-time PCR thanks to its unique rotary design. The tubes rotate in a chamber of moving air, which results in uniform and accurate temperatures for every sample. Because tubes rotate this machine eliminates the sample-to-sample variations that typically occur in block-based instruments due to the laser movement.

- **TaKaRa SYBR® Premix Ex TaqTM (Perfect Real Time).** RT-PCR is performed using TaKaRa SYBR® Premix Ex TaqTM (Perfect Real Time), a 2X concentration of premix reagent including the hot start enzyme TaKaRa Ex TaqTM HS, dNTPs and Mg buffer specific for this enzyme.

- **Qiagen QuantiTect Primer Assays.** Primers specific for gene of the osteoblastic lineage were obtained from the GeneGlobe Web Portal (Qiagen) (see table). Each tobe consists of a mix of specific forward and reverse primers that are derived from gene sequences contained in the NCBI Reference Sequence database and are validated for the costumer. They are designed in order to produce an amplicon which size is <150 bp and to cross exon/exon boundaries, where possible, enabling amplification of RNA sequences only. This prevents coamplification of genomic DNA, which can compromise assay sensitivity and efficiency by competition between the desired PCR product and the product derived from genomic DNA, or false positive results. They are standardized to work at the same temperature. To optimize the conditions of the experiment the better primer concentration was scanned with a primer matrix. The concentrations of the every pair of primers were 50, 300, and 900 nM, combined with various concentrations of cDNA.

All primers were tested for their efficiency with 4 cDNA dilutions (1/10, 1/50, 1/100, 1/500) and the dilution chosen to analyze the gene expression was 1/10 corresponding to 100 ng of cDNA as a starting concentration template. Each reaction was run in duplicate (technical replicates) and each gene was run together with its own GAPDH and a negative control. The gene expression levels were normalized to the expression of the housekeeping gene GAPDH used as endogenous reference gene. To quantify the samples was used the comparative CT method ($2^{-\Delta CT}$).

Table 6: Reaction Mixture.

Reagents	Volume	Final Concentration
SYBR® Premix Ex TaqTM (2X)	10 µl	1x
Primer F + R (10X)	2 µl	1x
cDNA 100 ng	1 µl (+ 4 µl H□O)	5 ng
H□O	3 µl	
Total volume	20 µl	

Table 7: Cycling conditions.

Step	Time	Temperature	Detection
Activation	3 min	95°C	OFF
Denaturation	5 sec	95°C	OFF
annealing/ extension	34 sec	60°C	ON
Number of cycles	40		

Because the SYBR green technique is not specific for the fragment produced, like explained before, at the end of every real time PCR was run a dissociation curve (melting ramp from 70 to 95°C)., to assure the amplification of a unique product (resulting in a unique peak).

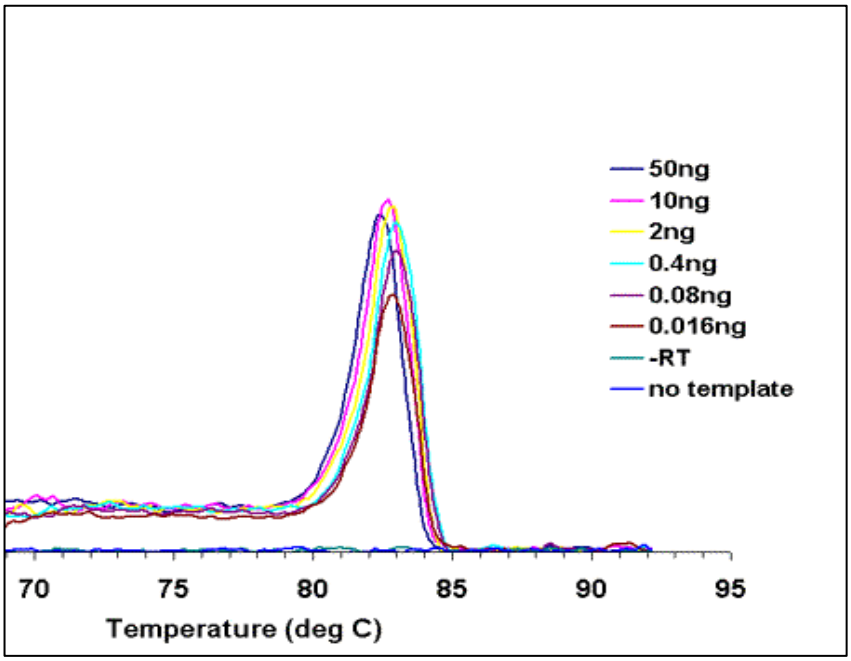

Fig. 33: Real Time PCR principle. Example of dissociation curve

A. Real Time PCR principle. The SYBR green I intercalates (and binds) all double-stranded DNA molecules synthesised by polymerase enzyme. While his quantum rate in free form is low, on binding emits a fluorescent signal of a defined wavelength. The excitation and emission wavelenghts of SYBR Green I are at 494 nm and 521 nm, respectively. Detection takes place in the extension step of real-time PCR. Signal intensity increases with increasing cycle number due to the accumulation of PCR product. Use of SYBR Green enables analysis of many different targets; however, non specific PCR products and primer-dimers, like the fragment size, will also contribute to the fluorescent signal.
B. Example of dissociation curve. This is very important to attest that the amplification product obtained by Real Time PCR is one.

3.12 INDIRECT IMMUNOFLUORESCENCE

Immunofluorescence is a technique that allows the visualization of a specific protein or antigen of the cell or a tissue section by the binding of a antibody directed to …... Distinguiamo tra (it is distinguish between): 1) direct immunofluorescence staining in which the primary antibody is labeled with a fluorescent dye, and the more common 2) indirect immunofluorescence staining in which a secondary antibody labeled with a fluorochrome recognize a primary antibody. Indirect immunofluorescence has a greater sensitivity than direct immunofluorescence, in fact there is an amplification of the signal because more than one secondary antibody can attach to each primary antibody. Commercially produced secondary antibodies are relatively inexpensive and available in an array of colors. Disadvantages of indirect immunofluorescence include the potential cross-reactivity between antibodies and the need to find primary and secondary antibodies that are not raised in different species. In this study was preferred the use of indirect immunofluorescence for laboratory antibodies availability and because this technique was just previously standardize.

Fixation step before staining is very important. Perfect fixation would immobilize the antigens, while retaining native cellular and subcellular architecture and permitting unhindered access of antibodies to all cells and subcellular compartments. To ensure access of the antibody to its intracellular citoplasmatic antigen, moreover cell membranes must be permeabilized. A large number of fixation (paraformaldeide, methanol) and permeabilization (alcohols, detergents such as Titon X-100 or SDS) techniques are available.

To fix and permeabilise at the same time in this study was choose the methanol-acetone fixation method. Methanol and Acetone remove lipids and dehydrate the cells, while precipitating the proteins on the cellular architecture. Removing membrane lipids the membrane becomes permeable to antibodies and preserves antigen epitopes characteristics (antigenicity), but they preserve cell structure less than cross-linking reagents.

Blocking step is en important passage, to avoid the inespecific unions of the antibody with other proteins. Samples are usually incubated with a BSA (Bovin serum albumin) solution or most specifically with the pre-immune serum from the donor specie of the secondary antibody (or if not possible serum from a different specie from the one in which has been developed the primary antibody). In this case was used goat serum, a serum different from the serums in which are developed all antibodies.

DAPI (DAPI or 4',6-diamidino-2-phenylindole) is a blue fluorescent probe that fluoresces brightly upon selectively binding to the minor groove of double stranded. DAPI has an absorption maximum at a wavelength of 358 nm (ultraviolet-UV) and its emission maximum is at 461 nm (blue). Therefore for fluorescence microscopy DAPI is excited with UV light and is detected through a blue/cyan filter.

Immunofluorescence stained samples are examined under a fluorescence microscope,

Procedure

Cell preparation:

Cells were grown up in 24-well plates until end time points established: 7, 14, 21, 28 days.

Culture medium was discarded from the wells, paying attention do not touch the biomaterials and the monolayer. Monolayers were washed three times with DPBS (at least 5 minutes each), and the excess DPBS removed.

Methanol-Acetone Fixation:

Ice-cold Methanol-Acetone solution (1:1) previously prepared and stored in -20 freezer, was added to every well and samples were incubated for 10 minutes at -20°C. The solution excess was discarded and the well let dry, by evaporation of the alcohol. Samples were stored at -20 ºC if it was not possible to stain them

immediately. When proceeding to staining only was required samples rehydratation in PBS for 5 minutes.

Triton Permeabilization:

To ensure good permeabilization, after methanol-acetone fixation-permeabilization step, samples were also treated with Triton X-100 1% in DPBS solution.

The cells were incubated with Triton X-100 1% in DPBS for 15 minutes at RT, the solution was discarded and wells washed three times with DPBS (at least 5 minutes each).

Blocking:

Samples were blocked in 10% normal goat serum in DPBS for 30 minutes at RT to block unspecific binding of the antibodies; and after the blocking solution discarded.

Samples staining:

Primary antibodies were diluted 1:100 in the blocking solution in DPBS solution and 200 µl (minimum volume necessary to cover a well of 24-well plate) were added to each well; every primary antibody was used to stain two wells (duplicates). Samples were incubated ON at 4°C, in a dark humidified chamber in agitation. The following day wells were washed three times with Triton 0,1% in DPBS (at least 5 minutes each).

Fluorochrome-conjugated secondary antibodies were diluted 1:500 in the DPBS and DAPI nuclear stainer were added at every dilution at a final concentration of 1µg/µl. 200 µl of each secondary antibody solution was added to the correspondent right previously incubated with the primary antibody wells (see table under); and samples incubated for 30 minutes at 37° C, in a dark humidified chamber.

The excess of staining was eliminated by washing with DPBS (three times at least 5 minutes each). Samples were stored at 4° C in the dark, until the moment of the analysis, covered wit a small amount of DPBS to avoid monolayers drying.

Evaluation:

Samples were inspected under a fluorescence microscope, and images taken. The Nikon Eclipse TE 2000-U is an EPI-inverted microscope, that permits analysis of 24 well-plates.

Tab. 8: Combinations of primary and secondary antibodies:

Primary Ab	**Dilution**	**Secondary Ab**	**Dilution**
Anti-collagen type I	1:100	Alexa Fluor® 488 goat anti-rabbit IgG	1:500
Anti-Osteocalcin	1:100	Alexa Fluor® 488 goat anti-rabbit IgG	1:500
Anti-Osteopontin	1:100	Alexa Fluor® 488 goat anti-rabbit IgG	1:500
Anti-Heparan Sulfate Proteoglycan	1:100	Alexa Fluor® 488 goat anti-rat IgG	1:500
Anti-β Tubulin	1:200	Alexa Fluor® 488 goat anti-mouse IgGA	1:500

3.13 SCANNING ELECTRON MICROSCOPY (SEM)

The scanning electron microscope (SEM) uses a focused beam of high-energy electrons to generate a variety of signals at the surface of solid specimens. The signals that derive from electron-sample interactions reveal information about the sample including external morphology, chemical composition, crystalline structure and orientation of materials making up the sample.

Scanning process

An electron beam is emitted from an electron gun fitted with a tungsten filament cathode. The electron beam, that has an energy ranging from 0.5 kV to 40 kV, is focused by condenser lenses to a spot about 0.4 nm to 5 nm in diameter. The beam passes through pairs of scanning coils or pairs of deflector plates in the electron column which deflects the beam in the *x* and *y* axes and scans in a raster fashion over a rectangular area of the sample surface. When the primary electron beam interacts with the sample, the electrons lose energy by repeated random scattering and absorption within the interaction volume of the sample, which extends from less than 100 nm to around 5 µm into the surface. This energy is dissipated as a variety of signals produced by electron-sample interactions when the incident electrons are decelerated in the solid sample. These signals include secondary electrons (that produce SEM images), backscattered electrons (BSE), diffracted backscattered electrons (EBSD that are used to determine crystal structures and orientations of minerals), photons (characteristic X-rays that are used for elemental analysis), visible light (cathodoluminescence), and heat.

Detection of secondary electrons

The most common imaging mode collects low-energy (<50 eV) secondary electrons that are ejected from the k-orbitals of the specimen atoms by inelastic scattering interactions with beam electrons. Due to their low energy, these electrons originate within a few nanometers from the sample surface. The electrons are detected by a scintillator-photomultiplier system. They are first attracted towards an electrically-biased grid at about +400 V, and then accelerated towards a scintillator positively biased to about +2,000 V. The accelerated secondary electrons are now sufficiently energetic to cause the scintillator to emit flashes of light (cathodoluminescence) which are conducted to a photomultiplier. The amplified electrical signal output is displayed as a two-dimensional intensity distribution that can be viewed and photographed on an analogue video display, or subjected to analog-to-digital conversion and displayed and saved as a digital image. The brightness of the signal depends on the number of secondary electrons reaching the detector.

Energy-dispersive X-ray spectroscopy (EDS)

Energy-dispersive X-ray spectroscopy is an analytical technique used for the elemental analysis or chemical characterization of a sample. It relies on the investigation of a sample through interactions between electromagnetic radiation and matter, analyzing X-rays emitted by the matter in response to being hit with charged particles. Its characterization capabilities are due to the fundamental principle that each element has a unique atomic structure allowing X-rays, that are characteristic of an element's atomic structure, to be identified uniquely from one another. To stimulate the emission of characteristic X-rays from a specimen, a high-energy beam of charged particles such as electrons is focused into the sample. At rest, an atom within the sample contains ground state electrons in discrete energy levels or electron shells bound to the nucleus. The incident beam may excite an electron in an inner shell, ejecting it from the shell while creating an electron hole. An electron from an outer, higher-energy shell then fills the hole, and the difference in energy between the higher-energy shell and the lower energy shell may be released in the form of an X-ray. As the energy of the X-rays are characteristic of the difference in energy between the two shells, and of the atomic structure of the element from which they were emitted, this allows the elemental composition of the specimen to be measured. The number and energy of the X-rays emitted from a specimen can be measured by an energy-dispersive spectrometer, however, EDS systems are most commonly found on scanning electron microscopes (SEM-EDS). A EDS spectrum is portrayed as a plot of x-ray counts vs. energy (in kV). Energy peaks correspond to the various elements in the sample. Generally they are narrow and readily resolved, but many elements yield multiple peaks. Elements in low abundance will generate x-ray peaks that may not be resolvable from the background radiation.

Magnification

SEM can reach a magnification of 500000X. Unlike optical and transmission electron microscopes, image magnification in the SEM is not a function of the power of the objective lens, which function is to focus the beam to a spot, and not to image

the specimen. In a SEM, magnification results from the ratio of the dimensions of the raster on the specimen and the raster on the display device. So it has a high resolving power and creates images that are a good tridimensional representation of the surface specimen.

Sample preparation (cells seeded on the biomaterials):

- Rinse the cells seeded over the biomaterial with DPBS.
- Fix in 3% glutaraldehyde in 0.1M cacodylate buffered (pH 7.2- 7.4) for one hour at 4°C. Living cells require chemical fixation to preserve and stabilize their structure.
- Rinse and postfix in osmium tetroxide (4% in H□O) for 1 hour.
- Dehydrate through a series of increasing concentrations of ethanol (30, 50, 70, 90 vol.%), with final dehydratation in absolute alcohol. Because air-drying causes collapse and shrinkage, dehydration is commonly achieved by critical point drying, that involves replacement of water in the cells with organic solvents.
- Replace ethanol with liquid CO□ at high pressure, drying samples by the critical point method in an acetone and CO□ bath in a Balzers Union CPDO2 chamber.
- Sputter coat samples with carbon (~200Å) in a Bio-Rad Polaron Division vaporiser. Coating with conductive materials prevents the accumulation of static electric charge on the specimen during electron irradiation.

The samples were observed with a Jeol JSM-6100 scanning electron microscope equipped with an EDS system (INCA; Oxford instruments UK) with an acceleration of 15 to 20 kV. The diameter of the sites of interest analyzed with the EDS-spectra is about 5-10 μm.

3.14 AHMSCS FLUORESCENT PROTEINS TRANSFECTION

The expression vector used in the present study were derived from p*IRES1hyg* (Clontech, Cambridge, UK). p(*eGFP*) I*RES1hyg* was generated by subcloning eGFP cDNA as a B*am*HI + N*ot*I insert from p*EGFP-N1* (Clontech, Cambridge, UK) into the B*am*HI + N*ot*I digested p*IRES1hyg*. Isolated cells were electroporated using the Electroporador Gene Pulser-II (Bio-Rad Laboratories, Inc). Electroporation was performed in a sterile cuvette with a 0.4 cm electrode gap (Bio-Rad Laboratories, Inc), using a single pulse of 270 V, 500µF. 5µg plasmid DNA was added to 1.5×10^6 viable hPDL-derived cells in 0.4 ml electroporation solution (α-MEM) before electrical pulsing. Drug selection of stable transfectants was performed with 50-100 µg/ml hygromycin B (hyg; Calbiochem, La Jolla, CA).

3.15 STATISTICAL ANALYSIS

To prove the distribution of the variables a Kolmogorov – Smirnoff test was done, to prove the normal distribution. After that parametrical tests were used to hypotesis contrast. Student t test for paired samples and ANOVA of one factor were used.

Results

4. RESULTS

4.1 INDUCTIVELY COUPLED PLASMA OPTICAL EMISSION SPECTROMETRY ANALYSIS

The behaviour of the scaffolds under acellular culture conditions was investigated in order to predict the ion concentrations the cells are exposed to, when cultured on the scaffolds as a function of time. Figure 1 shows the ICP-OES results for Ca release relative to EC1, EC2 and EC3. The trend of Ca elemental concentration that EC1 and EC2 release in the culture medium is comparable, in fact the Ca concentration is quite similar until 24 h incubation hours (~93 and ~73 ppm respectively). For both EC1 and EC2 it increases starting from 24 h and reach a pick at 4 days (~183 and ~143 ppm) when remains quite stable until the 24th day of incubation, when starts to decrease until the 32th day (~121 and ~88 ppm) when probably reach the minimum and maintains stable. The Ca concentration that EC3 release in the medium follow the same trend of the other two materials, in fact was found the higher concentrations between 4^{th} and 24^{th} day in medium soacking, but the difference resides in the numbers, Ca concentrations move from ~50 to ~80 ppm, that are lower than concentrations in EC1 and EC2 samples. Very interestingly are results obtained from the incubation of the bigger pieces, those used for PCR and Cytometry analysis (we remember that the volume of medium in which the pieces were soaked was calculated following … directions). For EC1 material was found a value of ~100 ppm al the starting point of 3 h, and release begin to increase from 4^{th} day (~230 ppm) study, the increase was very strong and maintain until day 16^{th} (~319 ppm), when starts to decrease and at 28^{th} days reach a minimum pick lower than starting values (~32 ppm). For EC2 was fin a pick before, at 4^{th} day, with a subsequent continuous decrease until day 12^{th} when didn't reach the stability and fluctuate between a range similar of the small pieces one. Finally EC3 bigger pieces Ca release is comparable with those of the smaller pieces, with a not important peak at 4^{th} day.

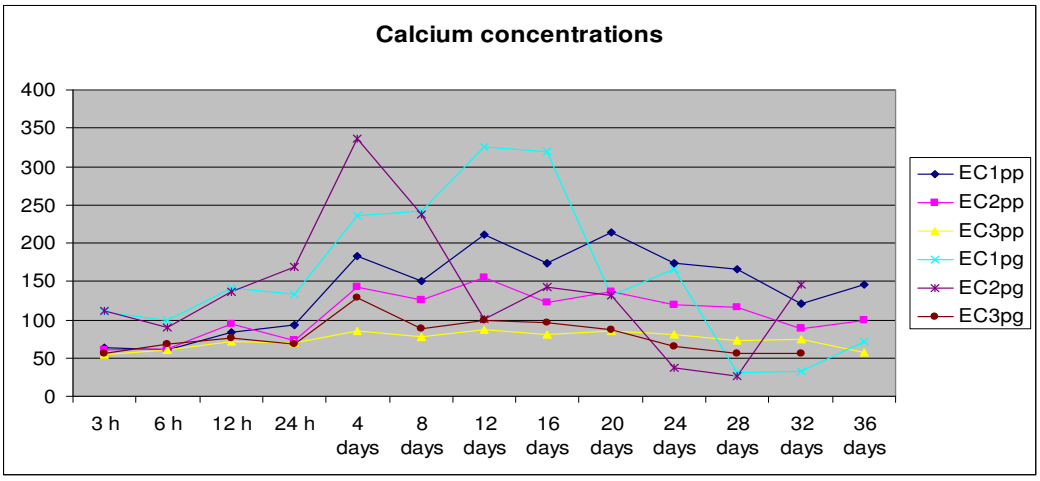

Fig. 1: Graph of Calcium concentrations plotted versus time. Values obtained by ICP-OES analysis after EC1, EC2 and EC3 smaller and bigger pieces soaking in growth medium. 36 days study.

For EC1 the P concentrations decreased during the whole incubation period from ~30 to ~10 ppm; for EC2 P concentrations registered were not very different and maintain close to 30 ppm and decreasing to ~20 ppm at 36th day. Very surprising were EC3 data: starting concentration registered was of ~53 ppm, and the release increased to reach the maximum (~85 ppm) at 4th day maintaining until 20th day when begins to fall down the release reaching the minimum (~57 ppm), similar to starting values, at 36th day. For bigger pieces values of P release registered were lower than for the smaller pieces of the corresponding material, and decrease when time passing.

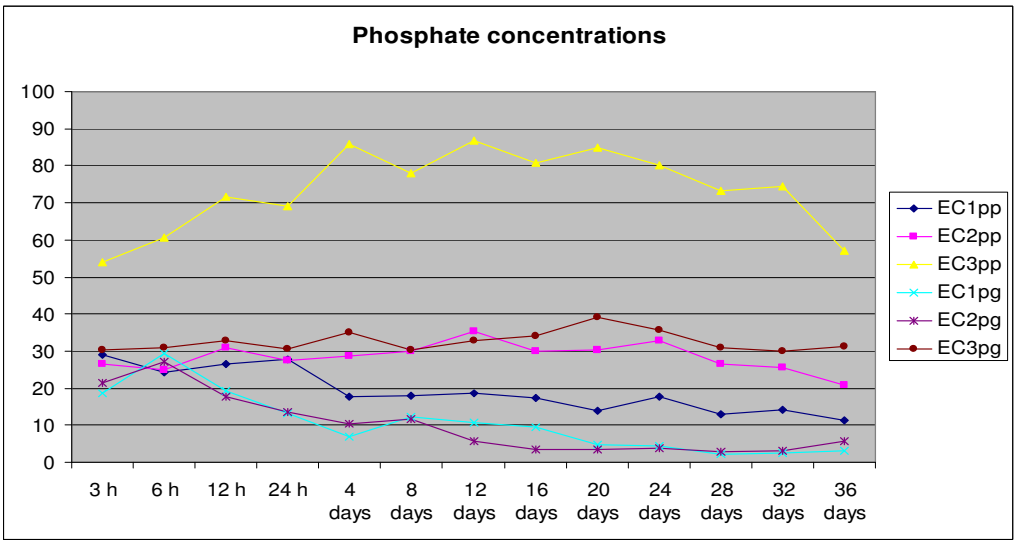

Fig. 34: Graph of Phosphate concentrations plotted versus time. Values obtained by ICP-OES analysis after EC1, EC2 and EC3 smaller and bigger pieces soaking in growth medium. 36 days study.

Analysis of Si release in medium for the three materials highlights differences more evident than in Ca and P graphs. The three materials material start release Si slowly, with very low values (in the range of 4 ppm); from 24 h for EC1 and EC2 is visible that starts the Si release increase, with a first peak at 4th day; but after EC1 follow Si release increase with some fluctuations but reaching a peak at day 20th (~78 ppm). In EC2 samples after the 4th day decrease Si concentrations in the medium and values maintain constant ~26 ppm until the last time point of the study, 36th day.

In EC3 samples conversely Si concentrations registered were very low or non detectable during the entire period, meaning no or low release from EC3 material.

For the bigger pieces samples of EC1 material the trend was respected, the curve has the same aspect than the one obtained for smaller pieces, but the values are higher (higher peak ~114 ppm at day 20th). EC2 bigger pieces samples showed the same trend of EC1 pieces with a maximum at 20th day (~134 ppm). And finally bigger pieces samples of EC3 material confirm data of smaller pieces, with values lower than EC1 and EC2, but was registered a ppeak at 4th day with subsequent slow but continuous decrease in bulk concentration.

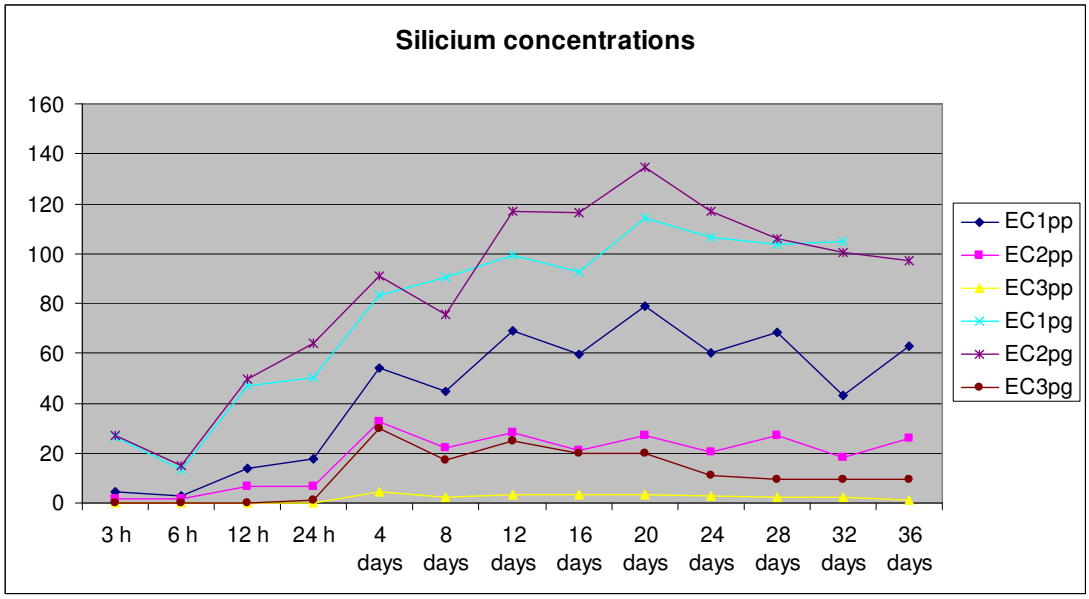

Fig. 35: Graph of Silicium concentrations plotted versus time. Values obtained by ICP-OES analysis after EC1, EC2 and EC3 smaller and bigger pieces soaking in growth medium. 36 days study.

It is important to bear in mind that cells in all the assays were seeded at day 7th, after the materials were maintained 1 week soaking, because was previously seen that during the first week the pH in the growth medium are more elevated than physiological pH required in cell cultures (~ 7 – 7.5). So first week ICP-OES data serve us to understand materials behaviour, but only the data from 8th day to 36th day are useful to comparative analysis with the other assays of this study. For this reason this assay extends until day 36th (and the other assays end at day 28th).

4.2. CELL VIABILITY AND GROWTH

Cells proliferation is investigated by measuring the metabolic activity of the cells with the MTT assay. The MTT assay permits to understand if the biomaterials tested influence cells growth. First of all, a calibration line is prepared, in order to determine absorbance values for known cell concentrations.

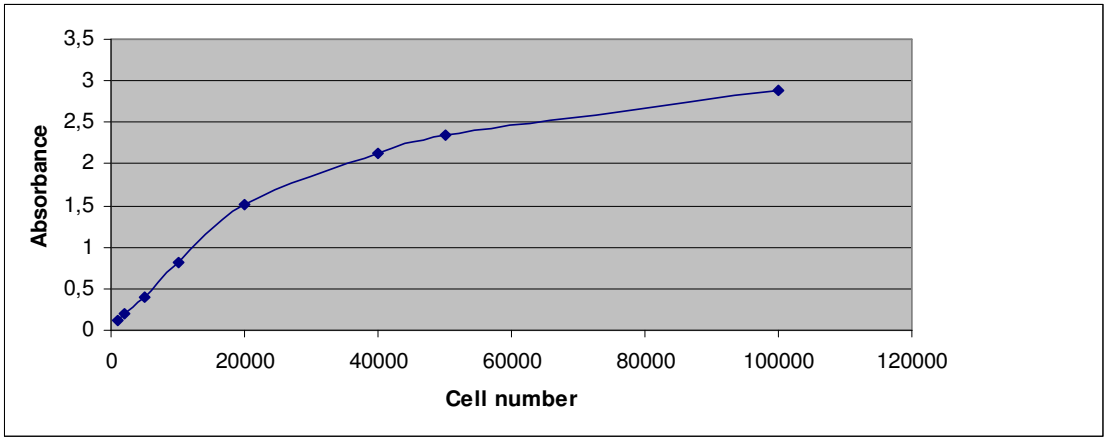

Fig. 36: Calibration line**.** Cells are seeded at different concentration and the MTT assay is performed after 24 h. The known cell concentrations are plotted against their value of absorbance to create a calibration line.

Figure 1 shows that the growth of the cell population used as control, progresses linearly with time; however the rate of proliferation is quite modest, the cells number didn't double during a week. The addition of the osteogenic medium, increases this

rate of about ~15-35% (compare 14d-21d vs 14d-21d OM and 21d- 28d vs 21d-28d OM).

The ECs biomaterials have limited deleterious effect on cell viability after the first 24h in culture, possibly because the cells have to adapt to the new environment.

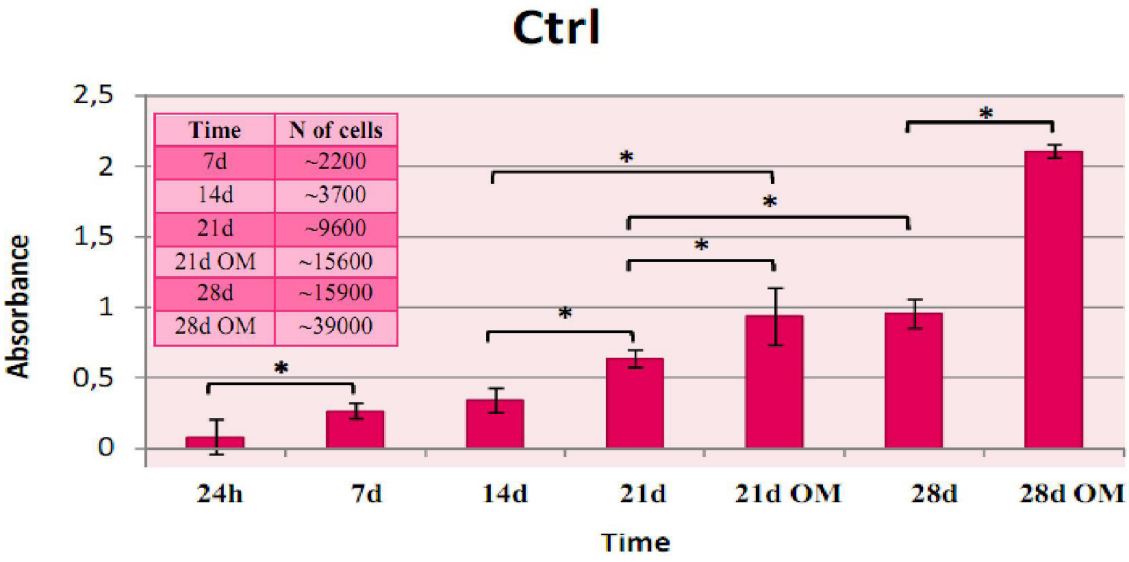

Fig. 37: Proliferation of cells seeded in plastic, used as control. * shows significance ($p < 0.05$) between the values of absorbance at the indicated days.

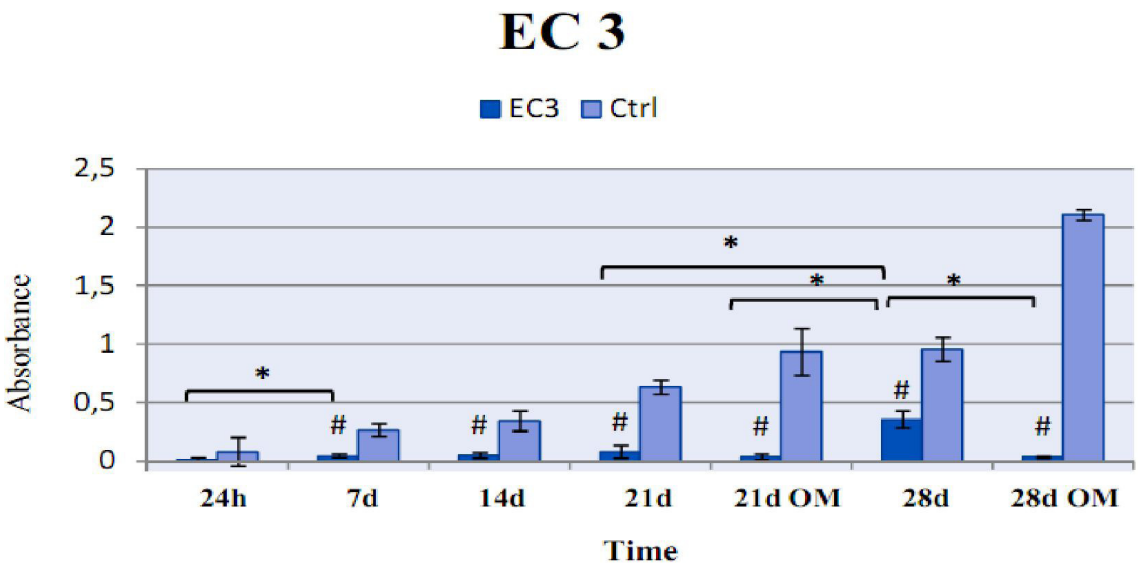

Fig. 38: Proliferation of cells seeded on EC 3 compared to the control, # shows significance at $p < 0.05$ for these samples. * shows significance at $p < 0.05$ between the values of absorbance at the indicated time points in the study.

EC1 and EC3 seem to prevent cell proliferation (figure 2, 3), with an exception for EC1 samples incubated also in the presence of the OM. The osteogenic supplements not only seem to stop the material inhibitory effects, but also enhance the positive effects on cell growth, as observed in the control.

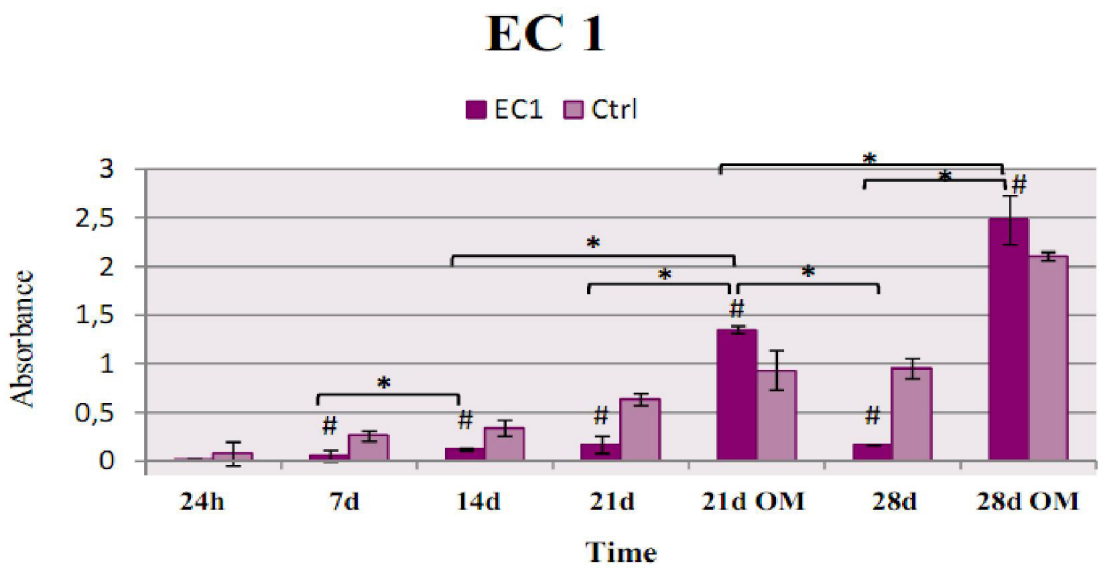

Fig. 39: Proliferation of cells seeded on EC1 compared to the control (# shows significance at $p < 0.05$ for these smaples) *shows significance at $p < 0.05$ between the values of absorbance at the indicated time points.

The most noteworthy result is the one obtained seeding ahMSC on EC 2 material (figure 4). At 24h, the low values of absorbance indicate that the number of cells initially adhered to EC2 was small. However the cells recover in a short period and, from the second week, their proliferation rate overtakes that of the control and remains constant during the whole incubation period. Starting with the second week in fact, the number of cells that grow on EC2 surface is always higher with the respect to the control. The OM increments growth of cells seeded on EC2 ceramic. This possibly is due to the calcium and phosphate ions that EC2 releases in the culture medium.

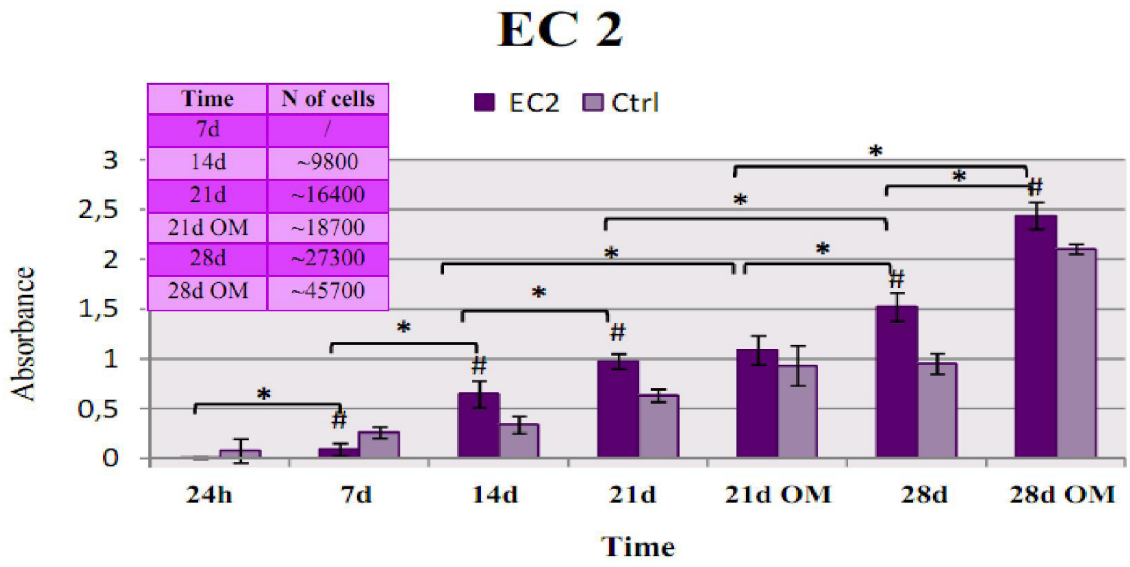

Fig. 40: Proliferation of cells seeded on EC 2compared to the control (# shows significance at $p < 0.05$ between these samples) *shows significance at $p< 0.05$ between the values of absorbance at the indicated times.

4.3 EXPRESSION OF OSTEOBLASTIC MARKERS

DNA COPY ANALYSIS

After retrotranscription, the integrity of cDNA (from total RNA) was checked by PCR. The gene amplified, as a housekeeping internal control, was the β-actin gene. A single 350 bp band was revealed in all the samples and corresponds to the amplification of the β-actin gene expected.

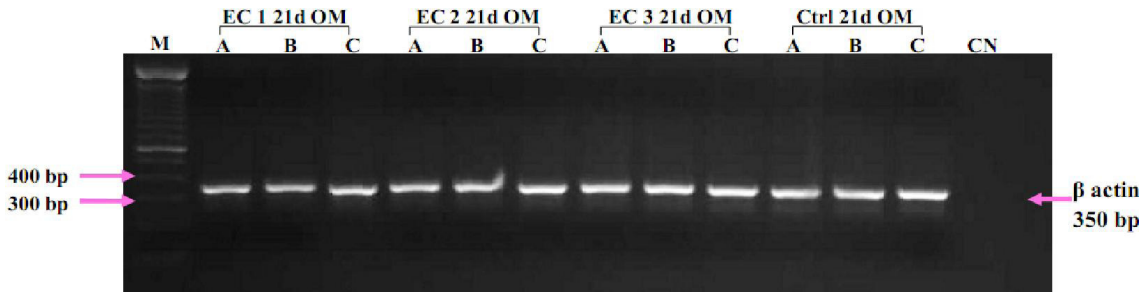

Fig. 41: Red Safe stained agarose gels of PCR products obtained from the amplification of 21 days samples in OM, using β-actin primers (F: 5' TGC GTC TGG ACC TGG CTG 3' and R: 5'GTC TTT

GCG GAT GTC CAC 3'). The left lane in each gel represents a 100-bp DNA marker (M). The letters A, B and C above the lanes refer to three distinct samples relative to the same material or the control (the triplicates). CN: negative control. The product of PCR obtained has a size of 350 bp.

These data suggest that the RNA has been correctly extracted and retrotranscribed and has a good quality because it was obtained a unique band in all the samples, with number of bp expected. In fact when degradation occurs, the recognition site of the primers may be lost and the primers would not be able to amplify the correct target and no band or smaller products would be visualized.

Then, to investigate the effect of ECs materials on MSCs differentiation, the transcription profile of a panel of osteoblastic markers of *ah*MSCs seeded on the biomaterials was examined by Real Time PCR.

RUNX2

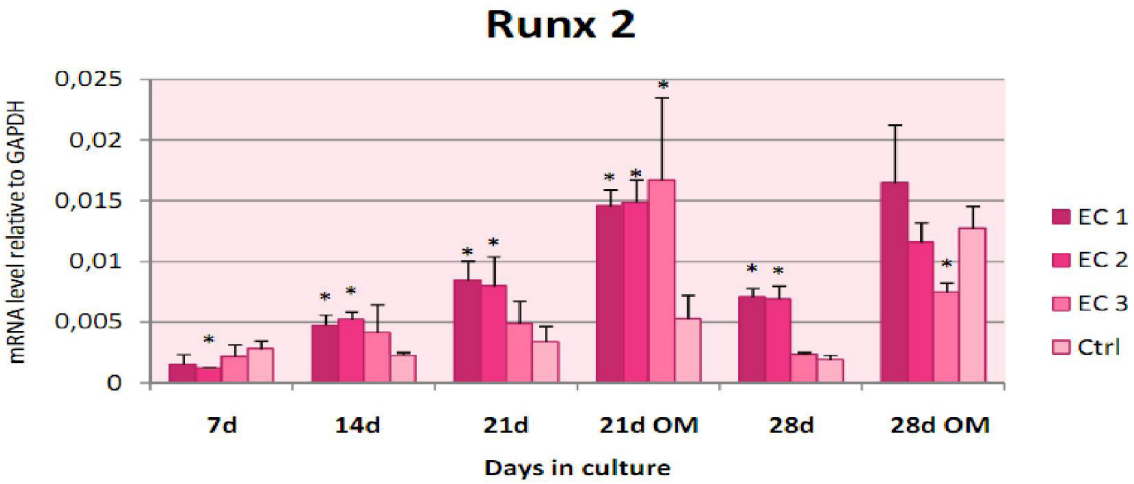

Fig.42. RUNX2 expression profile of *ah*MSCs cultured on plastic (control) and on EC materials. Data are RUNX2 mRNA levels normalized to the expression of the housekeeping gene GAPDH. The experiment was performed in triplicate and the Real Time PCR was run twice for each sample (technical duplicate). The quantification is obtained with the comparative CT method ($2\text{-}\Delta C^T$). * shows significance ($p < 0.05$) between cells seeded on the biomaterials and the control

Figure 42 shows the variation in the expression of the transcription factor RUNX2 during the whole incubation period of 28 days. Even if the activation of RUNX2

requires post-traslational modifications and its mRNA level is described to be not directly correlated with the protein levels, significant variations in its expression was detected in our work. Already from the second week, its expression augments in the cells seeded on EC1 and EC2 reaching the maximum value during the third week. The addition of the OM increments considerably RUNX2 expression relative to the ECs materials during the third week respect to the control. From the second week RUNX2 expression in the controls remains always significantly lower than EC1 and EC2, reaching a comparable expression during the fourth week of incubation in OM.

ALP

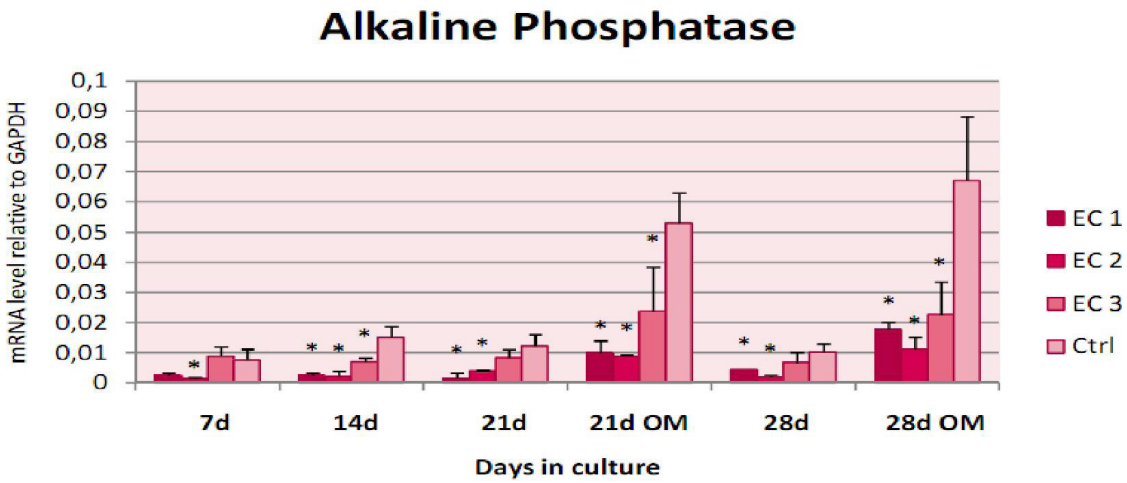

Fig.43: ALP expression profile of MSCs cultured on plates (control) and on EC materials. Data are ALP mRNA levels normalized to the expression of the housekeeping gene GAPDH. The experiment was performed in triplicate and the real time PCR was run twice for each sample (technical duplicate).The quantification is obtained with the comparative CT method ($2\text{-}\Delta C^T$). * shows significance at $p < 0.05$ between cells seeded on the biomaterials and the control.

In the case of alkaline phosphayase (ALP), the mRNA expression is apparently prevent by the biomaterials (figure 26). In fact, from the second week, its expression is always significantly lower in the cells cultured on EC1 and EC2 compared to the control. Conversely EC3 material gives results comparables with the control, in which ALP gene expression is not obstaculated. The addition of the osteogenic medium increases very much the expression in the control, which in turn remains constant in the cells cultured on ECs for 3 and 4 weeks.

A1(I) COLLAGEN

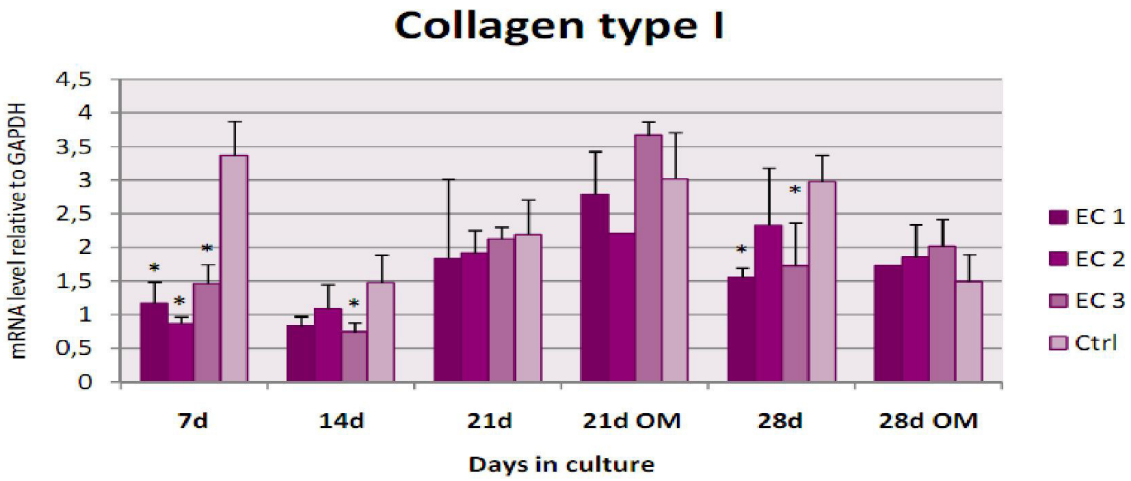

Fig.44. α1(I) collagen expression profile of MSCs cultured on plates (control) and on EC materials. Data are α1(I) collagen mRNA levels normalized to the expression of the housekeeping gene GAPDH. The experiment was performed in triplicate and the real time PCR was run twice for each sample (technical duplicate). The quantification is obtained with the comparative CT method ($2^{-\Delta C^T}$). * shows significance at $p < 0.05$ between cells seeded on the biomaterials and the control.

The expression of α1(I) collagen in the control is often superior to the ECs in presence of GM, and few significant differences are present (figure 27) during the four weeks studied. α1(I) collagen expression seems to decrease only at 21 days and 28 days in OM presence. OM presence seems to increase α1(I) collagen expression at 21 days when cells are seeded on EC2 material.

OSTEONECTIN

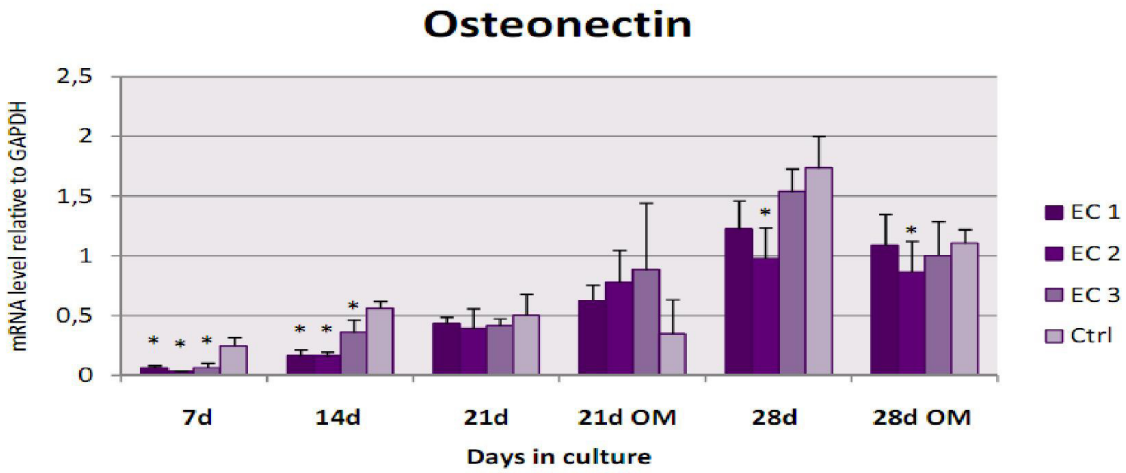

Fig.45: OSN expression profile of MSCs cultured on plates (control) and on EC materials. Data are OSN mRNA levels normalized to the expression of the housekeeping gene GAPDH. The experiment was performed in triplicate and the real time PCR was run twice for each sample (technical duplicate).The quantification is obtained with the comparative CT method ($2\text{-}\Delta C^T$). * shows significance at $p < 0.05$ between cells seeded on the biomaterials and the control.

Also in osteonectin (OSN) expression only few significant differences can be noted between cells seeded on the ECs materials and the controls (figure 28). The expression, that seems to increase with time, are not expected as the ON role as early marker in osteoblasts differentiation. This considerations suggest a regulation at the level of translation.

OSTEOPONTIN

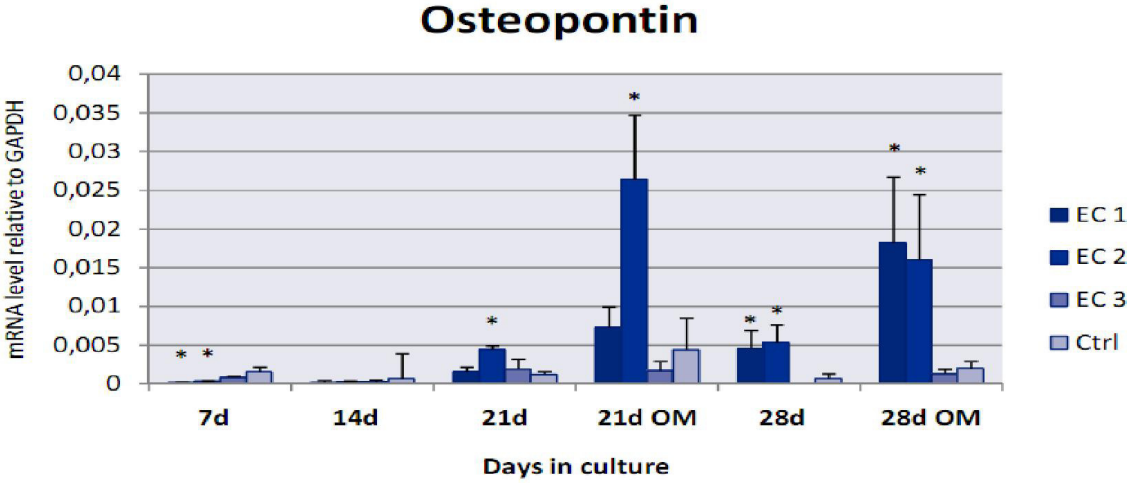

Fig.46. OPN expression profile of MSCs cultured on plates (control) and on EC materials. Data are OPN mRNA levels normalized to the expression of the housekeeping gene GAPDH. The experiment was performed in triplicate and the real time PCR was run twice for each sample (technical duplicate).The quantification is obtained with the comparative CT method ($2^{-\Delta C^T}$). * shows significance at $p < 0.05$ between cells seeded on the biomaterials and the control.

Osteopontin (OPN) seems to be stimulated by both EC1 and EC2 (figure 29). EC2 increases significantly OPN level starting from the third week, reaching its maximum value when OM is added, being the result very significant. OPN expression relative to EC1 incubated cells, is maximum during the fourth week and in presence of OMthe . OPN expression, almost absent during the first two weeks and increased in the last 2 weeks, confirms expected results, of OPN as a mature osteoblasts marker.

BONE SIALOPROTEIN

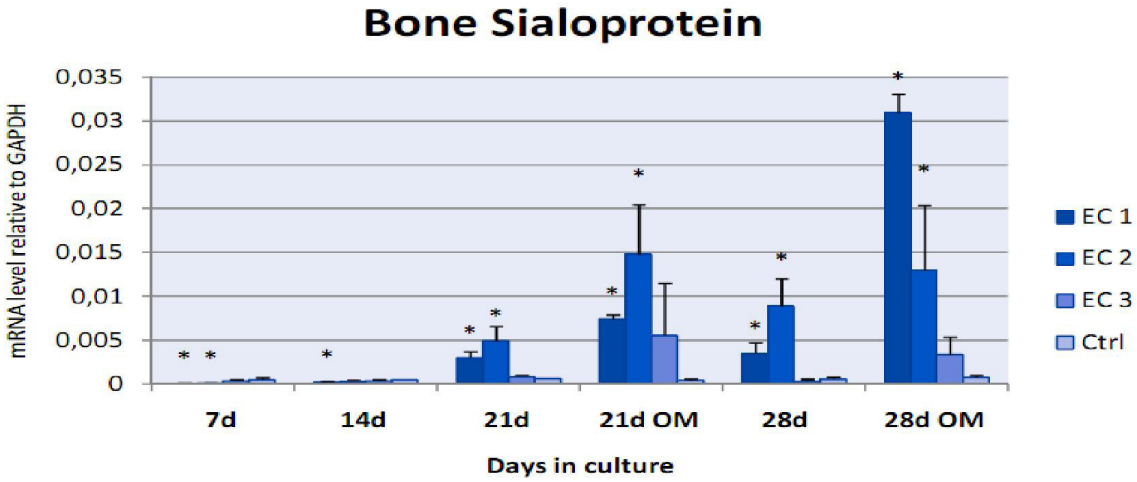

Fig.47. BSP expression profile of MSCs cultured on plates (control) and on EC materials. Data are BSP mRNA levels normalized to the expression of the housekeeping gene GAPDH. The experiment was performed in triplicate and the real time PCR was run twice for each sample (technical duplicate).The quantification is obtained with the comparative CT method ($2^{-\Delta C^T}$). * shows significance at $p < 0.05$ between cells seeded on the biomaterials and the control.

EC1 and EC2 are also able to upregulate the expression of bone sialoprotein (BSP) starting from the third week of incubation; the addition of the osteogenic supplements increments highly BSP expression level, reaching the maximum value

at 21 days for cells growth on EC2 ceramics and at 28 days for cells growth on EC1 ceramics (figure 30).

OSTEOPONTIN

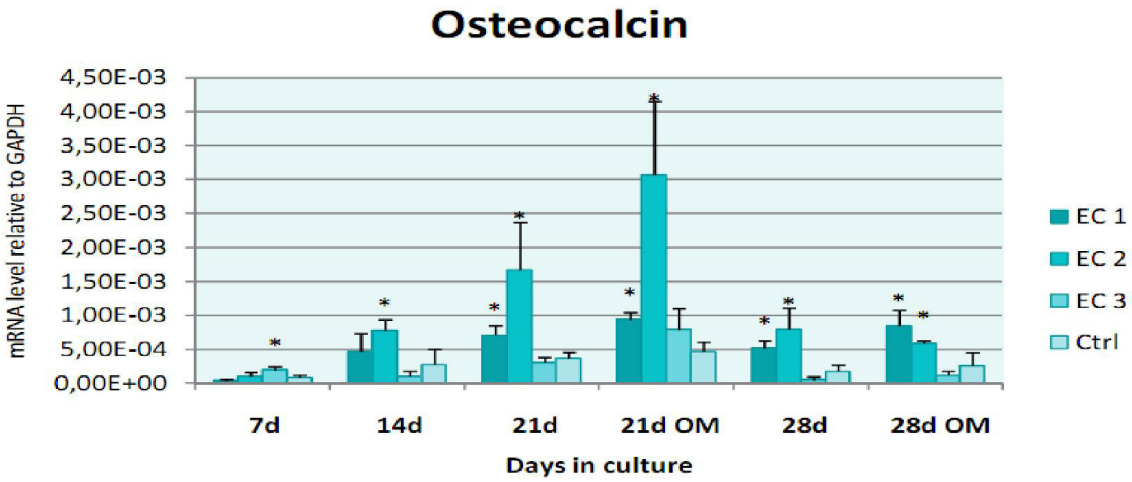

Fig.48. OSC expression profile of MSCs cultured on plates (control) and on EC materials. Data are OSC mRNA levels normalized to the expression of the housekeeping gene GAPDH. The experiment was performed in triplicate and the real time PCR was run twice for each sample (technical duplicate).The quantification is obtained with the comparative CT method ($2\text{-}\Delta C^T$). * shows significance at $p < 0.05$ between cells seeded on the biomaterials and the control.

Osteocalcin (OSC) is upregulated significantly, in comparison to the control, starting from the second week for the cells seeded on EC1 and EC2 ceramics. OC expression in EC2 samples increases until reaches its maximum level in the third week of incubation in OM. EC1 at 28 days in OM shows significant higher OC expression respect all the other samples.

4.4 ALKALINE PHOSPHATASE ACTIVITY

ALP is an important marker of osteoblastic differentiation, involved in the release of phosphate groups from many types of molecules and important for the mineralization of the extracellular matrix. ALP activity was measured by Alkaline phosphatase quantitation kit (Millipore) at 21 and 28 days. Results were processed statistically using t student test and ANOVA analysis. During the second week in culture no significant differences can be noted between cells incubated with the biomaterials and the control. After 28 days in culture, the enzyme activity in the control sample is significantly higher than in the other cases (EC1, EC2, EC3). The substitution of the normal growth medium per osteogenic medium changes the results. The activity of the enzyme in the samples incubated with EC2 and OM is higher than the control, like shown by the graph (Fig.) even if the differences are not significant. The value obtained for ALP activity in presence of EC2 material and OM, at the contrary, is significantly higher than the results obtained for the other materials (EC1, EC3) in presence of OM. Interestingly also the result for the control sample at and time point in OM is significantly higher than that obtained for EC1 material in the same study conditions.

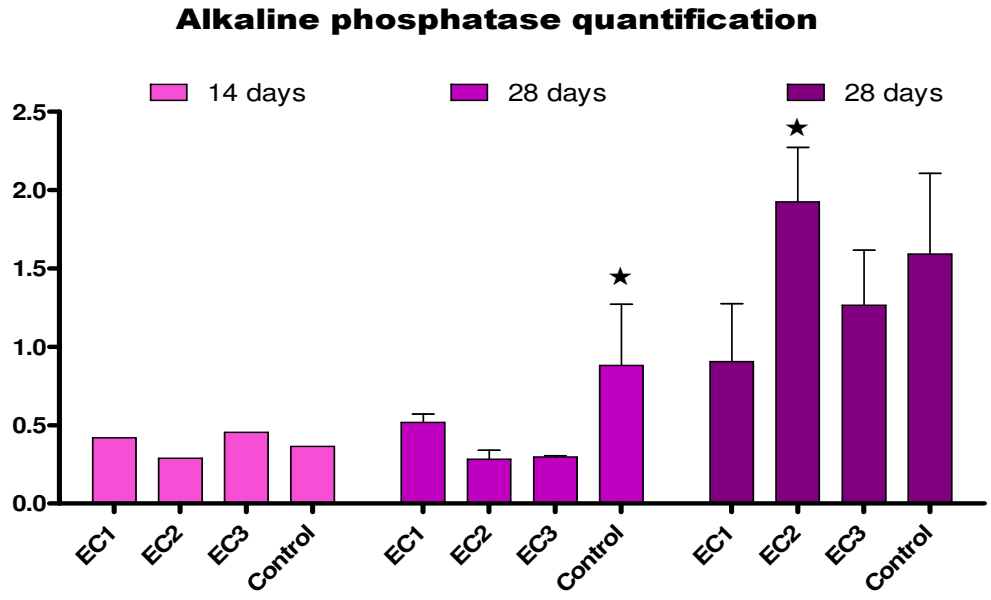

Fig. 49: Alkaline Phosphatase quantification of ahMSCs incubated with EC1, EC2, EC3 biomaterials and for the control (plastic culture). The experiment was performed in duplicate (two pieces per material) and samples were quantified twice (two elution from each sample are read). * shows

significance ($p < 0.05$, for ANOVA test) between ahMSCs incubated with biomaterials and the control.

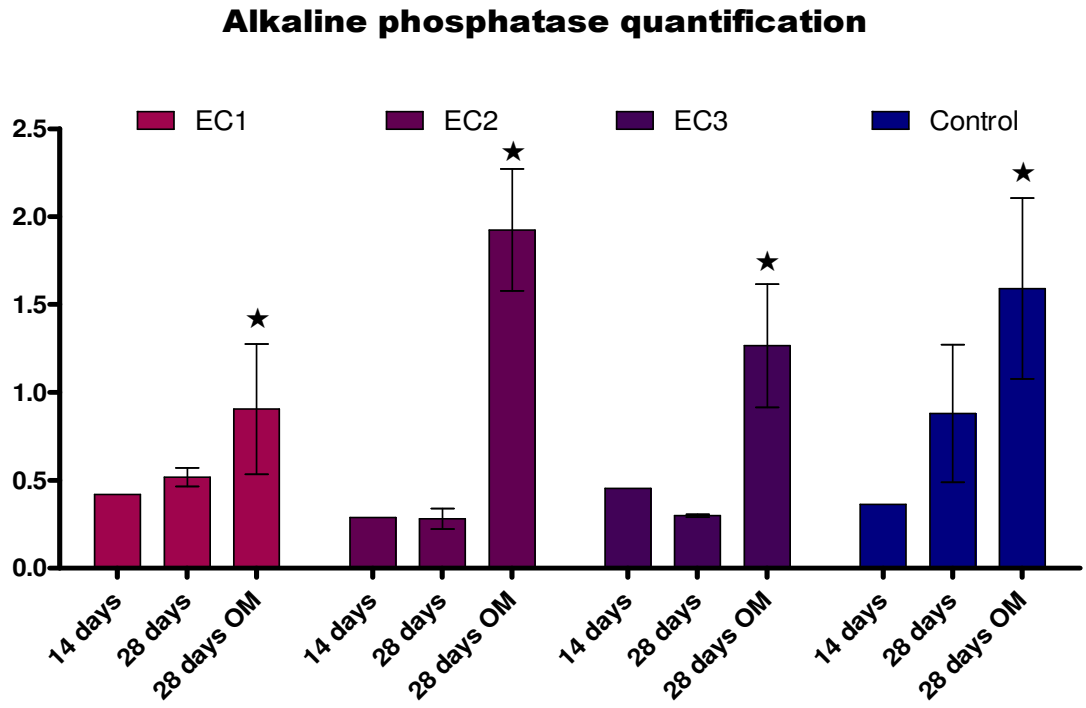

Fig. 50: Alkaline Phosphatase quantification of ahMSCs incubated with EC1, EC2, EC3 biomaterials and for the control (plastic culture). Results are shown in the graph divided by study groups (materials EC1, EC2, EC3 or control) instead by time.

* shows significance ($p < 0.05$, for ANOVA test) between ahMSCs incubated during 28 days, with biomaterials or the control in presence of GM, from the same samples incubated with OM .

Plotting the data of each material versus the time, results show better how in OM ALP activity increases significantly at 28 days compared to the values obtained at 14 days and 28 days in basal GM.

T student analysis data demonstrate a significant increase in ALP activity at 28 days for all the samples treated with OM instead of GM (in the presence of EC1, EC2, EC3 or in plastic control cultures), obtaining the great difference in samples containing the piece of EC2 biomaterial.

4.5 MINERAL CRYSTALS DEPOSITION

Mineralization nodules are visualized by staining with alizarin red dye, that permits to visualize calcium rich deposits in cell cultures, and can be also extracted to be quantified (Millipore osteogenesis kit).

During the second and third weeks of incubation with the biomaterials and/or the osteogenic supplements only few small spots spread in the monolayer can be visualized (data not shown). Conversely, a consistent red staining of cell cultures in the wells containing EC1 and EC2 biomaterial pieces was shown during the fourth week of incubation with the OM. Also cells of the control and cultured in the presence of EC3 biomaterial pieces show broad red stains but not as strong as occurs for the other two materials (figure , left column). To notice, after 28 days in culture with the normal growth medium and EC2 material, a modest red staining was identified, suggesting the beginning of the deposition of calcium crystals in samples cultivated in basal growth madium. The monolayers incubated with EC1 and EC2 materials in GM show only a weak staining, which is totally absent in the control (figure , right column).

The quantitative analysis shows a great increment in the alizarin red concentration during the fourth week of culture in OM for cells incubated with EC1 and EC2, with significant differences registered between these samples with and EC3 and control samples. No significant variations are detected with t student analysis between samples incubated with biomaterials and the control at the other time points of the study (Fig.).

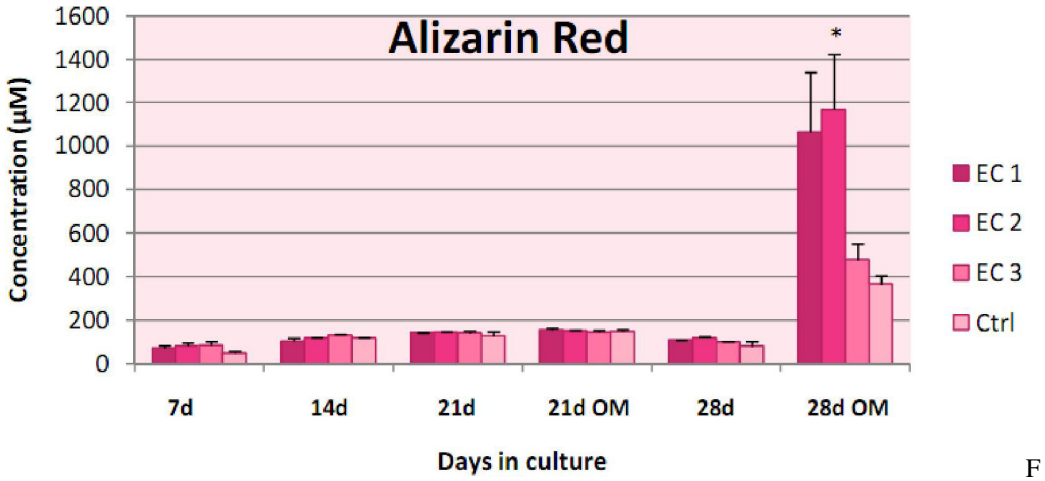

F

Fig. 51: Alizarin red dye quantification of ahMSCs incubated with or without EC1, EC2, EC3 biomaterials. The experiment was performed in duplicate (two pieces per material) and samples were quantified twice (two elutions from each sample were red).

* shows significance ($p < 0.05$ for ANOVA analysis) between ahMSCs incubated with biomaterials and the control.

Although this is roughly the situation revealed by the qualitative analysis, some limits of the technique used have to be considered. During the dye extraction with acetic acid from the monolayer, some aggregates of cells frequently form most of all during the last two weeks when the cells are very confluent and when the osteogenic medium is added. A sort of gelatinous layer seems to be deposited on surface monolayers in the presence of the osteogenic supplements, maybe because of the great amount of ECM production. These aggregates are very difficult to dissolve and often remain blocked within the tip during their movement to the eppendorf tube, resulting in a loss of extracted dye and underestimation of the calcium deposits. In addition, when cells are very confluent, the biomaterials remain encapsulated under the monolayer, and their removal implies an ulterior loss of cells that make the samples poorly comparable due to the different amount of starting material with which the quantification is effectuated. It would be better to incubate the cells only with the dissolution product of the respective materials. In conclusion, these results show that during the fourth week, in particular if the osteogenic medium is added, mineralization takes place in samples incubated with the biomaterials

It is also possible to appreciate, in the two graphs below, the significant differences, calculated by the ANOVA analysis, between the control and the samples cultivated with the three biomaterials at 14 and 21 days. Control values are more elevated respect to the values registered for cells cultivated in the presence of the biomaterials, indicating an inhibition of the mineral crystals deposition in the presence of the three biomaterials. Conversely OM addition upset the data, suggesting that OM acts strongly on the ahMSC when in culture are present also the biomaterials.

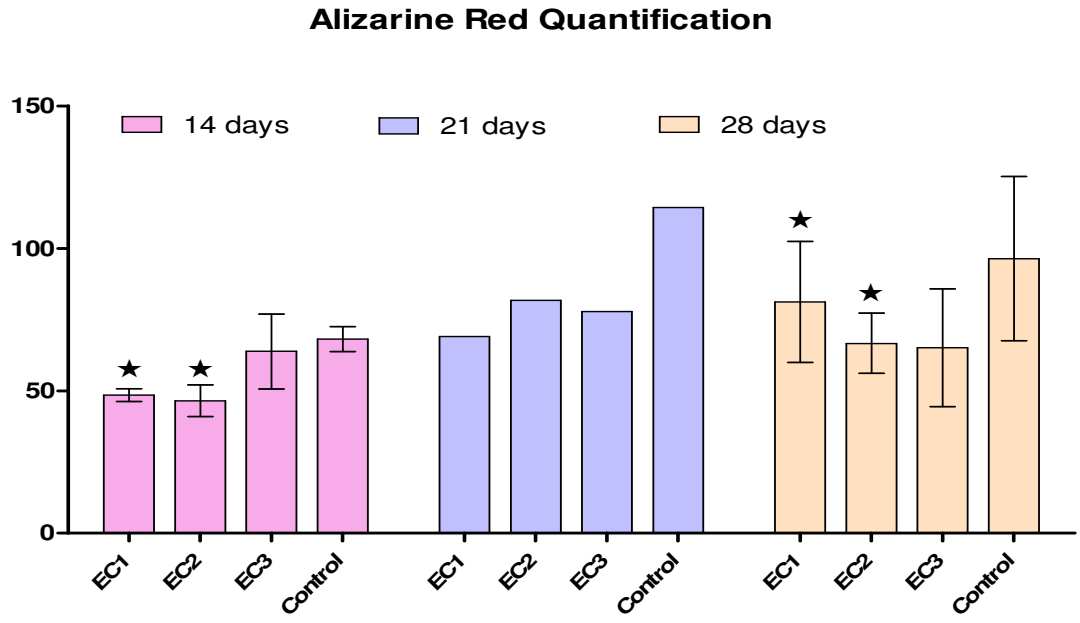

Fig. 52. Alizarin red dye quantification of ahMSCs incubated with or without EC1, EC2, EC3 biomaterials. Data grouped by weeks. It is possible to see as significant differences between control and other samples during first 3 weeks, disappear at 28 days.

* shows significance ($p < 0.05$ for ANOVA analysis) between ahMSCs incubated with biomaterials and the control.

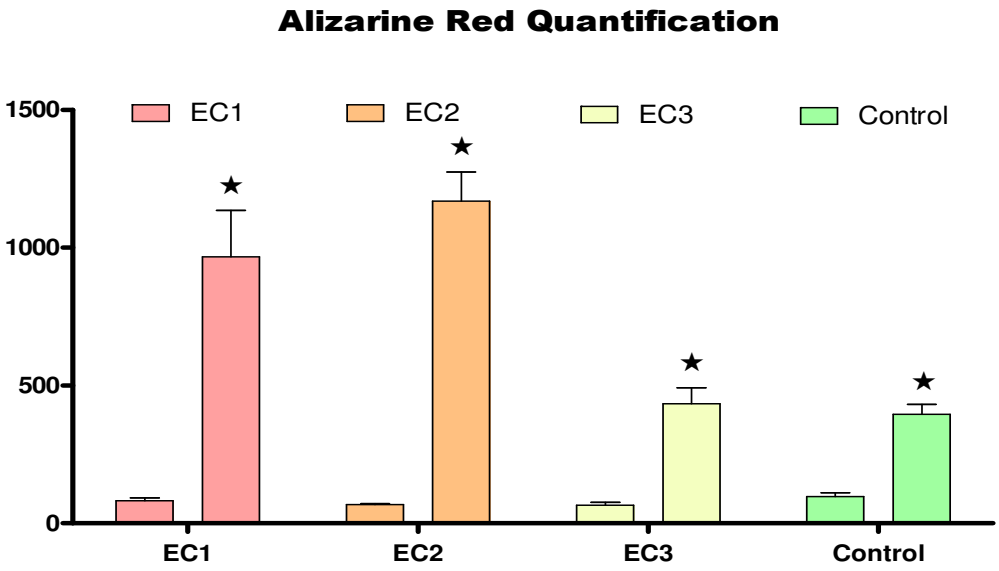

Fig. 53. Alizarin red dye quantification of ahMSCs incubated with or without EC1, EC2, EC3 biomaterials. Data highlight differences between same type of samples incubated in the presence of GM or OM. EC2 material shows the higher difference in mineralization when in these samples is added OM instead of normal GM.

* shows significance ($p < 0.05$ for ANOVA analysis) between ahMSCs incubated with biomaterials and the control.

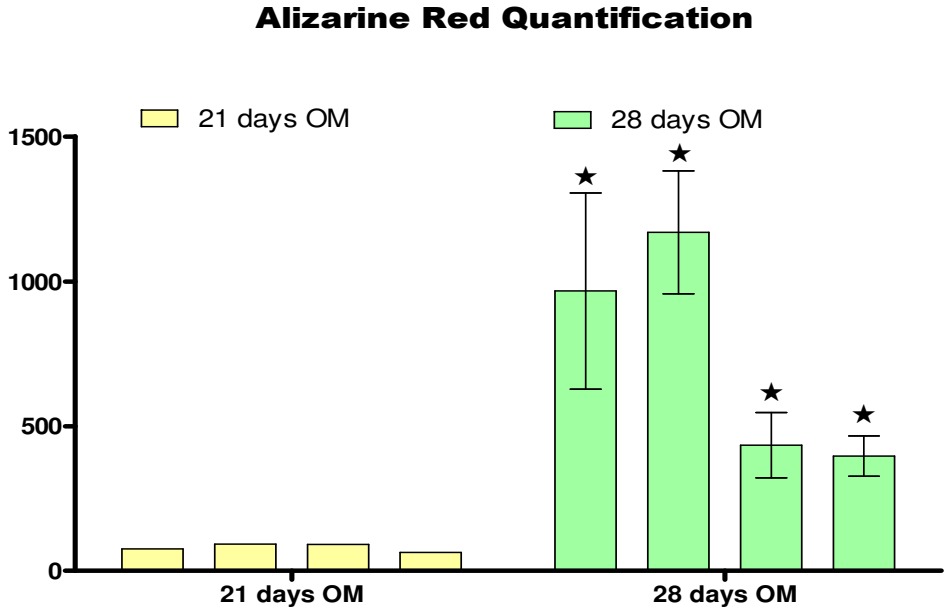

Fig. 54. Alizarin red dye quantification of ahMSCs incubated with or without EC1, EC2, EC3 biomaterials. Significant differences are shown between first and second week in culture with OM for all samples.

* shows significance ($p < 0.05$ for ANOVA analysis) between ahMSCs incubated with biomaterials and the control.

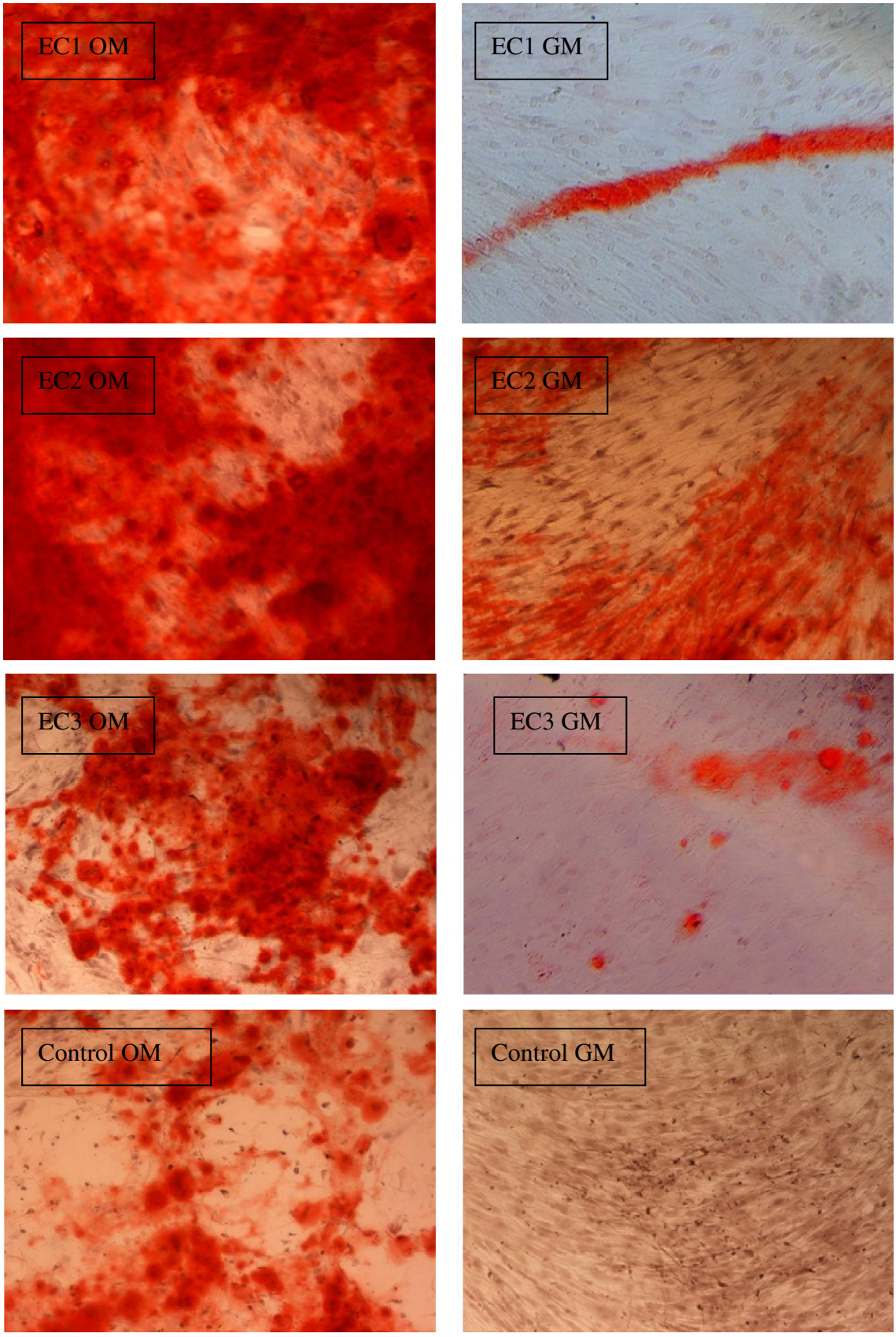

Fig. 55 Alizarin Red Staining of 28 days culture samples (EC1, EC2, EC3, Control from the top to the bottom), incubated with the osteogenic medium (left column) and growth medium (right column). Magnification 100X.

4.6 IMMUNOFLUORESCENCE STUDIES

Immunofluorescence is performed in order to detect the proteins of the extracellular matrix. This technique resulted not to be perfect to highlight differences between the cells incubated with different materials because of the elevated confluence of cells at 28 days in culture, the time when differentiation is more evident.

Collagen type I (ColI) is detected from the first weeks in culture. Figure .. is representative of the second week, many groups of cells express ColI in the samples incubated with EC1 and EC2; also samples incubated with EC3 express a little ColI and only few is express in the control. Also the Heparan Sulfate (HS) is expressed with no differences in all the samples considered. During the last two weeks of incubation, the situation in the samples incubated with the biomaterials is more homogeneous for ColI, the groups of positive cells augment also in the control but the general aspect of the control wells seems always less positive than the ones relative to biomaterials (figure 36). The HS signal is very high in all the samples considered and demonstrates the progression of the ECM deposition with time (figure 40). In this last period, also the osteoblast specific markers OPN and OSC are detected in the samples incubated with the biomaterials and significant differences between them are hard to be noted (figure 37a, b, c and 38a, b, c). OPN and OSC expression in the control is weak and suggests some aspecificities in the signals or low expression in groups of cells. The adding of the osteogenic medium increments the deposition of the extracellular matrix; a gelatinous layer in fact is visible on sample surfaces that make the capturing of the images quite hard. In this case, also the cells of the control are induced to express the osteoblast specific markers (figure 37d and 38d). Figure 39 shows very low populated areas in the wells. The monolayer has been damaged during the culture procedures and so few cells have migrated to repopulate the free area. This makes possible to visualize more clearly OPN and OSC expressed by cells incubated with EC 2 after three weeks in culture.

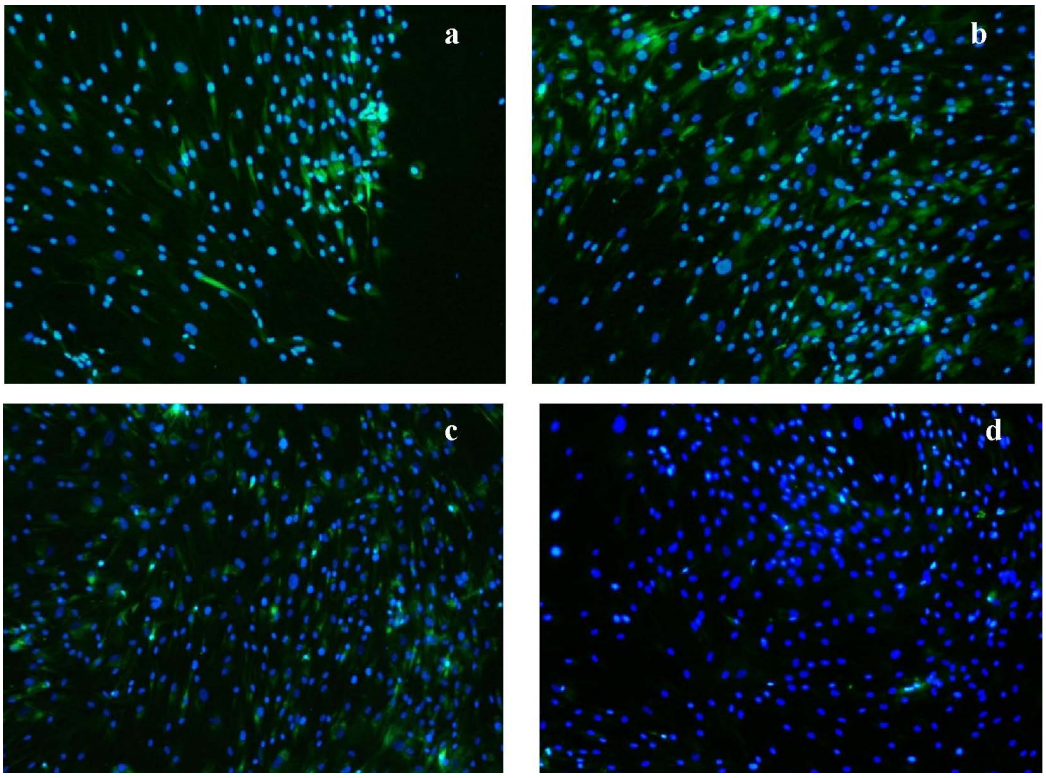

Fig. 56: Immunofluorescence images of cells i culture for four weeks incubated with EC1 (a), EC2 (b), EC3 (c) and control (d). Colagen I primary antibody and Alexa Fluor 488 secondary antibody. DAPI nuclei staining. Magnification 10X.

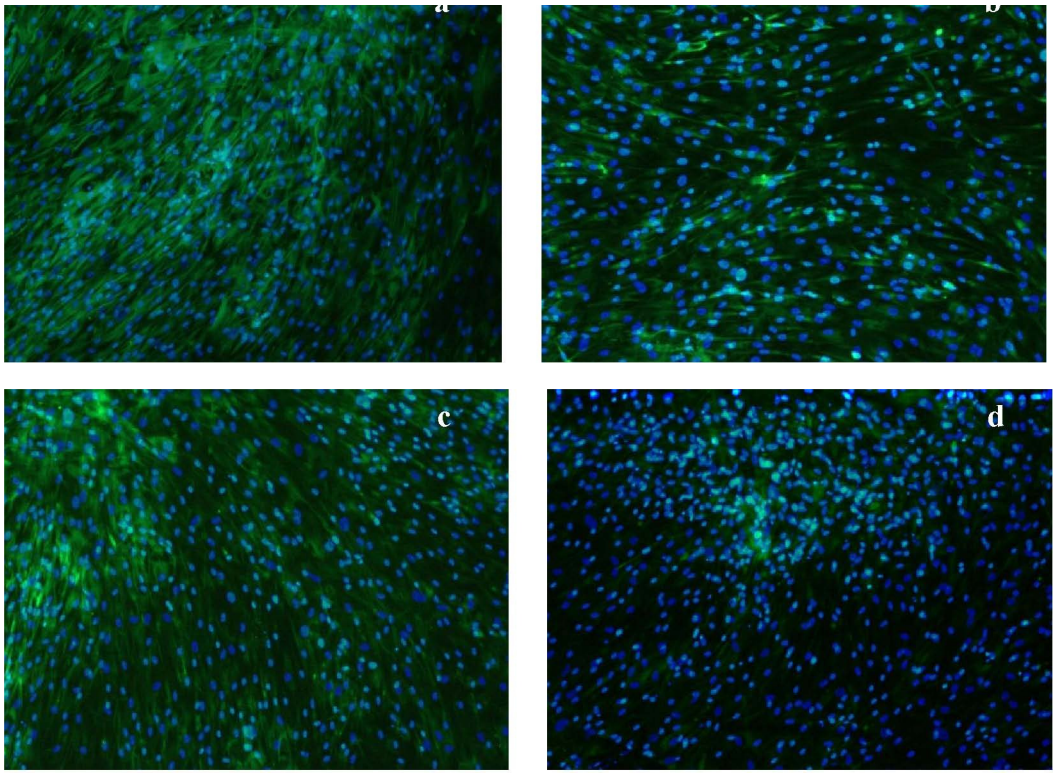

Fig. 57: Immunofluorescence images of cells i culture for four weeks incubated with EC1 (a), EC2 (b), EC3 (c) and control (d). Colagen I primary antibody and Alexa Fluor 488 secondary antibody. DAPI nuclei staining. Magnification 10X.

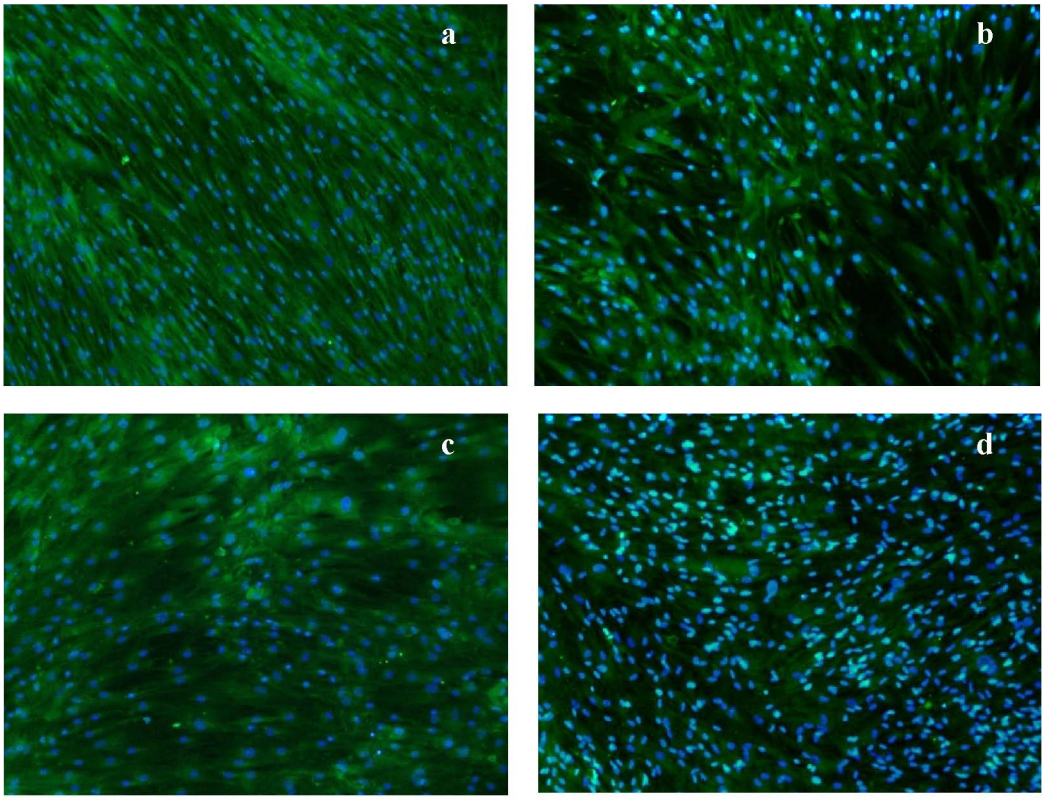

Fig. 57: Immunofluorescence images of cells i culture for four weeks incubated with EC1 (a), EC2 (b), EC3 (c) and control (d). Osteopontin primary antibody and Alexa Fluor 488 secondary antibody. DAPI nuclei staining. Magnification 10X.

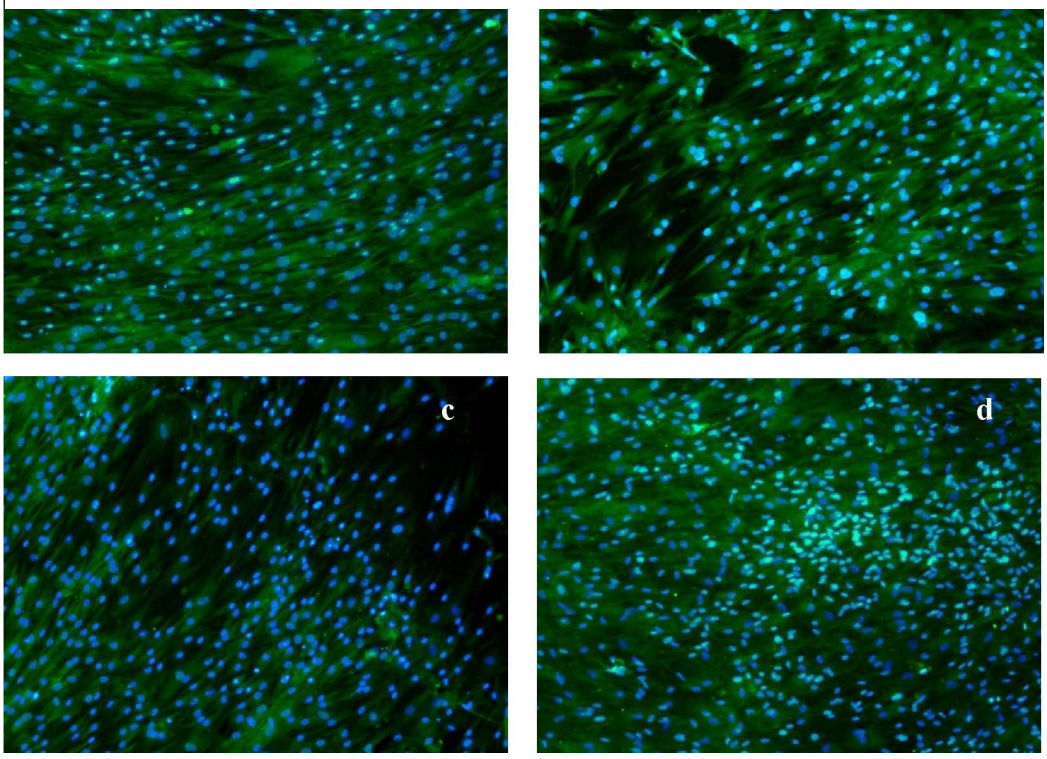

Fig. 58: Immunofluorescence images of cells i culture for four weeks incubated with EC1 (a), EC2 (b), EC3 (c) and control (d). Osteocalcin primary antibody and Alexa Fluor 488 secondary antibody. DAPI nuclei staining. Magnification 10X.

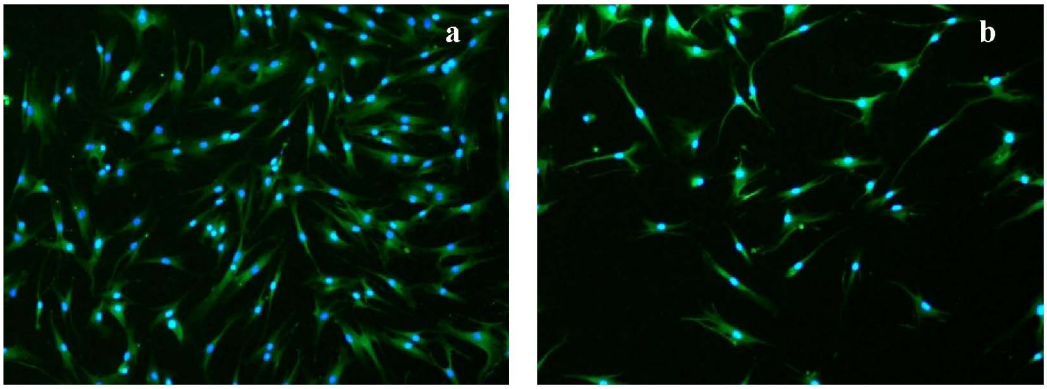

Fig. 59: Immunofluorescence images of cells i culture for four weeks incubated EC2 (b). Osteopontin (a) and osteocalcin (b) antibody and Alexa Fluor 488 secondary antibody. DAPI nuclei staining. Magnification 10X.

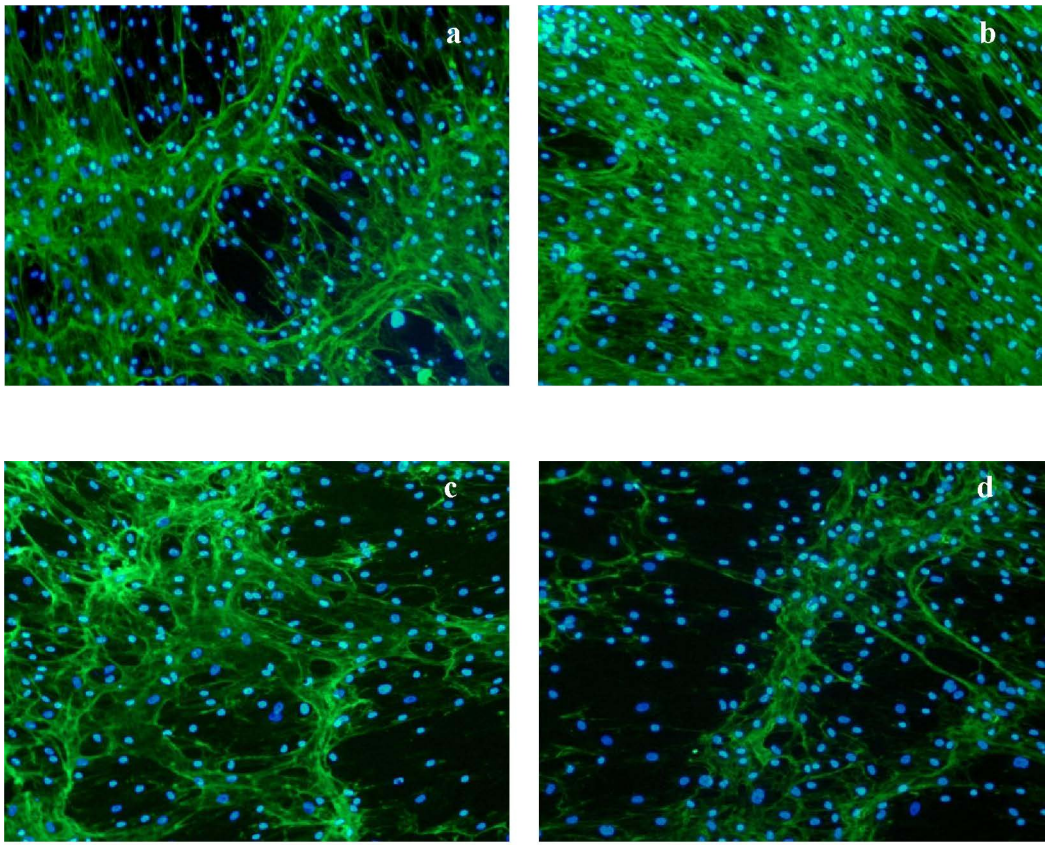

Fig. 60: Immunofluorescence images of cells i culture for four weeks incubated with EC1 (a), EC2 (b), EC3 (c) and control (d). Heparan Sulfate primary antibody and Alexa Fluor 488 secondary antibody. DAPI nuclei staining. Magnification 10X.

4.7 MORPHOLOGY AND BEHAVIOUR OF THE CELLS SEEDED ON THE BIOMATERIALS PIECES

SEM analysis permit to study cell attachment, proliferation and eventually differentiation by the deposition of collagenic proteins in the extracellular environment. Moreover permit us the validation of the bioactivity data given by the UMH Biomaterials Laboratory, in the presence of a basic growth medium and ahMSCs as cell line chosen.

At 24h ahMSCs seeded on EC1, EC2, EC3 biomaterials and feeded with normal GM, adhere to the materials surface, with flatted, round or polygonal shape and few cytoplasmatic prolongation, related with the material on which are seeded Fig. 1a-b-c). At this time point, it was observed that cells are isolated or form small disperse groups on materials surfaces. In the periphery and border of the EC2 pieces, were seen small isolated granules, in some occasions grouped (Fig. 1d). EDS microanalysis show Ca and P composition of these granules. These findings were more evident in EC2 material.

At 7 days, cells continue to adhere at materials surfaces. Some of the cells maintain a rounded globular aspect, above all in EC1 material. (Fig. 2a) and others show polygonal shape, principally in EC2 and EC3 materials (Fig. 2b-c). In this study phase, cell number grow up and was registered an increase in cytoplasmatic prolongations and cell-to-cell interactions, especially for cells seeded on EC2. At this time point, it is also considerable the mineralization nodules presence suggesting the continuity of their deposition on EC2 material surface; moreover granules are seen also above cells in contact with their membrane, so the granules form at the same time cells proliferate and cover the material surface (Fig. 2d).

At 14 days, wasn't observed relevant changes respect 7 days cultures samples, in the three materials.

At 21 days, was observed a general increase in cells number and number of interconnection established, for the three biomaterials; of the three biomaterials these results were found for EC2 (Fig. 3a), in the presence of GM as OM.
Cells that initially show rounded shape in EC1, appear more flatted at 21 days and start to show cytoplasmatic interconnections, seeming the ones observed until the moment on EC2, EC3 materials (Fig. 3b), without differences relives to the medium used. Cells remain adhered to materials surface during this period, conserving a morphology similar to the previous one. It is possible to observe more interconnections between cells, cells begin to adopt fibroblastic like shape (fusiform) and that cells cover almost all the materials pieces, with the worst trend for EC1. Intercellular spaces were filled with a fibrillar framework (with no organization), corresponding to extracellular matrix produced by cells. These findings were another time more evident in the EC2 samples (Fig. 3a) and with the best trend for those ones immersed in OM. During this period cells proliferate and cover almost all the pieces surface, with the best trend for EC2 and EC3, and showing that OM stimulate cell proliferation and not only differentiation, as the surface of the pieces in this cases are better covered by cells.

Finally, at 28 days time point, materials pieces were found to be totally covered for the cells, in GM and OM samples without differences. For EC2 and EC3 (Fig. 4a-b) samples, cells form a continuous layer (carpet), in which it is impossible to recognize single cells, covering the entire material surface (Fig. 4c). EC1 OM samples at this time point show fibrillar material in intercellular space, that is more dense and organized than in previous time points of the same samples (Fig. 4d).

At all time point cells show to adhere to biomaterials directly and firmly, and also to adhere on the neo-formed apatite layer (granules), shown to form above all on EC2 samples, with no difference between samples incubates with GM and OM. Adhesion was due principally to the cytoplasmatic prolongations of the cells (philopodia), which permit to increase cells contact surface with the biomaterials and other cells. These observations were more evident in the initial phases in EC2 and EC3 materials.

EDS MICROANALYSIS

Considering the surface evolution of the materials pieces, when in contact with the medium and the cells, it was different for the three materials and it is related with the material composition and the time immersion of the piece in the medium. The materials demonstrate to be active, to retain dynamic characteristics, when in contact with a solution like cells growth medium; they interchange ions with medium in which are immersed. These data corroborate the ones registered in ICP-OES analysis (Fig. 5a-b-c).

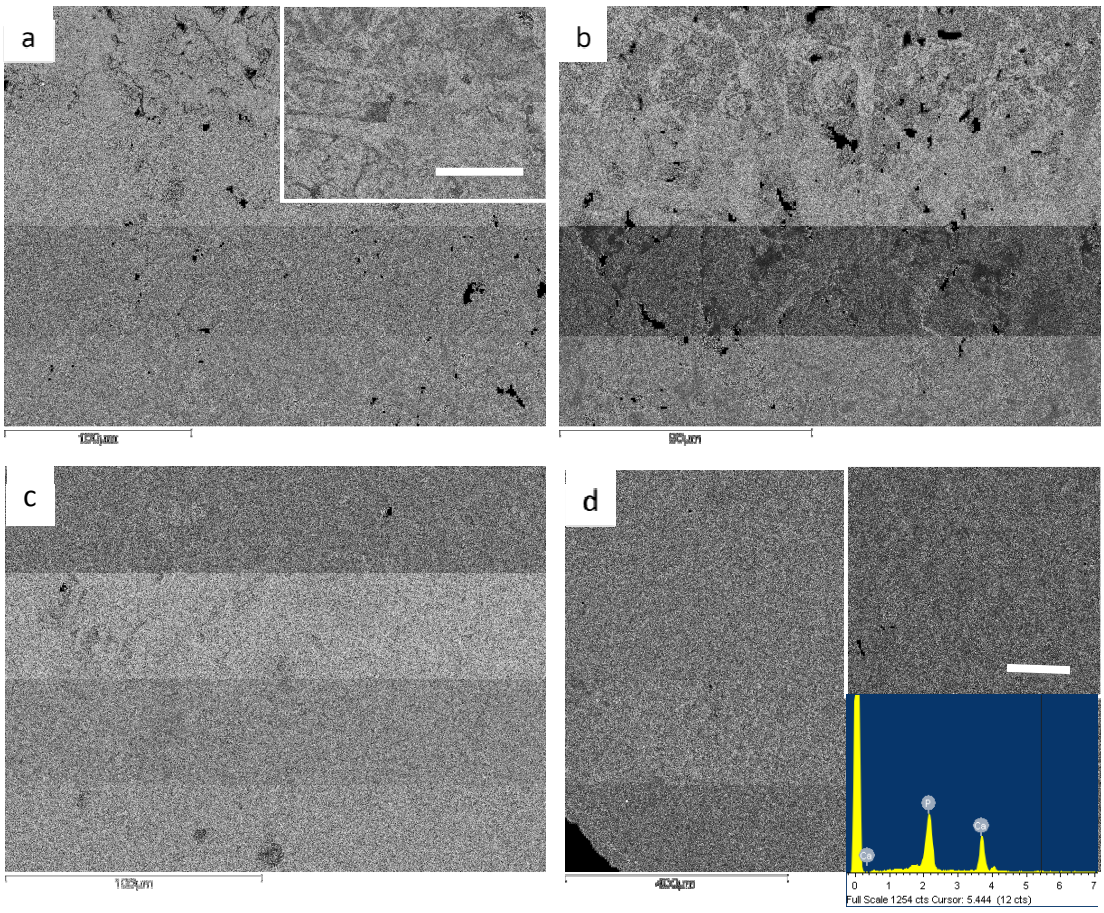

Fig. 61: SEM micrography of *ah*MSCs / MSCs ??? at 24 hours in culture showing: (a-b) cells started spreading, got enlarged and adhered firmly on both materials EC2 and EC3 (bar 100 µm. Inset bar 20 µm). (c) Rounded appearance of the cells attached to EC1 (bar 100 µm). (d) Microgranules on EC2 surface (bar 400 µm). Detail and spectrum in the inset (bar100 µm).

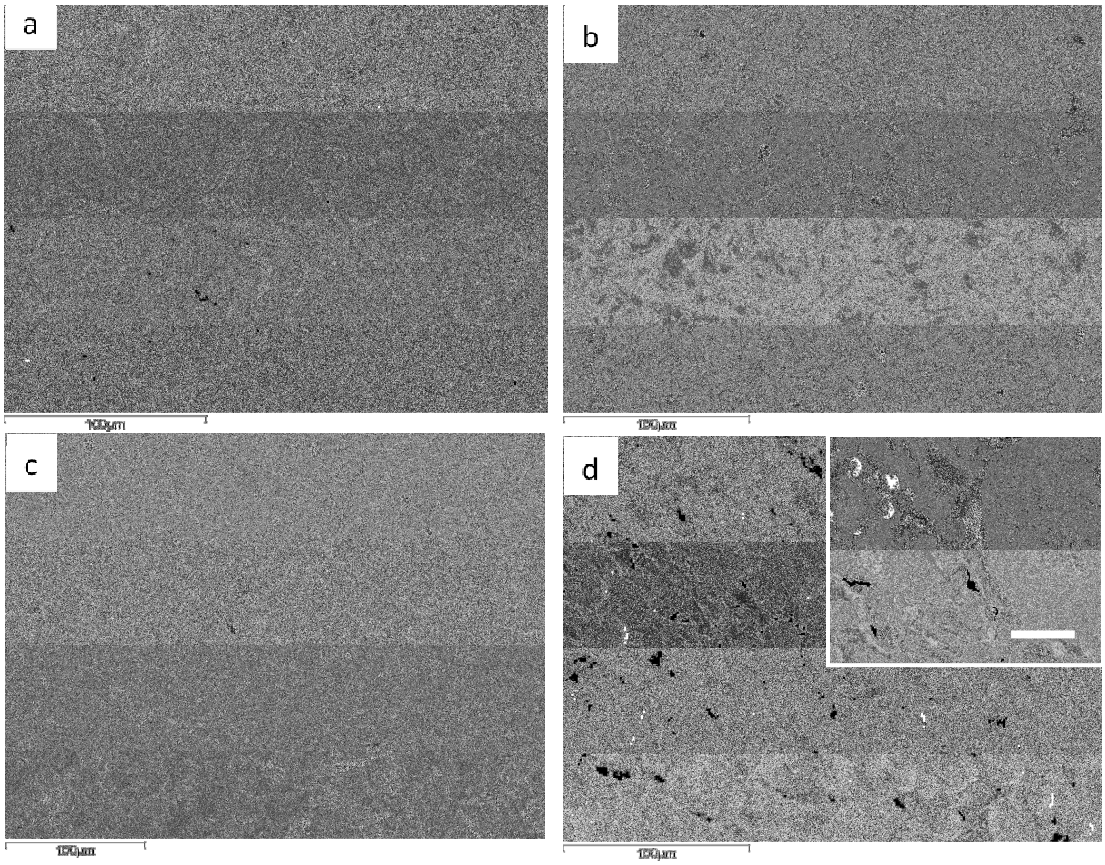

Fig. 62: SEM micrography of *ah*MSCs at 7 days. (a) Incresed number of rounded cells on EC1 and (b-c) cells with polygonal aspect on EC2 and EC3 as well. Extensive cytoplasmatic extensions, more evident on the material EC2. (d) Microgranules formation on the cell surface that grew on EC2 (bar 100 μm). Detail in the inset (bar 30 μm).

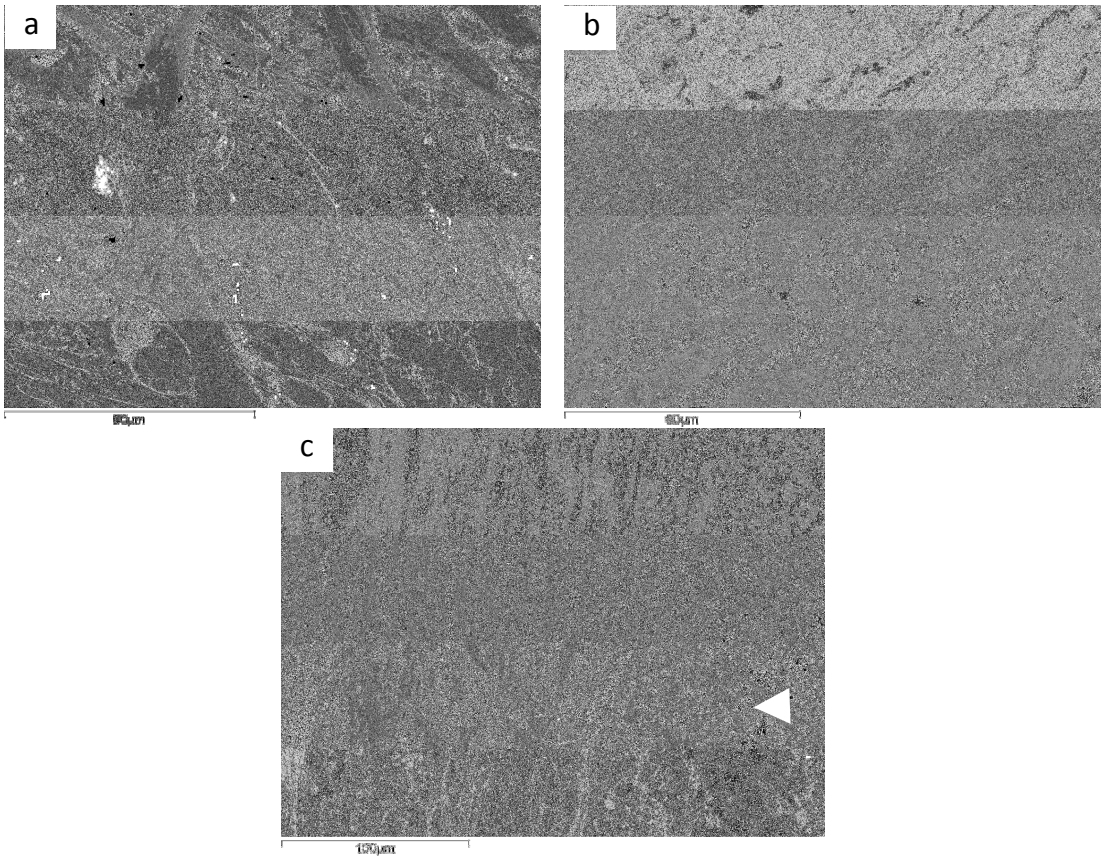

Fig. 63: SEM micrography of *ah*MSCs / MSCs ??? at 21 days. (a) Overall increase in the number of cells that grew on the three materials. Cel-cel interactions were also noted via microvillus extensions between cells, more evident in EC2. Note the presence of fibrillar structures to network mode corresponding to the extracellular matrix. (b) New morphological appareance of rounded cells on EC1. (c) Greater confluence of the cells which partially covers the surface of materials, less obvious on material EC1 (arrow head, uncovered material). (a-b, bar 60 μm; c, bar 100 μm).

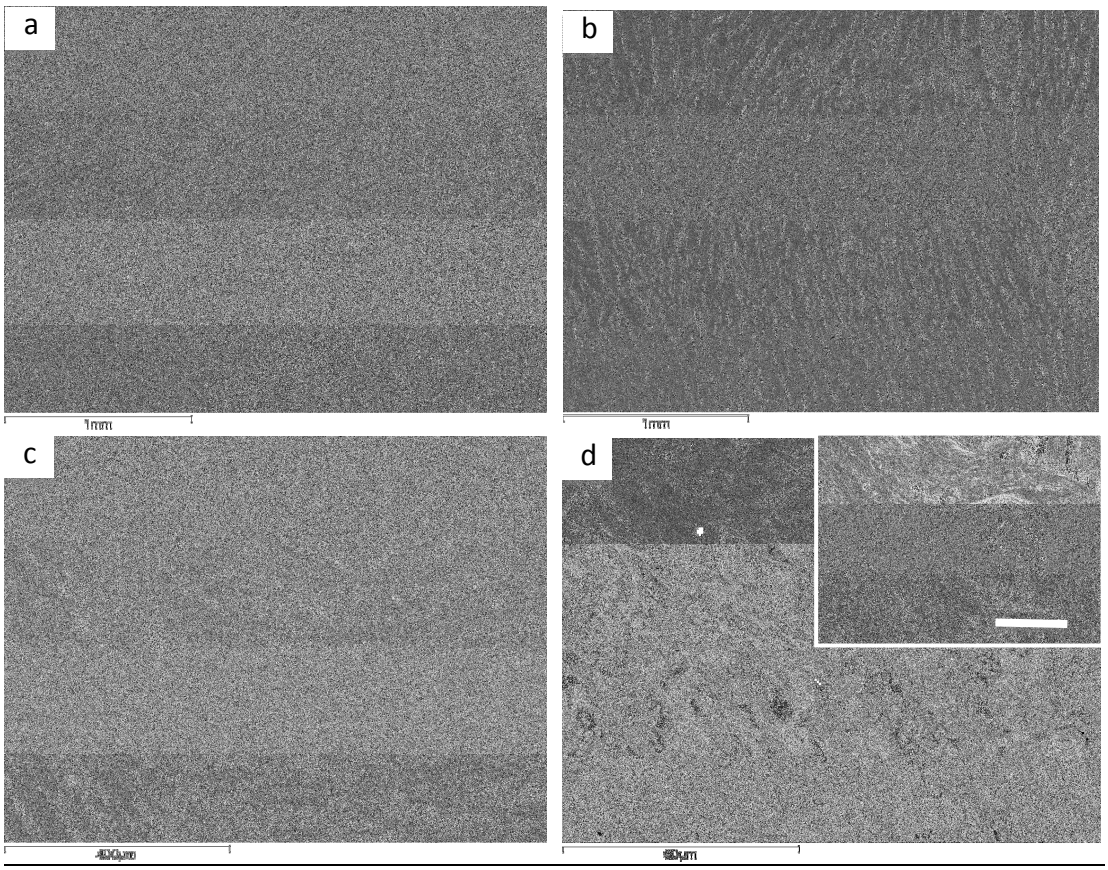

Fig. 64: SEM micrography of *ah*MSCs / MSCs ??? at 4 weeks. (a-b-c) Monolayer of cells covering the surface of materilas EC2 and EC3 (bar 1 mm) and tight junction between cells (barr 400 µm). (d) Less confluence in cells that grew on the material EC1 and intercellular spaces occupied by extracellular matrix (bar 60 µm, inset, bar 100 µm).

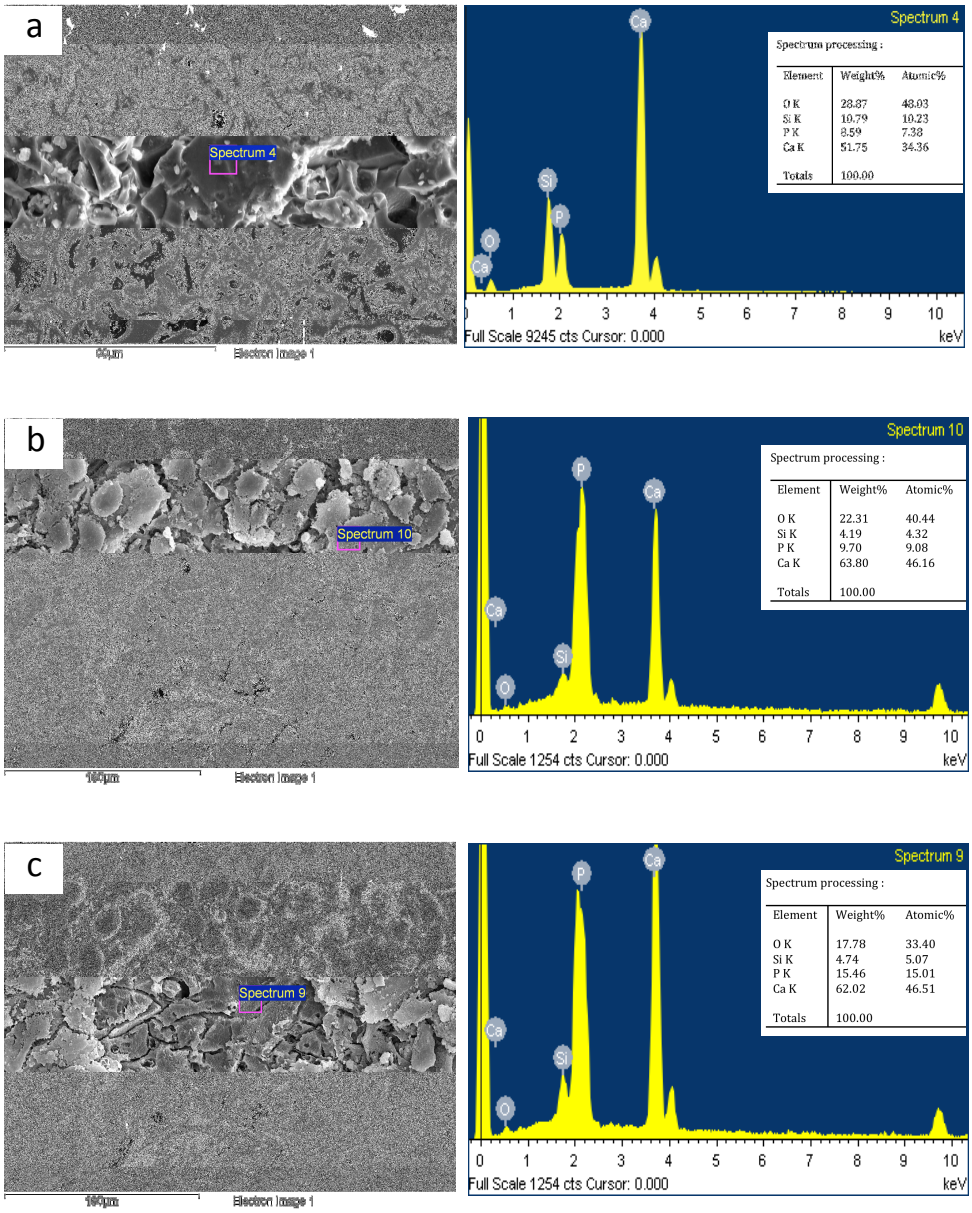

Fig. 65: Representatives images of EDS microanalysis of the surface of materials before (a) and after (b) immersion in culture media during one week. (bar 100 µm).

4.8. EXPRESSION OF *ah*MSCs SURFACE MARKERS

Flow cytometry is performed in order to analyze the expression of CD 105, 90,73 surface markers in cells seeded on the ECs, compared with a control, and cultivated for 7, 14, 21 and 28 days in basal GM and OM .

CD 105, 90, and 73 are considered a fundamental prerequisite of ahMSCs isolation; these markers were used previously by our laboratory to characterize ahMSCs from mononucleated fraction obtained by SEPAX isolation, and generally used in our experiments.

As figure 41 shows, starting from the second week the expression of CD 105 for cells seeded on EC2 and cultured in the normal growth medium is always significantly lower than the control, while it is comparable during the first week in culture; moreover with this material CD105 expression decrease in the time is significant at all the times. The situation is similar for cells cultivated on EC1, even if no significant differences are revealed after 28 days in culture and, surprisingly, the expression of the marker analyzed is significantly higher than the control after the first 7 days in culture. Otherwise the cells seeded on EC3 have the same behavior of the control (21 and 28 days of culture in growth medium) except for the first and the second week in culture, in which they show a significant reduction in CD 105 expression.

When the OM is added, even the expression in the control decreases resulting comparable to the materials (exception for EC 2 at 28 days, in which the antigen expression is significantly lower than the control). These data demonstrate that the activation of a program of differentiation is accompanied by a diminution of the expression of the 105 marker characteristic of the MSCs.

During the last week studied in GM CD105 marker expression don't change significantly respect the 3dt week in culture. It is possible that the cells will retain a minimal level of expression of this marker. Differences between the third week with OM and the forth week in OM aren't statistically significant. We conclude that CD105 expression didn't change after the third week.

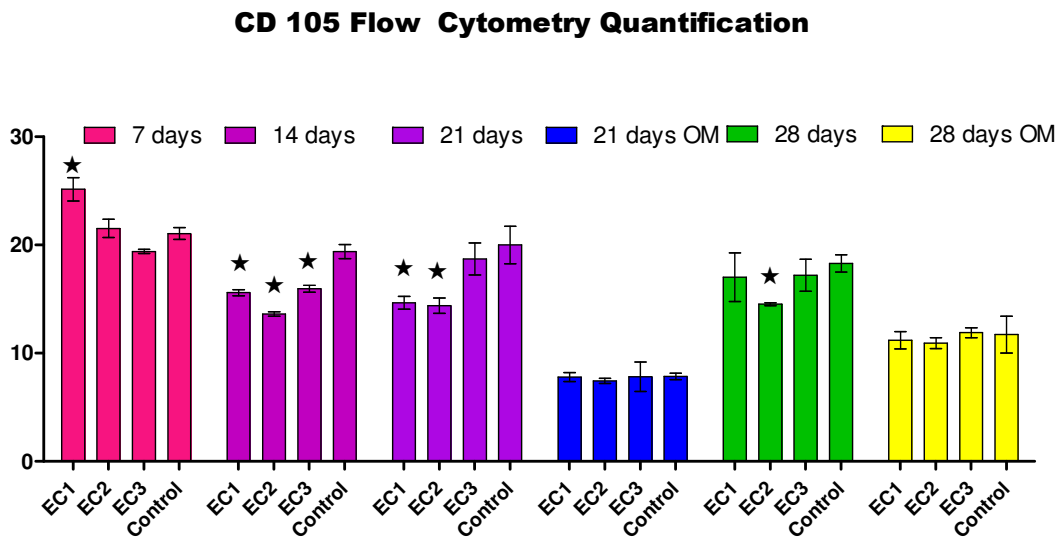

Fig. 66: **CD 105 expression of cells seeded on biomaterials compared to the control.** Data represents the level of fluorescence. The experiment was performed in triplicate. * indicates significant difference at p< 0.05 between cells cultivated on the material and the control at the same time.

CD90 expression didn't change significantly with the pass of the time nor with OM addition, though we can highlight a decrease in of its expression for all the samples at 21 days with OM, that it's the moment in which cells enter in the mature phase of the differentiation process.

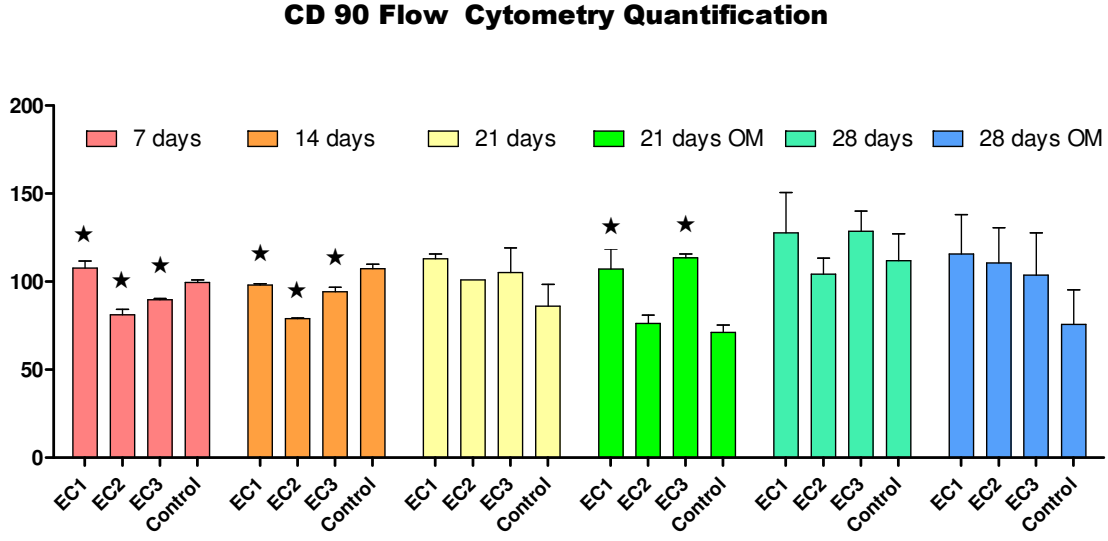

Fig. 67 **CD 90 expression of cells seeded on biomaterials compared to the control.** Data represents the level of fluorescence. The experiment was performed in triplicate. * indicates

significance difference at p< 0.05 between cells cultivated on the material and the control at the same time.

CD73 expression wasn't found to change significantly from the first to the last week of the study.

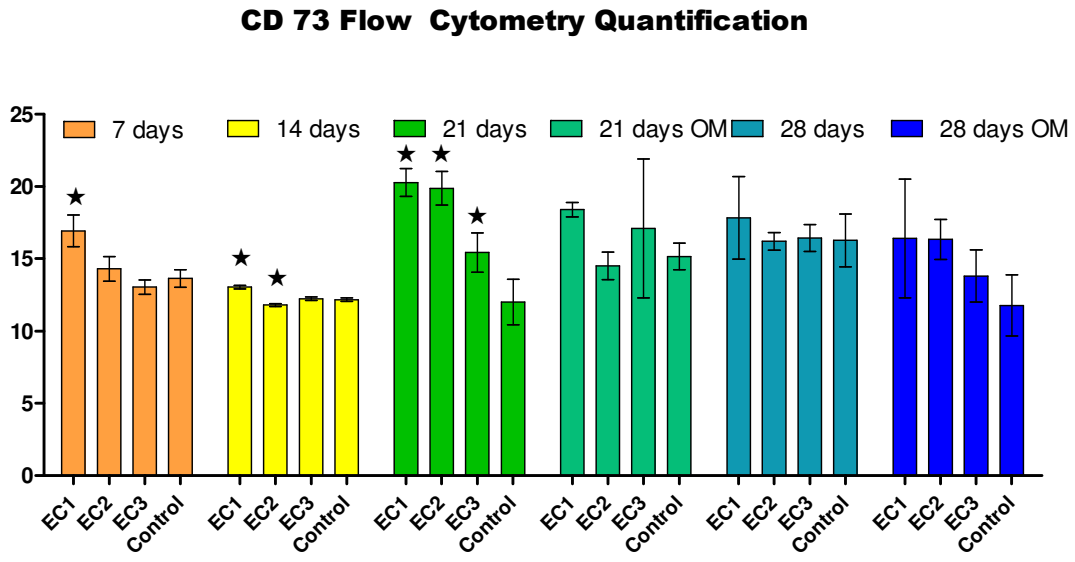

Fig. 68: **CD 73 expression of cells seeded on biomaterials compared to the control.** Data represents the level of fluorescence. The experiment was performed in triplicate. * indicates significance difference at p< 0.05 between cells cultivated on the material and the control at the same time.

4.9 CYTOTOXYCITY EVALUATION

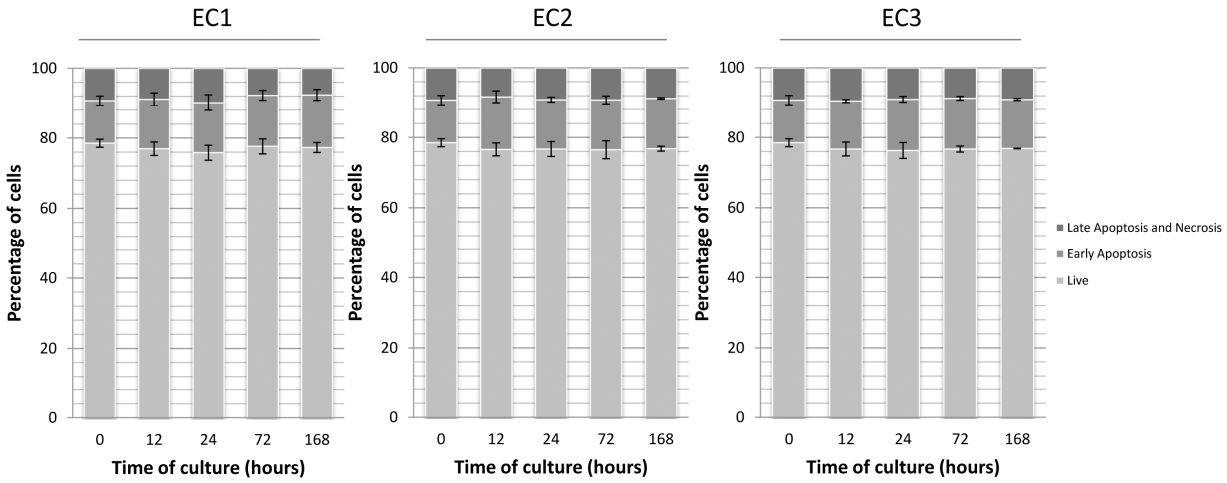

Fig. 69**: Effect of biomaterials on bone marrow-derived mesenchimal stem cells viability**. Mesenchimal stem cells was cultivated at 37ºC in complete culture medium (DMEM + 10% FBS) in the absence (time 0) or presence of biomaterials for the indicated times. Percentage of live (Annexin-V -/7-AAD -), early apoptotic (Annexin +/7-AAD -) or late apoptotic and necrotic cells (Annexin-V +/7-AAD +) was measured by flow cytometry. Mean values ± SD of three independent experiments is shown . * p<0,05 calculated using two-tailed Student's T test.

To assess the possible cellular cytotoxic effects of the different bioceramics, in addition to MTT proliferation studies, we measured the binding of Annexin-V to phosphatidil serine and 7-Amino-Actinomycin (7-AAD) incorporation; two color flow cytometry analysis usually used to determine the apoptosis stage of cells. This method allows to detect three populations: live, early apoptotic, and both late apoptotic and necrotic cells. All the ceramics studied induced an increase of the percentages of early or late apoptosis/necrosis lower than 5% compared with percentages shown by cells cultured in the absence of these ceramics (control at time 0), even in the longer times of culture tested (Fig. … A,B,C). Thus there aren't significant differences also between the three materials, EC1, EC2 and EC3, at different time points. These small differences were not statistically significant (P>0,05), according to two-tailed Student's T test. Moreover small values of early/late apoptosis/necrosis are normally met in cultures of all cell lines types, and are related with normal cell life cicle, samples manipulation and reaching of the confluency.

4.10 FLUORESCENT PROTEINS CELL CLONING FOR IF VISUALIZATION OVER THE MATERIALS SURFACES

Cells cloned with fluorescent (red and green) proteins, where used to confirm cells attachment over the materials, because with normal optic microscopy isn't possible visualize the cells due to the fact that cells are transparent and the materials white. Confirm cells attachment on the materials previously to start the experiment was very important for experiment design. If the cells don't attach on the surface don't live and moreover many experiments like MTT need to be changed and cells seeded on the plastic and materials only immersed in the well, i.e.

Here are reported two pictures of the cloned cells seeded on EC1, EC2 and EC3 materials after 10 days in culture.

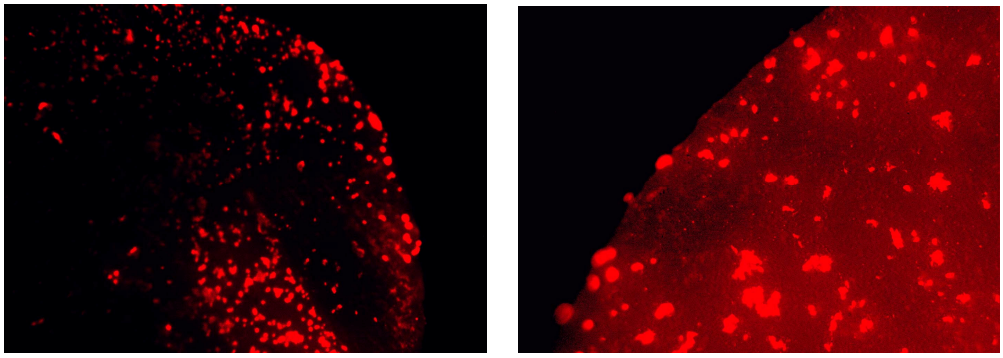

Fig. 70: ahMSCs cloned with RED fluorescent protein and seeded on EC1, EC2, EC3 biomaterials. Cells adhere and spread out.

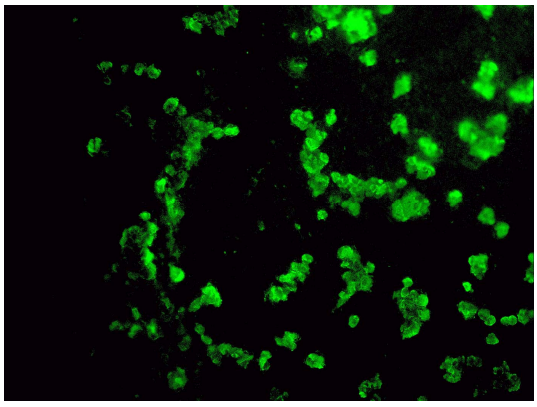

Fig. 71: ahMSCs cloned with GREEN fluorescent protein and seeded on EC1, EC2, EC3 biomaterials. Cells adhere and spread out.

Discussion

5. DISCUSSION

In this study three eutectoids materials (EC1, EC2, EC3) in the system dicalcium silicate-tricalcium phosphate, presenting different amounts of α-tricalcium phosphate and dicalcium silicate (EC1 31% TCP, 69% C_2S; EC2 55% TCP, 45% C_2S; EC3 83% TCP, 17% C_2S) are analyzed for their properties of biocompatibility, bioactivity and osteoinductivity. The cells used to perform the experiments were adult human bone marrow MSCs, chosen for their ability to differentiate into cells of the osteoblastic lineage if subjected to appropriate stimuli. When the ceramics are placed in contact with the culture medium, an intensive ion exchange occurs with the surrounding fluid. Ca, P and Si are the elements involved in this ion exchange process. The elements concentrations released in the medium follow a different trend for the three materials, justified probably because the differences in the materials composition. EC1 release Ca and Si at higher levels; EC3 release more P than EC1 and EC2 materials, doubling the data obtained for the other materials, that is very interestingly to bear in mind; instead its Si release is minimum.

Calcium and phosphate ions in the bulk are very important also for the apatite layer formation at the material-medium surface. In all cases an apatite layer forms on scaffold surfaces, as SEM microscopy demonstrated. Materials bioactivity was previously testes by the laboratory that produced the ceramics for the study, in a simulated body fluid (that resembles a physiologic solution in composition); and subsequently was proved in this study using basal growth medium as solution. SEM images show how ceramics surfaces result covered by small nodules already after few days of incubation; moreover the SEM-EDS analysis confirms these nodules nature, they were the first calcium-phosphate precipitates. The role of Si in this process is to help the nucleation of these crystals that converge and grow with time, consuming the calcium and phosphate ions of the surrounding fluid, so the concentration of the three ions is important, the right balance between them will

result in the best apatite layer formed. In this case EC1 and EC3 ceramics seem to be the ones that form more crystals precipitates. Changes occurring to the material surface enhance ahMSCs adherence, spreading, migration and proliferation over them. The MTT assay shows only few deleterious effects on cells viability during the first 24 hours in culture for the three materials. Citotoxycity assay performed using Annexin-V PE identification, confirms MTT data; the materials aren't cytotoxics for the cells and there aren't significant differences between them at any time point of the study. MTT results showed that these eutectoids materials influence cell proliferation in a different way. EC1 and EC3 seem to block cell proliferation, while EC 2 is able to stimulate cell proliferation. In fact already from the second week, the proliferation rate of cells seeded on EC2 overtakes that of the control and remains quite constant during the whole incubation period. Moreover this effect is increased with the addition of the osteogenic medium (OM). The different behavior of cells seeded on materials detected with the MTT assay is not confirmed by SEM observations, which show how after 28 days in culture the cells cover completely the surface of all the three materials. The MTT assay needs to be repeated to validate the results obtained, also because were used few replicates and MTT is an assays subjected at a high variability due to a lot of conditions intervening in the experiment. Also the osteoinductivity of the materials is tested, verifying their ability to lead ahMSCs toward an osteoblastic lineage differentiation. The results of the qPCR show that the RUNX2 gene is upregulated in cells seeded on EC1 and EC2 materials starting from the second week and that the addition of the osteogenic medium further increments its expression, confirming the role of this gene in giving an osteoblastic commitment to MSCs (contrasting many publications that don't find RUNX2 variations and justify their results with RUNX2 posttranscriptional or translational modifications). The biomaterials clearly seem to inhibit ALP mRNA expression, maybe because of the ions released. In particular, ALP role in osteoblast differentiation is to release inorganic phosphates to permit calcium-phosphate crystals formation. These crystals begin to form independently from ALP activity thanks to the bioactivity of the materials, and this may be the cause of the reduction in its mRNA expression. On the contrary, ALP activity quantification shows an increase in cells incubated with EC2 and the OM after 28 days in culture. The

discordance between mRNA expression and enzyme activity should be validated by other experiments with more replicates. The formation and maturation of the extracellular matrix was also observed. ColI and OSN are both markers of early osteoblast differentiation, but their mRNA expression seems to be poorly influenced by the ECs with slight significant variations during the whole incubation period that suggests a regulation at the level of translation. This suggestion is confirmed by ColI Immunofluorescence images. In fact ColI appeared to be synthesized since the first stages of ECM deposition in all the samples considered, but there more groups of cells expressing this protein for the samples incubated with EC1 and EC2, a little less were the ones incubated with EC3 and only a few were found in the control. This is maybe due to the major level of medium Si-concentration in samples incubated with EC1 and EC2, as Si favors the posttranslational modifications regarding the newly formed collagen pro-α chains. During the last weeks of incubation, the situations is more homogenous between the samples. During the third and the fourth week, EC1 and EC2 are also able to upregulate the markers of a more mature extracellular matrix as OPN, BSP and OCN whose role is to influence and regulate mineralization. The qPCR results show that cells seeded on EC2 reach the maximum expression of these markers during the third week of incubation with the OM, while cells cultured on EC1 reach it during the fourth week with the OM. These qPCR results are validated by immunofluorescence observations; during the last two weeks of culture in fact, OPN and OSC proteins are highly expressed in the samples incubated with the materials demonstrating that the ECM was maturing. Also SEM observations show that, during the same period, an abundant extracellular matrix is formed in all samples incubated with the ECs materials. The intercellular gaps are in fact occupied by fibrillar material (probably collagen), that retains deposits of mineral. In addition, Alizarin Red staining indicates a strong mineralization occurring during the fourth week when the cells are incubated with EC1 or EC2 and the OM. In the absence of the osteogenic supplements, only cells incubated with EC2 can retain in a consistent way mineral deposits within the monolayer. qPCR results in fact show that cells seeded on EC2 express the highest level of BSP and OSC, known to be able to nucleate minerals along the collagen fibers. Moreover, the analysis of the cell surface markers shows that cells seeded on EC2 and in part cells seeded on EC 1 present a

reduction of the expression of CD 105, a marker expressed in ahMSCs and whose expression decrease is considered a sign of a differentiation program activation. The expression of osteoblastic markers noted in the control samples may be due to several factors. First of all the population chosen may be constituted by a great amount of cells that already received a commitment or contaminated with other cell types. In fact samples of marrow extruded from bone can include osteoblast precursors eluted from trabecular bone or the inner surface of the bone itself. Even the culture conditions can influence ahMSCs spontaneous differentiation. The normal growth medium used in fact is the DMEM supplemented with SBF. DMEM contains Phenol Red as pH indicator, which is able to mimic the estrogens that are potent inducers of osteoblasts differentiation. Moreover, the SBF growth factors content preferentially induce ahMSC differentiation towards the osteogenic (77) lineage instead of the chondrogenic or adipogenic lineage. These observations highlight the need for a better characterization of the cells used and the improvement of the culture conditions, in order to contrast the normal induction of a differentiation program when cells are kept for a long period in culture and reach confluence.

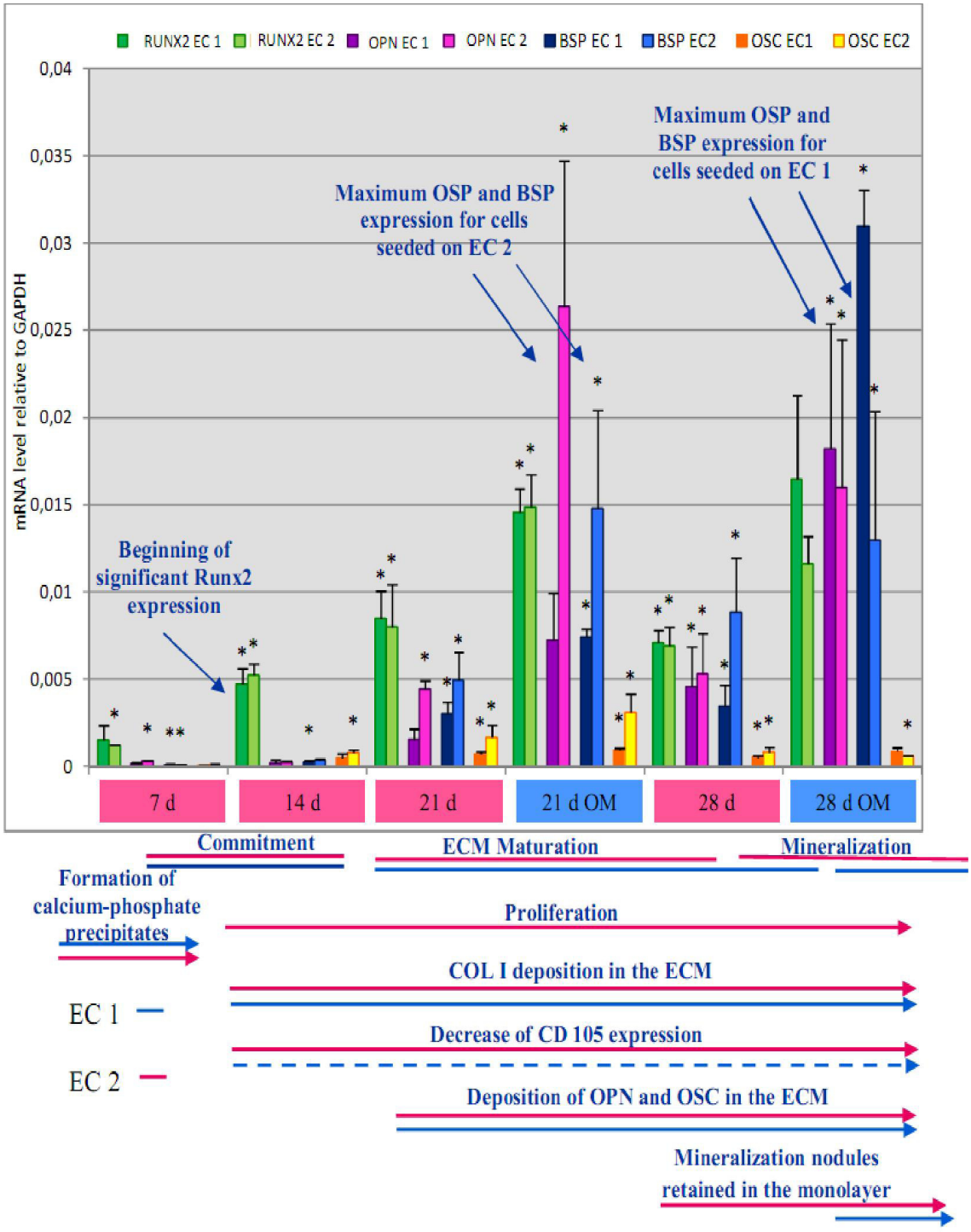

Fig.73. Graph that summarizes the effect of EC 1 and EC 2 on MSCs. The histograms show RUNX2, OPN, BSP and OSC mRNA expression relative to GAPDH. * shows significance at $p < 0.05$ between cells seeded

on the biomaterials and the control. The arrows show the progression in proliferation, in the deposition and mineralization of the ECM and in the loss of CD105 membrane antigen. The cells progress through three general phases: commitment, extracellular matrix deposition and maturation, and mineralization.

Conclusions

6. CONCLUSIONS

Taken together, these results show that EC2 accompanied by EC1, are the materials that have stronger effects on ahMSCs differentiation, but influence in a different way the temporal expression of markers typical of osteoblast differentiation. It seems in fact that EC2 increases the speed in which ahMSCs differentiate. Instead EC3 behaves, in most cases, as the control. EC2, especially if incubated with the osteogenic medium, is able not only to stimulate ahMSC proliferation, but exerts a positive effect on extracellular matrix formation and maturation, inducing the synthesis of proteins that are able to regulate the nucleation of apatite crystals along the collagen fibers leading to mineralization. Due to its bioactive properties, an apatite layer is formed on EC2 surface that reminds the mineralogical structure of the bones. On this surface, ahMSCs are able to adhere, grow and differentiate toward an osteoblastic phenotype, producing an extracellular matrix that can in turn mineralize and potentially be the substrate of the adhesion of new ahMSCs. These characteristic make EC2 the best candidate for further investigations concerning its application in bone tissue engineering.

Future Perspectives

7. FUTURE INVESTIGATIONS

The osteoinductive properties of EC2 are good but not excellent and need to be validated repeating the experiment with another cell pool. It would be interesting perform the same experiments incubating the ahMSCs with EC2 and selected concentration of growth factors, as BMP-2, that resemble the ones find in the bone. Nevertheless, EC2 could be potentially adopted as vehicle to introduce ahMSCs in the defective site of the patient. In this way the cells will be influenced in the activation of a differentiation program also by the local environment at the injury site. The next step to ensure its applicability in the field of bone tissue engineering is to test this biomaterial *in vivo* in an animal model, like a rabbit.

Bibliography

8. BIBLIOGRAPHY

Agrawal CM and Ray. Biodegradable polymeric scaffoldsfor musculoskeletal tissue engineering. J Biomed Mater Res 55: 141-150, 2001.

Albee F, Morrison H. Studies in bone growth — triple calcium phosphate as a stimulus osteogenesis. Ann Surg 1920;71:32–9.
Augello A and De Bari C. The Regulation of Differentiation in Mesenchymal Stem
B. A. Blenke, E. H. Pfeilbromer & H. H. Kas. Langenbechs Arch. Chir. Suppl. Forum 107 (1973).

Banfi A, Muraglia A, Dozin B. Proliferation kinatics and differentiation potential of ex-vivo expanded human bone marrow stromal cells: implications for their use in cell therapy. Exp Hematol 28: 707-15, 2000

Barbash IM, Chouraqui P, Baron J. Systemic delivery of bone marrow-derived mesenchymal stem cells to the infracted myocardium: feasibility, cell migration, and body distribution. Circulation 108: 863-868, 2003.

Barry FP, Boynton RE, Liu B, Murphy JM. Chondrogenesis differentiation of mesenchymal stem cells from bone marrow: differentiation-dependent gene expression of matrix components. Exp Cell Res 268: 189-200, 2001.

Barry FP, Murphy JM. Mesenchymal stem cells: clinical applications and biological characterization. Int J of Biochem and cell Biol 36: 568-84, 2004.

Beck GR, Zerler B, Moran E. Phosphate is a specific signal for induction of osteopontin gene expresión. Proc Natl Acad Sci USA 97: 8352-7, 2000.

Bellow CG, Aubin JE, Heersche JN. Initiation and progresión of mineralization of bone nodules formed in Vitro: the role of alkaline phosphatase and organic phosphate. Bone Miner 14: 27-40, 1991.

Berger, R. Sauer, G. Steinborn, F. Wihsmann, V. Thieme, St. Kholer & H. Dressel. «Clinical application of surface reactive apatite/wollastonite containig glass-ceramics». Pp. 120-26, in Proceedings of XV International Congress on Glass, Mazurin & O.V., Nauka, Editors, Leningrado (1989).

Best SM, Porter AE, Thian ES, Huang J. Bioceramics: past, present and for the future. J Eur Ceram Soc 28: 1319-1327, 2008

Best SM, Porter AE, Thian ES, Huang J. Bioceramics: past, present and for the future. J. Eur. Ceram. Soc. 28: 1319–1327, 2008.

Bianco P, Robey PG, Simmons PJ. Mesenchymal stem cells: revisiting history, concepts, and assays. Cell Stem Cell 2:313-319, 2008.

Bruder SP, Horowitz MC, Mosca JD, Haynesworth SE. Monoclonal antibodies reactive with human osteogenic cell surface antigens. Bone, 21: 225-235, 1997.

Bruder SP, Kurth AA, Shea M, Hayes WC, Jaiswal N, Kadiyal S. Bone regeneration by implantation of purified, culture-expanded human mesenchymal stem cells. J Orthop Res 16: 155-162, 1998.

Cancedda R, Dozin B, Giannoni P, Quarto R. Tissue engineering and cell therapy of cartilage and bone. Matrix Biol 22: 81-91, 2003.

Caplan AI. Adult mesenchymal stem cells for tissue engineering versus regenerative medicine. J Cell Physiol 213: 341-347, 2007.

Carlisle EM. A silicon requirement for normal skull formation in chicks. J Natr 110: 352-359, 1980.

Carlisle EM. Silicon: a posible factor in bone calcification. Science 167: 279–280, 1970.

Carlisle EM. Silicon: a positive factor in bone calcification. Science 167: 279-280, 1970.

Carlisle EM. Silicon: a possible factor in bone calcification. Science 1970;167: 279–80.

Carlisle EM. Silicon: an essential element for the chick, Science 178: 619–621, 1972.

Carlisle EM. Silicon: an essential element for the chick. Science 178: 619-621, 1972.

Carrodeguas RG, De Aza AH, Garcia-Paez I, De Aza S, Pena P. Revisiting the phase-equilibrium diagramo f the Ca3(PO4)2–CaMg(SiO3)2 system. J Am Ceram Soc 2010;93(2): 561–9.

Carrodeguas RG, De Aza HA, Jimènez J, De Aza PN, Pena P, Lopez-Bravo A, De Aza S. Preparation and in vitro characterization of wollastonite doped tricalcium phosphate ceramics. Key Eng Mater 361–363: 237–240 (2008).

Cells. Human Gene Therapy 21(10):1226-1238, 2010

Chen SL, Fang WW, Ye F. Effect on left ventricular function of intracoronary transplantation of autologous bone marrow mesenchymal stem cells in patients with acute myocardial infarction. Am J Cardiol 94: 92-5, 2004.

Cheung HS, & M. H. Haak. «Growth of osteoblasts on porous calcium phosphate ceramic: an in vitro model for biocompatibility study». Biomaterials 10 (1), 63-67 (1989).

Conget PA, Minguell JJ. Phenotypical and functional properties of human bone marrow mesenchymal progenitor cells. J Cell Physiol 181: 67-73, 1999.

De Aza HA, Velasquez P, Aleman MI, Penaa P, De Aza PN. In situ bone-like apatite formation from a bioeutectic® ceramic in SBF dynamic flow. J Am Ceram Soc 90(4): 1200-1207, 2007.

De Aza PN, De Aza AH, De Aza S. Crystalline bioceramic materials. Bol. Soc. Esp. Ceram. Vidr. 44 (3): 135–145 (2005).

De Aza PN, De Aza AH, Pena P, De Aza S. Bioactive glasses and glass–ceramics. Bol Soc Esp Ceram Vidr 2007;46(2):45–55.
De Aza PN, De Aza HA, Pena P, De Aza S. Bioactive glasses and glass ceramic materials. Bol Soc Esp Ceram Vidrio 468(2): 45-55, 2007.

De Aza PN, Guitian G, De Aza S. A new bioactive material which transforms in situ into hydroxyapatite. Acta mater 46(7): 2541-2549, 1998.

De Aza PN, Guitian G, De Aza S. Bioeutectic: a new ceramic material for human bone replacement. Biomaterials 18: 1285-1291, 1997.

De Aza PN, Luklinska Z, Santos C, Guitian F, De Aza S. Mechanism of bone like apatite formation on a bioactive implant. Biomaterials, 24(8): 1437-1445, 2003.

De Aza PN, Luklinska ZB, Anseau MR, Hector M, Guitian F, De Aza S. Reactivity of a wallostonite-tricalcium phosphate Boieutectic® ceramic in human parotid salivaa. Biomaterials 21: 1735-1741, 2000.

De Aza, Guitian F, De Aza S. A new bioactive material which transforms in situ into hydroxyapatite. Acta Mater, 46 (7): 2541-2549, 1998.

De Groot K. Medical application of calcium phosphate biocramics. The Centennial Issue, 99 (10), 943-953, 1991.

De Groot K. «Effect of Porosity and Physicochemical Properties on the Stability Resorption and Strength of Calcium Phosphate Bioceramics». Ann. N.Y. Acad. Sci., 523, 227 (1988).

Devine SM. Mesenchymal stem cells: willthey have a role in the clinic Cell Biochem Suppl 38: 73-79, 2002.

Digirolamo CM, Strokes D, Colter D, Phinney DG, Class R, Prockop DJ. Propagation and senescence of human marrow stromal cells in culture: a simple

colony forming assay identifies sample with the greatest potential to propagate and differentiate. Br J Haematol 107: 275-281, 1999.

Dominici M, Hofmann TJ, Horwitz EM. Bone marrow mesenchymal cells: biological properties and clinical application. J Biol Regul Homeosta Agents 15: 28-37, 2001.

Dorozhkin S. In vitro mineralization of silicon containing calcium phosphate bioceramics. J Am Ceram Soc 90: 244-249, 2007.

Driessens F, Verbeeck R. Biomaterials. Boca Raton: CRC Press; 1990.

Dubok VA. Bioceramics – Yesterday, today, tomorrow. Powder metal Met C+ 39 (7-8): 381-394, 2000.

Dvorak MM, Siddiqua A, Ward DT, Carter DH, Dallas SL, Nemeth EF, Riccardi D. Physiologicla changes in extracellular calcium concentration directly control osteoblast function in the absence of calciotropic hormones. Proc Natl Acad Sci USA 101: 5140-5, 2004.

Erices A, Conget P, Minguel JJ. Mesenchymal progenitor cells in human umbilical cord blood. Br J haematol 09: 235-42, 2000.

European Commission-Health and Consumer Protection Directorate-General. Technical requirements for the coding, processing, preservation, storage, and distribution of human tissues and cells. Directive 2004/23/EC.

Ferguson C, Alpern E, Miclau T, Helms JA. Does Adult Fracture Repair Recapitulate Embryonic Skeletal Formation? Mechanisms of Development. 87(1-
Fernandes JC, Martel-Pelletier J, Pelletier JP. The role of cytokines in osteoarthritis pathophysiology. Biorheology 39: 237-246, 2002.

Fibbe WE. Mesenchymal stem cells. A potential source for skeletal repair. Ann Rheum Dis 61: 29-31, 2002.
Friedenstein AJ, Chailakhjan RK, Lalykina KS. The development of fibroblast colonies in monolayer cultures of guinea-pig bone marrow and spleen cells. Cell tissue Kinet 3: 393-403, 1970.

Friedenstein AJ. Stromal mechanism of bone marrow: cloning in vitro and retransplantation in vivo. Haematol Blood Transfus 25: 19-29, 1980.

Galmiche MC, Koteliansky VE, Briere J, Herve P, Charbord P. Stromal cells from human long term marrow cultures are mesenchymal cells that differenciate following a vascular smooth muscle differentiation pathway. Blood 82: 66-76, 1993.

Ghosh SN, Rao PB, Paul AK, Raina K. The chemistry of dicalcium silicate mineral. J Mater Sci 14: 1554-66

Gibson IR, Best SM, Bonfield W. Chemical characterization of siliconsubstituted hydroxyapatite. J Biomed Mater Res 1999;44:422–8.

Goldring MB. Anticytokine therapy for osteoarthritis. Expert Opinion on Biological Therapy 1: 817-829, 2001.

Hayashi K, Matsuguchi N, Uenoyama K. Re-evaluation of the biocompatibility of bioinert ceramics in vivo. Biomaterials 13 (4), 195-200, 1992.

Haynesworth SE, Baber MA, Caplan AI. Cellsurface antigens on human marrow-derived mesenchymal cells are detected by monoclonal antibodies. Bone 13: 69.80, 1992.

Hench LL and Polak J. Third generationbiomedical materials. Science 295: 1014-1017, 2002.

Hench LL, Hench JW, Greenspan DC. Bioglass: a short history and bibliography. J Aust Ceram Soc 2004;40:1–42.

Hench LL. Bioceramics. J Am Ceram Soc 1998;81(7):1705–28.

Hench LL. Bioceramics. J Am Ceram Soc, 81(7): 1705-1728, 1998

Hench LL. Bioceramics: from concept to clinic, J. Am. Ceram. Soc. 74: 1487–1510, 1991.

Hench LL. Bioceramics: from concept to clinics. J Am Ceram Soc 74(7): 1487-1510, 1991.

Hench LL. Biomaterials. Science 208: 826-831, 1980.

Hench LL. Prosthetic implant materials. Ann Rev Mater Sci 5: 279-300, 1975.

Hing K, Revell P, Smith N, Buckland T. Effect of silicon level on rate, quality and progression of bone healing within silicate substituted porous hydroxyapatite scaffolds. Biomaterials 27: 5014-5026, 2006.

Horwitz EM, Prockop DJ, Fitzpatrick LA, Koo WW, Gordon PL, Neel M, Sussman M, Orchard P, Marx JC, Pyeritz RE, Brenner MK. Transplantability and therapeutic effects of bone marrow-derived mesenchymal stem cells in childrens with osteogenesis imperfecta. Nature Medicine, 5: 309-313, 1999.

Hulbert SF, Bokros JC, Hench LL, Wilson J, Heimke G. Ceramics in clinical applications: past, present and future. Pp. 189-213 in High Tech Ceramics, P. Vincenzini editor, Amsterdam, The Netherlands: Elsevier, 1987.

Hulbert SF, Hench LL, Forces D, Bowman L. Hystory of bioceramics. Pp. 3-29, in Ceramicss in surgery, P Vincenzini editor, Amsterdam, The Netherlands: Elsevier, 1983.

Hulbert SF, & J. T. Klawitter. «Potential of ceramic materials as permanently implantable skeletal prostheses». J. Biomed. Mater. Res. 4, 433-456 (1970).

Hutmacher T, Hurzeler MB, Schliephake H. A review of material properties of biodegradable and bioresorbable polymer for GTR and GBR. J Oral Maxillofac Implants 11: 667-678, 2000.

In't Anker PS, Noort WA, Scherjon SA, Kleijburg-van der Keur C, Kruisselbrink AB, van Bezooijen RL. Mesenchymal stem cells in human second-trimester bone marrow, liver, lung, and spleen exhibit a similar immunophenotype but a heterogeneous multilineage differentiation potential. Haematologica 88: 845-52, 2003.

In't Anker PS, Scherjon SA, Kleijburg-van der Keur, de Groot-Swings GM, Class FH, Fibbe WE. Isolation of mesenchymal stem cells of fetal and maternal origin from human placenta. Stem Cells 22: 1338-45, 2004.

Jiang Y, Jahagirdar BN, Reinhardt RE, Keene CD, Ortiz-Gonzalez XR, Reyes M, Lenvik T, Lund T, Blackstad M, Du J, Aldrich S, Lisberg A, Low WC, Largaespada DA, Verfaille CM. Pluripotency of mesenchymal stem cells derived from adult marrow. Nature, 418: 41-49, 2002.

Johnstone B, Hering TM, Caplan AI, Goldberg VM, Yoo JU. In vitro chondrogenesis of bone marrow-derived mesenchymal progenitor cells. Experimental Cell Research, 238: 265-272, 1998.

Julien M, Magne D, Masson M, Rolli-Derkinderen M, Chassandre O, Cario-Toumaniantz C, Cherel Y, Weiss P, Guicheux J. Phosphate stimulates matrix Gla protein expresión in chondrocytes through the extracellular signal regulated kinase signaling pathway. Endocrinology 148: 530-537, 2007.

K. H. Karlsson, K. Fröberg & T. Ringbom. «A structural approach to bone adhering of bioactive glasses». J. Non-Cryst. Solids, 112, 69-72 (1989).

Kamitakahara M, Ohtsuki C. Apatite formation on CaO-siO2-based glass-ceramics in a simulated body fluid. Phosphorus Research Bulletin 20: 101-110, 2006.

Kanatani M, Sugimoto T, Kano J, Chihara K. IGF-I mediates the stimulatory effect of high phosphate concentration on osteoblastic cell proliferation. J Cell Physiol 190: 306-312, 2002.

Khoshniat S, Bourgine A, Julien M, Petit M, Pilet P, Rouillon T, Masson M, Gatius M, Weiss P, Guicheux J, Beck L. Phosphate-dependent stimulation of MGP and

OPN expresión in osteoblasts via the ERK1/2 pathway is modulated by calcium. Bone 48: 894-902, 2011.

Kokubo T, Ito S, Huang ZT, Hayashi T, Sakka S, Kitsygi T, Yamamuro T. J Biomed Mater Res, 24: 331 and 721, 1990.

Kon E, Muraglia A, Corsi A, Bianco P, Marcacci P, Martin I. Autologous bone marrow stromal cells loaded onto porous hydroxyapatite ceramics accelerate bone repair in critical-size defects of sheep long bones. J Biomed Mater Res 49: 328-37, 2000.

Kopen GC, Prockop DJ, Phinney DG. Marrow stromal cells migrate throughout forebrain and cerebellum, and they differenciate into astrocytes after injection into neonatal mause brains. Proc Natl Acad Sci USA 96: 10711-10716, 1999.

Krampera M, Cosmi L, Angeli R, Pasini A, Liotta F, Andreini A. Role of the INF-ɤ in the immunomodulatory activity of human mesenchymal stem cells. Stem Cells 24: 386-98, 2006.

Krampera M, Glennie S, Dyson J, Scott D, Laylor R, Simpson E. Bone marrow mesenchymal stem cells inhibit the response of naïve and memory antigen-specific T cells to their cognate peptide. Blood 101: 3722-9, 2003.

Krebsbach PH, Kuznetsov SA, Satomura K. Bone formation in vivo: comparison of osteogenesis by transplanted mouse and human marrow stromal fibroblasts. Transplantation 63: 1059-69, 1997.

L. L. Hench &. D. E. Clark. «Physical chemistry of glass surfaces». J. Non- Cryst. Solids 28 (1) 83 (1978).

L. L. Hench, & J. Wilson. «Surface-active biomaterials». Science, 226, 630 (1984).

L. L. Hench, R. J. Splinter, W. C. Allen & T. K.Greenlee. «Bonding mechanisms at the interface of ceramic prosthetic materials». J. Biomed. Mater. Res. Symp. 2 (1), 117-41 (1971).

L. L. Hench. «Bioactive ceramics», pp. 54 in Bioceramics: Materials Characteristics Versus In Vivo Behaviour, Vol 523, Ducheyne, P. Lemons, J.E. editors. New York: Annals of New York Academy of Science (1988).

L. L. Hench. «Fundamental Aspects of Biocompatibility» .D.F. Williams, CRC Press. (1981).

Langstaff S, Sayer M, Smith TJ, Pugh SM, Hesp SA, Thompson WT. Resorbable bioceramics based on stabilized calcium phosphates. Part I: rational design, sample preparation and material characterization. Biomaterials 1999;20: 727–41.

Le Blanc K, Tammik C, Rosendahl K, Zetterberg E, Ringden O. HLA expression and immunologic properties of differentiated and undifferentiated mesenchymal stem cells. Experimental Haematology 31: 890-896, 2003.

Lee RH, Kim B, Choi I, Kim H, Choi SH, Suh K. Characterization and expression analysis of mesenchymal stem cells from human bone marrow and adipose tissue. Cell Physiol Biochem 14: 311-24, 2004.

Lennon DP, Caplan AI. Isolation of human marrow derived mesenchymal stem cells. Exp Hematol 34: 1604-5, 2006.

Lennon DP, Osdoby P, Carrino DA. Isolation and characterization of chondrocytes and non-chondrocytes from high-density chick limb bud cellcultures. J Craniofac Genet Dev Biol 3: 235-51, 1983.

Liu F, Malaval L, Gupta AK, Aubin JE. Simultaneous detection of multiple bone-related mRNAs and protein expression during osteoblast differentiation: polymerase chain reaction and immunocytochemical studies at the single cell level. Dev Biol 166: 220-234, 1994.

Liu X, Morra M, Carpi A, Li B. Bioactive calcium silicate ceramics and coatings. Biomedicine & Pharmacotherapy 62: 526-529, 2008.

Liu X, Xie Y, Ding C, Chu PK. Early apatite deposition and osteoblast growth on plasma-sprayed dicalcium silicate coating. J Biomed Mater Res 74A: 356-365, 2005
Long MW. Osteogenesis and bone marrow-derived cells. Blood Cells Mol Dis 27: 677-690, 2001.

Magne D, Bluteau G, Faucheux C, Palmer G, Vignes-Colombeix C, Pilet P, Rouillon T, Caverzasio J, Weiss P, Daculsi G, Guicheux J. Phosphate is a specific signal for ATDC5 chondrocyte maturation and apoptosis-associated mineralization: possible implications of apoptosis in the regulation of endochondral ossification. J Bone Miner Res 18: 1430-42, 2003.

Majumdar MK, Keane-Moore M, Buyaner D, Hardy WB, Moorman MA, McIntosh KR, Mosca JD. Characterization and functionality of cell surface molecules on human mesenchymal stem cells. Juornal of Biomedical Science 10: 228-241, 2003.

Martinez IM, Velásquez PA, De Aza PN. Synthesis and stability of a α-tricalcium phosphate doped with dicalcium silicate in the system $Ca_3(PO_4)_2$-Ca_2SiO_4.

Martinez IM. Preparation and characterization of novel bioactive a-Tricalcium Phosphate doped with Dicalcium Silicate ceramics. Materials Science and Engineering C, In press.

Meirelles LS, Chagastelles PC, Nardi NB. Mesenchymal stem cells reside in virtually all post-natal organs and tissues. J Cell Sci 119: 2204-2213, 2006.

Mermet, J. M. Is it still possible, necessary and beneficial to perform research in ICP-atomic emission spectrometry?"Anal. At. Spectrom. 20: 11–16, 2005.

Minarelli-Gaspar AM, Saska S, Carrodeguas RG, De Aza HA, Pena P, De Aza PN, De Aza S. Biological response to wollastonite doped a-tricalcium phosphate implants in hard and soft tissues in rats. Key Eng. Mater. 396–398: 7–10, 2009.

Minguell JJ, Erices A, Conget P. Mesenchymal stem Cells. Minireview. Exp Biol Med Vol 226(6): 507-520, 2001.

Modder UI, Khosla S. Skeletal stem/osteoprogenitor cells: current concepts, alternate hypotheses, and relationship to the bone remodeling compartment. L Cell Biochem 103: 393-400, 2008.

Mosmann T . Rapid colorimetric assay for cellular growth and survival: application to proliferation and cytotoxicity assays". *Journal of Immunological Methods* **65** (1–2): 55–63, 1983.

Muraglia A, Cancedda R, Quato R. Clonal mesenchymal progenitors from human bone marrow differentiate in vitro according to a hierarchical model. J Cell Sci 113: 1161-6, 2000.

Murphy JM, Fink DJ, Hunziker EB, Barry FP. Stem cell therapy in a caprine model of osteoarthritis. Arthritis Rheumatism 48: 3464-3474, 2003.

Na K, Kim SW, Sun BK. Osteogenic differentiation of rabbit mesenchymal stem cells in thermo reversible hydrogel constructs containing hydroxyapatite and bone morphogenic protein-2 (BMP-2). Biomaterials 28: 2631-37, 2007.

Navarro M, Michiardi A, Castaño O, Planell JA. Biomaterials in orthopaedics. J R Soc Interface 5: 1137-1158, 2008.

Nurse RW, Welch JH, Gutt W. High temperature phase equilibra in the system dicalcium silicate-tricalcium phosphate. J Chem Soc 1077-1083, 1959.
Ö. H. Anderson, K. H. Karlsson &. K. Kanganiemi. «Calcium phosphate formation at the surface of bioactive in vivo». J. Non-Cryst. Solids, 119, 290-296, 1990.

Ohtsuki C, Kokubo T, Takatsuka K, Yamamuro T. J Ceram Soc. Japan, 99: 1, 1991.
Ohtsuki C, Kokubo T, Yamamuro T, J Non-Cryst. Solids, 143: 84, 1992.

Palermo AT, Labarge MA, Doyonnas R. Bone marrow contribution to skeletal muscle: a physiological response to stress. Dev Biol 279: 336-344, 2005.

Petersen BE, Bowen WC, Patrene KD, Mars WM, Sullivan AK, Murase N, Boggs SS, Greenberger JS, Goff JP. Bone marrow as a potential source of hepatic oval cells. Science 284: 1168-1170, 1999.

Petit H, Viateau V, Bensaid W, Meunier A, de Pollak C, Bourguignon M. Tissue-engineering bone regeneration. Nat Biotecnol 18: 959-63, 2000.

Pietak AM, Reid JW, Stott MJ, Sayer M. Silicon substitution in the calcium phosphate bioceramics. Biomaterials 2007;28:4023–32.

Pittenger MF, Mackay AM, Beck SC, Jaiswal RK, Douglas R, Mosca JD, Moorman MA, Simonetti DW, Craig S, Marshak DR. Multilineage potential of adult human mesenchymal stem cells. Science 284: 143-147, 1999.

Porter AE, Patel N, Skepper JN, Best SM, Bonfield W. Comparison of in vivo dissolution processes in hydroxyapatite and silicon-substituted hydroxyapatite bioceramics. Biomaterials 24: 4609–4620, 2003.

Pountos I, Giannoudis PV. Biologi of mesenchymal stem cells. Injury 36: S8-S12, 2005.

Pountos I, Jones E, Tzioupis C. Growing bone and cartilage. The role of mesenchymal stem cells. J Bone Joint Surg Br. 88: 421-425, 2006.

Prockop DJ. Marrow stromalcellsas stem cells for nonhematopoietic tissues. Science 276: 71-74, 1997.

Quarto R, Mastrogiacomo M, Cancedda R, Kutepov SM, Mukhachev V, Lavroukov A. Repair of large bone defects with the use of autologous bone marrow stromal cells. N Engl J Med 344: 385-6, 2001.

Reading L, Still K, Bishop N, Scutt A. Peripheral blood as an alternative source of mesenchymal stem cells. Bone 26(Suppl): 9S, 2000.

Refitt DM, Ogston N, Jugdaohsingh R, Cheung HFJ. Orthosilicic acid stimulates collagen type I synthesis and osteoblastic differentiation in human osteoblast-like cells in vitro. Bone 32: 127-135, 2003.
Reid JW, Tuc L, Sayer M, Fargo K, Hendry JA. Synthesis and characterization of single-phase silicon-substituted a-tricalcium phosphate. Biomaterials 27: 2916–2925, 2005.

Reyes M, Verfaillie CM. Turning marrow into brain: generation of glial and neuronal cells from adult bone marrow mesenchymal stem cells. Blood 94: 10(S1):377a, 1999.
Rose FR, Oreffo RO. Bone tissue engineering: hope vs hype. Biochem Biophys Res Commun 292: 1-7, 2002.

Roufosse CA, Direkze NC, Otto WR, Wright NA. Circulating masenchymal stem cells. Int J Biochem Cell Biol 36: 585-97, 2004.

Roy S, Basu B. Mechanical and tribological characterization of human tooth. Mater Charact 2008;59:747–56.

Rubio D, Garcia-Castro J, Martin MC. Spontaneous human adult stem cell transformation. Cancer Res 65: 3035-9, 2005.

Ruys AJ. Silicon-doped hydroxyapatite. J Aust Ceram Soc 1993;29:71–80.

Schipani E, Kronenberg M. Adult mesenchymal stem cells. StemBook, ed. The stem Cell Research Community (www.stembook.org), 2009.

Schwarz KA. A bound form of silicon in glycosaminoglycans and polyuronides. Proc Natl Acad Sci USA 70: 1608-12, 1973.

Seaborn CD and Nielsen FH. Silicon deprivation decreases collagen formation in wounds and bone, and ornithine transaminase enzyme activity in liver. Bio Trace Elem Res 89: 251-261, 2002.

Shackelford JF. Bioceramics: current status and future trenes. Mater Sci Forum 293: 99-106, 1999.

Shih DT, Lee DC, Chen SC, Tsai RY, Huang CT, Tsai CC. Isolation and characterization of neurogenic masenchymal stem cells in human scalptissue. Stem Cells 23: 1012.20, 2005.

Simmons PJ, Torok-Storb B. Identification of stromal cell precursors in human bone marrow by a novel monoclonal antibody, Stro-1. Blood 78: 55-62, 1991.

Stefánsson A, Gunnarsson I, Giroud N. New methods for the direct determination of dissolved inorganic, organic and total carbon in natural waters by Reagent-Free Ion Chromatography and inductively coupled plasma atomic emission spectrometry. Anal. Chim. Acta 582 (1): 69–74, 2007.

Stenderup K, Justesen J, Clausen C, Kassem M. Aging is associated with decreased maximal life span and accelerated senescence of bone marrow stromal cells. Bone 33: 919-26, 2003.

T. Kokubo, S. Ito, S. Sakkay & Y. Yamamuro. «Formation of a High Strengh Bioactive Glass-Ceramic in the System MgO-CaO-SiO2-P2O5». J. Mater. Sci., 21, 536-540 (1986).
T. Kokubo. .«A-W Glass-Ceramic: Processing and Properties», pp.75.88, in An Introduction to Bioceramcs, L.L.Hench & J. Wilson Editors. Singapore (1993).

T. Kokubo. «Novel Ceramics for Biomedical Applications» pp.1-16, in Third Euro Ceramics. Vol. 3, P. Durán & J.F. Fernandez Editors. (1993).

Tavian M, Zheng B, Oberlin E, Crisan M, Sun B, Huard J, Peault B. The vascular wall as a source of stem cells. Ann NY Acad Sci 1044: 41-50, 2005.

Temenoff JS and Mikos AG. Tissue engineering for regeneration of articular cartilage. Biomaterials 21: 431-440, 2000.

Terkeltaub RA. Inorganic pyrophosphate generation and disposition in pathophysiology. Am J Physiol Cell Physiol 281: C1-11, 2001.

Thomas CB, Kellam JF, Burg KL. Comparative study of bone cell culture methods for tissue engineering applications. J of ASTM international 1: 1-17, 2004.

Trömel G. Beiträge zur Kenntnis des Systems Kalziumoxyd-Phosphorpentoxyd, Mitt Kaiser-Wilhelm-Inst Eisenforschg. Düsseldorf 1932;14:25–34.

Trubiani O, Di Primio R, Traini T, Pizzicannella J, Scarano A, Piattelli A. Morphological and cytofluorimetric analysis of adult mesenchymal stem cells expanded ex vivo from periodontal ligament. Int J Immunopathol Pharmacol 18: 213.21, 2005.

Tuan RS, Boland G, Tuli R. Adult mesenchymal stem cell and cell-based tissue engineering. Arthritis Res Ther 5: 32-5, 2003.

U. Gross, R. Kinne, H. J. Schmitz & V. Strunz. «The response of bone to surface active glass/glass-ceramics» CRC. Crit. Rev. Biocompat. (4 - 2) (1988).

U. M. Gross &. V. Strunz. «Clinical Application of Biomaterials», pp. 237, Ed. A.J.C. Lee, T. Albrektsson & P. Branemark.,New York: John Wiley & Son (1982).
U. M. Gross, C. Müller-Mai & C Voigt. «Ceravital bioactive Glass-Ceramic», pp.105-124, in An introduction to bioceramics. Hench LL, &Wilson J, Editors. Singapore: World Scientific Publishing Co (1993).

Vallet-Regí M and Ruiz-Hernández E. Bioceramics: From bone regeneration to cancer nanomadicine. Adv Mater 5177-5218, 2011.

Vallet-Regí M, Chem Eng 2008 137, 1

Vallet-Regí M. Ceramics for medical applications. J Chem Soc Dalton 2: 97-108, 2001.

Vats A, Tolley NS, Polak JM, Gough JE. Scaffolds and biomaterials for tissue engineering: a review of clinical applications. Clin Otolaringol 28: 165-172, 1003.
Wan C, He Q, MacCaigue M, Marsh D, Li G. Nonadherent cell population of human marrow colture is a complementary source of mesenchymal stem cells (MSCs). J Orthop Res 24: 21-28, 2006.

Wang L, Li Y, Chen X, Chen J, Gautam SC, Xu Y, Chopp M. Ischemic cerebral tissue enhance human bone marrow stromal cell migration in interface culture. Hematology 7: 113-117, 2002.

Warnke PH, Springer IN, Wiltfang J, Acil Y, Eufinger H, Wehmoller M. Growth and transplantation of a custom vascularised bone graft in a man. Lancet 364: 766-770, 2004.

Watt FM, Hogan BL. Out of Eden: Stem cells and their niches. Science 287: 1427-1430, 2000.

Welch JH, Gutt JH. High-temperature studies of the system calcium oxide–phosphorus pentoxide. J Chem Soc 1961: 4442–4.

Williams DF. The biocompatibility and clinical uses of calcium-phosphate ceramics. Biocompatibility of tissue analogs (II 43-66), William DF editor, Boca Raton, FL: CRC Press, 1985.

Williams FD. Biomaterials 2009, 30, 5897

Williams FD. Definitions of biomaterials. Elsevier, Amsterdam, 1987.

Wiessmann HP, Meyer U, Plate U, Hohling HJ. Aspects of collagen mineralization in hard tissue formation. Int Rev Cytol 242: 121, 2005).
Wong GL, Frantz K, Lam C. Isolation and characterization of highly serum-dependent cells released early from collagenase digested calvaria. J Bone Miner Res 1: 417-24, 1986.

Xi Chen, Haibo Xu, Chao Wan. Bioreactor expansion of human adult bone marrow-derived mesenchymal stem cells. Stem Cells 24: 2052-59, 2006.

Xiao Y, Mareddy S, Crawford R. Clonal Characterization of Bone Marrow Derived Stem Cells and Their Application for Bone Regeneration. International Journal of Oral Science 2(3): 127-135, 2010.

RESUMEN

El objetivo de este trabajo, ha sido evaluar la aplicabilidad de tres materiales eutectoides en el sistema dicalcio silicato-tricalcio fosfato (EC1, EC2, EC3) en el campo de la ingeniería del tejido óseo. Por eso es necesario evaluar la biocompatibilidad de estas cerámicas a través de estudios in vitro , la posibilidad de utilizarlas como matrices para suportar el crecimiento celular y al mismo tiempo la capacidad osteoinductora de lo los materiales de estimular la diferenciación de células indiferenciadas (ahMSCs) hacia osteoblastos.

LA BIO-INGENIERÍA DEL TEJIDO ÓSEO

La bio-ingeniería es un nuevo campo inter-disciplinar que se propone de combinar los principios de la biología y de la ingeniería. Esta disciplina se propone reparar daños óseos utilizando como soportes para el crecimiento celular biomateriales que una vez introducidos en el sito defectivo permitirian a los precursores celulares diferenciarse bajo la influencia de los factores de crecimiento y de los iones presentes.

Los precursores no cometidos mas utilizados para estos estudios son las células mesenquimales adultas humanas (ahMSCs) aisladas de aspirados completos de medula ósea, através de varios protocolos entre los cuales la centrifugación en gradientes de densidad como el Ficoll. Las ahMSCs son células multipotentes capaces de originar progenitores de diferentes tejidos mesenquimales como el óseo, cartilagíneo, adiposo o muscular. Por este motivo y por la baja imunogenicidad presentada son las celulas mas deseadas. Al día de hoy hay algunas normas para la caracterización de las ahMSCs como la adherencia al plástico y la expresión de algunos marcadores como CD105, CD73, CD90; porque los cultivos primarios de

células mononucleadas separadas por centrifugacion en Ficoll, se ha demostrado contener células de la línea hematopoyética y un conjunto de progenitores mesenquimales con diferentes grados de staminalidad. El mayor o menor contenido de células no comisionadas varia de muestra a muestra y está relacionado con factores dependientes del donador como edad o condiciones físicas y del método de extracción o separación.

LOS MATERIALES CERAMICOS (EC1, EC2, EC2)

Los materiales utilizados en este trabajo los ha producido Isabel Martinez de la Universidad de Helche. Son ceramicas contenientes diferentes cantidades de fosfato tricalcico $Ca_3(PO_4)_2$ (TCP) y dicalcio silicato Ca_2SiO_4 (C_2S) (EC 1: 31% TCP e 69% C_2S, EC 2: 55% TCP e 45% C_2S, EC 3: 83% TCP e 17% C_2S). La hipótesis es que estos materiales sean biocompatibles, y debido a su bioactividad (comprobada anteriormente por el laboratorio que los produce) que estimulen la regeneración ósea integrándose al hueso através de la formación de una capa de hydroxuapatita y promocionando el diferenciamiento osteogenico de las ahMSCs através de la liberación de iones al medio de cultivo celular. Calcio i Fosfato son iones que actúan como moléculas señal, capaces de estimular la proliferación y el diferenciamiento celular actuando sobre la vía de señalización ERK1/2. En cambio el Silicio es un cofactor de la prolina idroxilasa, que actúa sobre las cadenas alfa del colágeno promocionando su síntesis y secreción extracelular.

MARCADORES DE LA DIFERENCIACIÓN OSTEOBLASTICA

Las capacidades regeneradoras del hueso dependen de la re-activación de vías activadas durante la esqueletogenesis en el embrión. En la osteogenesis endocondral como intramembranosa, la generación de nuevo tejido óseo pasa por la formación de agregados de células mesenquimales previamente al inicio de su inducción al diferenciamiento en osteoblastos. El factor de trascripción RUNX2 se ha determinado por varios estudios ser importante para el comisionamiento de las MSCs en osteoblastos. RUNX2 fosforilado por la vía de ERK1/2 junto con otros cofactores se une a la secuencia OSE presente en los promotores de genes expresados en la

diferenciación osteoblastica como la alcalina fosfatasa el colágeno tipoI, la osteopontina, osteocalcina y la sialoproteina.

RESULTADOS Y DISCUSION

Las ahMSC fueron aisladas a partir de aspirados de medula ósea de pacientes intervenidos de hernia discal. Las células fueron expandidas en plástico hasta el pase 2 antes de empezar el experimento. Las ahMSCs fueron entonces sembradas sobre la superficie de los materiales o sobre plástico y los materiales introducidos en los pocillos contenientes las células. El periodo de estudio fue de 4 semanas, y a partir de la tercera semana las muestras fueron divididas en dos grupos y todos los materiales y los controles cultivados en paralelo en presencia de medio de crecimiento normal e medio osteogenico. Los resultados de los análisis de ICP demostraron que los tres materiales intercambian con el medio de cultivo iones Calcio, Fospato y Silicio, de manera diferente para cada material. Los resultados de la microscopia electronica combinados con los microanalisis EDS (Energydispersive X-ray spectroscopy) confirmaron la formación de nódulos de Ca-P sobre la superficie de todos los materiales, nucleación de la capa de hydroxyapatita. Estas formaciones son muy importantes para las ahMSCs, porque le permiten adherir mejor, proliferar y migrar encima de ellos.

El estudio de proliferación con MTT demostró que los materiales solo débilmente afectaron la proliferación celular durante las primeras 24 horas; pero no hay indicios de toxicidad por parte de los materiales. El estudio de apoptosis por Annexina V-Fosfatidil Serina confirmó que la apoptosis en las muestras incubadas con los materiales era comparable en cada momento con las muestras control. El material EC2 demostró estimular la proliferación de ahMSCs a partir de la segunda semana, superando la muestra control, y aumentando mucho mas en presencia del medio osteogenico, probablemente debido al elevado contenido de fosfatos introducido por este medio. Las imágenes de SEM confirmaron en parte que el material EC2 estimuló mas eficazmente la proliferación de las ahMSCs, pero demostraron que también los otros dos materiales permiten el crecimiento normal de las células. La osteoinductividad de los tres materiales fue comprobada evaluando la expresión de marcadores osteoblasticos por las ahMSCs con el pasar del tiempo. Los resultados de

la PCR cuantitativa mostraron el aumento de la expresión del gen RUNX2 a partir de la segunda semana en las células cultivadas sobre los materiales EC1 y EC2; el medio osteogenico aumentó ulteriormente su expresión en estas muestras, confirmando la hipótesis que este marcador es importante para dirigir las celulas hacia la diferenciación osteoblastica. Siempre según los resultados obtenidos por qPCR, se observó la inhibición de la expresión del gen que codifica por la fosfatasa alcalina para estos materiales, siendo la fosfatasa un clasico marcador de las células osteoblastica. La fosfatasa aumenta a los 28 dias de estudio cuando las ahMSCs fueron incubadas en EC2 en presencia de medio osteogenico. Fueron estudiadas también la formación y la maduración de la matriz extracelular. El colágeno de tipo I y la osteonectina son marcadores precoces de la diferenciación hacia osteoblastos; sin embargo no hubo cambios significativos en la expresión de su mRNA en presencia de los materiales, sugiriendo una regulación de estas proteínas postraducional. Esta hipótesis seria confirmada por las imágenes de inmunofluorescencia del Colageno I. De hecho por inmunofluorescencia el colágeno I se detectó a partir de los primeros momentos en cultivo y en las muestras control, aunque se detectó un mayor numero de grupos celulares que expresaban ColI en las muestras de EC1 y EC2. Este dato podría estar relacionado con la mayor liberacion de Si registrada por estos materiales, sabiendo que el Si interviene en las modificaciones post-traduccionales de las cadenas alfa del colágeno. A partir de la tercera y quarta semana, EC1 y EC2 se demostró que eran capaces de estimular la expresión de genes codificantes por proteínas de la matriz extracelular como osteopontina, osteocalcina, bone sialoprotein, que regulan también la mineralización. Los datos de q-PCR mostraron que las células sembradas sobre el material EC2 expresaban los mayores niveles de estas proteínas a los 21 días con medio osteogenico; las células cultivadas sobre EC1 mostraron en cambio la mayor expresión a las 4 semanas. Los datos de q-PCR además fueron confirmados por las inmunofluorescencias, demostrando maduración de la matriz extracelular durante las últimas dos semanas de experimento con medio osteogenico. Las imágenes de SEM confirmaron la síntesis de matriz extracelular: en los espacios intercelulares se pudo fotografiar material fibrilar que aumenta en los dichos periodos. Las tinciones de alizarin red para el estudio de la mineralizacion mostraron datos significativos solo

para las muestras incubadas in medio osteogenico. Solo el material EC2 parece estimular la mineralización también en presencia de medio de cultivo basal. El análisis de los marcadores mesenquimales demostró la disminución con el paso del tiempo de la expresión del CD105 para las muestras sembradas sobre los materiales EC1 y EC2, significativa respecto al control, sugiriendo perdida de la staminalidad. En conjunto los resultados enseñan que los materiales EC1 y EC2, y el EC2 en particular manera, son los dos materiales que mejor activan la diferenciación osteogenica; aunque el EC2 obtiene esto en menor tiempo.

El material EC2, sobre todo en presencia de medio osteogenico, demostró estimular la proliferación de las ahMSCs y tener un efecto positivo sobre la formación y maduración de la matriz extracelular, induciendo la síntesis de proteínas que dirigen la nucleación de los cristales de apatita. La formación de una capa de hydroxyapatita en la superficie del material es importante porque reproduce las características del hueso. Esta superficie estimula la adhesión, proliferación y diferenciamiento de las ahMSCs, y durante este proceso la producción de matriz extracelular. Por eso definimos la cerámica EC2 como la que tiene mejores características osteoinductoras y lo proponemos para ulteriores estudios previos al utilizo como implante en bio-ingeniería del tejido óseo.